

PUBLICATIONS OF
THE UNIVERSITY OF EASTERN FINLAND



UNIVERSITY OF
EASTERN FINLAND

Dissertations in Health Sciences

METTE HEISKANEN

CIRCULATING PLASMA microRNAs AND NEUROFILAMENT LIGHT CHAIN AS BIOMARKERS FOR INJURY SEVERITY AND POST-TRAUMATIC EPILEPTOGENESIS AFTER AN EXPERIMENTAL TRAUMATIC BRAIN INJURY

**CIRCULATING PLASMA microRNAs AND
NEUROFILAMENT LIGHT CHAIN AS BIOMARKERS
FOR INJURY SEVERITY AND POST-TRAUMATIC
EPILEPTOGENESIS FOLLOWING AN
EXPERIMENTAL TRAUMATIC BRAIN INJURY**

Mette Heiskanen

**CIRCULATING PLASMA microRNAs AND
NEUROFILAMENT LIGHT CHAIN AS BIOMARKERS
FOR INJURY SEVERITY AND POST-TRAUMATIC
EPILEPTOGENESIS AFTER AN EXPERIMENTAL
TRAUMATIC BRAIN INJURY**

To be presented by permission of the Faculty of Health Sciences,
University of Eastern Finland for public examination in MS300
Auditorium, Kuopio on June 14th, 2024, at 12 o'clock noon

Publications of the University of Eastern Finland
Dissertations in Health Sciences
No 823

A.I. Virtanen Institute for Molecular Sciences
University of Eastern Finland, Kuopio
2024

Series Editors

Professor Tomi Laitinen, M.D., Ph.D.
Institute of Clinical Medicine, Clinical Physiology and Nuclear Medicine
Faculty of Health Sciences

Professor Ville Leinonen, M.D., Ph.D.
Institute of Clinical Medicine, Neurosurgery
Faculty of Health Sciences

Professor Tarja Malm, Ph.D.
A.I. Virtanen Institute for Molecular Sciences
Faculty of Health Sciences

Lecturer Veli-Pekka Ranta, Ph.D.
School of Pharmacy
Faculty of Health Sciences

Lecturer Tarja Välimäki, Ph.D.
Department of Nursing Science
Faculty of Health Sciences

PunaMusta Oy
Joensuu, 2024
Distributor: University of Eastern Finland
Kuopio Campus Library

ISBN: 978-952-61-5193-9 (print/nid.)

ISBN: 978-952-61-5194-6 (PDF)

ISSNL: 1798-5706

ISSN: 1798-5706

ISSN: 1798-5714 (PDF)

Author's address: A.I. Virtanen Institute for Molecular Sciences
University of Eastern Finland
KUOPIO
FINLAND

Doctoral programme: Doctoral Programme in Molecular Medicine

Supervisors: Professor Asla Pitkänen, M.D., Ph.D., D.Sc.
A.I. Virtanen Institute for Molecular Sciences
University of Eastern Finland
KUOPIO
FINLAND

Docent Kirsi Rilla, Ph.D., D.Sc.
Institute of Biomedicine
University of Eastern Finland
KUOPIO
FINLAND

Jenni Karttunen, Ph.D.
Department of Veterinary Medicine
University of Cambridge
CAMBRIDGE
UK

Reviewers: Cristina Reschke, Ph.D.
School of Pharmacy and Biomolecular Sciences
RCSI University of Medicine and Health Sciences
DUBLIN
IRELAND

Professor Olli Tenovuo, M.D., Ph.D.
Department of Clinical Neurosciences
University of Turku
TURKU
FINLAND

Opponent:

Professor Merab Kokaia, Ph.D.
Epilepsy Center, Department of Clinical Sciences
Lund University
LUND
SWEDEN

Heiskanen, Mette

Circulating plasma microRNAs and neurofilament light chain as biomarkers for injury severity and post-traumatic epileptogenesis following an experimental traumatic brain injury

Kuopio: University of Eastern Finland

Publications of the University of Eastern Finland

Dissertations in Health Sciences 823. 2024, 159 p.

ISBN: 978-952-61-5193-9 (print)

ISSNL: 1798-5706

ISSN: 1798-5706

ISBN: 978-952-61-5194-6 (PDF)

ISSN: 1798-5714 (PDF)

ABSTRACT

Traumatic brain injury (TBI) is a disturbance in brain function caused by an external force, which is suffered globally by 60–70 million people each year. More than half of patients with moderate-to-severe TBI experience long-term disabilities, and even in mild TBI, more than 15% of patients display symptoms that have still not resolved 1 year after their injury. In addition, TBI patients are at an increased risk of post-traumatic epilepsy (PTE), which is a seizure disorder that can develop months or even years after the TBI. The PTE risk increases with the severity of the injury; it is around 2% for mild, 4% for moderate, and 17% for severe TBI. There are currently no treatments which can either prevent or minimize the epileptogenic process. The search for new antiepileptogenic treatments is hindered by the lack of biomarkers to identify those patients with a high PTE risk. Due to the low incidence and long latency period of PTE, preclinical and clinical treatment trials are currently very laborious and expensive. For this reason, reliable biomarkers of epileptogenesis could be used to enrich the number of patients at an increased PTE risk to be recruited into treatment trials.

This thesis aimed to identify circulating molecular biomarkers to allow the evaluation of the severity of the brain injury as well as the prediction of the development of post-traumatic epileptogenesis. Previous investigations have detected alterations in the levels of circulating microRNAs (miRNAs) and proteins both in TBI and in epilepsy, indicating that they may represent a potential source for PTE biomarkers. The miRNAs in the blood circulation are associated with extracellular vesicles (EVs), lipoproteins and carrier proteins. First, it was investigated whether a precipitation-based EV isolation method could be used to isolate EVs from a small volume of rat plasma to obtain EV-associated miRNAs for further analysis. Next, TBI-induced alterations in the plasma miRNA profile were investigated in a preclinical model of PTE, in which 25% of injured rats developed PTE during a 6-month follow-up. The relationship was examined between the post-injury miRNA profile with the cortical lesion severity and post-traumatic epileptogenesis. Finally, the levels of neurofilament light chain (NF-L), a marker of axonal injury, were explored in TBI rat plasma, and the ability of NF-L levels to predict structural and functional outcome in rats after TBI was investigated.

In the first study, an analysis of the isolated EVs revealed that lipoproteins and other plasma proteins, including their miRNA cargo, were co-precipitated during the procedure. Since the EV yield was low and the EV pellet contained both EV-associated and protein-associated miRNAs, the precipitation method was found to be unsuitable for our subsequent studies and therefore, the second study investigated total plasma miRNAs. It was found that elevated levels of 7 circulating miRNAs (miR-9a-3p, miR-124-3p, miR-323-3p, miR-434-3p, miR-136-3p, miR-132-3p, and miR-212-3p) distinguished the TBI rats from sham-operated and naïve controls 2 days after the injury. Further, 6 out of the 7 miRNAs distinguished the sham group from naïve controls. Higher expression levels of the circulating miRNAs were correlated with a larger cortical lesion area, but the miRNA profile did not differentiate between rats with or without PTE. In the third study, increased levels of plasma NF-L 2 days after injury distinguished TBI rats from sham-operated controls and baseline samples. Further, the NF-L

levels differentiated sham-operated rats from baseline samples, indicating NF-L as sensitive marker for a mild injury. Acutely increased plasma NF-L levels were associated with a larger cortical lesion area, but they did not predict somatomotor recovery, cognitive impairment, or PTE development.

In conclusion, the miRNA profile or NF-L levels were not able to predict post-traumatic epileptogenesis. On the other hand, acutely increased amounts of plasma miRNAs and NF-L were demonstrated to be sensitive markers of brain injury, and higher miRNA and NF-L levels were associated with a worse structural outcome in the cortex of the TBI rats. Importantly, circulating miR-323-3p and miR-212-3p have not been previously investigated after a TBI, and very little information is available about miR-132-3p, warranting further validation in patients with TBI.

Keywords: biomarker, epilepsy, epileptogenesis, extracellular vesicles, microRNA, neurofilament, plasma, traumatic brain injury

Heiskanen, Mette

Veriplasmassa kiertävät mikroRNA:t ja neurofilamentin kevytketju biomarkkereina aivovaurion vakavuudelle ja posttraumaattiselle epileptogeneesille aivovamman prekliinisessä mallissa

Kuopio: Itä-Suomen yliopisto

Publications of the University of Eastern Finland

Dissertations in Health Sciences 823. 2024, 159 s.

ISBN: 978-952-61-5193-9 (nid.)

ISSNL: 1798-5706

ISSN: 1798-5706

ISBN: 978-952-61-5194-6 (PDF)

ISSN: 1798-5714 (PDF)

TIIVISTELMÄ

Traumaattinen aivovamma on ulkoisen voiman aiheuttama muutos aivojen toiminnassa, ja sen saa maailmanlaajuisesti vuosittain 60–70 miljoonaa ihmistä. Yli puolet keskivaikean tai vaikean aivovamman saaneista potilaista kärsii pitkäaikaisista toiminnanvajauksista, ja yli 15 %:lla lievän aivovamman saaneista potilaista on jälkioireita, jotka eivät parane vuoden sisällä vammasta. Lisäksi aivovampapotilailla on kohonnut riski sairastua posttraumaattiseen epilepsiaan (PTE), joka voi kehittyä kuukausia tai jopa vuosia aivovamman jälkeen. PTE:n riski kasvaa aivovamman vakavuusasteen mukaan, ja on noin 2 % lievässä, 4 % keskivaikeassa ja 17 % vaikeassa aivovammassa. PTE:n kehittymiseen johtavan prosessin, epileptogeneesin, ehkäisyyn tai minimointiin ei tällä hetkellä ole olemassa hoitokeinoja. Uusien hoitojen kehittäminen on vaikeaa, koska ei ole olemassa biomarkkereita, joiden avulla voitaisiin tunnistaa potilaat, joilla on kohonnut epilepsiariski. PTE:n matalan ilmaantuvuuden ja pitkän latenssiajan vuoksi prekliiniset ja kliiniset lääketutkimukset ovat tällä hetkellä erittäin työläitä ja kalliita. Epileptogeneesin tunnistavien biomarkkereiden avulla voitaisiin tunnistaa korkean epilepsiariskin potilaat ja kasvattaa heidän määräänsä lääketutkimuksissa.

Tämän väitöskirjatutkimuksen tavoitteena oli tunnistaa verenkierrosta molekulaarisia biomarkkereita, joiden avulla voitaisiin arvioida aivovaurion vakavuutta ja ennustaa PTE:n kehittymistä. Aiemmissa tutkimuksissa on havaittu, että sekä aivovamma että epilepsia aiheuttavat muutoksia mikroRNA:iden ja proteiinien tasoissa verenkierrossa, joten ne ovat lupaavia lähteitä uusille PTE:n biomarkkereille. MikroRNA:t kiertävät veressä solunulkoisten vesikkelien ja kuljettajaproteiinien mukana. Väitöskirjan ensimmäisessä osatyössä tutkittiin saostukseen perustuvan vesikkelien eristysmenetelmän soveltuvuutta vesikkelien eristämiseen pienestä määrästä rotan plasmaa. Tarkoituksena oli eristää verenkierrosta vesikkeleitä niiden kuljettamien mikro-RNA:iden tutkimusta varten. Toisessa osatyössä tutkittiin aivovamman aiheuttamia muutoksia veren mikro-RNA-profiilissa PTE:n prekliinisessä mallissa, jossa 25 % koe-eläiminä käytetyistä rotista sairastui epilepsiaan puolen vuoden seurantajakson aikana. Tutkimus selvitti veriplasman mikroRNA-profiilin yhteyttä aivokuoren vaurion laajuuteen ja aivovamman jälkeiseen epileptogeneesiin. Väitöskirjan viimeisessä osatyössä tutkittiin hermosolujen aksonivauriosta kertovan proteiinin, neurofilamentin kevytketjun (NF-L:n), pitoisuuksia rotan veri-plasmassa aivovamman jälkeen. Tutkimus selvitti, ennustavatko NF-L-proteiinin tasot plasmassa aivovamman rakenteellista ja toiminnallista lopputulosta aivovamman saaneissa rotissa.

Rotan plasmasta saostamalla eristettyjen solunulkoisten vesikkelien karakterisointi paljasti, että menetelmä saosti vesikkelien lisäksi lipoproteiineja ja muita plasman proteiineja. Koska vesikkelien määrä oli pieni ja näyte sisälsi vesikkelien kuljettamien mikroRNA:iden lisäksi myös proteiinien kuljettamia mikroRNA:ita, menetelmä ei ollut sopiva myöhempisiin tutkimuksiimme. Tämän vuoksi toisessa osatyössä tutkittiin vesikkelien sisältämien miRNA:iden sijaan kaikkia plasman mikroRNA:ita. Tutkimuksessa havaittiin, että seitsemän mikroRNA:n (miR-9a-3p, miR-124-3p, miR-323-3p, miR-434-3p, miR-136-3p, miR-132-3p ja miR-212-3p) kohonneet arvot plasmassa erottivat aivovamman saaneet rotat verrokiryhmistä 2 päivää vaurion jälkeen. Lisäksi kuusi seitsemästä

tutkitusta mikroRNA:sta erotti kirurgisen verrokkiryhmän ryhmästä, jolle ei tehty toimenpiteitä. Plasman mikroRNA:iden kohonneet arvot 2 päivää aivovamman jälkeen korreloivat laajemman aivokuoren vaurion kanssa, mutta mikroRNA-tasot eivät erottaneet epilepsiaan sairastuneita rottia niistä, joille ei kehittynyt epilepsiaa. Kolmannessa osatyössä havaittiin, että NF-L-proteiinin kohonneet arvot plasmassa 2 pv aivovamman jälkeen erottivat aivovamman saaneet rotat sekä kirurgisesta verrokkiryhmästä että ennen vammaa otetuista näytteistä. Lisäksi veren NF-L-arvot erottivat kirurgisen verrokkiryhmän ennen toimenpidettä otetuista näytteistä, mikä osoitti NF-L:n olevan herkkä mittari lievälle vauriolle. Akuutisti kohonneet plasman NF-L-arvot korreloivat laajemman aivokuoren vaurion kanssa, mutta ne eivät ennustaneet somatomotorista toipumista, kognitiivisia häiriöitä tai PTE:n kehittymistä.

Tutkimuksen loppupäätelmä on, että aivovamman seurauksena kohonneet mikroRNA:t ja NF-L-proteiinin tasot verenkierrassa eivät ennustaneet epilepsian kehittymistä. Tutkimuksessa kuitenkin havaittiin, että akuutisti kohonneet mikroRNA:t ja NF-L verenkierrassa ovat herkkiä aivovamman merkkiaineita, ja korkeammat mikroRNA- ja NF-L-tasot aivovamman saaneissa rotissa ennustavat huonompaa aivokuoren rakenteellista lopputulosta vamman jälkeen. Veressä kiertäviä miR-323-3p:tä ja miR-212-3p:tä ei ole aiemmin tutkittu aivovamman jälkeen, ja miR-132-3p:sta on vain vähän aikaisempaa tietoa, joten niitä on syytä tutkia lisää tulevaisuudessa aivovammapotilailta kerätyillä näytteillä.

Avainsanat: aivovamma, biomarkkeri, epilepsia, epileptogeneesi, mikroRNA, neurofilamentti, plasma, solunulkoiset vesikkelit

ACKNOWLEDGEMENTS

This work was conducted in the Epilepsy Research laboratory of the A.I. Virtanen Institute for Molecular Sciences, University of Eastern Finland, Kuopio.

I sincerely thank my principal supervisor, Professor Asla Pitkänen, M.D., Ph.D., for offering me the opportunity to join her laboratory back in 2016, when I first arrived in Kuopio to undertake a master's thesis project, and for providing me with the possibility to continue with a Ph.D. project. I am truly grateful for all the lessons in the field of TBI and epilepsy and for the excellent guidance on conducting the research. I also thank my second supervisor, Docent Kirsi Rilla, Ph.D., for the useful comments on the thesis. I am truly grateful to my third supervisor, Jenni Karttunen, Ph.D., for the inspiring introduction to the world of extracellular vesicles and for the extensive guidance especially during the first years of the project.

My sincere gratitude to Professor Olli Tenovuo, M.D., and Cristina Reschke, Ph.D., for acting as reviewers for this thesis and for their important comments. I sincerely thank Professor Merab Kokaia, Ph.D., for kindly accepting to be the opponent to for this thesis. I also thank Ewen MacDonald for revising the language of the thesis book.

I thank all the co-authors of the articles in this thesis, Vicente Navarro-Ferrandis, Shalini Das Gupta, Anssi Lipponen, Noora Puhakka, Arto Koistinen, James D. Mills, Erwin A. van Vliet, Eppu Manninen, Robert Cizek, Pedro Andrade, Eleonora Aronica, Olli Jääskeläinen, Olli Gröhn, and Sanna-Kaisa Herukka, for their significant contribution.

I thank all the present and former members of the "EpiClub": Natallie Kajevu, Meheli Banerjee, Pedro Andrade, Noora Puhakka, Elina Hämäläinen, Jarmo Hartikainen, Johanna Tiilikainen, Jenni Kyyriäinen, Merja Lukkari, Xavier Ekolle Ndode-Ekane, Shalini Das Gupta, Mehwish Anwer, Niina Vuokila, Anssi Lipponen, Niina Lapinlampi, Ivette Bañuelos, Leonardo Lara, Jenni Karttunen, Tomi Paananen, Robert Cizek, Vicente Navarro-Ferrandis, Amna Yasmin, Ying Wang, Diana Miszczuk, and Francesco Noé. My special thanks to Natallie Kajevu for being my peer support in the office

during these years. I am grateful to Jenni Kyyriäinen for all the advice during the thesis book process. I thank Shalini Das Gupta, Niina Vuokila, Jenni Kyyriäinen, Mehwish Anwer, and Anssi Lipponen for setting me a good example. I am grateful to Noora Puhakka for all the help with scientific and other questions regarding the research.

I thank all the present and former participants of our weekly relaxed floorball in Studentia, especially Eppu, Oskari, Tommi, Raghu, Natallie, Isidore, Lenka, Anssi, and Jenni. This weekly activity has given me a lot of energy, and it has been one of the highlights of my week.

Finally, I thank my family for showing interest in my work and for supporting me. I am forever grateful to my partner Tommi for being my constant support throughout these years. You always managed to find ways to motivate me to reach my goals when I needed it. I could not have done this without you. Finally, I thank our daughter Helmi for giving me extra motivation to finalize the thesis.

This thesis was funded by Academy of Finland, Sigrid Jusélius Foundation, European Union's Seventh Framework Programme, the European Infrastructure for Translational Medicine, University of Eastern Finland, Biocenter Finland, the National Institute of Neurological Disorders and Stroke (NINDS) Center without Walls of the National Institutes of Health (NIH), Doctoral Programme in Molecular Medicine (DPMM), Foundation for Research on Epilepsy (Epilepsiatutkimussäätiö), the Paulo Foundation, Juhani Aho Foundation for Medical Research, Instrumentarium Science Foundation, and Finnish Brain Foundation. The figures in the literature review were created with BioRender.com.

Kuopio, March 2024



Mette Heiskanen

LIST OF ORIGINAL PUBLICATIONS

This dissertation is based on the following original publications:

- I Karttunen, J, Heiskanen, M, Navarro-Ferrandis, V, Das Gupta, S, Lipponen, A, Puhakka, N, Rilla, K, Koistinen, A and Pitkänen, A. Precipitation-based extracellular vesicle isolation from rat plasma co-precipitate vesicle-free microRNAs. *Journal of Extracellular Vesicles*, 8(1): 1555410, 2018.
- II Heiskanen, M, Das Gupta, S, Mills, J.D, van Vliet, E.A, Manninen, E, Cizek, R, Andrade, P, Puhakka, N, Aronica, E and Pitkänen, A. Discovery and Validation of Circulating microRNAs as Biomarkers for Epileptogenesis after Experimental Traumatic Brain Injury – The EPITARGET Cohort. *International Journal of Molecular Sciences*, 24(3): 2823, 2023.
- III Heiskanen, M, Jääskeläinen, O, Manninen, E, Das Gupta, S, Andrade, P, Cizek, R, Gröhn, O, Herukka, S.-K, Puhakka, N and Pitkänen, A. Plasma Neurofilament Light Chain (NF-L) Is a Prognostic Biomarker for Cortical Damage Evolution but Not for Cognitive Impairment or Epileptogenesis Following Experimental TBI. *International Journal of Molecular Sciences*, 23(23): 15208, 2022.

The publications were adapted with the permission of the copyright owners.

CONTENTS

ABSTRACT	7
TIIVISTELMÄ	11
1 INTRODUCTION	27
2 REVIEW OF THE LITERATURE	29
2.1 Traumatic brain injury and post-traumatic epilepsy.....	29
2.1.1 Traumatic brain injury	29
2.1.2 Pathophysiology of TBI.....	30
2.1.3 Post-traumatic epilepsy.....	31
2.1.4 Epileptogenesis after TBI.....	32
2.1.5 Animal models of PTE.....	33
2.1.6 Definition of biomarkers	34
2.1.7 Biomarkers for epileptogenesis.....	35
2.2 Circulating miRNAs as disease biomarkers.....	36
2.2.1 miRNA biogenesis and function	36
2.2.2 miRNAs as disease biomarkers	38
2.2.3 miRNA carriers in blood	38
2.2.4 Extracellular vesicle associated miRNAs	40
2.2.5 Circulating miRNAs as TBI biomarkers.....	42
2.2.6 Circulating miRNAs in epilepsy	54
2.3 Circulating proteins as disease biomarkers.....	57
2.3.1 Circulating proteins as TBI biomarkers.....	57
2.3.2 Clinical use of circulating TBI biomarkers.....	63
2.3.3 Circulating proteins as biomarkers of epilepsy.....	65
3 AIMS OF THE STUDY	69
4 MATERIALS AND METHODS	71
4.1 Animals.....	71
4.2 Animal experiments	72
4.2.1 TBI induction by lateral fluid-percussion injury	73
4.2.2 Video-EEG monitoring	74
4.3 Molecular biology methods.....	74

4.4 Bioinformatics methods	75
4.5 Statistical analysis.....	75
5 RESULTS.....	77
5.1 Evaluation of a commercial precipitation-based method in the isolation of EVs from rat plasma for miRNA analysis (I).....	77
5.1.1 The precipitated EV pellet from rat plasma contained circulating lipoproteins and plasma proteins.....	77
5.1.2 SEC separated particles and proteins into different fractions, but the EV fractions also contained lipoproteins.	78
5.1.3 The precipitation method excluded the majority of plasma proteins from the EV pellet.	78
5.1.4 The EV pellet acquired by the precipitation method contained both EV-enriched and vesicle-free miRNAs.	79
5.2 The circulating miRNA profile at an acute time-point after TBI as a biomarker for post-traumatic epileptogenesis in rats (II).....	80
5.2.1 The plasma miRNA profile from small RNA-seq separated TBI rats from sham-operated controls at 2 days but not at 9 days after the TBI.....	80
5.2.2 Circulating miRNA profile from small RNA sequencing on 2 d or 9 d after TBI did not separate rats with or without PTE.	81
5.2.3 Differentially expressed plasma miRNAs were identified between the TBI and sham groups, but not between the TBI+ and TBI- groups.....	81
5.2.4 Upregulation of plasma miR-136-3p, miR-323-3p, miR-434-3p, and miR-9a-3p 2 d after TBI was validated by RT-qPCR.....	82
5.2.5 Analysis in the large EPITARGET animal cohort confirmed 7 plasma miRNAs as injury biomarkers.	83
5.2.6 Plasma miRNAs at the acute time-point after TBI did not predict the epilepsy outcome.	85
5.2.7 The expression levels of plasma miRNAs at the acute time-point after TBI correlated with the severity of the cortical lesion at different time points after TBI.	86
5.3 Circulating NF-L as a prognostic biomarker for the structural and functional outcome in rats after TBI (III).....	87

5.3.1 Plasma NF-L levels increased after the LFP-induced TBI, and a slight elevation was observed even 6 months after TBI.	87
5.3.2 Plasma NF-L levels correlated with cortical lesion severity at acute and chronic time-points after TBI.	87
5.3.3 Circulating NF-L functioned as biomarker for TBI and sham-operation.	88
5.3.4 The plasma NF-L levels did not predict somatomotor recovery after TBI.	89
5.3.5 The plasma NF-L levels did not predict the cognitive impairment after TBI.	90
5.3.6 Plasma NF-L levels did not predict post-traumatic epileptogenesis.	90
6 DISCUSSION	93
6.1 Isolation of EVs by the precipitation method co-precipitated plasma proteins, lipoproteins, and vesicle-free miRNAs.....	93
6.2 Circulating miRNAs are markers of brain injury and predict the severity of cortical pathology but not epileptogenesis	97
6.3 Circulating NF-L predicts the evolution of cortical damage but not cognitive impairment or epileptogenesis.....	102
7 CONCLUSIONS	107
REFERENCES.....	109

ABBREVIATIONS

Ago	Argonaute	EEG	Electroencephalography
ASC	Apoptosis-associated speck-like protein containing a caspase recruit domain	ELISA	Enzyme-linked immunosorbent assay
AUC	Area under the curve	EV	Extracellular vesicle
BBB	Blood-brain barrier	FLE	Frontal lobe epilepsy
BDNF	Brain-derived neurotrophic factor	FPI	Fluid percussion injury
BEST	Biomarkers, EndpointS, and other Tools	GCS	Glasgow Coma Scale
CCI	Controlled cortical impact	GFAP	Glial fibrillary acidic protein
CNS	Central nervous system	GGE	Genetic generalized epilepsy
CSF	Cerebrospinal fluid	HC	Healthy control
CT	Computed tomography	HDL	High-density lipoprotein
D	Day	HMGB-1	High mobility group 1
ddPCR	Droplet digital polymerase chain reaction	ICAM-1	Intercellular adhesion molecule 1
DRE	Drug-resistant epilepsy	IFN- γ	Interferon gamma
EC	Extracranial injury	IL	Interleukin

ISEV	International Society for Extracellular Vesicles	NSE	Neuron-specific enolase
LDL	Low-density lipoprotein	NTA	Nanoparticle tracking analysis
LFPI	Lateral fluid percussion injury	PCA	Principal component analysis
MAP-2	Microtubule-associated protein 2	PCR	Polymerase chain reaction
MCP	Monocyte chemoattractant protein	PNES	Psychogenic nonepileptic seizures
miRISC	MiRNA-induced silencing complex	pNF-H	Phosphorylated neurofilament heavy chain
miRNA	MicroRNA		
MMP-3	Matrix metalloproteinase-3	pre-miRNA	Precursor miRNA
moTBI	Moderate traumatic brain injury	pri-miRNA	Primary miRNA
MRI	Magnetic resonance imaging	PTE	Post-traumatic epilepsy
mRNA	Messenger RNA	PTSD	Post-traumatic stress disorder
mTBI	Mild traumatic brain injury	ROC	Receiver operating characteristic
mTLE-HS	Mesial temporal lobe epilepsy with hippocampal sclerosis	RT-qPCR	Reverse transcription quantitative PCR
NF-H	Neurofilament heavy chain	S100B	S100 calcium-binding protein beta
NF-L	Neurofilament light chain	SE	Status epilepticus
NRGN	Neurogranin	SEC	Size-exclusion chromatography

SEM	Scanning electron microscopy	TIMP-1	Tissue inhibitor matrix metalloproteinase 1
seq	Sequencing	TLE	Temporal lobe epilepsy
sICAM5	Soluble intercellular adhesion molecule 5	TNF-R1	Tumor necrosis factor-receptor 1
SIMOA	Single molecule array	TNF- α	Tumor necrosis factor alpha
sTBI	Severe traumatic brain injury	TRAIL	Tumor necrosis factor-related apoptosis-inducing ligand
TARC	Thymus activation regulated chemokine	UC	Ultracentrifugation
TBI	Traumatic brain injury	UCH-L1	Ubiquitin C-terminal hydrolase L1
TCC	Terminal complement complex		
TEM	Transmission electron microscopy		

1 INTRODUCTION

Traumatic brain injury (TBI) is a neurological disorder that is caused by an external force impacting on the brain (Menon et al., 2010), which is commonly caused by falls and traffic accidents (Maas et al., 2022). Many TBI survivors suffer from long-term consequences such as physical limitations, cognitive deficits, headaches, and emotional dysfunctions (Dixon, 2017). Post-traumatic epilepsy (PTE) is one of the major consequences of TBI; it develops in from 2% up to 17% of patients with TBI depending on the injury severity (Annegers et al., 1998). PTE is a result of a chronic process called epileptogenesis in which the TBI-induced changes in the brain network lead to increased seizure susceptibility (Pitkänen et al., 2015). Currently, there are no treatments that can prevent or minimize the epileptogenic process (Klein & Tyrlikova, 2020). Due to the low incidence rate of PTE and its long latency period, treatment trials for potential antiepileptogenic drug candidates are difficult and very expensive (Engel et al., 2013; Klein & Tyrlikova, 2020). For this reason, biomarkers that could predict PTE are urgently needed, as they could be used to stratify study subjects into different PTE risk groups, making preclinical and clinical trials more cost-effective. In addition, PTE biomarkers could help to identify those patients that require closer monitoring, and aid in the choice of the most appropriate treatment option.

TBI investigators have described alterations in the microRNA (miRNA) and protein signatures in cerebrospinal fluid (CSF) and blood circulation, indicating that miRNAs and proteins may represent potential brain injury biomarkers (Pitkänen et al., 2021). For example, an assay of a brain-enriched protein S100B from a blood sample is already being used in the clinic in the initial evaluation of the injury severity in patients with mTBI (Undén et al., 2013). In contrast, no miRNA biomarkers of TBI have yet been developed for clinical use. MiRNAs are small non-coding RNAs that regulate gene expression by binding to target mRNAs (Lee et al., 1993). Circulating miRNAs are protected from degradation due to their association with

carrier proteins and extracellular vesicles (EVs), which are small membrane-bound vesicles secreted by cells (Colombo et al., 2014). Their protection by carrier proteins and EVs means that circulating miRNAs are rather stable which is a clear advantage over proteins if they are to be used as biomarkers (Mitchell et al., 2008; Balakathiresan et al., 2015). In addition to the situation in TBI, alterations in circulating proteins and miRNAs have also been reported in epilepsy patients (see review by Pitkänen et al., 2021). Whether circulating brain-derived miRNAs or proteins can predict the development of PTE, however, has not been investigated.

This study aims to identify circulating miRNA and protein biomarkers that can be used to evaluate injury severity and predict post-traumatic epileptogenesis, using a recognized animal model of human PTE. In the first study, a commercial precipitation-based EV isolation kit was tested as a method to capture circulating EVs from a small volume of rat plasma for subsequent analysis of EV-associated miRNAs. In the second study, small RNA sequencing was used to reveal miRNA alterations in the plasma of lateral fluid percussion injury (FPI)-induced TBI rats at 2 d and 9 d after injury, to identify potential miRNA biomarkers for the evaluation of injury severity and prediction of post-traumatic epileptogenesis. The rats underwent a 6 months' long follow-up that included a 1-month video-electroencephalography (video-EEG) monitoring to detect PTE. In the third study, levels of a protein marker of axonal injury, neurofilament light chain (NF-L), were measured with single molecule array (SIMOA) in rat plasma at 2 d, 9 d and 6 months after TBI. Correlation analyses were conducted to investigate the relation of plasma NF-L levels with structural and functional outcome after TBI, including PTE.

2 REVIEW OF THE LITERATURE

2.1 TRAUMATIC BRAIN INJURY AND POST-TRAUMATIC EPILEPSY

2.1.1 Traumatic brain injury

The position statement by Menon et al. (2010) defined TBI as “an alteration in brain function, or other evidence of brain pathology, caused by an external force”. The estimated global incidence of TBI is around 60–70 million people per year (Dewan et al., 2019), and the cost of TBI to the global economy has been estimated to be around 400 billion US dollars each year (Maas et al., 2022). In Finland, the incidence rate of hospitalized TBI among the working-age population (16–69 years of age) is 69/100,000 overall (Posti et al., 2022). The incidence rate is more than twice as high in men (94/100,000) than in women (44/100,000). Globally, the most common causes of TBI include falls and traffic accidents (Maas et al., 2022). In addition, TBIs are caused by violence, conflicts, and activities that have an increased risk of head impact, such as contact sports.

By using the Glasgow Coma Scale (GCS), TBI can be classified as mild (GCS 13–15), moderate (GCS 9–12), or severe (GCS 3–8) (Teasdale et al., 2014). Most TBIs, 70–90%, are mild (Cassidy et al., 2004), however, mild TBI can still cause physical symptoms such as headaches and dizziness, and deficits in cognitive functions (Daneshvar et al., 2011; McInnes et al., 2017). In most cases, the functional deficits become resolved within 3 months to 1 year from the injury (Carroll et al., 2004). On the other hand, a significant minority of people with mTBI experience persistent symptoms, such as cognitive impairment, that last > 1 year after the injury (McInnes et al., 2017; Machamer et al., 2022). In moderate to severe TBI, the mortality of hospitalized patients is around 10–30% (Wilson et al., 2017; Jochems et al., 2021; Niemyer et al., 2022; Raj et al., 2022). In addition, more than 50% of moderate-to-severe TBI survivors suffer from long-term functional disabilities (Whitnall et al., 2006; McCrea et al., 2021). Furthermore, even mild TBI increases the risk of neurodegenerative diseases, such as chronic

traumatic encephalopathy (McKee et al., 2013), Parkinson's disease (Gardner et al., 2018), and post-traumatic epilepsy (PTE) (Annegers et al., 1998). Moreover, repetitive mild TBIs are a health concern especially in contact sports such as ice-hockey, soccer, and American football (Senaratne et al., 2022). For instance, recent studies have detected an increased risk of neurodegenerative disease in former professional soccer players (Mackay et al., 2019; Russell et al., 2021), which have led to proposals to reduce head impacts in soccer among children.

2.1.2 Pathophysiology of TBI

TBI is caused by primary and secondary injury mechanisms (**Figure 1**). The primary injury consists of the direct consequences of the external forces impacting the brain, such as axonal shearing and stretching (Dixon, 2017; Kaur & Sharma, 2018). Further, the initial injury may damage the blood vessels in the brain, causing hemorrhage. The initial impact may also lead to a rupture of the blood-brain barrier (BBB), allowing the recruitment of blood-borne immune cells to reach the injured site (Kumar & Loane, 2012). The secondary injury refers to events that occur in response to the primary injury hours to days after the initial injury, such as excitotoxicity, mitochondrial dysfunction, oxidative stress, inflammation, axon degeneration, and apoptotic cell death (Kaur and Sharma, 2018; Jarrahi et al., 2020). In some cases, the primary injury can be mitigated by preventive actions, for example by wearing a helmet in sports that are known to have an elevated TBI risk (Maas et al., 2022). However, so far, there are no neuroprotective treatments available for TBI that could stop the injury's progression (Kaur and Sharma, 2018). There is a clear unmet clinical need to develop new therapeutic strategies for TBI i.e., treatments that could block or mitigate the secondary injury mechanisms (Loane and Faden, 2010; Jarrahi et al., 2020).

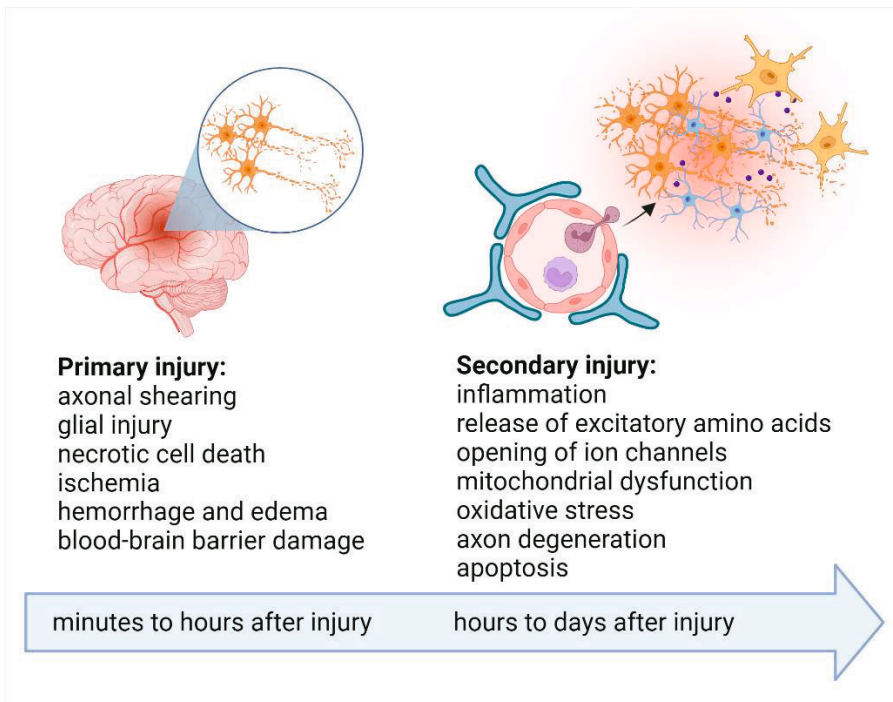


Figure 1. Primary and secondary injury mechanisms of TBI.

2.1.3 Post-traumatic epilepsy

TBI is a major cause of epilepsy, as it is responsible for 10–20% of symptomatic epilepsies and around 5% of all epilepsies (Herman, 2002; Agrawal et al., 2006). Post-traumatic epilepsy (PTE) is defined as the occurrence of spontaneous late seizures >1 week after TBI (Christensen, 2015). The risk of PTE increases with the severity of the TBI. The 30-year cumulative incidence rate for PTE is around 2% for mild TBI, 4% for moderate TBI, and 17% for severe TBI (Annegers et al., 1998). The time from injury to the appearance of the first spontaneous seizure varies from weeks or months, even to years (Annegers et al., 1998; Englander et al., 2003; Yu et al., 2021). Englander et al. (2003) reported that 80% of patients with TBI that developed PTE within 2 years from injury experienced the first seizure ≤ 1 year after the injury. According to Yu and colleagues (2021), the latency to the first spontaneous late seizure was ≤ 1 year in 46% of patients with PTE, whereas around 13% of patients experienced the first seizure >10 years after the injury. Seizures recurrence is common after the appearance

of the first seizure; most of the patients that experience a late seizure (82%) suffer a second seizure within 1 year from the injury (Haltiner et al., 1997).

2.1.4 Epileptogenesis after TBI

Epileptogenesis is a process in which the brain tissue develops the capability to generate spontaneous seizures, resulting in the development of an epileptic condition, and/or progression of established epilepsy (Pitkänen, 2010). Neuropathological events of TBI, such as inflammation, breakdown of the BBB, epigenetic alterations, and reorganization of neural circuits have been associated with the progression of post-traumatic epileptogenesis (Golub & Reddy, 2022). For instance, the presence of inflammation increases the levels of cytokines such as interleukin-1 β (IL-1 β), which exerts excitatory effects on the neurons (Vezzani et al., 2011). Furthermore, the increased permeability of the BBB due to the initial injury or subsequent inflammation permits the leakage of serum albumin from the bloodstream into the brain parenchyma, contributing to excitatory synaptogenesis (Weissberg et al., 2015). Epigenetic alterations refer to several changes for example, histone modifications, DNA methylation or changes in the regulation of gene expression caused by miRNAs (Younus and Reddy, 2017; Golub and Reddy, 2022). Alterations in miRNA expression in the brain tissue have been detected both in TBI and epilepsy (Di Pietro et al., 2018; Brennan and Henshall, 2020; Kumar, 2023), however, the role of miRNAs in post-traumatic epileptogenesis is still a mystery. In summary, the TBI-induced pathological mechanisms result in neuronal losses and a reorganization of neuronal connections, which lead to changes in excitatory and inhibitory circuits (Hunt et al., 2013; Golub and Reddy, 2022). For instance, in the dentate gyrus of the hippocampus, TBI was reported to induce a loss of inhibitory interneurons (Pitkänen et al., 2019; Klein and Tyrlikova, 2020).

2.1.5 Animal models of PTE

Animal models of PTE have been developed to investigate the mechanisms underpinning post-traumatic epileptogenesis and to test potential anti-epileptogenic treatments. Similar to human PTE, the experimental animals develop recurrent spontaneous seizures after a latency period following the injury (Ostergard et al., 2016). A fluid percussion injury (FPI) and a controlled cortical impact (CCI) have been the two most commonly exploited PTE models (Ostergard et al., 2016; Santana-Gomez et al., 2021), with either rats or mice as the experimental animals.

FPI model. In FPI, a small craniotomy is performed under general anesthesia to expose the dura, after which the animal is connected to a fluid-percussion device that consists of a saline-filled tube and a pendulum (see review Ostergard et al., 2016). As the mallet of the pendulum hits the other end of the saline-filled tube, it triggers a fluid pulse that travels through the tube and induces an injury on the brain of the animal connected to the device. The severity of the injury can be modified by changing the height from which the pendulum is released. In lateral FPI (LFPI), the craniotomy is performed laterally to the parietal bone to mimic a rotational force vector (McIntosh et al., 1989). LFPI induces a focal cortical contusion and diffuse subcortical neuronal injury, which also includes damage in the hippocampus and thalamus, and in this respect, it models human TBI without a skull fracture (Xiong et al., 2013). At the pressure pulse of ≥ 3 atmospheres (atm), which causes severe TBI, the mortality of rats is around 30% (Kharatishvili et al., 2006). Around one in every four of the surviving rats will develop PTE within 6 months and 50% within 1 year from the injury. Other comorbidities associated with the LFPI model include impairments in cognitive and sensorimotor functions (Pitkänen et al., 2009).

CCI model. In CCI, the dura is exposed by performing a small craniotomy under general anesthesia, after which the dura is struck directly by a pneumatic or electromagnetic impactor (Lighthall, 1988; Ostergard et al., 2016). The method was initially developed for ferrets (Lighthall, 1988) but has since been adapted for rats and mice (Dixon et al., 1991; Smith et al.,

1995). The severity of the injury can be modified by adjusting the depth of the impactor. The CCI models a penetrating brain injury and while it induces mostly a focal cortical injury (Ostergard et al., 2016), signs of neurodegeneration have also been observed in the hippocampus (Hall et al., 2005). In contrast to the FPI model, the CCI model has a very low mortality (Osier & Dixon, 2016). The percentage of mice that develop late spontaneous seizures after CCI-induced TBI has been reported to vary from 9% to 20% at an injury depth of 0.5 mm (Hunt et al., 2009; Bolkvadze and Pitkänen, 2012) and from 36% to 50% at an injury depth of ≥ 1.0 mm (Hunt et al., 2009; Guo et al., 2013; Brady et al., 2019). With rats, late seizures have been reported in about one in every five animals (Kelly et al., 2015). As with FPI, the CCI-induced injury causes impairments in cognitive and sensorimotor functions of the animals (Fox et al., 1998; Washington et al., 2012).

2.1.6 Definition of biomarkers

The BEST (Biomarkers, EndpointS, and other Tools) Resource defines a biomarker as “a defined characteristic that is measured as an indicator of normal biological processes, pathogenic processes, or biological responses to an exposure or intervention, including therapeutic interventions” (FDA-NIH Biomarker Working Group, 2016). The characteristic can be molecular, histologic, radiographic, or physiologic. According to the BEST Resource, there are 7 biomarker categories: susceptibility/risk biomarker, diagnostic biomarker, monitoring biomarker, prognostic biomarker, predictive biomarker, response biomarker, and safety biomarker. For example, a prognostic biomarker is a biomarker that can be used to evaluate the probability of a clinical event or disease progression, such as the development of PTE after TBI. In contrast, a response biomarker is a biomarker that can be used to identify biological response to a treatment, for example, a reduction in epileptiform activity in the EEG after administration of anti-seizure medication.

2.1.7 Biomarkers for epileptogenesis

Since only a small percentage of patients with TBI develop PTE and the latency period may be months or even years, antiepileptogenic treatment studies would need to recruit such a large patient cohort with a long follow-up duration that they are too laborious and expensive to carry out (Engel et al., 2013; Klein and Tyrlikova, 2020). Even in preclinical models of PTE, only a minority of the animals develop spontaneous seizures (Kharatishvili and Pitkänen, 2010; Golub and Reddy, 2022). Therefore, there is a high demand to discover prognostic biomarkers that could be used to stratify subjects at the highest PTE risk into different groups in preclinical and clinical studies, as this would be beneficial in the development of antiepileptogenic treatments (Pitkänen et al., 2021).

Several investigators have searched for imaging, electrographic, genetic, and molecular biomarkers which could predict epileptogenesis after TBI (Pitkänen et al., 2021; Golub and Reddy, 2022). With respect to imaging biomarkers of post-traumatic epileptogenesis, there are a few preclinical reports describing parameters detected in the analysis of brain magnetic resonance imaging (MRI) scans that do seem to be indicative of an elevated seizure susceptibility (Pitkänen & Immonen, 2014) or an increased probability of PTE after LFP-induced TBI (Manninen et al., 2021). Electrographic biomarkers refer to abnormal patterns evident in an EEG analysis. There are studies indicating that electrographic findings such as an increased occurrence of high-frequency oscillations (Reid et al., 2016) and the length of sleep spindles (Andrade et al., 2017) may be associated with epileptogenesis after LFPI. Genetic biomarkers refer to DNA sequences that are associated with disease susceptibility (Pitkänen et al., 2021; Golub and Reddy, 2022). Clinical studies have identified several genes, such as the glutamate transporter encoding *SLC1A3*, in which a single nucleotide polymorphism leads to an increased risk of the individual developing post-traumatic seizures (Kumar et al., 2019; Pitkänen et al., 2021). Molecular biomarkers refer to factors such as proteins and miRNAs that can be measured in biological samples such as blood, CSF, or a tissue biopsy (Golub and Reddy, 2022). Currently, no molecular biomarkers have

been discovered for PTE. Blood-based biomarkers of post-traumatic epileptogenesis would be especially useful, as blood sampling is minimally invasive and routinely performed in hospitals, allowing simple longitudinal monitoring.

2.2 CIRCULATING miRNAs AS DISEASE BIOMARKERS

2.2.1 miRNA biogenesis and function

MicroRNAs are small non-coding RNAs with a length of around 22 nucleotides, and they function in the post-transcriptional regulation of gene expression (Lee et al., 1993; Wightman et al., 1993). Currently, >2600 mature miRNAs are known for humans, and >800 mature miRNAs have been detected in rats (Kozomara et al., 2019) (<https://mirbase.org/>, accessed on 5.10.2023). Most of the mammalian miRNAs (~50%) are located in the intergenic regions of the genome and are therefore transcribed independently of a host gene, whereas around 40% are located in introns and 10% within the exons of other genes (O'Carroll & Schaefer, 2013).

In the canonical miRNA biogenesis pathway (**Figure 2**), a primary miRNA (pri-miRNA) is first transcribed in the nucleus by RNA polymerase II (Lin & Gregory, 2015; O'Brien et al., 2018). Next, the pri-miRNA is processed into a precursor-miRNA (pre-miRNA) by a microprocessor complex that consists of ribonuclease III enzyme Drosha and RNA-binding protein DGCR8 (Denli et al., 2004). The pre-miRNA is exported from the nucleus to the cytoplasm by a complex formed by exportin 5 and RanGTP (Lund et al., 2004). In the cytoplasm, the pre-miRNA is further processed by RNase III endonuclease Dicer, which cleaves the terminal loop, producing a mature miRNA duplex (Ketting et al., 2001). The miRNA duplex is incorporated into the Argonaute (Ago) protein. Next, either the 5p strand or the 3p strand, i.e., the strands originating from the 5' end or the 3' end of the pre-miRNA, remains with Ago as a guide miRNA while the other strand is discarded (Meijer et al., 2014). In addition to the canonical miRNA biogenesis pathway, there are

also pathways that are independent of processing by Drosha/DGCR8 or Dicer (O'Brien et al., 2018; Shang et al., 2023).

Together, the miRNA strand and the Ago protein form a miRNA-induced silencing complex (miRISC) that regulates gene expression by miRNA-guided binding to the target mRNA, which blocks translation of the target mRNA and leads to mRNA degradation (Jonas & Izaurralde, 2015). One miRNA can regulate the expression of hundreds of proteins (Selbach et al., 2008). The target specificity is defined by the miRNA "seed" region, i.e., the bases 2–8 of the miRNA, which are usually perfectly complementary to the sequence of the target mRNA (Lewis et al., 2003). The binding sites for miRNAs are typically located in the 3' untranslated region of the target mRNA. In addition to transcription inhibition in the cytoplasm, miRNAs can also function as transcriptional regulators in the nucleus by binding to gene promoters or enhancers (Liu et al., 2018). Furthermore, some miRNAs are actively secreted out of cells (Mori et al., 2019). In vitro and in vivo studies have indicated that the secreted miRNAs are taken up by other cells, and they can affect gene expression in the recipient cell (Valadi et al., 2007; Makarova et al., 2016).

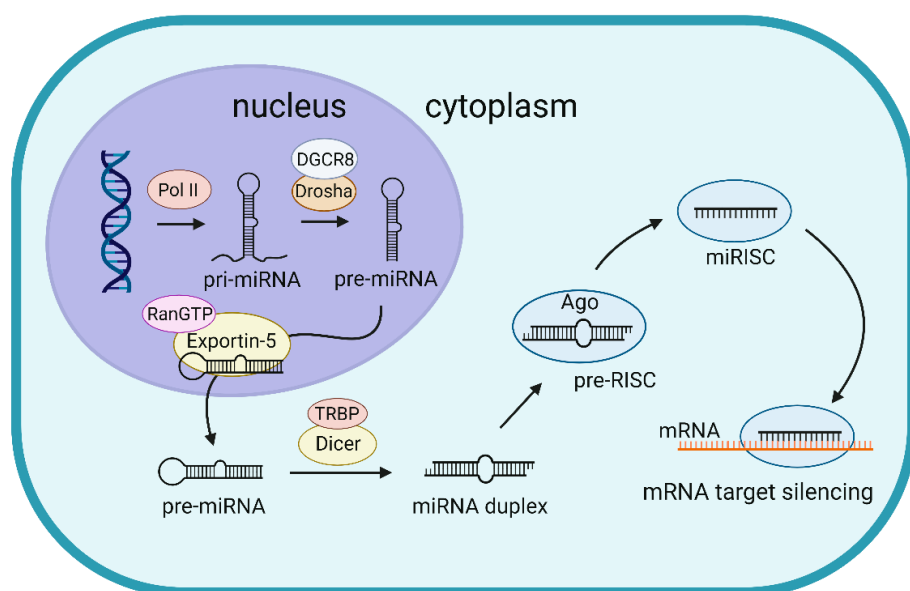


Figure 2. Canonical pathway of miRNA biogenesis. The figure is based on the figures in Lin & Gregory (2015) and O'Brien et al. (2018).

2.2.2 miRNAs as disease biomarkers

Since the discovery of miRNAs around 30 years ago, numerous investigators have reported alterations in miRNA expression in different diseases, including neurodegenerative diseases and epilepsy (Paul et al., 2018; Juźwik et al., 2019). In addition to tissues, alterations in miRNA expression in pathological conditions have been detected in blood and other biofluids (Juźwik et al., 2019), making biofluid miRNAs an attractive source for new disease biomarkers. Moreover, many miRNAs are specifically expressed in certain tissues. For example, miR-122 is considered as a liver-specific miRNA, whereas miR-124 and miR-9 are specifically expressed in the brain (Landgraf et al., 2007; Minami et al., 2014; Ludwig et al., 2016; Bushel et al., 2018). Since in diseases of the central nervous system (CNS), a tissue biopsy is rarely possible, an analysis of brain-derived miRNAs in a biofluid such as blood could provide a minimally invasive method for aiding in disease diagnosis or for monitoring the progression of the disease. Multiple studies have investigated circulating miRNAs as potential biomarkers for CNS disorders (Sheinerman et al., 2013; Condrat et al., 2020; Pitkänen et al., 2021), however, none of them are yet in clinical use.

2.2.3 miRNA carriers in blood

MiRNAs are secreted from cells through two main routes: transport in extracellular vesicles (EVs) and transport in protein-miRNA complexes such as lipoproteins and Argonaute2 (Ago2) (Mori et al., 2019). MiRNAs can also leak from damaged or broken cells, a process which likely occurs in TBI. In blood, circulating miRNAs are associated with EVs (Hunter et al., 2008), lipoproteins (Vickers et al., 2011; Wagner et al., 2013), and Ago2 protein (Arroyo et al., 2011; Turchinovich et al., 2011) (**Figure 3**). The association of circulating miRNAs with the carriers protects them from degradation by ribonucleases and increases their stability; it has been demonstrated that plasma miRNA levels remain stable during multiple freeze-thaw cycles or a 24-h incubation at room temperature (Mitchell et al., 2008).

Circulating miRNAs are not evenly distributed between the different carriers. Arroyo and colleagues analyzed 375 miRNAs in human serum and plasma and showed that most of the circulating miRNAs were vesicle-free, with only 15% being associated with EVs (Arroyo et al., 2011). In another study, only 11 out of 130 (~8%) miRNAs detected in human plasma were found to be mainly associated with carriers other than Ago2 (Geekiyanaage et al., 2020). The distribution into different carriers varies between the miRNAs; some are predominantly associated with EVs, some are carried by both EVs and Ago2, and some are mainly associated with the Ago2 complexes (Arroyo et al., 2011). In addition, the 3' and 5' strands of the same miRNA can have different carriers. For example, miR-142-3p associated mainly with EVs in rat plasma, whereas miR-142-5p was enriched in the protein fractions (Korotkov et al., 2020b). It has also been reported that circulating miRNAs are also carried by high-density lipoproteins (HDL), and to a lesser extent by low-density lipoproteins (LDL) (Vickers et al., 2011; Wagner et al., 2013) but the percentage of circulating miRNAs carried by lipoproteins is not known. Vickers and colleagues reported miR-223 as the most abundant HDL-bound miRNA, however, Wagner and colleagues found that HDL-bound miR-223 accounted for only ~8% of all circulating miR-223. The distribution of individual miRNAs between the different carriers may also differ between the healthy and the disease states. For instance, it was claimed that the proportion of Ago2-bound circulating miR-328-3p increased after an epileptic seizure in TLE patients (Raouf et al., 2018).

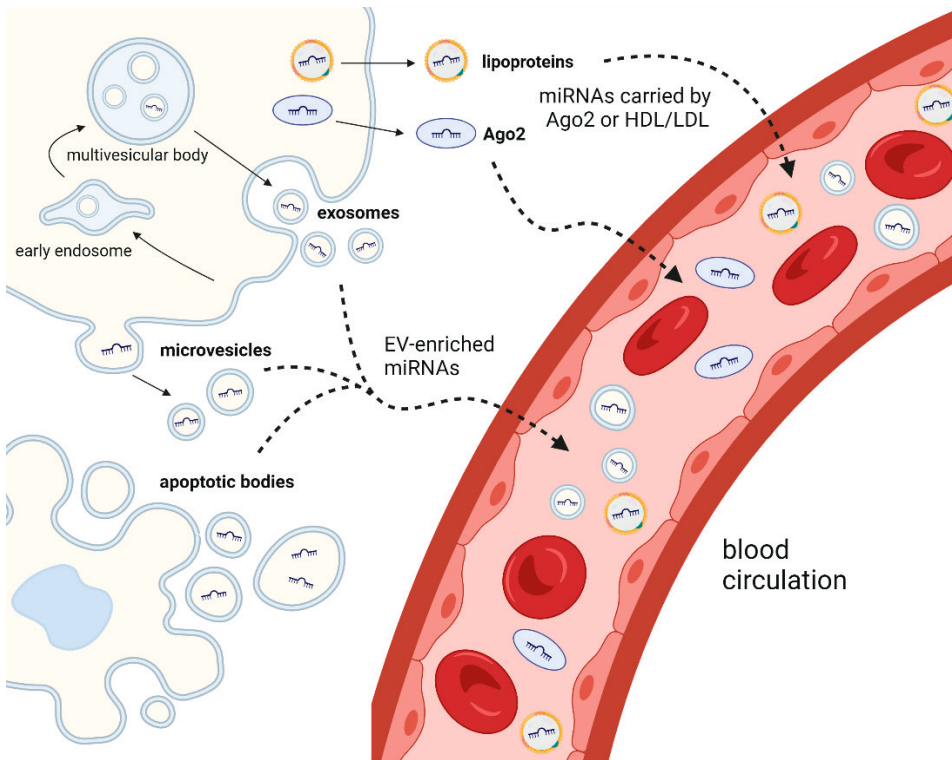


Figure 3. Secretion of extracellular miRNAs and their carriers.

2.2.4 Extracellular vesicle associated miRNAs

EVs are lipid bilayer-enclosed vesicles secreted by cells, and they are present in multiple biofluids including blood, CSF, urine, and saliva (Colombo et al., 2014; Yáñez-Mó et al., 2015). Based on their biogenesis pathway, EVs are traditionally classified into 3 classes, which are exosomes, microvesicles and apoptotic bodies (El Andaloussi et al., 2013) (**Figure 3**). Exosomes have a size of around 40–120 nm, and they are formed within the endosomal network. Exosomes are released from the cell when a multivesicular body fuses with the plasma membrane. In contrast, microvesicles (size 50–1000 nm) originate from the cell surface and are formed by an outward budding of the plasma membrane. The third class of EVs, apoptotic bodies, is formed by an outward budding of cell membrane of an apoptotic cell, and their size ranges from 500 to 2000 nm. Since there do not seem to be specific markers that could distinguish the EVs with different subcellular origins, the International Society for

Extracellular Vesicles (ISEV) recommends use of the generic term “EVs” (Théry et al., 2018).

EVs function as transporters of biological information between different cells (Valadi et al., 2007; Colombo et al., 2014). In addition to cell-to-cell transport, EVs function in cellular clearance of unwanted proteins (Vidal, 2019). The cargo of EVs consists of proteins, lipids, and multiple forms of RNA, such as mRNA, miRNA, and long non-coding RNA (Valadi et al., 2007; Kogure et al., 2013; Colombo et al., 2014; Yáñez-Mó et al., 2015). In the CNS, EVs are secreted by all kinds of cells, and they have important functions both in neurogenesis during early development and in the maintenance of normal functions of the mature brain (Schnatz et al., 2021). For example, miRNA transferred in the EVs secreted by neurons regulate the uptake of glutamate by astrocytes in the synaptic cleft (Morel et al., 2013), whereas EVs secreted by astrocytes protect neurons from oxidative stress and promote neuronal survival (Upadhya et al., 2020).

Many researchers have investigated the potential of EV-enriched miRNAs in blood and other body fluids as biomarkers for different diseases, including neurodegenerative diseases (Thompson et al., 2016). EVs can enter the systemic circulation from the CNS after crossing the BBB (Alvarez-Erviti et al., 2011; García-Romero et al., 2017; Shi et al., 2019). Other suggested routes for EV transport from the CNS include transport from the brain tissue to CSF through the choroid plexus, and transport from the brain to blood via the lymphatic system (Shi et al., 2019). Importantly, EVs have features that can improve the biomarker performance of EV-associated miRNAs compared to an analysis of the total miRNA pool (Guedes et al., 2020). First, it was postulated that cells actively sort miRNAs into EVs for secretion, whereas the secretion of Ago2-bound extracellular miRNAs has been considered as a more of a passive process that occurs during cell death or disruption of the plasma membrane (Turchinovich et al., 2012; Makarova et al., 2021). Therefore, EV-associated miRNAs may provide information from different cell populations compared with vesicle-free miRNAs, for example, healthy tissue vs. damaged tissue. Second, the proteins on the surface of the EVs reflect the identity of the

parental cell (Hallal et al., 2022), which enables the specific capture of EV subpopulations by immunoprecipitation methods and thereby offers a possibility to investigate the cargo of EVs originating from specific tissues or cells (Mustapic et al., 2017; Shi et al., 2019; Newman et al., 2022).

So far, there are a few studies investigating various diseases that have found evidence of potential improved biomarker performance of EV-miRNAs compared to protein-associated miRNAs or the total miRNA pool in the blood or CSF (Raouf et al., 2017; Sohn et al., 2015; Yang et al., 2017). Since different miRNAs have different carriers and their distribution between the carriers may change from the healthy to the disease state, it still needs to be clarified whether an analysis of EV-miRNAs improves diagnostic accuracy and most likely this will need to be determined on a case-by-case approach.

It is also important to bear in mind that the EV isolation methods can affect the composition of the resulting EV population, as the methods only capture a subpopulation of the total EVs. For example, depending on the isolation method, the discriminating factor can be size, density, or the presence of a specific protein on the EV membrane (Konoshenko et al., 2018). Importantly, it has been shown that the isolation of circulating EVs from plasma or serum with different methods does result in different miRNA profiles (Rekker et al., 2014; Tang et al., 2017; Buschmann et al., 2018; Ding et al., 2018).

2.2.5 Circulating miRNAs as TBI biomarkers

There are multiple preclinical and clinical studies describing TBI-induced alterations in miRNA expression levels in blood, CSF, and saliva (Atif and Hicks, 2019; Toffolo et al., 2019; Huibregtse et al., 2021; Ghaith et al., 2022). A summary of published studies on miRNA levels in blood circulation after a TBI is presented in **Table 1**. As seen in the table, there is extensive variability in these studies where the levels of the miRNAs have changed. The variability may result from many factors such as differences in samples (serum vs. plasma), cause and severity of the injury, age of the patients, sampling time-point, sample processing, and miRNA analysis methods (e.g. miRNA sequencing, different miRNA arrays) (Di Pietro et al., 2018; Atif and

Hicks, 2019). The exact mechanisms leading to alterations in miRNA expression after TBI are not known, but they likely include the release of miRNAs from damaged neurons and the disrupted BBB, and if there has been an inflammatory response to the injury (Atif and Hicks, 2019; Korotkov et al., 2020b).

Ideally, a clinically useful biofluid biomarker of TBI should 1) be rapidly and conveniently accessed, 2) show considerably elevated levels at the acute time-point after injury as compared to controls, 3) have a low background expression in a healthy control population, 4) be mainly derived from the injured brain rather than from other sources, 5) be related to the TBI severity defined by other diagnostic tools [GCS, computed tomography (CT), and MRI] (Wang et al., 2018). Furthermore, an ideal biomarker should be detectable with more than one assay, show a similar profile in more than one animal model of TBI, correlate with TBI outcome, and respond to therapeutic interventions (Wang et al., 2018). Although TBI studies have identified a few potential circulating miRNA biomarkers that meet several of the listed requirements, none has yet been translated into clinical use.

Table 1. Circulating miRNA biomarkers of TBI.

Species, sample	Study design	Alteration	ROC AUC	Reference
human plasma	patients with mTBI or sTBI vs. healthy controls or patients with orthopedic injury	mTBI vs. HC: miR-16 ↑ miR-92a ↑ sTBI vs. HC: miR-16 ↓ miR-92a ↓ miR-765 ↑	mTBI vs. HC: miR-16: 0.82 miR-92a: 0.78 sTBI vs. HC: miR-16: 0.89 miR-92a: 0.82 miR-765: 0.86 sTBI vs. OI: miR-16: 0.92 miR-92a: 0.83 miR-765: 0.79	(Redell et al., 2010)

rat serum	rats with blast-induced TBI vs. controls	TBI vs. controls: miR-let-7i ↑	no ROC analysis	(Balakathiresan et al., 2012)
mouse serum	mice with weight-drop-induced mTBI vs. sham-operated controls	mTBI vs. controls: miR-376a ↑ miR-214 ↑ miR-199a-3p ↑	no ROC analysis	(Sharma et al., 2014)
human serum	patients with mild to severe TBI, orthopedic injury controls, and healthy controls	TBI vs. HC: miR-195 ↑ miR-30d ↑ miR-451 ↑ miR-328 ↑ miR-92a ↑ miR-486 ↑ miR-505* ↑ miR-362 ↑ miR-151 ↑ miR-20a ↑	TBI vs. HC: miR-195: 0.81 miR-30d: 0.75 miR-451: 0.82 miR-328: 0.73 miR-92a: 0.88 miR-486: 0.81 miR-505*: 0.82 miR-362: 0.79 miR-151: 0.66 miR-20a: 0.78	(Bhomia et al., 2016)
human serum	patients with TBI vs. healthy controls	TBI vs. HC: miR-93 ↑ miR-191 ↑ miR-499 ↑	TBI vs. HC: miR-93: 1.00 miR-191: 0.73 miR-499: 0.80 mTBI vs. HC: miR-93: 1.00 miR-191: 0.74 miR-499: 0.82	(Yang et al., 2016)
human serum	patients with extracranial injury (EC), patients with mTBI+EC, patients with	mTBI+EC vs. others (≤ 1h): miR-425 ↓ miR-502 ↓ sTBI vs. others (≤ 1h):	mTBI+EC vs. others (≤ 1h): miR-425: 0.91–1.00 miR-502: 0.99–1.00	(Di Pietro et al., 2017)

	sTBI+EC, and healthy controls	miR-335 ↑ sTBI+EC vs. others (4–12h): miR-21 ↑	sTBI vs. others (≤ 1h): miR-335: 0.78–0.99 sTBI+EC vs. others (4–12h): miR-21: 0.90–0.96	
human plasma	patients with mild to severe TBI vs. healthy controls	TBI vs. HC: miR-6867-5p ↑ miR-3665 ↑ miR-328-5p ↑ miR-762 ↑ miR-3195 ↑ miR-4669 ↑ miR-2861 ↑	TBI vs. HC: miR-6867: 0.85 miR-3665: 0.88 miR-328-5p: 0.89 miR-762: 0.92 miR-3195: 0.90 miR-4669: 0.91 miR-2861: 0.91 mTBI vs. HC: miR-6867: 0.77 miR-3665: 0.92 miR-328-5p: 0.86 miR-762: 0.92 miR-3195: 0.86 miR-4669: 0.89 miR-2861: 0.90	(Qin et al., 2018)

mouse plasma	mice with single or repeated blast-induced TBI vs. controls	TBI vs. controls: miR-127 ↑	no ROC analysis	(Sajja et al., 2018)
rat plasma	weight-drop induced TBI rats vs. sham-operated controls	TBI vs. sham: miR-23b ↓	no ROC analysis	(Sun et al., 2018)
human plasma	patients with TBI vs. healthy controls	TBI vs. HC: miR-23b ↓	no ROC analysis	(Sun et al., 2018)
human serum	athletes with sport-related concussion (baseline vs. post-concussion)	mTBI vs. baseline: miR-153 ↑ miR-223-3p ↑ miR-let-7a-5p ↑	no ROC analysis	(Svingos et al., 2019)
human serum	martial arts fighters pre-fight vs. post-fight	pre-fight vs. post-fight: 9 miRNAs ↑ 5 miRNAs ↓	no ROC analysis	(LaRocca et al., 2019)
human serum	patients with sTBI, blood samples collected at different post-injury time-points	12h vs. 2h: 10 miRNAs ↑ 3 miRNAs ↓ 24h vs. 2h: 8 miRNAs ↑ 3 miRNAs ↓ 48h vs. 2h: 5 miRNAs ↑ 1 miRNA ↓ 72h vs. 2h: 7 miRNAs ↑ 1 miRNA ↓	no ROC analysis	(Ma et al., 2019)
human serum	patients with mTBI or sTBI vs.	TBI vs. HC: miR-103a-3p ↑	mTBI or sTBI vs. HC:	(Yan et al., 2019)

	healthy controls	miR-219a-5p ↑ miR-302d-3p ↑ miR-422a ↑ miR-518f-3p ↑ miR-520d-3p ↑ miR-627 ↑	miR-103a-3p: 0.81–0.82 miR-219a-5p: 0.79–0.86 miR-302d-3p: 0.80–0.84 miR-422a: 0.80–0.83 miR-518f-3p: 0.75 miR-520d-3p: 0.85 miR-627: 0.79–0.80	
human serum	patients with TBI vs. healthy controls	TBI vs. HC: miR-219a-5p ↑ miR-9-5p ↑ miR-9-3p ↑ miR-137 ↑ miR-124-3p (n.s) ↑ miR-128-3p (n.s) ↑	TBI vs. HC: miR-219a-5p: 0.89 miR-9-5p: 0.89 miR-9-3p: 0.78 miR-137: 0.81	(O’Connell et al., 2020b)
human serum	athletes pre-season vs. post-season vs. non-athlete controls	pre-season vs. post-season: miR-505* ↑ miR-362-3p ↑ miR-30d ↑ miR-92a ↑ miR-486 ↑ miR-195 ↑	concussed vs. non-concussed: miR-505*: 0.83 miR-362-3p: 0.75 miR-30d: 0.86 miR-92a: 0.92 miR-195: 0.92	(Papa et al., 2019)
human serum	patients with mTBI vs.	mTBI vs. HC: miR-151 ↑ miR-362-3p ↑	no ROC	(Polito et al., 2020)

	healthy controls	miR-486 ↑ miR-499 ↑ miR-505 ↑ miR-381 ↑ miR-625 ↑ miR-638 ↑		
human serum	patients with isolated TBI, patients with polytrauma and sTBI, patients with polytrauma, and healthy controls	TBI vs. HC: miR-423-3p ↑ miR-124-3p ↑	injury severity prediction: miR-423-3p: 0.79	(Schindler et al., 2020)
rat plasma	LFPI-induced TBI rats vs. sham-operated controls	TBI vs. sham: miR-124-3p ↑	TBI vs. sham: miR-124-3p: 0.73–0.88 (multiple cohorts)	(Vuokila et al., 2020)
human serum	patients with TBI vs. uninjured controls	TBI vs. HC: 16 miRNAs ↑ 7 miRNAs ↓	no ROC	(Weisz et al., 2020)
rat plasma	LFPI-induced mTBI or sTBI rats vs. sham-operated controls and naive rats	mTBI or sTBI vs. controls: miR-9-3p ↑ miR-136-3p ↑ miR-434-3p ↑	sham vs. naïve: miR-434: 0.90 mTBI vs. sham: miR-9-3p: 0.98 miR-434-3p: 0.71 sTBI vs. mTBI:	(Das Gupta et al., 2021)

			miR-9-3p: 1.00 miR-434-3p: 1.00 miR-136-3p: 0.91	
human plasma	patients with mTBI or sTBI	mTBI patients with high S100B vs. HC: miR-9-3p ↑ miR-136-3p ↑	no ROC analysis	(Das Gupta et al., 2021)
human plasma	recovered mTBI patients vs. non-recovered mTBI patients	recovered vs. non-recovered mTBI patients: miR-32-5p ↑ miR-142-3p ↓ miR-223-3p ↓ miR-423-3p ↓	recovered vs. non-recovered (7d): miR-32-5p: 0.81 miR-223-3p: 0.85 miR-423-3p: 0.81 recovered vs. non-recovered (28d): miR-32-5p: 0.67 miR-142-3p: 0.77 miR-223-3p: 0.69 miR-423-3p: 0.71	(Mitra et al., 2022)
human plasma	Australian football players before	post-injury (6d, 13d) vs. baseline:	no ROC analysis	(Shultz et al., 2022)

	concussion vs. after concussion	miR-221 ↓ miR-27a ↓		
--	---------------------------------------	------------------------	--	--

EV-associated circulating miRNAs in TBI. In addition to total circulating miRNAs in blood, several investigators have identified TBI-induced alterations in circulating EV-associated miRNAs in preclinical models or in patients with TBI (see **Table 2**). In most instances, the EVs were isolated from human or rodent plasma by commercial membrane-based affinity-binding columns (Devoto et al., 2020; Wang et al., 2020; Vorn et al., 2021) or precipitation-based methods (Ghai et al., 2020; Guedes et al., 2021), whereas one research group used density gradient ultracentrifugation (Puffer et al., 2021). In addition, Ko and colleagues developed a surface protein-based immunocapture approach to allow the specific capture of brain-derived EVs (Ko et al., 2018, 2020). They reported that an EV-miRNA panel identified from small RNA-sequencing of brain-derived (GluR2-positive) plasma EVs was able to differentiate patients with TBI from controls with an AUC value of 0.84 (Ko et al., 2020), however, they did not validate their miRNA alterations by applying PCR methods. In addition, it was not investigated how well the biomarker performance of EV-miRNAs compared to the analysis of total circulating miRNAs. Importantly, it should be noted that many of the studies presented in the table have failed to fully characterize the isolated EVs, and even in those which have, they often did not control for possible co-isolation of other miRNA carriers, such as Ago2 or lipoproteins.

Table 2. Circulating EV-associated miRNA biomarkers of TBI.

Species	Injury	Sample	EV isolation and characterization	Alteration	Reference
mouse, human	mouse: blast TBI human: TBI	plasma	isolation: immunomagnetic capture of GluR1/GluR2-positive EVs characterization: Western blot for EV markers (Alix, Tsg101, CD9) (mouse EVs only)	TBI vs. sham (mouse): miR-129-5p ↑, miR-212-5p ↑, miR-9-5p ↑, miR-152-5p ↓, miR-21 ↓, miR-374b-5p ↓, miR-664-3p ↓ TBI patients vs. HC: miR-212-5p ↑, miR-9-5p ↑, miR-152-5p ↓	(Ko et al., 2018)
human	single or repetitive mTBI	plasma	isolation: membrane-based affinity binding column (exoRNeasy Serum/Plasma Kit) characterization: no characterization described	TBI vs. HC: 16 miRNAs ↑, 1 miRNA ↓ single vs. repetitive mTBI: 13 miRNAs ↑, 3 miRNAs ↓ repetitive mTBI vs. HC: ↑ 30 miRNAs ↑, 2 miRNAs ↓	(Devoto et al., 2020)
human	blast-related chronic mTBI	plasma	isolation: precipitation by Total Exosome Isolation Kit characterization: no characterization described	war veterans with mTBI vs. HC: miR-139-5p ↓, miR-146a-5p ↓, miR-21-5p ↓, miR-143-3p ↓, miR-192-5p ↓, miR-203a-3p ↓, miR-423-5p ↓	(Ghai et al., 2020)

mouse, human	<p>mouse: blast or CCI-induced TBI</p> <p>human: TBI (mainly mTBI)</p>	plasma	<p>isolation: immunomagnetic capture of GluR2-positive EVs</p> <p>characterization: no characterization described</p>	<p>TBI vs. sham (mouse): miR-488-3p ↑, miR-9-5p ↑, miR-219a.2-3p ↑, miR-22-5p ↓, miR-150-5p ↓, miR-669c-5p ↓, miR-6236 ↓, miR-351-3p ↓</p> <p>miRNA panel: AUC 0.74</p> <p>TBI patients vs. HC: miR-206 ↑, miR-185-5p ↑, miR-203b-5p ↓, miR-203a-3p ↓</p> <p>miRNA panel: AUC 0.84</p>	(Ko et al., 2020)
rat	weight-drop-induced moTBI	plasma	<p>isolation: membrane-based affinity binding column (exoEasy Maxi kit)</p> <p>characterization: Western blot for EV markers (CD63, HSP79), NTA, TEM</p>	<p>TBI vs. sham: miR-124-3p ↑, miR-142-3p ↑, miR-374-5p ↑, miR-532-5p ↑, miR-29b-3p ↑, miR-106-5p ↑, miR-92a-3p ↑, miR-451-5p ↑, miR-145-3p ↓</p>	(Wang et al., 2020)
human	mTBI patients with or without PTSD	plasma	<p>isolation: precipitation by ExoQuick Plasma Prep and Exosome Precipitation Kit</p> <p>characterization: Analysis of EV marker TSG101 by ELISA</p>	<p>+mTBI/-PTSD vs. HC: miR-204-5p ↑, miR-372-3p ↑, miR-509-3-5p ↑, miR-615-5p ↑, miR-1277-3p ↑, miR-139-5p ↓</p>	(Guedes et al., 2021)

				<p>+mTBI/+PTSD vs. HC: miR-3190-3p ↑, miR-615-5p ↑, miR-1185-1-3p ↑, miR-3196 ↑, miR-372-3p ↑, miR-139-5p ↓</p> <p>+mTBI/+PTSD vs. +mTBI/-PTSD: miR-374a-3p ↓</p>	
human	mTBI, moTBI, sTBI	plasma	<p>isolation: density gradient UC</p> <p>characterization: Western blot for EV markers (CD63, CD9, Alix), NTA</p>	<p>TBI patients vs. HC: miR-9a-3p ↑, miR-1-3p ↑, miR-143-3p ↑, miR-29a-3p ↑, miR-27a-3p ↑, miR-99a-5p ↑, miR-99b-5p ↑, miR-151b ↑, miR-328-3p ↑, miR-155-5p ↓, miR-30c-5p ↓</p>	(Puffer et al., 2021)
human	chronic mTBI	plasma	<p>isolation: membrane-based affinity binding column (exoRNeasy Serum/Plasma Kit)</p> <p>characterization: no characterization described</p>	<p>chronic mTBI patients vs. HC: 4 miRNAs ↑ 21 miRNAs ↓</p>	(Vorn et al., 2021)

2.2.6 Circulating miRNAs in epilepsy

To date, no circulating miRNA biomarkers have been discovered for PTE. However, several investigators have reported alterations in miRNA expression in blood circulation in patients with epilepsy and preclinical models of epileptogenesis (Enright et al., 2018; Pitkänen et al., 2021). A summary of the published circulating miRNA studies with respect to epilepsy is presented in **Table 3**.

One approach to search for potential PTE biomarkers is to identify those miRNAs that are dysregulated both in epilepsy and in TBI (Pitkänen et al., 2021). In general, there has been little overlap between altered miRNAs in TBI and epilepsy. Interestingly, a recent systematic review on dysregulated miRNAs in human TBI and epilepsy identified 10 miRNAs (miR-27a, miR-502, miR-130b, miR-9, miR-625, miR-660, miR-138, miR-21, miR-30a, miR-1307) that were common to both diseases, hinting at their potential dysregulation in PTE (Kumar, 2023). It remains to be clarified whether the listed miRNAs could function as biomarkers for post-traumatic epileptogenesis.

Table 3. Circulating miRNA biomarkers of epilepsy.

Species	Disease or model	Sample	Alteration	Reference
rat	SE	blood	SE vs. controls: 21 miRNAs ↑ 10 miRNAs ↓	(Liu et al., 2010)
rat	SE	blood	SE vs. controls: miR-34a ↑, miR-22 ↑, miR-125a ↑, miR-21 ↓	(Hu et al., 2011)
rat	TLE	plasma	SE vs. controls: miR-142-5p ↑ (24 h post-SE) miR-21-5p ↑ (1 w post-SE) miR-146a-3p ↑ (1 mo post-SE)	(Gorter et al., 2014)
rat	TLE	plasma	SE vs. controls: early latency: miR-9a-3p ↑, miR-598-5p ↓ late latency: miR-300-3p ↓	(Roncon et al., 2015)

			<p>first seizure: miR-300-3p ↓</p> <p>chronic time-point: miR-142-3p ↓</p>	
human	drug-resistant epilepsy (DRE)	serum	DRE vs. responsive epilepsy: miR-194-5p ↓, miR-301a-3p ↓, miR-30b-5p ↓, miR-342-5p ↓, miR-4446-3p ↓	(Wang et al., 2015a)
human	epilepsy	serum	epilepsy patients vs. controls: let-7d-5p ↑, miR-106b-5p ↑, miR-130a-3p ↑, miR-146a-5p ↑, miR-15a-5p ↓, miR-194-5p ↓	(Wang et al., 2015b)
human	epilepsy	serum	epilepsy patients vs. controls: miR-106b ↑, miR-146a ↑, miR-301a ↑, miR-194-5p ↓	(An et al., 2016)
human	mTLE	plasma	mTLE patients vs. surgical controls: miR-153 ↓	(Li et al., 2016)
human	TLE	plasma	refractory TLE vs. controls: miR-129-2-3p ↑	(Sun et al., 2016)
human	mTLE	serum	after seizure vs. before seizure: miR-143-3p ↑, miR-145-5p ↑, miR-365a-3p ↑, miR-532-3p ↑	(Surges et al., 2016)
human	TLE	serum	refractory TLE vs. controls: miR-4521 ↑	(Wang et al., 2016)
human	mTLE	plasma	mTLE patients vs. controls: miR-134 ↑	(Avansini et al., 2017)
human	epilepsy	plasma	new-onset epilepsy vs. controls: miR-134 ↑	(Wang et al., 2017)
human	mTLE	plasma	mTLE patients vs. surgical controls: miR-153 ↓	(Gong et al., 2018)
human	TLE, GGE, FLE, SE	plasma	TLE patients vs. controls: miR-27a-3p ↓, miR-328-3p ↓ after seizure vs. baseline: miR-27a-3p ↓, miR-328-3p ↓ GGE vs. controls: miR-27a-3p ↓, miR-654-3p ↓	(Raouf et al., 2018)
human	mTLE-HS	blood	mTLE-HS patients vs. controls:	(Antônio et al., 2019)

			miR-145 ↑, miR-181c ↑, miR-199a ↑, miR-1183 ↑	
human	pediatric epilepsy	plasma	children with epilepsy vs. controls: miR-146a ↑, miR-106b ↑	(Elnady et al., 2019)
human	epilepsy	plasma	refractory epilepsy vs. controls: miR-145-5p ↓ mTLE patients vs. controls: miR-145-5p ↓	(Shen et al., 2019)
mouse, rat, human	TLE	plasma	rodent models: miR-93-5p ↑, miR-182-5p ↑, miR-142-5p ↑, miR-199a-3p ↑, miR-574-3p ↓ TLE patients vs. controls: miR-93-5p ↑, miR-199a-3p ↑, miR-574-3p ↓	(G. P. Brennan et al., 2020)
mouse	TLE	SE	SE vs. no SE miR-434-3p ↑, miR-133a-3p ↑	(M. Chen et al., 2020)
human	pediatric epilepsy	serum	children with epilepsy vs. controls: miR-34c-5p ↓ DRE vs. responsive epilepsy: miR-34c-5p ↓	(Fu et al., 2020)
human	mTLE-HS	serum	mTLE-HS patients vs. controls: miR-328-3p ↑	(Ioriatti et al., 2020)
human	epilepsy	serum	DRE vs. responsive epilepsy: miR-134 ↑, miR-146a ↑	(Leontariti et al., 2020)
human	GGE	serum	GGE patients vs. controls: miR-146a ↑, miR-155 ↑	(Martins-Ferreira et al., 2020)
human	TLE	serum	TLE patients vs. controls: miR-142 ↑, miR-146a ↑, miR-223 ↑ DRE vs. responsive epilepsy: miR-142 ↑, miR-223 ↑	(De Benedittis et al., 2021)
human	mTLE-HS	blood	mTLE-HS patients vs. controls: miR-629-3p ↑, miR-1202 ↑, miR-1225-5p ↑	(Gattás et al., 2022)
human	epilepsy	plasma	epilepsy patients vs. controls: miR-146a ↑, miR-132 ↑	(Huang et al., 2022)

human	pediatric epilepsy	plasma EVs	children with epilepsy vs. controls: miR-584-5p ↑, miR-342-5p ↑, miR-150-3p ↑, miR-125b-5p ↑	(Wang et al., 2022)
rat	SE	plasma	SE models (electrical, chemical, kindling) vs. sham controls: miR-429 ↑	(von Rüden et al., 2023)

2.3 CIRCULATING PROTEINS AS DISEASE BIOMARKERS

2.3.1 Circulating proteins as TBI biomarkers

Several potential biofluid-based protein biomarkers have been discovered for TBI (Wang et al., 2018; Ghaith et al., 2022). They are linked to the pathophysiologic processes associated with TBI, such as neuronal injury, astrogliosis, and inflammation (Wang et al., 2018; Huibregtse et al., 2021). The possible uses of biofluid protein biomarkers of TBI have included an evaluation of injury severity, monitoring of disease progression, and a prediction of the disease outcome (Sharma & Laskowitz, 2012). The biomarker proteins are typically measured from CSF or blood, although, serum or plasma would be preferred over CSF especially in mild-to-moderate TBI due to the convenience and good accessibility of blood (Wang et al., 2018). While many of the potential biomarker proteins are present in blood at very low concentrations, nonetheless, the development of very sensitive detection methods, such as single molecule array (SIMOA) (Rissin et al., 2010) has enabled the measurement of concentrations as low as < 1 pg/ml. A summary of published clinical studies on serum or plasma protein biomarkers of TBI is presented in **Table 4**.

Neuronal biomarkers. The markers of neuronal injury include proteins such as ubiquitin C-terminal hydrolase L1 (UCH-L1), neuron-specific enolase (NSE), and neurofilament subunits (Wang et al., 2018; Huibregtse et al., 2021). UCH-L1 is a cytoplasmic enzyme that functions in the ubiquitination of proteins, and it is abundantly present in neurons (Bishop et al., 2016). Like UCH-L1, NSE is also a cytoplasmic enzyme specific to

neurons, and it is involved in the glycolytic energy metabolism in the brain (Isgrò et al., 2015). Neurofilaments are cytoskeletal proteins that provide structural support to axons and are involved in synapse formation; their major components include neurofilament light (NF-L), medium (NF-M), and heavy (NF-H) subunits (Gafson et al., 2020). An increase in the levels of UCH-L1 and NSE in biofluids indicate the presence of damage to the neuronal cell body, whereas increased levels of the neurofilament subunits reflect axonal damage (Wang et al., 2018).

Of the neuronal markers, especially UCH-L1 has been widely examined in TBI, and multiple studies have indicated that UCH-L1 appears to be a sensitive marker of brain injury and as such, is useful in the initial assessment of injury severity and outcome prediction (Papa et al., 2012; Diaz-Arrastia et al., 2014; Posti et al., 2016; Welch et al., 2017; Bazarian et al., 2018; O'Connell et al., 2020a; Korley et al., 2022). In addition, during the past 10 years, the neurofilament subunits NF-L and pNF-H, a phosphorylated form of NF-H, have also emerged as potential biomarkers for TBI diagnostics (Al Nimer et al., 2015; Shahim et al., 2016, 2017; Shibahashi et al., 2016; Gill et al., 2018; Thelin et al., 2019). While the highest levels of UCH-L1 are evident in human blood during the first ≤ 12 h after TBI (Papa et al., 2016; Metzger et al., 2018), the peak concentrations for circulating NF-L and pNF-H in humans are observed around 10–14 days after the injury (Shahim et al., 2016; Otani et al., 2020), offering a later time-point for biomarker analysis. Importantly, although the concentration peak is reached slowly, an increase in neurofilament levels in patients with TBI in comparison to controls can already be detected ≤ 24 h after the injury (Gatson et al., 2014; Shahim et al., 2016), meaning that neurofilaments can also function as acute injury biomarkers.

Astroglial biomarkers. Astroglial injury marker proteins include glial fibrillary acidic protein (GFAP) and S100B (Wang et al., 2018; Ghaith et al., 2022). GFAP is an intermediate filament protein that is a part of the cytoskeleton of astrocytes and is responsible for maintaining their mechanical strength (Yang & Wang, 2015), and high levels of circulating GFAP after TBI have been linked to a worse outcome (Pelinka et al., 2004;

Di Battista et al., 2015; Takala et al., 2016; T.N. Anderson et al., 2020; Thelin et al., 2019; Korley et al., 2022). S100B is a calcium-binding protein. An increase in the extracellular concentration of S100B triggers the pro-inflammatory activation of astrocytes and microglia (Michetti et al., 2019). In contrast to GFAP, S100B is not exclusively expressed in astrocytes, as it has been also detected outside of the CNS, for example in adipocytes. Furthermore, S100B is not specific to TBI as its levels are also increased in the serum of trauma patients without head injuries (R.E. Anderson et al., 2001). Nonetheless, circulating S100B concentrations have been demonstrated to be useful not only in the evaluation of injury severity but also in the prediction of TBI outcome (Pelinka et al., 2004; Di Battista et al., 2015; Heidari et al., 2015; Çevik et al., 2019).

Inflammation biomarkers. The markers of neuroinflammation include cytokines, such as IL-1 β , IL-6, and TNF- α ; these are agents that are secreted by activated microglia and immune cells in response to the TBI (Kumar & Loane, 2012; Huibregtse et al., 2021). While on one hand, circulating inflammatory biomarkers have shown some potential in injury detection and the prediction of TBI outcome (Stein et al., 2011; Raheja et al., 2016; Visser et al., 2022; Yue et al., 2023), on the other hand, circulating levels of inflammatory biomarkers are not specific to TBI as they can be increased in other diseases associated with cellular damage (Visser et al., 2022). Therefore, the optimal use of inflammatory biomarkers of TBI may be when they are assessed together with established markers of neuronal and astroglial injuries (Woodcock & Morganti-Kossmann, 2013; Visser et al., 2022).

Table 4. Circulating protein biomarkers of TBI.

Study design	Sample	Time-point	Alteration	Reference
TBI non-survivors vs. TBI survivors	serum	< 12 h, 12–108 h after injury	GFAP \uparrow S100B \uparrow	(Pelinka et al., 2004)
sTBI patients with poor outcome vs.	serum	\leq 6 h after injury	Tau \uparrow	(Liliang et al., 2010)

patients with good outcome				
patients with TBI vs. healthy controls, and TBI patients with positive CT vs. negative CT	serum	≤ 4 h after injury	TBI patients vs. HC: UCH-L1 ↑ CT+ vs. CT-: UHC-L1 ↑	(Papa et al., 2012)
TBI patients with positive CT vs. negative CT	plasma	≤ 24 h after injury	GFAP breakdown products ↑	(Okonkwo et al., 2013)
patients with TBI vs. healthy controls	serum	≤ 24 h after injury	UCH-L1 ↑ GFAP ↑	(Diaz-Arrastia et al., 2014)
mTBI patients vs. healthy controls, mTBI patients with positive CT vs. negative CT	serum	1 d and 3 d after injury	mTBI vs. HC: pNF-H ↑ CT+ vs. CT-: pNF-H ↑	(Gatson et al., 2014)
TBI non-survivors vs. TBI survivors	plasma	≤ 24 h after injury	TIMP-1 ↑	(Lorente et al., 2014)
ice-hockey players before and after concussion	plasma	1 h, 12 h, 36 h, 144 h after concussion	T-tau ↑	(Shahim et al., 2014)
TBI patients with unfavorable vs. favorable outcome	plasma	6 h, 12 h, 24 h after injury	GFAP ↑ S100B ↑ MCP-1 ↑	(Di Battista et al., 2015)
patients with TBI vs. patients without TBI	serum	≤ 24 h after injury	BDNF ↓	(Korley et al., 2016)

TBI patients with positive CT vs. negative CT	plasma	0 d, 1 d, 2 d, 3 d, 7 d after injury	UCH-L1 ↑ GFAP ↑	(Posti et al., 2016)
TBI patients with poor outcome vs. TBI patients with good outcome	serum	0 d, 7 d after admission	at admission: NSE ↓ IL-6 ↓ at 7 d: GFAP ↑ IL-6 ↑ progesterone ↓	(Raheja et al., 2016)
sTBI patients vs. healthy controls	serum	0–12 d after injury	NF-L ↑	(Shahim et al., 2016)
patients with sTBI vs. mTBI, patients with unfavorable vs. favorable outcome	serum	24 h, 72 h after injury	pNF-H ↑	(Shibahashi et al., 2016)
TBI patients with poor outcome vs. TBI patients with good outcome	serum	0 d, 1 d, 2 d, 3 d, 7 d after admission	UCH-L1 ↑ GFAP ↑	(Takala et al., 2016)
athletes with concussion vs. athletes without concussion vs. nonathlete controls	plasma	6 h, 24 h, 72 h, 7 d after concussion	concussed athletes vs. control athletes: Tau ↓ athletes vs. controls: Tau ↑	(Gill et al., 2017)
amateur boxers after bout vs. after rest vs. controls	serum	7–10 d after bout and after 3 mo rest	boxers vs. controls: NF-L ↑	(Shahim et al., 2017)

professional ice-hockey players vs. controls	serum	1 h, 12 h, 36 h, 144 h after concussion	NF-L ↑	(Shahim et al., 2017)
TBI patients with positive CT vs. negative CT	serum	≤ 24 h after injury	UCH-L1 ↑ GFAP ↑ S100B ↑	(Welch et al., 2017)
mTBI patients with positive CT vs. negative CT	serum	≤ 12 h after injury	UCH-L1 ↑ GFAP ↑	(Bazarian et al., 2018)
mTBI patients with positive CT vs. negative CT	serum	≤ 4 h after injury	CT+ vs. CT-: GFAP ↑ S100B ↑ NRGN ↑	(Çevik et al., 2019)
patients with suspected mTBI vs. healthy controls	plasma	≤ 48 after injury	UCH-L1 ↑ GFAP ↑ NF-L ↑ Tau ↑	(Gill et al., 2018)
patients with TBI vs. healthy controls,	serum	1 d, 2 d after injury	ASC ↑ caspase-1 ↑	(Kerr et al., 2018)
TBI patients with unfavorable vs. favorable outcome	serum	≤ 2 weeks from injury	S100B ↑ NSE ↑ GFAP ↑ UCH-L1 ↑ Tau ↑ NF-L ↑	(Thelin et al., 2019)
prediction of TBI outcome	serum	median 1.4 h after injury	CT+ vs. CT-: UCH-L1 ↑ GFAP ↑ MAP-2 ↑	(T.N. Anderson et al., 2020)
patients with TBI vs. neurologically normal controls	serum	≤ 24 h after injury	NF-L ↑ Tau ↑	(O'Connell et al., 2020a)
TBI patients with unfavorable vs.	plasma	≤ 24 h after injury	UCH-L1 ↑ GFAP ↑	(Korley et al., 2022)

favorable outcome, and non-survivors vs. survivors				
patients with TBI vs. healthy controls	plasma	≤ 24 h after injury	IL-6 ↑ IL-10 ↑ HMGB-1 ↑ IL-4 ↑ IL-9 ↑ IL-5 ↑ IL-16 ↑ IL-1b ↑ IL-7 ↓ TARC ↓	(Yue et al., 2023)

2.3.2 Clinical use of circulating TBI biomarkers

One of the major aims of TBI biomarker studies has been to develop diagnostic tools to permit an initial stratification of patients based on the severity of their injury. Several researchers have indicated that circulating protein biomarkers are able to distinguish between patients with a minor head injury who do not require brain imaging and patients that are likely to display abnormal findings in the CT scan (Heidari et al., 2015; Welch et al., 2016). Consequently, in 2018, the U.S. Food and Drug Administration (FDA) approved the first blood test for the prediction of absence of intracranial injury in patients with mTBI. The test is based on the levels of circulating UCH-L1 and GFAP, which are upregulated in patients that have an intracranial injury detectable in a head CT scan (Bazarian et al., 2018). In addition to UCH-L1 and GFAP, acutely elevated levels of circulating S100B have also been shown to predict abnormal CT findings after mTBI (Heidari et al., 2015; Welch et al., 2016). Importantly, an analysis of serum S100B levels ≤ 6 h from injury when the clinician evaluates the need for a CT scan is recommended by the Scandinavian guidelines for initial management of mild head injuries (Undén et al., 2013).

Although circulating proteins have proven useful in the evaluation of the need for brain imaging in patients with mild TBI, there is still an unmet need for other biomarkers, for example for monitoring of disease progression and recovery, as well as the prediction of the outcome after the injury (Bogoslovsky et al., 2016). For instance, in the field of sports, biomarkers are needed to evaluate when a player who has sustained a concussion can safely return to play, as a prematurely early return increases his/her risk of further injury as well as long-term consequences such as chronic deficits in neurocognitive functions (Senaratne et al., 2022). Studies on circulating proteins in contact sports athletes have demonstrated that the levels of neuronal and astroglial injury markers are increased after a concussion (Shahim et al., 2014, 2017; McCrea et al., 2020; Senaratne et al., 2022). For example, acute serum NF-L levels after a concussion distinguished between ice-hockey players with prolonged post-concussive symptoms from rapidly recovering players, indicating that measurements of circulating NF-L may be potentially useful and aid in decision making (Shahim et al., 2017).

Nonetheless, there is an urgent need for a molecular biomarker in which an increase or decrease of its levels in blood circulation would reflect the response to treatment. This kind of biomarker would be most beneficial both in preclinical and clinical trials that aim to develop treatments to improve the recovery after TBI (Bogoslovsky et al., 2016). Furthermore, prognostic biomarkers that could predict the long-term outcome of TBI would help in decision making to help the clinician choose the best therapeutic option and it would also be an advantage when performing a stratification of subjects being recruited into treatment trials (Korley et al., 2022). Several brain-derived circulating proteins, especially UCH-L1 and GFAP, have shown some promise in TBI outcome prediction (see **Table 4**), however, no prognostic circulating biomarkers are yet in clinical use.

2.3.3 Circulating proteins as biomarkers of epilepsy

Several investigators have detected alterations in circulating proteins in patients suffering from epilepsy. A summary of the published clinical studies that have included a ROC analysis is presented in **Table 5**. As seen in the table, there is only a slight overlap with the TBI biomarkers used in the acute phase, however, a few studies on epilepsy patients have reported increased levels of circulating proteins such as UCH-L1, S100B, and cytokines indicating tissue damage and neuroinflammation caused by the seizures (Simani et al., 2020; Banote et al., 2022). Brain inflammation is also one of the pathological processes contributing to epileptogenesis (Vezzani et al., 2013; Webster et al., 2017). However, it has not been determined whether the injury and inflammatory biomarker proteins detected in blood circulation can predict the appearance of post-traumatic epileptogenesis. For example, in FPI-induced TBI rats, the epileptogenic focus was reported to develop at the perilesional cortex (Bragin et al., 2016). Therefore, whether the circulating levels indicators of neuronal injury, such as NF-L, are related to the extent of the cortical lesion and the risk of PTE development, would be worthwhile investigating. Furthermore, in patients with TBI, it is well established that the risk of PTE increases with the severity of the injury (Annegers et al., 1998). Since several circulating proteins have been shown to reflect injury severity (see **Table 4**), the biomarker proteins of TBI can potentially aid in patient stratification into PTE risk groups. Due to the low incidence rate of PTE after TBI and the long latency period before the disease onset, the initial screening for potential epileptogenesis biomarkers is most feasible in preclinical models (Engel et al., 2013). After an initial screening in preclinical models, the potential biomarkers still need to be validated in humans before their translation into clinical use.

Table 5. Circulating protein biomarkers of epilepsy.

Disease	Sample	Alteration	ROC AUC	Reference
Drug-resistant epilepsy	plasma	Epilepsy patients vs. controls: sICAM5 ↓, IL-12p70↓, IL-1β ↑, IL-2 ↑, IL-6 ↑, IL-8 ↑, IFN-γ ↑	Epilepsy vs. controls: sICAM5: 0.87 IL-6: 0.81 TARC/sICAM5: 1.00 IL-6/sICAM5: 0.90 IL-8/sICAM5: 0.88	(Pollard et al., 2012)
Epilepsy (idiopathic, symptomatic, cryptogenic)	serum	Epilepsy patients vs. controls: No difference in BDNF levels	Daily seizures vs. less frequent seizures: BDNF: 0.86	(Hong et al., 2014)
Epilepsy (idiopathic, symptomatic, cryptogenic)	serum	Epilepsy patients vs. controls: MMP-3 ↓	Epilepsy vs. controls: Males < 20 y/o: 0.56 Females < 20 y/o: 0.66 Males 20–40 y/o: 0.77 Females 20–40 y/o: 0.73 Males > 40 y/o: 0.64 Females > 40 y/o: 0.93	(Wang et al., 2016)
Epilepsy (many diagnoses)	plasma	Epilepsy patients vs. controls: factor H ↑, TCC ↑	Epilepsy vs. controls: Combination of complement analytes (C3, C4, Properdin,	(Kopczynska et al., 2018)

			factor H, C1 inhibitor and clusterin): 0.80	
New-onset childhood epilepsy	serum	Epilepsy patients vs. controls: HMGB-1 ↑, IL-1β ↑, S100B ↑, GFAP ↑	Prediction of seizure frequency: HMGB-1: 0.95 IL-1β: 0.83	(Zhu et al., 2018)
Focal seizures	serum	Patients with focal seizures vs. controls: S100B ↑	Prediction of focal seizure positivity: S100B: 0.96	(Maiti et al., 2018)
Epilepsy	serum	Epileptic seizure (ES) vs. psychogenic nonepileptic seizures (PNES): GFAP ↑	ES vs. PNES: GFAP: 0.68	(Simani et al., 2018)
Epilepsy	serum	ES vs. PNES: UCH-L1 ↑, S100B ↑	ES vs. PNES: UCH-L1: 0.68 S100B: 0.59	(Asadollahi & Simani, 2019)
Epilepsy	plasma	Epilepsy patients vs. patients with PNES: MCP-2 ↑, TNF-R1 ↑, TRAIL ↓, ICAM-1 ↓	Epileptic seizures vs. PNES: Combination of MCP-2, TRAIL, ICAM-1 and TNF-R1: 0.94	(Gledhill et al., 2021)
Temporal lobe epilepsy	plasma	TLE vs. controls: BDNF ↓, TNF-α ↓	TLE vs. controls: BDNF: 0.98 TNF-α: 0.90	(Panina et al., 2023)

3 AIMS OF THE STUDY

The overall aim of this thesis study was to identify circulating miRNA and protein biomarkers to evaluate the severity of TBI and predict the development of epileptogenesis after TBI, by using a rat model in which the TBI was induced by lateral fluid percussion.

The specific aims of this study were as follows:

1. To evaluate the performance of a precipitation-based method in extraction of EV-specific circulating miRNAs from a small volume of rat plasma.
2. To discover differentially expressed circulating miRNAs in rat plasma after TBI, and to investigate whether the altered miRNA profile can be used as a biomarker to assess the severity of cortical damage and to predict epileptogenesis after TBI.
3. To investigate whether circulating NF-L levels act as a biomarker to predict the functional outcome (somatomotor recovery, cognitive decline, and epileptogenesis) as well as the evolution of cortical damage after TBI.

The hypotheses of this study were as follows:

1. The precipitation-based EV isolation method can isolate circulating EVs from rat plasma for subsequent analysis of EV-associated miRNAs.
2. Alterations in the levels of circulating miRNAs at acute time-point after TBI will present prognostic biomarkers for TBI and post-traumatic epileptogenesis.
3. Higher levels of circulating NF-L at an acute time-point after TBI will associate with a worse somatomotor recovery, impaired cognitive functions, a larger cortical lesion area, and an increased probability of PTE development.

4 MATERIALS AND METHODS

Materials and methods used in this thesis are summarized in the following tables. The detailed descriptions of materials and methods can be found in the original publications (I–III).

4.1 ANIMALS

All studies in this thesis used adult male Sprague-Dawley rats which were housed in individual cages in a controlled environment (temperature 22 ± 1 °C, humidity 50–60%) with 12-hour light/dark cycle (lights on 7:00–19:00) and ad libitum access to food and water. All animal procedures were approved by the Animal Ethics Committee of the Provincial Government of Southern Finland and performed in accordance with the guidelines of the European Community Council Directives 2010/63/EU.

Table 6. An overview of the animal cohorts used in the studies included in this thesis.

Study	Number of animals used	Animal groups
I	5 Sprague-Dawley rats	Naïve (n=5)
II	EPITARGET cohort: 150 epilepsy-phenotyped Sprague-Dawley rats	Epilepsy-phenotyped rats (n=150): Naïve (n=13) Sham (n=23) TBI (n=114), including 29 TBI+ and 85 TBI-
		miRNA discovery cohort (n=20) Sham (n=4*) TBI (n=16*), including 7 TBI+ and 9 TBI-
		miRNA validation cohort (n=115): Naïve (n=8) Sham (n=17*) TBI (n=90*), including 21 TBI+ and 69 TBI-

III	Subcohort of the EPITARGET cohort: 34 Sprague-Dawley rats	NF-L analysis cohort (n=34): Sham (n=8) TBI (n=26), including 13 TBI+ and 13 TBI-
-----	---	--

* 2 samples from sham-operated and 5 samples from injured animals (2 TBI+, 3 TBI-) were included both in the discovery and validation cohorts

4.2 ANIMAL EXPERIMENTS

Table 7. Summary of in vivo methods and experiments.

Method / experiment	Purpose	Publication
Lateral fluid-percussion injury (LFPI)	Model severe TBI and epileptogenesis in rats	II, III
Blood collection	Plasma samples for EV isolation and biomarker analyses	I, II, III
Video-EEG monitoring	Diagnosis of post-traumatic epilepsy	II, III
Magnetic resonance imaging (MRI)	Analysis of cortical lesion area after TBI	II, III
Composite neuroscore	Evaluation of somatomotor recovery	III
Morris water-maze	Evaluation of cognitive functions	III
Nissl staining and cortical unfolded maps	Assessment of cortical lesion area and damage to different cytoarchitectonic cortical areas after TBI	II, III

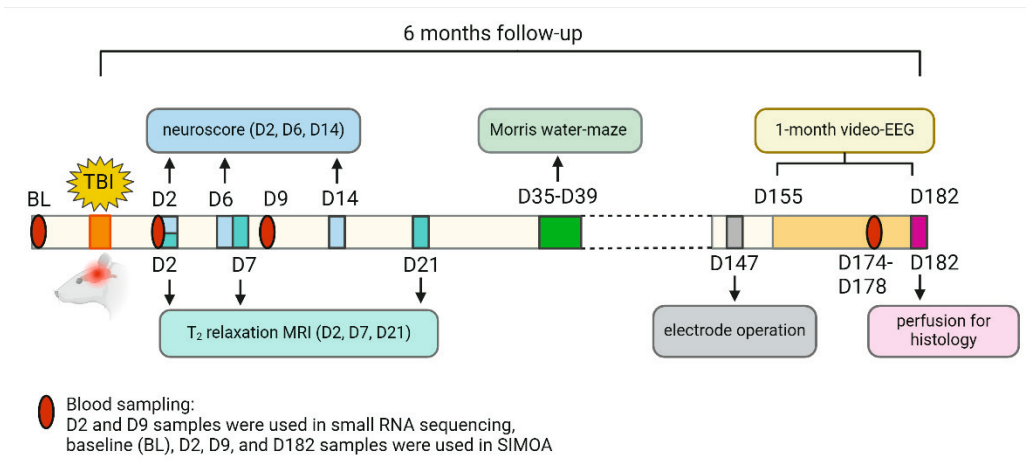


Figure 4. Timeline of the experiments conducted to EPITARGET animal cohort during the follow-up.

4.2.1 TBI induction by lateral fluid-percussion injury

TBI was induced to rats by lateral fluid-percussion injury (McIntosh et al., 1989, Kharatishvili et al., 2006). Briefly, rats were anesthetized with an anesthesia cocktail (for details, see Lapinlampi et al., 2020) and placed in a Kopf stereotactic frame. The skull was exposed with a midline skin incision and the periosteum was extracted. The left temporal muscle was gently detached from the lateral ridge. A circular craniectomy (diameter 5 mm) was performed over the left parietal cortex midway between lambda and bregma (center coordinates: 4.5 mm posterior and 2.5 mm lateral from bregma). The dura was left intact. Next, a modified Luer-Lock cap was placed into the site of craniectomy, and its edges were sealed with tissue adhesive. The cap was covered with dental acrylate and filled with sterile saline. Finally, the rat was connected to the fluid-percussion device via the Luer-Lock fitting, and lateral FPI was induced at 90 min after administration of the anesthesia cocktail. The impact pressure (approximately 3.0 atm) was adjusted to produce severe TBI. Sham-operated controls underwent the same surgical procedures without TBI induction.

4.2.2 Video-EEG monitoring

PTE was diagnosed by video-EEG. Electrode implantation for the video-EEG monitoring was conducted at 5 months after the TBI (D147). Rats were anesthetized and implanted with 3 skull electrodes. The 4-week continuous (24/7) video-EEG monitoring of the rats was started one week after electrode implantation (D154). Rats were defined as having epilepsy if ≥ 1 unprovoked electrographic seizure was detected. The electroencephalographic seizure was defined as a high-amplitude rhythmic discharge that clearly represented an atypical EEG pattern that lasted > 10 seconds (Kharatisvili et al., 2006).

4.3 MOLECULAR BIOLOGY METHODS

Table 8. Summary of molecular biology methods.

Method	Purpose	Publication
Extracellular vesicle precipitation by miRCURY Exosome Isolation Kit - Serum and Plasma	Extraction of EVs from rat plasma	I
Size-exclusion chromatography (SEC)	Separation of EV-enriched and protein-enriched fractions in rat plasma	I
Protein concentration assay	Measurement of protein concentration	I
Small RNA extraction	RNA for small RNA-sequencing, RT-qPCR, and ddPCR	I, II
Nanoparticle Tracking Analysis (NTA)	Measurement of particle concentration and size distribution	I
SDS-PAGE and Western blot	Quality control of EV isolation	I
Scanning electron microscopy (SEM)	Characterization of EVs isolated by precipitation method	I
Transmission electron microscopy (TEM)	Characterization of EVs isolated by precipitation method or SEC	I
Droplet digital PCR (ddPCR)	Measurement of the levels of specific miRNAs	I, II
Small RNA sequencing	Expression profile of plasma miRNAs after TBI or sham-operation	II

Reverse transcription qPCR (RT-qPCR)	Measurement of the levels of specific miRNAs	II
Spectrometry by NanoDrop ND-1000	Plasma quality control by measuring hemolysis	II
Qubit miRNA assay	Measurement of small RNA concentration	I, II
Single Molecule Array (SIMOA)	Measurement of plasma NF-L levels	III

4.4 BIOINFORMATICS METHODS

Table 9. Summary of bioinformatics methods and software

Method / software	Purpose	Publication
RStudio and R	Statistical analyses and preparation of graphs	II, III
DESeq2 R package	Identification of differentially expressed miRNAs in small RNA sequencing	II
pROC R package	Receiver operating characteristic (ROC) analysis	II, III
cutpointR R package	Definition of an optimal cut-off value for different parameters to categorize study subjects	II, III
Machine learning	Identification of differences in the miRNA expression pattern	II
Glmnet logistic regression	Investigation of miRNAs for inclusion in an optimal biomarker panel	II
Ingenuity Pathway Analysis (IPA)	Investigation of miRNA target genes and their function	II
GraphPad Prism	Statistical analyses and preparation of graphs	I, II, III

4.5 STATISTICAL ANALYSIS

Table 10. Summary of statistical analyses.

Statistical test	Purpose	Publication
Mann-Whitney U test	Analysis of differences between groups (unpaired data)	II, III

Wilcoxon matched-pairs signed rank test	Analysis of differences between groups (paired data)	III
Kruskal-Wallis test	Comparison of variables, such as miRNA levels, between naïve, sham and TBI groups	II
Friedman test	Evolution of NF-L levels and composite neuroscore in the same animals over different time points	III
Spearman correlation test	Analysis of relationship between miRNA or NF-L levels and disease outcome parameters	II, III
ROC analysis	Assessment of biomarker performance (sensitivity and specificity)	II, III

5 RESULTS

5.1 EVALUATION OF A COMMERCIAL PRECIPITATION-BASED METHOD IN THE ISOLATION OF EVs FROM RAT PLASMA FOR miRNA ANALYSIS (I)

5.1.1 The precipitated EV pellet from rat plasma contained circulating lipoproteins and plasma proteins.

First, the performance of a precipitation-based EV isolation kit was evaluated according to ISEV guidelines. EVs were isolated from 350 μ l of rat trunk plasma by a commercial precipitation-based EV isolation kit. The size and concentration of particles in the resulting EV pellet were measured by Nanoparticle Tracking Analysis (NTA). NTA indicated that most of the particles were in the size range of 60–120 nm (**I, Figure 1 B**). The EV pellet was further analyzed by scanning electron microscopy (SEM), which revealed round particles that had a similar size range as observed with NTA. In addition to the approximately 100 nm particles, numerous smaller particles were evident in the background (**I, Figure 1 A**).

The purity of EVs in the precipitated pellet was investigated by Western blot by comparing the EV pellet to the original plasma and the remaining supernatant. Antibodies against TSG101 (EV marker), ApoA1 (HDL marker) and albumin (marker of plasma protein contamination) were used. Western blotting revealed the presence of ApoA1 and albumin in the EV pellet. In contrast, the EV marker TSG101 was not detected in the plasma, EV pellet, or the remaining supernatant (**I, Figure 1 D**).

To further investigate the morphology of the extracted particles and to differentiate between lipoproteins and EVs, another EV pellet extracted from 250 μ l rat trunk plasma was imaged by transmission electron microscopy (TEM). In TEM, EVs typically display a cup-shaped morphology (van der Pol et al., 2012; Böing et al., 2014; Jeurissen et al., 2017; Rikkert et al., 2019), whereas lipoproteins remain round (Böing et al., 2014; Yuana et al., 2014), which makes it possible to distinguish between these particles.

TEM showed that the EV pellet contained mostly round particles, corresponding to lipoproteins, and a few cup-shaped particles, corresponding to EVs (**I, Figure 2 A**). Most particles had a size ranging from approximately 50 nm to 100 nm. In addition, TEM revealed the presence of a “dense smudge” that corresponded to aggregated proteins (Böing et al., 2014).

5.1.2 SEC separated particles and proteins into different fractions, but the EV fractions also contained lipoproteins.

SEC was conducted on 250 µl rat trunk plasma to investigate the separation of particles and proteins into different fractions. Larger particles, such as EVs, were expected to elute in the earlier fractions whereas smaller particles, such as HDL and plasma proteins, were expected to elute in the later fractions (Boing et al., 2014).

A total of 25 fractions were collected during SEC. The highest particle concentrations were detected by NTA in the fractions 12–15, whereas the protein concentration peaked in fractions 18–20 (**I, Figure 2 B**). NTA showed a progressive decrease in the particle size from the earlier to later fractions (**I, Figure 2 F-H**). A Western blot analysis of the HDL marker ApoA1 in SEC fractions revealed an intensity profile similar to the particle concentration profile in NTA (**I, Supplementary Fig. 3C**). The strongest ApoA1 bands were detected in fractions 14–16. TEM analysis revealed that most of the particles observed in the pooled fractions 6–7, 8–10, and 12–13 were round-shaped lipoproteins (**I, Figure 2 C-E**). In addition, a few particles with a cup-shaped morphology characteristic of EVs were found in fractions 6–7.

5.1.3 The precipitation method excluded the majority of plasma proteins from the EV pellet.

Next, we used SEC to compare the particle and protein concentration profile of the precipitated EV pellet to original plasma. EV precipitation was conducted with two 800-µl samples of rat trunk plasma, and the

precipitated EV pellets were further processed with SEC. The particle and protein concentrations in the resulting EV pellet SEC fractions (EV-SEC) were then compared with fractions from parallel 800- μ l plasma samples that underwent only SEC (plasma-SEC) (**I, Figure 3 A**). A comparison of the protein concentration in the EV-SEC and plasma-SEC fractions showed that the precipitation method had removed 85% to 91% of the total plasma proteins (**I, Figure 3 B**). In contrast, the particle concentration profile was comparable between the fractions acquired with both methods, indicating that the precipitation method did not remove particles that were measurable with NTA. In plasma-SEC, the particle count peaked in fraction 15, whereas in EV-SEC, the particle count peaked in fraction 16 (**I, Figure 3 C**).

5.1.4 The EV pellet acquired by the precipitation method contained both EV-enriched and vesicle-free miRNAs.

Finally, we investigated differences in miRNA profiles between the EV-SEC fractions and plasma-SEC fractions. In plasma-SEC, the highest miRNA concentration was detected in fractions 18–21 (**I, Figure 4 A**), which were also the fractions with the highest protein concentration (**I, Figure 3 B**). In contrast, in EV-SEC, miRNAs were evenly distributed across the early and late fractions (**I, Figure 4 A**). The miRNA concentration in the EV-SEC fractions 16–21 was from 51% up to 70% of that in the corresponding plasma-SEC fractions.

The presence of EV-enriched and vesicle-free miRNAs in the EV-SEC and plasma-SEC fractions was further investigated by ddPCR analysis of 4 miRNAs: miR-142-3p, miR-124-3p, miR-23a, and miR-122. Of these, miR-142-3p has been previously shown to elute mainly in the EV-enriched early fractions and in smaller quantities in the late protein fractions, whereas miR-23a and miR-122 elute mainly in the late protein fractions (Arroyo et al., 2011). The distribution of miR-124-3p in SEC fractions was previously unknown. The ddPCR analysis revealed the presence of miR-142-3p in the early fractions (f. 6–11) both in plasma-SEC and EV-SEC (**I, Figure 4 B**). The concentration of miR-142-3p in EV-SEC fractions 6–11 was only from 14% to

23% of that in plasma-SEC fractions, indicating a loss of the carrier of this miRNA during the precipitation procedure. In one of the plasma-SEC samples, there was also a smaller miR-142-3p peak in the protein fractions (f. 16–21). In contrast, miR-124-3p, miR-23a, and miR-122 peaked in the protein fractions (f. 16–23) not only in plasma-SEC but also in EV-SEC (**I, Figure 4 C–E**), indicating that the precipitated EV pellet contained vesicle-free miRNAs.

5.2 THE CIRCULATING miRNA PROFILE AT AN ACUTE TIME-POINT AFTER TBI AS A BIOMARKER FOR POST-TRAUMATIC EPILEPTOGENESIS IN RATS (II)

5.2.1 The plasma miRNA profile from small RNA-seq separated TBI rats from sham-operated controls at 2 days but not at 9 days after the TBI.

Since the isolation of EVs from rat plasma for miRNA analysis was found unfeasible, an analysis of circulating miRNAs in TBI rats was conducted from total plasma. In order to identify potential circulating biomarker miRNAs capable of differentiating between the experimental groups, miRNAs in rat plasma were first investigated by small RNA-sequencing (RNA-seq). The small RNA-seq was conducted with a subset of the EPITARGET cohort (discovery cohort, see **Table 6**), which contained samples from 20 rats. RNA for small RNA-seq was extracted from 200 µl of plasma collected at 2 days (D2) and 9 days (D9) after the TBI (n=16) or the sham-operation (n=4). On D2, small RNA-seq detected a total of 565 miRNAs in at least one sample, out of which 471 were common between sham and TBI rats (**II, Figure 1 A**). On D9, small RNA-seq detected a total of 541 miRNAs in at least one sample, 377 of which were common between sham and TBI rats (**II, Figure 1 B**). On D2, the number of reads mapping to miRNAs did not differ between the groups. On D9, the number of mapped reads in the sham-operated control rats was only 17% of that in the TBI rats (**II, Supplementary Fig. 1 A–B**).

Principal component analysis (PCA) revealed that the plasma miRNA expression profile separated TBI from the sham group on D2 but not on D9 (**II, Fig. 1 E–F**). Similarly, the heatmap analysis of miRNA expression profile in all samples achieved a separation between TBI and sham rats on D2 but not on D9 (**II, Supplementary Fig. 3**). Pairwise comparison heatmaps revealed a clear separation between sham and TBI groups on D2, but there was no separation on D9 (**II, Supplementary Fig. 4 & Supplementary Fig. 5**).

5.2.2 Circulating miRNA profile from small RNA sequencing on 2 d or 9 d after TBI did not separate rats with or without PTE.

The 16 animals in the TBI group consisted of 7 rats with epilepsy (TBI+) and 9 rats without epilepsy (TBI-). PCA detected no separation between the TBI+ and TBI- groups on D2 or on D9 (**II, Fig. 1 G–H**). A heatmap analysis of all samples (**II, Supplementary Fig. 3**) or a pairwise comparison heatmaps (**II, Supplementary Fig. 4 and 5**) did not achieve a separation between TBI+ and TBI- groups on either D2 or D9.

5.2.3 Differentially expressed plasma miRNAs were identified between the TBI and sham groups, but not between the TBI+ and TBI- groups.

Differential expression analysis by DESeq2 was used to identify miRNAs that were either upregulated or downregulated between the different experiment groups. DESeq2 analysis detected 45 differentially expressed plasma miRNAs between the TBI and sham groups on D2 (28 upregulated, 17 downregulated) (**Supplementary Table 1**). On D9, DESeq2 detected 17 differentially expressed miRNAs (6 upregulated, 11 downregulated) (**Supplementary Table 4**). No differentially expressed miRNAs were detected between the TBI+ and TBI- groups on either D2 or D9.

Logistic regression analysis for miRNA candidates differentiating sham and TBI groups yielded 30 miRNAs on D2, and 23/30 of these miRNAs were common with DESeq2 analysis (**Supplementary Fig. 6**). On D9, a logistic

regression analysis of sham and TBI groups yielded 29 miRNAs, however, none of them were common with DESeq2. Furthermore, the logistic regression analysis could not differentiate between the TBI+ and TBI- groups at either time-point.

5.2.4 Upregulation of plasma miR-136-3p, miR-323-3p, miR-434-3p, and miR-9a-3p 2 d after TBI was validated by RT-qPCR.

Selection of miRNAs for validation. Since a differential expression analysis did not identify any miRNAs which could distinguish the rats with epilepsy from their non-epileptic counterparts, a further analysis was conducted focusing on the miRNAs that had been found to be upregulated in TBI rats as compared to sham-operated controls. Furthermore, as the circulating miRNA profile from small RNA sequencing achieved a poor separation of TBI and sham groups on D9, the subsequent validation of the small RNA-seq results focused on those miRNAs that were differentially expressed at the D2 time-point. A differentially expressed miRNA was selected for RT-qPCR validation if it met the following criteria: i) an adequately large difference in the expression between TBI and sham groups ($\log_2FC \geq 1.0$) ii) a low adjusted p-value, and iii) a sufficient abundance of the miRNA to allow detection by PCR methods (count per million reads, CPM ≥ 30). Based on the criteria, 3 miRNAs, miR-136-3p, miR-323-3p and miR-129-5p, were selected for technical validation by RT-qPCR. There were more miRNAs that met the criteria, but due to the limited amount of sample they were not included in the initial RT-qPCR validation. In addition to miR-136-3p, miR-323-3p, and miR-129-5p, the RT-qPCR analysis was complemented with two other miRNAs, miR-434-3p and miR-9a-3p, which had earlier been observed to be strongly upregulated 2 d after TBI (Das Gupta et al., 2021) but were not detected in the small RNA-seq of the EPITARGET rats. The expression levels in RT-qPCR were normalized to the endogenous control miR-28-3p by the $2^{-\Delta Ct}$ method.

Validation of miRNAs by RT-qPCR. Validation by RT-qPCR was performed with different plasma aliquots from the same rats that were used in small RNA sequencing (discovery cohort: 4 sham, 16 TBI). Increased levels of miR-

136-3p and miR-323-3p were validated in the TBI group in comparison to the sham group ($p < 0.05$ for both), whereas the difference in miR-129-5p levels did not reach statistical significance ($p > 0.05$). In addition, miR-434-3p and miR-9a-3p that were not detected by sequencing showed increased levels in the TBI group when compared to the sham group ($p < 0.01$ for miR-434-3p, $p < 0.001$ for miR-9a-3p) (**II, Figure 2**). No differences were detected in the levels of the 5 assessed miRNAs between rats with epilepsy (TBI+, $n=7$) and rats without epilepsy (TBI-, $n=9$) ($p > 0.05$ for all).

5.2.5 Analysis in the large EPITARGET animal cohort confirmed 7 plasma miRNAs as injury biomarkers.

Selection of miRNAs for ddPCR analysis. After the technical validation in the smaller discovery cohort, differentially expressed miRNAs were validated in the whole EPITARGET cohort (validation cohort, see **Table 6**). The validation in the larger cohort was performed by ddPCR, which is a more sensitive method than RT-qPCR. The selection criteria for candidate miRNAs for the ddPCR analysis in the validation cohort were the same as for the technical validation by RT-qPCR. In addition, the selected candidate miRNAs were brain-specific or brain-enriched in miRNA databases and in a literature search. Based on the selection criteria and preliminary experiments, a total of 7 upregulated miRNAs (miR-434-3p, miR-9a-3p, miR-136-3p, miR-323-3p, miR-124-3p, miR-132-3p, and miR-212-3p) were selected for ddPCR validation. Preliminary experiments with ddPCR were also performed with miRNAs downregulated in the TBI group compared with the sham group (miR-455-5p, miR-140-3p, and miR-149-5p). Since the preliminary analysis by ddPCR did not detect differences in the levels of miR-455-5p, miR-140-3p, and miR-149-5p between the TBI and sham groups, downregulated miRNAs were not included in further analysis (**II, Supplementary Fig. 7**).

ddPCR analysis. A total of 115 out of the 150 plasma samples available on D2 from the epilepsy-phenotyped rats in the EPITARGET cohort had sufficient volume and quality to be included into the ddPCR analysis. The validation cohort included 8 naïve, 17 sham, and 90 TBI rats (21 TBI+, 69

TBI-). The target miRNA expression levels were normalized to the endogenous control miR-28-3p (target copy number / miR-28-3p copy number). No correlation was detected between the plasma A414 value and the unnormalized miRNA expression levels of the 7 analyzed miRNAs ($p>0.05$ for all), indicating that hemolysis had not affected the miRNA expression levels.

DdPCR showed increased levels of all 7 analyzed miRNAs in the TBI group as compared with naïve or sham-operated controls ($p<0.001$ for all) (**II, Figure 3**). In comparison to naïve controls, the largest increase in the TBI group was detected for miR-9a-3p (41.1-fold), followed by miR-124-3p (20.8-fold), miR-323-3p (30.6-fold), miR-434-3p (11.2-fold), miR-136-3p (10.6-fold), miR-132-3p (3.1-fold), and miR-212-3p (2.4-fold). In the comparison between the TBI and sham groups, the largest increases were detected for miR-9a-3p (22-fold), followed by miR-124-3p (18.2-fold), miR-323-3p (7.3-fold), miR-136-3p (4.4-fold), miR-434-3p (4.2-fold), miR-132-3p (2.2-fold), and miR-212-3p (1.5-fold).

The levels of 6 out of 7 miRNAs were also increased in the sham-operated group in comparison with the naïve group. The largest increase was observed for miR-323-3p (4.2-fold, $p<0.01$), followed by miR-9a-3p (3.4-fold, $p<0.05$), miR-136-3p (2.9-fold, $p<0.01$), miR-434-3p (2.3-fold, $p<0.001$), miR-212-3p (1.6-fold, $p<0.05$), and miR-132-3p (1.4-fold, $p<0.05$). The levels of miR-124-3p did not differ between the naïve and sham groups ($p>0.05$).

ROC analysis. ROC analysis was used to evaluate the performance of each miRNA to differentiate between the TBI, sham, and naïve groups, and to determine optimal cut-offs for the normalized miRNA expression levels. The summary of the AUCs, sensitivity, specificity, and optimal cut-off values is presented in **II, Supplementary Table 7**. All 7 investigated miRNAs separated TBI rats from naïve rats and sham-operated controls. In the separation of TBI rats from sham-operated controls, 6 miRNAs had AUC values ≥ 0.94 ($p<0.001$ for all), whereas miR-212-3p had AUC 0.76 ($p<0.001$). In the separation between TBI rats and naïve rats, all 7 miRNAs had AUC ≥ 0.95 ($p<0.001$ for all). In the differentiation of sham-operated controls from naïve rats, all miRNAs except miR-124-3p (AUC 0.49, $p>0.05$) separated the

two groups with AUC values ranging from 0.76 (miR-9a-3p, $p < 0.05$) to 0.96 (miR-434-3p, $p < 0.001$) (**II, Figure 4**).

5.2.6 Plasma miRNAs at the acute time-point after TBI did not predict the epilepsy outcome.

The group of 90 TBI rats analyzed by ddPCR included 21 rats with (TBI+) and 69 rats without epilepsy (TBI-). No differences in plasma miRNA levels at 2 d after TBI were detected between the two groups (**II, Figure 5**).

To investigate whether the miRNA levels depended on the severity of epilepsy, the 21 rats in the TBI+ group were categorized according to their seizure frequency and the occurrence of seizure clusters. The categorization by seizure frequency was conducted by dividing the TBI+ rats into two groups according to the total number of seizures during the 1-month video-EEG monitoring (≥ 3 seizures, $n=15$ vs. < 3 seizures, $n=6$). The categorization by seizure clusters was conducted by dividing the TBI+ rats into two groups according to whether they experienced seizure clusters (≥ 3 seizures within 24 hours) (clusters, $n=8$, no clusters, $n=13$). However, no differences in plasma miRNA expression levels were detected between the rats with many seizures and those animals with few seizures ($p > 0.05$), or between the rats with seizure clusters or those without clusters ($p > 0.05$) (**II, Figure 6**). The ROC analysis showed that none of the miRNAs differentiated between the TBI+ and TBI- groups, or the epilepsy severity groups (**II, Figure 7**).

In addition, an elastic net regularized logistic regression (glmnet) was used to determine whether a set of miRNAs rather than an individual miRNA could separate TBI+ and TBI- rats, and the rats in different epilepsy severity groups. The glmnet analysis did not identify any combination of miRNAs which could differentiate TBI+ rats from their TBI- counterparts. Interestingly, glmnet analyses of epilepsy severity groups identified candidate miRNA sets capable of separating those rats with many seizures from those with few seizures, or rats with or without seizure clusters. However, the AUCs in all ROC analyses had large confidence intervals, and $p > 0.05$ (**II, Figure 8**).

5.2.7 The expression levels of plasma miRNAs at the acute time-point after TBI correlated with the severity of the cortical lesion at different time points after TBI.

To determine whether the levels of circulating miRNAs were related to the severity of the cortical injury after TBI, the correlation was estimated between miRNA levels on D2 and the severity of the cortical lesion at acute, subacute, and chronic time-points.

First, data from an earlier T₂ MRI analysis of the whole EPITARGET cohort (Manninen et al., 2020) was used to assess the correlation of D2 miRNA levels and the volume of cortical lesion on D2, D7 and D21 after the TBI. MRI data was available for all 90 TBI rats that were included in the ddPCR analysis. The correlation analysis showed that for 6 out of 7 miRNAs (all except miR-212-3p), the increased plasma miRNA levels were associated with a larger cortical lesion on both D2 and D7. In addition, levels of all 7 miRNAs associated with a larger cortical lesion on D21. The strongest correlation coefficients at all time-points were observed for miR-124-3p ($\rho = 0.522-0.582$, $p < 0.001$) and miR-9a-3p ($\rho = 0.507-0.571$, $p < 0.001$), followed by miR-323-3p ($\rho = 0.418-0.489$, $p < 0.001$), miR-132-3p ($\rho = 0.433-0.463$, $p < 0.001$), miR-434-3p ($\rho = 0.342-0.581$, $p < 0.001$), miR-136-3p ($\rho = 0.287-0.394$, $p < 0.001$), and miR-212-3p ($\rho = 0.269$ on D21, $p < 0.05$) (II, **Figure 9**).

Next, to investigate the correlation between miRNA levels on D2 and the cortical lesion area at a chronic time-point (D182) after TBI, unfolded cortical maps were created for all 90 TBI rats included in the ddPCR analysis. The correlation analysis showed that in 6 out of 7 miRNAs (all except miR-212-3p), increased plasma miRNA levels on D2 associated with a larger cortical lesion area on D182. The highest correlation coefficients were observed for miR-124-3p ($\rho = 0.433$, $p < 0.001$) and miR-9a-3p ($\rho = 0.408$, $p < 0.001$), followed by miR-323-3p ($\rho = 0.277$, $p < 0.01$), miR-434-3p ($\rho = 0.248$, $p < 0.05$), miR-132-3p ($\rho = 0.240$, $p < 0.05$), and miR-136-3p ($\rho = 0.230$, $p < 0.05$) (II, **Figure 10**).

5.3 CIRCULATING NF-L AS A PROGNOSTIC BIOMARKER FOR THE STRUCTURAL AND FUNCTIONAL OUTCOME IN RATS AFTER TBI (III)

5.3.1 Plasma NF-L levels increased after the LFP-induced TBI, and a slight elevation was observed even 6 months after TBI.

The plasma NF-L study cohort included 34 rats (8 sham, 26 TBI) from the total of 137 rats (23 sham, 114 TBI) that completed the 6-month-long EPITARGET project. The temporal profile of NF-L protein in rat plasma after LFP-induced TBI was investigated by measuring NF-L levels in the TBI group by SIMOA 6 days before TBI (baseline), and on 2 d (D2), 9 d (D9), and at 6 months after TBI (D176). In the sham group, NF-L levels were measured at baseline and on D2 after the sham-operation.

On D2, the TBI group showed a 483-fold increase in the mean plasma NF-L levels in comparison with the baseline levels from the same rats, and a 21-fold increase compared with the sham-operated group ($p < 0.001$ for both) (**III, Figure 1**). On D9, the plasma NF-L levels decreased on average to 20% of that on D2 but remained 89-fold elevated when compared to baseline ($p < 0.001$ for both). Plasma NF-L levels on D9 in the TBI group were 4-fold higher than in sham-operated group on D2 ($p < 0.001$). On D176, the plasma NF-L levels in the TBI group were still approximately 3-fold higher when compared with the baseline samples ($p < 0.001$). The NF-L levels on D176 in the TBI group were only 13% of that in the sham-operated group on D2 ($p < 0.001$). In the sham group, the mean plasma NF-L levels on D2 were 25-fold higher than baseline levels ($p < 0.01$).

5.3.2 Plasma NF-L levels correlated with cortical lesion severity at acute and chronic time-points after TBI.

A correlation analysis was performed to investigate whether plasma NF-L levels predicted the severity of the cortical lesion at both the acute and chronic time points. The analysis used data on the cortical lesion volumes on D2, D7 and D21 after the TBI or the sham-operation from the earlier

quantitative T₂ MRI analysis of the EPITARGET cohort (Manninen et al., 2020). In addition, unfolded cortical maps on D182 after TBI were used in the estimation of the correlation between NF-L levels and the severity of the cortical lesion at a chronic time-point.

Quantitative T₂ MRI data were available for all rats included in the NF-L analysis. The correlation analysis showed that the higher the plasma NF-L levels on D2 after TBI, the larger the cortical lesion volume as assessed by MRI on D2 ($\rho = 0.401$, $p < 0.05$) (**III, Figure 2**). However, no correlation was detected between the D2 NF-L levels and the cortical lesion volume on D7 or D21 ($p > 0.05$). In addition, no correlation was evident between the D9 NF-L levels and the cortical lesion volume on D7 or D21 ($p > 0.05$).

The correlation analysis of plasma NF-L levels and the lesion area in cortical unfolded maps indicated that the higher the plasma NF-L levels on D2 and D9, the larger the cortical lesion area on D182 ($\rho = 0.437$ for D2, $\rho = 0.393$ for D9, $p < 0.05$ for both). In contrast, plasma NF-L levels at the chronic time point (D176) did not correlate with the presence of a larger cortical lesion area on D182 ($p > 0.05$).

5.3.3 Circulating NF-L functioned as biomarker for TBI and sham-operation.

The performance of plasma NF-L levels to distinguish between the injury groups was evaluated by conducting an ROC analysis. Baseline samples from both TBI and sham-operated controls were used in the analysis as a naïve control group. The ROC analysis showed that on D2, a cut-off of 2291 pg/ml differentiated TBI rats from naïve rats with 100% sensitivity and 100% specificity (AUC 1.00, $p < 0.001$) (**III, Figure 3**). On D9, a cut-off of 442 pg/ml differentiated TBI rats from naïve rats with 100% sensitivity and 100% specificity (AUC 1.00, $p < 0.001$). Even on D176, a cut-off of 15.8 pg/ml differentiated TBI rats from naïve rats with 100% sensitivity and 97% specificity (AUC 0.999, $p < 0.001$). In addition, the TBI group was perfectly separated from the sham-operated controls on D2 with a cut-off of 2201 pg/ml (AUC 1.00, 100% sensitivity and 100% specificity, $p < 0.001$). Interestingly, plasma NF-L levels also perfectly separated sham-operated

controls from the naïve group with a cut-off of 49.1 pg/ml (AUC 1.00, 100% sensitivity and 100% specificity, $p < 0.001$).

5.3.4 The plasma NF-L levels did not predict somatomotor recovery after TBI.

The severity of somatomotor and vestibular deficits after the TBI was evaluated by the composite neuroscore test on D2, D6, and D14 after the TBI. The more severe the somatomotor impairment, the lower the neuroscore (the range of the scale was 0–28). In the sham-operated control group, the mean neuroscore slightly improved from 26.5 (D2) to 27.5 (D14) during the follow-up ($p < 0.01$). In the TBI group, the mean neuroscore improved from 7.9 (D2) to 14.2 (D14) ($p < 0.001$) (**III, Figure 4 A**). The correlation analysis showed that higher plasma NF-L levels on D2 were associated with a lower neuroscore on D2 ($\rho = -0.480$, $p < 0.05$) (**III, Figure 4 C**). However, no correlation was found between D2 NF-L levels and the neuroscore at subsequent time-points ($p > 0.05$).

Importantly, the rats subjected to TBI demonstrated extensive variation in the severity of somatomotor impairment at all post-injury time-points. The neuroscore range was 3.0–13.0 on D2, 7.0–19.7 on D6, and 9.7–22.7 on D14. An analysis of the overall recovery during the post-TBI follow-up showed that some rats experienced a notable improvement in their neuroscore from D2 to D14, whereas some rats demonstrated only a slight improvement (**III, Figure 4 D**). However, the correlation analysis revealed that the plasma NF-L levels at any investigated time point (D2, D9, D176) did not correlate with the recovery index ($p > 0.05$). In addition, the ROC analysis indicated that plasma NF-L levels at any time point did not differentiate between the rats with a good somatomotor recovery from those experiencing a poor recovery.

5.3.5 The plasma NF-L levels did not predict the cognitive impairment after TBI.

Morris water-maze data of the whole EPITARGET cohort (23 sham, 118 TBI) was used to identify the best parameter with which to differentiate between cognitively impaired (CI+) and non-impaired (CI-) rats. It was found that the latency to reach the platform on D37 after the TBI separated the TBI rats from sham-operated controls with 84% sensitivity and 100% specificity (AUC 0.94, $p < 0.001$, cut-off 19.2 seconds) (**III, Figure 5 A**). Next, the selected parameter and cut-off were used to categorize the rats with TBI in the whole EPITARGET cohort into CI+ and CI- groups. In the NF-L analysis cohort, 19/26 (73%) of rats with TBI were classified as CI+, and 7/26 (27%) as CI-, which was comparable with the division in the whole EPITARGET cohort.

Plasma NF-L levels did not differ between the CI+ and CI- rats at any time-point ($p > 0.05$) (**III, Supplementary Fig. 3 B**). No correlation was detected between the NF-L levels on D2 and the latency to reach the platform on D37 after TBI ($p > 0.05$) (**III, Figure 5 B**). ROC analysis showed that plasma NF-L levels on D2 after TBI did not distinguish the CI+ rats from their CI- counterparts (**III, Figure 5 C**).

5.3.6 Plasma NF-L levels did not predict post-traumatic epileptogenesis.

The 26 selected TBI rats included in the NF-L analysis consisted of 13 rats with epilepsy (TBI+) and 13 rats without epilepsy (TBI-). No differences in plasma NF-L levels were detected between the TBI+ and TBI- rats at any investigated time-point ($p > 0.05$) (**III, Figure 6 A**). In addition, no differences in the evolution of plasma NF-L levels from D2 to D9, or from D9 to D176, were detected between the TBI+ and TBI- groups ($p > 0.05$). No correlation was found between the total number of seizures and plasma NF-L levels at any time-point ($p > 0.05$). In addition, NF-L levels did not differ between rats that experienced seizure clusters and those that did not ($p > 0.05$). The ROC

analysis indicated that plasma NF-L levels did not distinguish between TBI+ and TBI- rats at any investigated time-point (**III, Figure 6 B**).

6 DISCUSSION

The aim of this thesis was to find circulating miRNA and protein biomarkers for the evaluation of TBI severity and the prediction of PTE development by using a preclinical model of PTE in which TBI was induced in rats by lateral FPI, with vEEG being used to define the epilepsy phenotype.

6.1 ISOLATION OF EVs BY THE PRECIPITATION METHOD CO-PRECIPITATED PLASMA PROTEINS, LIPOPROTEINS, AND VESICLE-FREE miRNAs

In the first part of this thesis, the aim was to find an EV extraction method suitable for subsequent studies which would make it possible to detect alterations in circulating EV-enriched miRNAs in a preclinical model of PTE. Therefore, the performance of a commercial precipitation-based kit in the isolation of circulating EVs from rat plasma was evaluated.

The EV precipitation method was selected because it has several qualities that make it appealing for biomarker studies. First, there are multiple commercial kits available, such as miRCURY Exosome Isolation kit (QIAGEN), Total Exosome Isolation (Invitrogen), and ExoQuick (System Biosciences), and their protocols are simple, not requiring expensive equipment, and they enable simultaneous processing of a large number of samples. Second, the precipitation protocols are fast (< 2 h) when compared to more time-consuming methods such as ultracentrifugation or density gradient centrifugation, which may last from 3 h up to around 20 h (Raposo et al., 1996; Van Deun et al., 2014). Third, the manufacturers of the precipitation kits claim that EV isolation will be successful from plasma samples as small as 100–300 µl. This was important here, as the volume of a blood sample that can be obtained from a rat is very limited, and a small starting volume enables longitudinal studies in which sampling could be conducted at several time-points. In contrast, the typical starting volume of

plasma in other EV isolation methods varies from $\geq 500 \mu\text{l}$ in size-exclusion chromatography (SEC) (Böing et al., 2014; Dong et al., 2020) to several milliliters in ultracentrifugation (Serrano-Pertierra et al., 2019; Dong et al., 2020).

EVs were isolated from naïve rat plasma by the precipitation-based miRCURY Exosome Isolation Kit. However, the characterization by Western blot revealed the presence of albumin and ApoA1 in the pellet, indicating co-precipitation of plasma proteins and lipoproteins. An analysis of the EV pellet by TEM confirmed that most of the observed particles corresponded to lipoproteins (Böing et al., 2014; Yuana et al., 2014; Karimi et al., 2018) whereas only a few EVs were detected. The small number of EVs and the observed contamination by lipoproteins and plasma proteins in the resulting sample raised two important questions, i.e. whether the precipitation method had succeeded in enriching EV-associated miRNAs from plasma, and whether the EV pellet also contained vesicle-free miRNAs. Previously, Arroyo et al. used SEC with human serum and plasma to investigate the distribution of circulating miRNAs in vesicular and non-vesicular fractions. In our study, SEC was used to investigate the miRNA profile of the precipitated EV pellet (EV-SEC) and SEC fractions acquired directly from plasma (plasma-SEC).

As expected, miR-142-3p, the miRNA that Arroyo et al. reported to be mainly EV-associated in humans, was detected mainly in the early SEC fractions both in EV-SEC and in plasma-SEC. The levels of miR-142-3p, however, were lower in EV-SEC than in plasma-SEC, suggesting that some of the EVs and their miRNA cargo had been lost during the precipitation process. Importantly, we detected two known Ago2-associated miRNAs, miR-23a and miR-122 (Arroyo et al., 2011), in the late SEC fractions both in EV-SEC and plasma-SEC. This indicated that although a protein concentration analysis showed that precipitation removed $\sim 90\%$ of total plasma proteins, the EV pellet still contained protein complexes that were carrying miRNAs.

In addition to the known EV or protein-associated miRNAs, we investigated the distribution of miR-124-3p in rat plasma. The brain-

enriched miR-124-3p was selected for the analysis, since an earlier study from our laboratory revealed that miR-124-3p was chronically downregulated after TBI in the perilesional cortex and dentate gyrus of rats and human patients (Vuokila et al., 2018). Furthermore, a subsequent study detected increased levels of miR-124-3p in rat plasma 2 d after TBI (Vuokila et al., 2020). In our study, the fractionation of rat plasma by SEC revealed that miR-124-3p peaked in the protein fractions, suggesting that at least in naïve rat plasma, miR-124-3p was mainly vesicle-free. Interestingly, several investigators have detected miR-124-3p to be associated with EVs. For example, one group found miR-124-3p as the third most common miRNA in serum exosomes obtained from healthy humans (Huang et al., 2013). Wang et al. (2020) reported a TBI-induced increase in miR-124-3p levels in rat plasma EVs 24 h after a weight-drop injury. Increased levels of miR-124 in serum exosomes were also found in patients with acute ischemic stroke (Ji et al., 2016), and in patients with glioblastoma (Santangelo et al., 2018). On the other hand, a recent study detected miR-124 to be both vesicle-free and exosome-associated in plasma of lung cancer patients (Sanchez-Cabrero et al., 2023). However, since these studies used a precipitation method for EV isolation and none of them controlled for plasma protein or lipoprotein contamination, one must speculate whether the resulting EV products were not completely depleted of vesicle-free miRNAs. In addition, the distribution of circulating miRNAs in disease state may also differ from the healthy state.

In summary, the precipitation method did not enrich EV-associated circulating miRNAs, with co-precipitation of plasma proteins and, consequently, vesicle-free miRNAs, being a major drawback. Incomplete depletion of circulating lipoproteins and proteins with a precipitation method has also been demonstrated in human plasma samples by other investigators (K. Brennan et al., 2020; Dong et al., 2020). Furthermore, similarly to our findings, these investigators had encountered difficulties in detecting EV marker proteins in the EVs isolated by precipitation methods, indicating a low EV yield that was confirmed by TEM imaging.

Since the polymer-based precipitation method seems unsuitable for EV isolation from blood, this raises the question, what other methods can be used to extract circulating EVs to achieve a reliable miRNA analysis? In this thesis, the SEC protocol of Boing et al. (2014) was used to separate plasma EVs from proteins. However, SEC did not separate EVs from lipoproteins that had an overlapping size with the EVs. The co-isolation of lipoprotein particles with EVs in SEC has also been described in several other publications (Karimi et al., 2018; Brennan et al., 2020; Benayas et al., 2023). The purity of EVs can be improved by undertaking additional purification steps, for example, by conducting a density gradient UC before or after SEC (Karimi et al., 2018; Vergauwen et al., 2021). Another research group utilized density gradient UC followed by bind-elute chromatography to isolate high-purity EVs from rat plasma (Onódi et al., 2018). These studies required a minimal 2–6 ml volume of plasma, which is not feasible in longitudinal rat studies, as the maximal blood volume that can be collected from rats is around 1 ml per week (<https://www.nc3rs.org.uk/3rs-resources/blood-sampling/blood-sampling-rat>, accessed on 27.11.2023). Another possible approach would be to selectively capture EVs from plasma by immunoaffinity purification techniques (He et al., 2014; Ko et al., 2018). By using antibodies against tissue-specific membrane proteins, immunoaffinity methods may make it possible to achieve a selective capture of circulating EVs derived from different tissues, such as the brain (Mustapic et al., 2017; Sun et al., 2017; Ko et al., 2018). According to Ko and colleagues, the isolation of brain-derived EVs from mouse plasma by an immunocapture method resulted in an adequate RNA yield to permit analysis of EV-miRNAs by small RNA sequencing and RT-qPCR. On the other hand, one challenge associated with immunoaffinity methods is finding membrane proteins that are specific to the desired EV population. For instance, several investigators have used L1CAM protein as a marker for neuronal-derived EVs (Gomes & Witwer, 2022), but the presence of L1CAM in the EVs in plasma and CSF has been recently criticized (Norman et al., 2021).

All in all, it is evident that the isolation of circulating EVs for miRNA analysis is challenging. In preclinical studies, EV isolation is further complicated by the limited sample volume. As our study demonstrates, whatever method is used for EV isolation, it is essential to conduct a thorough quality control for possible contaminants in order to avoid erroneous conclusions in the downstream analyses. Since the precipitation method was not suitable for our further studies and there were no alternative EV isolation methods available for small plasma volumes, the analysis of circulating miRNAs in rat plasma in the second part of this thesis was conducted from total plasma instead of from EVs.

6.2 CIRCULATING miRNAs ARE MARKERS OF BRAIN INJURY AND PREDICT THE SEVERITY OF CORTICAL PATHOLOGY BUT NOT EPILEPTOGENESIS

Currently, there are no biomarkers that could predict the development of PTE after TBI. The lack of prognostic biomarkers for PTE has hampered the development of anti-epileptogenic treatments, as there are no tools which could help to stratify the study subjects, pinpointing those that have the highest risk of PTE (Engel et al., 2013). In the second part of the thesis, the objective was to discover if there are circulating miRNA biomarkers that would be useful when assessing injury severity and predict post-traumatic epileptogenesis in a rat model of PTE. Since the extraction of EV-associated miRNAs from rat plasma had proved to be unfeasible, TBI-induced alterations in all circulating miRNAs were investigated. In this part of the project, we used the EPITARGET rat cohort, in which the animals underwent a 6-month follow-up including 1-month of continuous vEEG monitoring to determine PTE (for details, see Lapinlampi et al., 2020).

As the small RNA-seq analysis of plasma samples did not identify any miRNAs which could distinguish the rats with or without PTE, a further analysis was conducted with the miRNAs that were upregulated in TBI rats in comparison to sham-operated controls. Based on the sequencing results, a literature review, and preliminary experiments, a total of 7

miRNAs (miR-9a-3p, miR-124-3p, miR-323-3p, miR-136-3p, miR-434-3p, miR-132-3p, and miR-212-3p) were selected for ddPCR analysis in the whole EPITARGET cohort. The ddPCR analysis demonstrated an upregulation of all 7 miRNAs in rat plasma at 2 d after TBI when compared with either sham-operated or naïve controls. All 7 miRNAs distinguished TBI rats from both control groups with high AUCs, showing excellent performance as biomarkers for a brain injury. Further, differences in plasma miRNA levels between the sham-operated (craniotomy) and naïve rats were investigated. It has been previously shown that craniotomy can induce structural and functional damage in the brain (Cole et al., 2011) and alter the levels of circulating miRNAs (Das Gupta et al., 2021). We found that 6 out of 7 analyzed miRNAs (all except miR-124-3p) separated sham-operated controls from naïve controls, indicating them as potential biomarkers for mild TBI.

Of the miRNAs investigated in our study, the levels of miR-434-3p, miR-9a-3p, miR-136-3p, and miR-124-3p have been previously reported both by our laboratory and others to be elevated in rat plasma at an acute time-point after TBI (Vuokila et al., 2020; Wang et al., 2020; Das Gupta et al., 2021). Upregulation of miR-434-3p has also been detected in mouse plasma after mild TBI (Sharma et al., 2014). In addition to preclinical studies, the miRNAs have been investigated in a few clinical studies. One study reported 4-fold and 3-fold increases in the levels of miR-9-3p and miR-124-3p levels in patient serum samples \leq 24 h post-TBI (O'Connell et al., 2020b). There is another report of a slight elevation in circulating miR-124-3p levels at 6 h after a severe TBI (Schindler et al., 2020). A previous study from our laboratory identified circulating miR-9-3p and miR-136-3p as potential biomarkers for mild TBI in rats (Das Gupta et al., 2021). In the same study, the upregulation of miR-9-3p, but not that of miR-136-3p, was validated in plasma samples from patients with severe TBI, but the number of samples was small. In contrast, miR-434-3p is rodent-specific and has not been detected in humans (Das Gupta et al., 2021). With respect to miR-132-3p, one clinical study reported elevated serum miR-132-3p levels at 12 h and 48 h post-TBI compared to the 2 h time-point (Ma et al., 2019).

Importantly, to the best of our knowledge, there are no prior clinical studies on circulating miR-323-3p and miR-212-3p after TBI, a situation warranting further validation in humans.

Next, we investigated whether the circulating miRNA profile at acute time-point after TBI could be used to predict the progression of cortical pathology. The increased levels of 6 out of 7 miRNAs (all except miR-212-3p) on D2 after TBI correlated with the development of a larger lesion volume in MRI during the first 3 weeks after injury. Furthermore, a histologic analysis revealed that the elevated circulating miRNA levels on D2 correlated with an enlarged cortical lesion area at 6 months after the TBI. In both the MRI and histological analyses, miR-124 and miR-9 demonstrated the strongest correlation with cortical pathology. Increased plasma miR-124-3p levels have been reported to correlate with a larger cortical lesion area as detected with MRI also at 2 months after the TBI (Vuokila et al., 2020). In addition to being observed after a TBI, elevated blood miR-124 or miR-9 levels have been associated with a larger lesion or infarct volume and worse outcome in clinical stroke studies (Ji et al., 2016; Rainer et al., 2016). In contrast, one study reported that acute ischemic stroke patients with a larger infarct volume had decreased levels of miR-124 and miR-9 in their serum (Liu et al., 2015).

In the EPITARGET cohort, 25% of the TBI rats developed PTE during the 6-month follow-up. Nonetheless, it was evident that small RNA sequencing of plasma samples collected either at 2 d or at 9 d after TBI did not identify differentially expressed miRNAs between the rats with (TBI+) or without epilepsy (TBI-). Since the risk of PTE increases with the severity of the injury (Annegers et al., 1998), it was investigated whether the 7 miRNAs that were upregulated in plasma at 2 d after the TBI could predict the development of PTE. Furthermore, TBI+ rats were divided into different groups based on the epilepsy severity (total number of seizures and presence of seizure clusters). However, none of the miRNAs distinguished the TBI+ and TBI- rats or the rats allocated to the different epilepsy severity groups. Next, we applied a glmnet analysis to assess whether a combination of the acutely upregulated miRNAs would be one way to improve the differentiation of

the groups, but no miRNA sets were identified capable of separating TBI+ from their TBI- counterparts. Interestingly, glmnet identified a set of miRNAs which could potentially identify rats in the epilepsy severity groups. Unfortunately, the number of animals per group was small, and the results did not reach statistical significance. The findings suggest that further studies with more animals are warranted.

All 7 of the investigated miRNAs are known to be neuronally enriched (Coolen et al., 2013; Jovičić et al., 2013). MiR-9 and miR-124 function in embryonic neurogenesis and neuronal differentiation (Krichevsky et al., 2006). MiR-9 also participates in the regulation of synaptic plasticity and memory (Sim et al., 2016). In contrast, the functions of miR-323 are largely unknown. There is one study that reported elevated circulating miR-323 levels in patients with mild cognitive impairment (Sheinerman et al., 2013), and another study detected an upregulation of miR-323 in the brain as being associated with depression (Fiori et al., 2021). MiR-136 is specifically enriched in neurons (Miska et al., 2004; Jovičić et al., 2013). On the other hand, the expression of miR-136 outside the central nervous system has also been reported (Kitahara et al., 2013; Chen et al., 2020). In addition to TBI, upregulation of miR-136 was reported in the blood of patients with Parkinson's disease (Ravanidis et al., 2020). According Jovičić et al. (2013), miR-434 is specifically expressed in rat cortical neurons. Interestingly, miR-434 has also been detected in rodent skeletal muscles (Shang et al., 2016; Jung et al., 2017; Pardo et al., 2017). The last two miRNAs, miR-132 and miR-212, are closely related and are located in the same miRNA cluster (Wanet et al., 2012). They regulate neurite outgrowth, dendrite maturation, and synaptic plasticity (Vo et al., 2005; Wayman et al., 2008; Magill et al., 2010; Luikart et al., 2011; Remenyi et al., 2013). MiR-132 and miR-212 have also been detected in astrocytes and microglia in rat and human TLE (Korotkov et al., 2020a).

Of the 7 miRNAs, miR-132 and miR-212 have been the most extensively studied in epilepsy. Increased levels of miR-132 and/or miR-212 in hippocampal tissue in rodent models of SE have been reported in multiple publications (Nudelman et al., 2010; Jimenez-Mateos et al., 2011; Bot et al.,

2013; Gorter et al., 2014; Guo et al., 2014; Korotkov et al., 2020a; Venø et al., 2020; Bencurova et al., 2021). Furthermore, two clinical studies detected increased miR-132 expression in the hippocampal tissue of patients with TLE (Peng et al., 2013; Korotkov et al., 2020a). In contrast, there are two reports of a downregulation of miR-212 in the hippocampus of TLE patients (Haenisch et al., 2015; Cai et al., 2020). Interestingly, Cai et al. detected a downregulation of circulating miR-212 in TLE patients (Cai et al., 2020), whereas Huang et al. reported increased circulating miR-132 levels at 2 h after seizure onset in epilepsy patients (Huang et al., 2022). Furthermore, there are several studies which have investigated miR-124 expression in epilepsy; three reported a downregulation of miR-124 in rat hippocampus after SE induction by kainic acid (Brennan et al., 2016; Ambrogini et al., 2018) or amygdala stimulation (Vuokila et al., 2018). In contrast, an upregulation of miR-124 in rat hippocampus was described by two research groups where the SE had been induced by administration of pilocarpine (Hu et al., 2011; Peng et al., 2013).

With respect to the 4 remaining miRNAs, miR-9, miR-323, miR-434, and miR-136, little information exists on their expression in the context of epilepsy. Brennan et al. (2016) did not detect changes in miR-9 expression in rat hippocampus after SE. An upregulation of miR-323 was observed in miRNA screening of mouse hippocampus after SE by Jimenez-Mateos et al. (2011), but miR-323 was not subjected to a further validation by PCR. Increased levels of miR-434 were reported in mouse blood after pilocarpine-induced SE (Chen et al., 2020). Finally, a downregulation of miR-136 was detected in the rat hippocampus after pilocarpine-induced SE (Cui & Zhang, 2022). Alterations in miR-124, miR-9, miR-323, and miR-136 levels in patients with epilepsy remain to be investigated.

To the best of our knowledge, this study was the first to investigate the expression of circulating miRNAs in a PTE model. Although alterations in the expression of some miRNAs, especially miR-132 and miR-212, have been previously linked to epileptogenesis in experimental models in which epileptogenesis has been induced by chemoconvulsants or electrical stimulation, none of the circulating miRNAs examined here were useful in

the prediction of post-TBI epileptogenesis. One explanation could be that the alterations in miRNA expression are specific to the different epileptogenesis etiologies. In addition, the possible alterations in miRNA expression in the brain during epileptogenesis may be too small to allow for their detection in blood. We investigated samples from acute (day 2) and subacute (day 9) time-points after injury in order to discover circulating miRNAs that would predict the subsequent development of PTE at an early post-injury time-point. On the other hand, the time-point at which PTE develops after TBI is variable, and it is not known exactly when the epileptogenic process starts before there is the appearance of late seizures. It remains to be clarified whether a different post-TBI time-point would be more optimal for the circulating miRNA analysis for the identification of potential biomarkers of post-TBI epileptogenesis.

6.3 CIRCULATING NF-L PREDICTS THE EVOLUTION OF CORTICAL DAMAGE BUT NOT COGNITIVE IMPAIRMENT OR EPILEPTOGENESIS

Several circulating protein biomarkers exist for TBI but no biomarkers have been discovered for PTE (Agoston & Kamnaksh, 2019; Pitkänen et al., 2021). Previously, it has been demonstrated that the levels of NF-L in blood and CSF are associated with TBI severity and can be used in the prediction of the clinical outcome after the injury (Al Nimer et al., 2015; Shahim et al., 2016, 2020; Ljungqvist et al., 2017; Thelin et al., 2019). It has not been previously investigated whether circulating NF-L levels can predict the development of PTE. The aim of our study was to determine the levels of NF-L in rat plasma after LFPI-induced TBI, and to clarify whether the NF-L levels could act as a biomarker for predicting the structural and behavioural outcomes as well as the appearance of epileptogenesis after the injury.

A 483-fold increase in the plasma NF-L concentration was observed on D2 after TBI as compared to the baseline samples. The mean concentration on D2 was around 5000 pg/ml, which is in line with the NF-L levels reported

on D2 post-TBI in another rat study (Wong et al., 2021). By D9, NF-L levels had declined to around 900 pg/ml, which was still 89-fold higher than the baseline. The temporal profile of NF-L levels detected here were comparable to those described in a rat study which examined NF-L levels after a mild TBI, in which the serum NF-L levels peaked on 1 d after the injury, and though they subsequently decreased, they remained elevated at 14 d after the injury (O'Brien et al., 2021). In our study, around a 3-fold increase in plasma NF-L levels was observed as long as 6 months after a severe TBI when compared to the baseline values. In another study, elevated levels of serum NF-L at 4 months after injury were reported in 50% of rats exposed to a blast overpressure injury (Dickstein et al., 2020). The elevated NF-L levels at a late time-point after an injury point to an ongoing chronic release of NF-L into the systemic circulation from the injured brain. In humans, elevated blood NF-L levels were reported as long as 5 years after a TBI (Shahim et al., 2020). In another study, blood NF-L levels were increased at 8 months but not >5 years post-TBI, however, higher NF-L levels around the 8-month time-point predicted a brain white matter volume loss at later time-points (Newcombe et al., 2022). Interestingly, the time scale and the magnitude of change in circulating NF-L levels after TBI seem to differ between rats and humans. In humans, NF-L levels were reported to peak in serum at 10–12 d after a severe TBI with a concentration of around 2000 pg/ml (Shahim et al., 2016), whereas in our study, the NF-L levels had declined by D9 to only 18% of those assayed on D2 (900 pg/ml vs. 5000 pg/ml).

There are clinical studies which have suggested circulating NF-L to be a potential diagnostic biomarker for mild and severe TBI (Shahim et al., 2016; 2020a). New diagnostic biomarkers would be especially useful for mild TBI, as mild TBI often remains undetected in a CT scan (Maas et al., 2022). In our study, plasma NF-L levels on D2 after an injury differentiated severe TBI rats from the baseline samples and from sham-operated controls with 100% sensitivity and 100% specificity. A similar performance was reported earlier for serum NF-L in a model of moderate TBI (Wong et al., 2021). Importantly, we found that the craniotomy performed in sham-operated

rats increased plasma NF-L levels from an average 9.6 pg/ml to 244 pg/ml, which was around a 25-fold difference. A concentration cut-off of 49 pg/ml differentiated sham-operated controls from baseline samples with 100% sensitivity and 100% specificity. MRI analysis detected mild T₂ relaxation abnormalities in the sham-operated controls. The results suggest that craniotomy causes a subtle axonal injury that is detected as increased circulating NF-L levels, indicating that NF-L is a sensitive marker for a mild injury.

One aim of the study was to determine whether circulating NF-L levels could predict the structural outcome after the TBI. It was found that higher plasma NF-L levels on D2 after the TBI were reflected in a larger volume of abnormal T₂ in the MRI analysis on the same day. In contrast, the NF-L levels on D2 did not predict lesion volume in MRI at later time points (D7 or D21). This was not surprising, as a previous study from our laboratory reported that the volume of abnormal cortical T₂ decreased significantly from D2 to D7 and then slightly increased from D7 to D21 (Manninen et al., 2020). On the other hand, we found that the higher plasma NF-L levels on D2 and D9 correlated with a larger cortical lesion area in a histological analysis conducted at 6 months after the TBI. Taken together, the results suggest that circulating NF-L levels when assessed at an acute post-injury time-point reflect the injury severity after LFPI-induced TBI and may predict the progression of the cortical lesion at more chronic time-points.

In addition to the structural outcome, we examined whether circulating NF-L levels reflected somatomotor impairment and recovery after TBI. Previous studies on single or repeated mild TBI have reported that higher serum NF-L levels at the acute post-TBI time-point are associated with a poorer performance in the beam-walking test soon after the injury (O'Brien et al., 2021; Pham et al., 2021). In our study, higher NF-L levels on D2 after severe TBI correlated with a more severe impairment in the neuroscore test on the same day but did not predict the somatomotor performance on subsequent time points. Furthermore, we investigated whether NF-L levels at an acute post-TBI time-point would be able to predict the development of a cognitive impairment. Previously, an association has been described

between high NF-L levels and cognitive impairment in neurodegenerative diseases (Mattsson et al., 2017; Lin et al., 2019; Mattioli et al., 2020; Zhu et al., 2021). In the LFP-induced TBI model, TBI rats have been shown to experience long-lasting deficits in hippocampus-dependent memory (Thompson et al., 2006). Furthermore, it is known that TBI induces the death of interneurons and hippocampal principal cells, and the rats also suffer from a hippocampal atrophy (Pitkänen and McIntosh, 2006; Huusko et al., 2015; Sierra et al., 2015). In contrast to our expectations, plasma NF-L levels after TBI did not distinguish between those rats with and those without signs of a cognitive impairment at 37 d after the injury.

To the best of our knowledge, circulating NF-L levels have not been previously investigated in PTE models or in patients with PTE. Unfortunately, no differences were detected in the plasma NF-L levels between the rats with or without PTE at any time-point, indicating that circulating NF-L levels would be of little value in predicting the appearance of epileptogenesis after a TBI. Previously, it has been reported that there was a very small elevation in plasma NF-L levels in patients with post-stroke epilepsy in comparison to patients who had experienced a single seizure (Eriksson et al., 2021). Furthermore, a retrospective study conducted by Giovannini and colleagues detected increased serum NF-L levels in patients with SE as compared to epilepsy patients or healthy controls (Giovannini et al., 2021). They reported that NF-L levels were higher in patients with refractory epilepsy than in those with drug-responsive epilepsy, and higher NF-L levels associated with a worse clinical outcome. Increased serum NF-L levels in drug-refractory epilepsy patients were also evident in another study (Ouédraogo et al., 2021). In contrast, elevated serum NF-L levels in autoimmune epilepsy were reported to be attributable to the older age of the patients rather than the disease (Nass et al., 2021a). Interestingly, another study by Nass and colleagues described a small and statistically non-significant (< 1 pg/ml) increase in serum NF-L levels immediately after a tonic-clonic seizure (Nass et al., 2021b). Of the 13 TBI+ rats in our study, 3 had experienced a seizure on the day before blood sampling at the 6-month time-point. Plasma NF-L levels

in these rats did not differ from the other rats, indicating that the seizure did not have a measurable effect on the circulating NF-L levels on the following day. Taken together, it does seem that circulating NF-L levels reflected the injury severity and predicted structural outcome at chronic time points. In contrast, the NF-L levels did not predict the signs of a cognitive impairment or the development of epileptogenesis.

7 CONCLUSIONS

This study aimed to identify miRNA and protein biomarkers in the systemic circulation to evaluate TBI severity and predict post-traumatic epileptogenesis in an experimental PTE model. The study also evaluated the performance of a precipitation-based method to isolate circulating EV from rat plasma for subsequent analysis of EV-associated miRNAs. The key findings of this thesis can be summarized as follows:

1. During the isolation of EVs from rat plasma by a precipitation-based method, circulating lipoproteins and other plasma proteins are co-precipitated into the EV pellet. As a result, the precipitated EV pellet does not contain solely EV-associated miRNAs as there are also vesicle-free miRNAs, such as the miRNAs carried by Ago2.
2. Circulating miR-124-3p is carried by proteins rather than EVs in naïve rat plasma.
3. Elevated levels of miR-9a-3p, miR-124-3p, miR-323-3p, miR-434-3p, miR-136-3p, miR-132-3p, and miR-212-3p in rat plasma at 2 d after an injury can differentiate TBI rats from sham-operated or naïve controls.
4. Elevated levels of miR-9a-3p, miR-323-3p, miR-434-3p, miR-136-3p, miR-132-3p, and miR-212-3p differentiate sham-operated rats from naïve controls, suggesting that they may represent potential markers for mild TBI.
5. Higher expression levels of miR-9a-3p, miR-124-3p, miR-323-3p, miR-434-3p, miR-136-3p and miR-132-3p 2 d after TBI are associated with a larger cortical lesion at acute, subacute, and chronic time-points.
6. The circulating miRNA signature at 2 d or 9 d after TBI does not predict the development of post-traumatic epileptogenesis.
7. Plasma NF-L levels, when assayed at 2 d after the injury, are able to differentiate between TBI/sham/naïve groups. Furthermore, the NF-L levels remain slightly increased even 6 months after TBI.

8. Higher plasma NF-L levels 2 d after TBI associate with a larger cortical lesion at acute and chronic post-injury time-points.
9. Plasma NF-L levels 2 d after TBI cannot predict the somatomotor recovery, cognitive impairment or post-traumatic epileptogenesis.

To summarize, due to the low EV yield and the co-precipitation of lipoproteins and other plasma proteins during the preparation of the EVs, a precipitation-based method is not optimal for EV isolation from rat plasma. An analysis of total circulating miRNAs in rat plasma after a lateral FPI-induced TBI identified a set of elevated miRNAs that could differentiate injured animals from controls and furthermore they were associated with the severity of the cortical lesion. Especially, circulating miR-323-3p, miR-132-3p, and miR-212-3p warrant further studies in patients with TBI; in fact, miR-323-3p and miR-212-3p have not previously investigated in TBI, and very little information is available on the properties of miR-132-3p. In addition to the miRNAs, elevated levels of NF-L in the systemic circulation were also found to associate with a larger cortical lesion. However, neither the miRNA signature nor the NF-L levels could predict the development of post-traumatic epileptogenesis.

REFERENCES

- Agoston, D. V., & Kamnaksh, A. (2019). Protein biomarkers of epileptogenicity after traumatic brain injury. *Neurobiology of Disease*, 123, 59–68. <https://doi.org/10.1016/j.nbd.2018.07.017>
- Agrawal, A., Timothy, J., Pandit, L., & Manju, M. (2006). Post-traumatic epilepsy: An overview. *Clinical Neurology and Neurosurgery*, 108(5), 433–439. <https://doi.org/https://doi.org/10.1016/j.clineuro.2005.09.001>
- Al Nimer, F., Thelin, E., Nyström, H., Dring, A. M., Svenningsson, A., Piehl, F., Nelson, D. W., & Bellander, B. M. (2015). Comparative assessment of the prognostic value of biomarkers in traumatic brain injury reveals an independent role for serum levels of neurofilament light. *PLoS ONE*, 10(7), 1–19. <https://doi.org/10.1371/journal.pone.0132177>
- Alvarez-Erviti, L., Seow, Y., Yin, H., Betts, C., Lakhai, S., & Wood, M. J. A. (2011). Delivery of siRNA to the mouse brain by systemic injection of targeted exosomes. *Nature Biotechnology*, 29(4), 341–345. <https://doi.org/10.1038/nbt.1807>
- Ambrogini, P., Albertini, M. C., Betti, M., Galati, C., Lattanzi, D., Savelli, D., Di Palma, M., Saccomanno, S., Bartolini, D., Torquato, P., Ruffolo, G., Olivieri, F., Galli, F., Palma, E., Minelli, A., & Cuppini, R. (2018). Neurobiological Correlates of Alpha-Tocopherol Antiepileptogenic Effects and MicroRNA Expression Modulation in a Rat Model of Kainate-Induced Seizures. *Molecular Neurobiology*, 55(10), 7822–7838. <https://doi.org/10.1007/s12035-018-0946-7>
- An, N., Zhao, W., Liu, Y., Yang, X., & Chen, P. (2016). Elevated serum miR-106b and miR-146a in patients with focal and generalized epilepsy. *Epilepsy Research*, 127, 311–316. <https://doi.org/10.1016/j.eplepsyres.2016.09.019>
- Anderson, R. E., Hansson, L. O., Nilsson, O., Dijlai-Merzoug, R., & Settergren, G. (2001). High serum S100B levels for trauma patients without head injuries. *Neurosurgery*, 48(6), 1255–1260. <https://doi.org/10.1097/00006123-200106000-00012>

- Anderson, T. N., Hwang, J., Munar, M., Papa, L., Hinson, H. E., Vaughan, A., & Rowell, S. E. (2020). Blood-based biomarkers for prediction of intracranial hemorrhage and outcome in patients with moderate or severe traumatic brain injury. *Journal of Trauma and Acute Care Surgery*, *89*(1), 80–86. <https://doi.org/10.1097/TA.0000000000002706>
- Andrade, P., Nissinen, J., & Pitkänen, A. (2017). Generalized Seizures after Experimental Traumatic Brain Injury Occur at the Transition from Slow-Wave to Rapid Eye Movement Sleep. *Journal of Neurotrauma*, *34*(7), 1482–1487. <https://doi.org/10.1089/neu.2016.4675>
- Annegers, J. F., Hauser, W. A., Coan, S. P., & Rocca, W. A. (1998). A population-based study of seizures after traumatic brain injuries. *The New England Journal of Medicine*, *338*(1), 20–24. <https://doi.org/10.1056/NEJM199801013380104>
- Antônio, L. G. L., Freitas-Lima, P., Pereira-da-Silva, G., Assirati, J. A. J., Matias, C. M., Cirino, M. L. A., Tirapelli, L. F., Velasco, T. R., Sakamoto, A. C., Carlotti, C. G. J., & Tirapelli, D. P. da C. (2019). Expression of MicroRNAs miR-145, miR-181c, miR-199a and miR-1183 in the Blood and Hippocampus of Patients with Mesial Temporal Lobe Epilepsy. *Journal of Molecular Neuroscience : MN*, *69*(4), 580–587. <https://doi.org/10.1007/s12031-019-01386-w>
- Arroyo, J. D., Chevillet, J. R., Kroh, E. M., Ruf, I. K., Pritchard, C. C., Gibson, D. F., Mitchell, P. S., Bennett, C. F., Pogosova-Agadjanyan, E. L., Stirewalt, D. L., Tait, J. F., & Tewari, M. (2011). Argonaute2 complexes carry a population of circulating microRNAs independent of vesicles in human plasma. *Proceedings of the National Academy of Sciences of the United States of America*, *108*(12), 5003–5008. <https://doi.org/10.1073/pnas.1019055108>
- Asadollahi, M., & Simani, L. (2019). The diagnostic value of serum UCHL-1 and S100-B levels in differentiate epileptic seizures from psychogenic attacks. *Brain Research*, *1704*(July 2018), 11–15. <https://doi.org/10.1016/j.brainres.2018.09.028>

- Atif, H., & Hicks, S. D. (2019). A Review of MicroRNA Biomarkers in Traumatic Brain Injury. *Journal of Experimental Neuroscience*, *13*, 1179069519832286. <https://doi.org/10.1177/1179069519832286>
- Avansini, S. H., de Sousa Lima, B. P., Secolin, R., Santos, M. L., Coan, A. C., Vieira, A. S., Torres, F. R., Carvalho, B. S., Alvim, M. K. M., Morita, M. E., Yasuda, C. L., Pimentel-Silva, L. R., Dogini, D. B., Rogerio, F., Cendes, F., & Lopes-Cendes, I. (2017). MicroRNA hsa-miR-134 is a circulating biomarker for mesial temporal lobe epilepsy. *PloS One*, *12*(4), e0173060. <https://doi.org/10.1371/journal.pone.0173060>
- Balakathiresan, N., Bhomia, M., Chandran, R., Chavko, M., McCarron, R. M., & Maheshwari, R. K. (2012). MicroRNA let-7i is a promising serum biomarker for blast-induced traumatic brain injury. *Journal of Neurotrauma*, *29*(7), 1379–1387. <https://doi.org/10.1089/neu.2011.2146>
- Balakathiresan, N. S., Bhomia, M., Gupta, P., Chandran, R., Sharma, A., & Maheshwari, R. K. (2015). *MicroRNAs as Brain Injury Biomarker BT - General Methods in Biomarker Research and their Applications* (V. R. Preedy & V. B. Patel, Eds.; pp. 1081–1112). Springer Netherlands. https://doi.org/10.1007/978-94-007-7696-8_6
- Banote, R. K., Akel, S., & Zelano, J. (2022). Blood biomarkers in epilepsy. *Acta Neurologica Scandinavica*, *146*(4), 362–368. <https://doi.org/10.1111/ane.13616>
- Bazarian, J. J., Biberthaler, P., Welch, R. D., Lewis, L. M., Barzo, P., Bogner-Flatz, V., Gunnar Brolinson, P., Büki, A., Chen, J. Y., Christenson, R. H., Hack, D., Huff, J. S., Johar, S., Jordan, J. D., Leidel, B. A., Lindner, T., Ludington, E., Okonkwo, D. O., Ornato, J., ... Jagoda, A. S. (2018). Serum GFAP and UCH-L1 for prediction of absence of intracranial injuries on head CT (ALERT-TBI): a multicentre observational study. *The Lancet Neurology*, *17*(9), 782–789. [https://doi.org/10.1016/S1474-4422\(18\)30231-X](https://doi.org/10.1016/S1474-4422(18)30231-X)
- Benayas, B., Morales, J., Egea, C., Armisén, P., & Yáñez-Mó, M. (2023). Optimization of extracellular vesicle isolation and their separation

- from lipoproteins by size exclusion chromatography. *Journal of Extracellular Biology*, 2(7). <https://doi.org/10.1002/jex2.100>
- Bencurova, P., Baloun, J., Hynst, J., Oppelt, J., Kubova, H., Pospisilova, S., & Brazdil, M. (2021). Dynamic miRNA changes during the process of epileptogenesis in an infantile and adult-onset model. *Scientific Reports*, 11(1), 9649. <https://doi.org/10.1038/s41598-021-89084-9>
- Bhomia, M., Balakathiresan, N. S., Wang, K. K., Papa, L., & Maheshwari, R. K. (2016). A Panel of Serum MiRNA Biomarkers for the Diagnosis of Severe to Mild Traumatic Brain Injury in Humans. *Scientific Reports*, 6, 28148. <https://doi.org/10.1038/srep28148>
- Bishop, P., Rocca, D., & Henley, J. M. (2016). Ubiquitin C-Terminal hydrolase L1 (UCH-L1): Structure, distribution and roles in brain function and dysfunction. *Biochemical Journal*, 473(16), 2453–2462. <https://doi.org/10.1042/BCJ20160082>
- Bogoslovsky, T., Gill, J., Jeromin, A., Davis, C., & Diaz-Arrastia, R. (2016). Fluid biomarkers of traumatic brain injury and intended context of use. *Diagnostics*, 6(4), 1–22. <https://doi.org/10.3390/diagnostics6040037>
- Böing, A. N., van der Pol, E., Grootemaat, A. E., Coumans, F. A. W., Sturk, A., & Nieuwland, R. (2014). Single-step isolation of extracellular vesicles by size-exclusion chromatography. *Journal of Extracellular Vesicles*, 3(1). <https://doi.org/10.3402/jev.v3.23430>
- Bolkvadze, T., & Pitkänen, A. (2012). Development of post-traumatic epilepsy after controlled cortical impact and lateral fluid-percussion-induced brain injury in the mouse. *Journal of Neurotrauma*, 29(5), 789–812. <https://doi.org/10.1089/neu.2011.1954>
- Bot, A. M., Dębski, K. J., & Lukasiuk, K. (2013). Alterations in miRNA levels in the dentate gyrus in epileptic rats. *PloS One*, 8(10), e76051. <https://doi.org/10.1371/journal.pone.0076051>
- Brady, R. D., Casillas-Espinosa, P. M., Agoston, D. V, Bertram, E. H., Kamnaksh, A., Semple, B. D., & Shultz, S. R. (2019). Modelling traumatic brain injury and posttraumatic epilepsy in rodents. *Neurobiology of Disease*, 123, 8–19. <https://doi.org/10.1016/j.nbd.2018.08.007>

- Bragin, A., Li, L., Almajano, J., Alvarado-Rojas, C., Reid, A. Y., Staba, R. J., & Engel, J. J. (2016). Pathologic electrographic changes after experimental traumatic brain injury. *Epilepsia*, *57*(5), 735–745.
<https://doi.org/10.1111/epi.13359>
- Brennan, G. P., Bauer, S., Engel, T., Jimenez-Mateos, E. M., Del Gallo, F., Hill, T. D. M., Connolly, N. M. C., Costard, L. S., Neubert, V., Salvetti, B., Sanz-Rodriguez, A., Heiland, M., Mamad, O., Brindley, E., Norwood, B., Batool, A., Raoof, R., El-Naggar, H., Reschke, C. R., ... Henshall, D. C. (2020). Genome-wide microRNA profiling of plasma from three different animal models identifies biomarkers of temporal lobe epilepsy. *Neurobiology of Disease*, *144*, 105048.
<https://doi.org/10.1016/j.nbd.2020.105048>
- Brennan, G. P., Dey, D., Chen, Y., Patterson, K. P., Magnosta, E. J., Hall, A. M., Dube, C. M., Mei, Y.-T., & Baram, T. Z. (2016). Dual and Opposing Roles of MicroRNA-124 in Epilepsy Are Mediated through Inflammatory and NRSF-Dependent Gene Networks. *Cell Reports*, *14*(10), 2402–2412.
<https://doi.org/10.1016/j.celrep.2016.02.042>
- Brennan, G. P., & Henshall, D. C. (2020). MicroRNAs as regulators of brain function and targets for treatment of epilepsy. *Nature Reviews. Neurology*, *16*(9), 506–519. <https://doi.org/10.1038/s41582-020-0369-8>
- Brennan, K., Martin, K., FitzGerald, S. P., O'Sullivan, J., Wu, Y., Blanco, A., Richardson, C., & Mc Gee, M. M. (2020). A comparison of methods for the isolation and separation of extracellular vesicles from protein and lipid particles in human serum. *Scientific Reports*, *10*(1), 1–13.
<https://doi.org/10.1038/s41598-020-57497-7>
- Buschmann, D., Kirchner, B., Hermann, S., Märte, M., Wurmser, C., Brandes, F., Kotschote, S., Bonin, M., Steinlein, O. K., Pfaffl, M. W., Schelling, G., & Reithmair, M. (2018). Evaluation of serum extracellular vesicle isolation methods for profiling miRNAs by next-generation sequencing. *Journal of Extracellular Vesicles*, *7*(1), 1481321.
<https://doi.org/https://doi.org/10.1080/20013078.2018.1481321>
- Bushel, P. R., Caiment, F., Wu, H., O'Lone, R., Day, F., Calley, J., Smith, A., & Li, J. (2018). RATEmiRs: the rat atlas of tissue-specific and enriched

- miRNAs database. *BMC Genomics*, 19(1), 825.
<https://doi.org/10.1186/s12864-018-5220-x>
- Cai, X., Long, L., Zeng, C., Ni, G., Meng, Y., Guo, Q., Chen, Z., & Li, Z. (2020). LncRNA ILF3-AS1 mediated the occurrence of epilepsy through suppressing hippocampal miR-212 expression. *Aging*, 12(9), 8413–8422. <https://doi.org/10.18632/aging.103148>
- Carroll, L. J., Cassidy, J. D., Peloso, P. M., Borg, J., von Holst, H., Holm, L., Paniak, C., & Pépin, M. (2004). Prognosis for mild traumatic brain injury: Results of the WHO Collaborating Centre Task Force on Mild Traumatic Brain Injury. *Journal of Rehabilitation Medicine, Supplement*, 43, 84–105. <https://doi.org/10.1080/16501960410023859>
- Cassidy, J. D., Carroll, L. J., Peloso, P. M., Borg, J., von Holst, H., Holm, L., Kraus, J., & Coronado, V. G. (2004). Incidence, risk factors and prevention of mild traumatic brain injury: Results of the WHO Collaborating Centre Task Force on Mild Traumatic Brain Injury. *Journal of Rehabilitation Medicine, Supplement*, 43, 28–60. <https://doi.org/10.1080/16501960410023732>
- Çevik, S., Özgenç, M. M., Güneyk, A., Evran, Ş., Akkaya, E., Çalış, F., Katar, S., Soyalp, C., Hanımoğlu, H., & Kaynar, M. Y. (2019). NRG1, S100B and GFAP levels are significantly increased in patients with structural lesions resulting from mild traumatic brain injuries. *Clinical Neurology and Neurosurgery*, 183(November 2018), 105380. <https://doi.org/10.1016/j.clineuro.2019.105380>
- Chen, M., Zhao, Q.-Y., Edson, J., Zhang, Z. H., Li, X., Wei, W., Bredy, T., & Reutens, D. C. (2020). Genome-wide microRNA profiling in brain and blood samples in a mouse model of epileptogenesis. *Epilepsy Research*, 166, 106400. <https://doi.org/10.1016/j.eplepsyres.2020.106400>
- Chen, Y., Yu, H., Zhu, D., Liu, P., Yin, J., Liu, D., Zheng, M., Gao, J., Zhang, C., & Gao, Y. (2020). miR-136-3p targets PTEN to regulate vascularization and bone formation and ameliorates alcohol-induced osteopenia. *FASEB Journal: Official Publication of the Federation of American Societies for Experimental Biology*, 34(4), 5348–5362. <https://doi.org/10.1096/fj.201902463RR>

- Christensen, J. (2015). The epidemiology of posttraumatic epilepsy. *Seminars in Neurology*, 35(3), 218–222. <https://doi.org/10.1055/s-0035-1552923>
- Cole, J. T., Yarnell, A., Kean, W. S., Gold, E., Lewis, B., Ren, M., McMullen, D. C., Jacobowitz, D. M., Pollard, H. B., O'Neill, J. T., Grunberg, N. E., Dalgard, C. L., Frank, J. A., & Watson, W. D. (2011). Craniotomy: true sham for traumatic brain injury, or a sham of a sham? *Journal of Neurotrauma*, 28(3), 359–369. <https://doi.org/10.1089/neu.2010.1427>
- Colombo, M., Raposo, G., & Théry, C. (2014). Biogenesis, secretion, and intercellular interactions of exosomes and other extracellular vesicles. *Annual Review of Cell and Developmental Biology*, 30, 255–289. <https://doi.org/10.1146/annurev-cellbio-101512-122326>
- Condrat, C. E., Thompson, D. C., Barbu, M. G., Bugnar, O. L., Boboc, A., Cretoiu, D., Suci, N., Cretoiu, S. M., & Voinea, S. C. (2020). miRNAs as Biomarkers in Disease: Latest Findings Regarding Their Role in Diagnosis and Prognosis. *Cells*, 9(2). <https://doi.org/10.3390/cells9020276>
- Coolen, M., Katz, S., & Bally-Cuif, L. (2013). miR-9: a versatile regulator of neurogenesis. *Frontiers in Cellular Neuroscience*, 7, 220. <https://doi.org/10.3389/fncel.2013.00220>
- Cui, H., & Zhang, W. (2022). The Neuroprotective Effect of miR-136 on Pilocarpine-Induced Temporal Lobe Epilepsy Rats by Inhibiting Wnt/ β -Catenin Signaling Pathway. *Computational and Mathematical Methods in Medicine*, 2022, 1938205. <https://doi.org/10.1155/2022/1938205>
- Daneshvar, D. H., Riley, D. O., Nowinski, C. J., McKee, A. C., Stern, R. A., & Cantu, R. C. (2011). Long-term consequences: effects on normal development profile after concussion. *Physical Medicine and Rehabilitation Clinics of North America*, 22(4), 683–700, ix. <https://doi.org/10.1016/j.pmr.2011.08.009>
- Das Gupta, S., Cizek, R., Heiskanen, M., Lapinlampi, N., Kukkonen, J., Leinonen, V., Puhakka, N., & Pitkänen, A. (2021). Plasma miR-9-3p and miR-136-3p as Potential Novel Diagnostic Biomarkers for Experimental

- and Human Mild Traumatic Brain Injury. *International Journal of Molecular Sciences*, 22(4). <https://doi.org/10.3390/ijms22041563>
- De Benedittis, S., Fortunato, F., Cava, C., Gallivanone, F., Iaccino, E., Caligiuri, M. E., Castiglioni, I., Bertoli, G., Manna, I., Labate, A., & Gambardella, A. (2021). Circulating microRNA: The Potential Novel Diagnostic Biomarkers to Predict Drug Resistance in Temporal Lobe Epilepsy, a Pilot Study. *International Journal of Molecular Sciences*, 22(2). <https://doi.org/10.3390/ijms22020702>
- Denli, A. M., Tops, B. B. J., Plasterk, R. H. A., Ketting, R. F., & Hannon, G. J. (2004). Processing of primary microRNAs by the Microprocessor complex. *Nature*, 432(7014), 231–235. <https://doi.org/10.1038/nature03049>
- Devoto, C., Lai, C., Qu, B.-X., Guedes, V. A., Leete, J., Wilde, E., Walker, W. C., Diaz-Arrastia, R., Kenney, K., & Gill, J. (2020). Exosomal MicroRNAs in Military Personnel with Mild Traumatic Brain Injury: Preliminary Results from the Chronic Effects of Neurotrauma Consortium Biomarker Discovery Project. *Journal of Neurotrauma*, 37(23), 2482–2492. <https://doi.org/10.1089/neu.2019.6933>
- Dewan, M. C., Rattani, A., Gupta, S., Baticulon, R. E., Hung, Y. C., Punchak, M., Agrawal, A., Adeleye, A. O., Shrimel, M. G., Rubiano, A. M., Rosenfeld, J. V., & Park, K. B. (2019). Estimating the global incidence of traumatic brain injury. *Journal of Neurosurgery*, 130(4), 1080–1097. <https://doi.org/10.3171/2017.10.JNS17352>
- Di Battista, A. P., Buonora, J. E., Rhind, S. G., Hutchison, M. G., Baker, A. J., Rizoli, S. B., Diaz-Arrastia, R., & Mueller, G. P. (2015). Blood biomarkers in moderate-to-severe traumatic brain injury: Potential utility of a multi-marker approach in characterizing outcome. *Frontiers in Neurology*, 6(MAY), 1–9. <https://doi.org/10.3389/fneur.2015.00110>
- Di Pietro, V., Ragusa, M., Davies, D., Su, Z., Hazeldine, J., Lazzarino, G., Hill, L. J., Crombie, N., Foster, M., Purrello, M., Logan, A., & Belli, A. (2017). MicroRNAs as Novel Biomarkers for the Diagnosis and Prognosis of Mild and Severe Traumatic Brain Injury. *Journal of Neurotrauma*, 34(11), 1948–1956. <https://doi.org/10.1089/neu.2016.4857>

- Di Pietro, V., Yakoub, K. M., Scarpa, U., Di Pietro, C., & Belli, A. (2018). MicroRNA Signature of Traumatic Brain Injury: From the Biomarker Discovery to the Point-of-Care. *Frontiers in Neurology*, 9, 429. <https://doi.org/10.3389/fneur.2018.00429>
- Diaz-Arrastia, R., Wang, K. K. W., Papa, L., Sorani, M. D., Yue, J. K., Puccio, A. M., McMahon, P. J., Inoue, T., Yuh, E. L., Lingsma, H. F., Maas, A. I. R., Valadka, A. B., Okonkwo, D. O., Manley, G. T., Casey, I. S. S., Cheong, M., Cooper, S. R., Dams-O'Connor, K., Gordon, W. A., ... Vassar, M. J. (2014). Acute biomarkers of traumatic brain injury: Relationship between plasma levels of ubiquitin C-terminal hydrolase-11 and glial fibrillary acidic protein. *Journal of Neurotrauma*, 31(1), 19–25. <https://doi.org/10.1089/neu.2013.3040>
- Dickstein, D. L., De Gasperi, R., Gama Sosa, M. A., Perez-Garcia, G., Short, J. A., Sosa, H., Perez, G. M., Tschiffely, A. E., Dams-O'Connor, K., Pullman, M. Y., Knesaurek, K., Knutsen, A., Pham, D. L., Soleimani, L., Jordan, B. D., Gordon, W. A., Delman, B. N., Shumyatsky, G., Shahim, P. P., ... Elder, G. A. (2020). Brain and blood biomarkers of tauopathy and neuronal injury in humans and rats with neurobehavioral syndromes following blast exposure. *Molecular Psychiatry*. <https://doi.org/10.1038/s41380-020-0674-z>
- Ding, M., Wang, C., Lu, X., Zhang, C., Zhou, Z., Chen, X., Zhang, C.-Y., Zen, K., & Zhang, C. (2018). Comparison of commercial exosome isolation kits for circulating exosomal microRNA profiling. *Analytical and Bioanalytical Chemistry*, 410(16), 3805–3814. <https://doi.org/10.1007/s00216-018-1052-4>
- Dixon, C. E., Clifton, G. L., Lighthall, J. W., Yaghmai, A. A., & Hayes, R. L. (1991). A controlled cortical impact model of traumatic brain injury in the rat. *Journal of Neuroscience Methods*, 39(3), 253–262. [https://doi.org/10.1016/0165-0270\(91\)90104-8](https://doi.org/10.1016/0165-0270(91)90104-8)
- Dixon, K. J. (2017). Pathophysiology of Traumatic Brain Injury. *Physical Medicine and Rehabilitation Clinics of North America*, 28(2), 215–225. <https://doi.org/10.1016/j.pmr.2016.12.001>

- Dong, L., Zieren, R. C., Horie, K., Kim, C. J., Mallick, E., Jing, Y., Feng, M., Kuczler, M. D., Green, J., Amend, S. R., Witwer, K. W., de Reijke, T. M., Cho, Y. K., Pienta, K. J., & Xue, W. (2020). Comprehensive evaluation of methods for small extracellular vesicles separation from human plasma, urine and cell culture medium. *Journal of Extracellular Vesicles*, *10*(2). <https://doi.org/10.1002/jev2.12044>
- El Andaloussi, S., Mäger, I., Breakefield, X. O., & Wood, M. J. A. (2013). Extracellular vesicles: Biology and emerging therapeutic opportunities. *Nature Reviews Drug Discovery*, *12*(5), 347–357. <https://doi.org/10.1038/nrd3978>
- Elnady, H. G., Abdelmoneam, N., Eissa, E., Hamid, E. R. A., Zeid, D. A., Abo-Shanab, A. M., Atta, H., & Kholoussi, N. M. (2019). MicroRNAs as Potential Biomarkers for Childhood Epilepsy. *Open Access Macedonian Journal of Medical Sciences*, *7*(23), 3965–3969. <https://doi.org/10.3889/oamjms.2019.634>
- Engel, J., Pitkanen, A., Loeb, J. A., Dudek, F. E., Bertram, E. H., Cole, A. J., Moshé, S. L., Wiebe, S., Jensen, F. E., Mody, I., Nehlig, A., & Vezzani, A. (2013). Epilepsy biomarkers. *Epilepsia*, *54*(SUPPL.4), 61–69. <https://doi.org/10.1111/epi.12299>
- Englander, J., Bushnik, T., Duong, T. T., Cifu, D. X., Zafonte, R., Wright, J., Hughes, R., & Bergman, W. (2003). Analyzing risk factors for late posttraumatic seizures: A prospective, multicenter investigation. *Archives of Physical Medicine and Rehabilitation*, *84*(3 SUPPL. 1), 365–373. <https://doi.org/10.1053/apmr.2003.50022>
- Enright, N., Simonato, M., & Henshall, D. C. (2018). Discovery and validation of blood microRNAs as molecular biomarkers of epilepsy: Ways to close current knowledge gaps. *Epilepsia Open*, *3*(4), 427–436. <https://doi.org/10.1002/epi4.12275>
- Eriksson, H., Banote, R. K., Larsson, D., Blennow, K., Zetterberg, H., & Zelano, J. (2021). Brain injury markers in new-onset seizures in adults: A pilot study. *Seizure*, *92*, 62–67. <https://doi.org/10.1016/j.seizure.2021.08.012>

- FDA-NIH Biomarker Working Group. (2016). *BEST (Biomarkers, Endpoints, and other Tools) Resource*. Food and Drug Administration (US).
<https://www.ncbi.nlm.nih.gov/books/NBK326791/>
- Fiori, L. M., Kos, A., Lin, R., Th eroux, J.-F., Lopez, J. P., K uhne, C., Eggert, C., Holzapfel, M., Huettl, R.-E., Mechawar, N., Belzung, C., Ibrahim, E. C., Chen, A., & Turecki, G. (2021). miR-323a regulates ERBB4 and is involved in depression. *Molecular Psychiatry*, 26(8), 4191–4204.
<https://doi.org/10.1038/s41380-020-00953-7>
- Fox, G. B., Fan, L., Levasseur, R. A., & Faden, A. I. (1998). Sustained sensory/motor and cognitive deficits with neuronal apoptosis following controlled cortical impact brain injury in the mouse. *Journal of Neurotrauma*, 15(8), 599–614.
<https://doi.org/10.1089/neu.1998.15.599>
- Fu, M., Tao, J., Wang, D., Zhang, Z., Wang, X., Ji, Y., & Li, Z. (2020). Downregulation of MicroRNA-34c-5p facilitated neuroinflammation in drug-resistant epilepsy. *Brain Research*, 1749, 147130.
<https://doi.org/10.1016/j.brainres.2020.147130>
- Gafson, A. R., Barth elmy, N. R., Bomont, P., Carare, R. O., Durham, H. D., Julien, J. P., Kuhle, J., Leppert, D., Nixon, R. A., Weller, R. O., Zetterberg, H., & Matthews, P. M. (2020). Neurofilaments: Neurobiological foundations for biomarker applications. *Brain*, 143(7), 1975–1998.
<https://doi.org/10.1093/brain/awaa098>
- Garc a-Romero, N., Carri on-Navarro, J., Esteban-Rubio, S., L azaro-Ib a nez, E., Peris-Celda, M., Alonso, M. M., Guzm an-De-Villoria, J., Fern andez-Carballal, C., de Mendivil, A. O., Garc a-Duque, S., Escobedo-Lucea, C., Prat-Ac ın, R., Belda-Iniesta, C., & Ayuso-Sacido, A. (2017). DNA sequences within glioma-derived extracellular vesicles can cross the intact blood-brain barrier and be detected in peripheral blood of patients. *Oncotarget*, 8(1), 1416–1428.
<https://doi.org/10.18632/oncotarget.13635>
- Gardner, R. C., Byers, A. L., Barnes, D. E., Li, Y., Boscardin, J., & Yaffe, K. (2018). Mild TBI and risk of Parkinson disease: A Chronic Effects of

- Neurotrauma Consortium Study. *Neurology*, 90(20), E1771–E1779.
<https://doi.org/10.1212/WNL.0000000000005522>
- Gatson, J. W., Barillas, J., Hynan, L. S., Diaz-Arrastia, R., Wolf, S. E., & Minei, J. P. (2014). Detection of neurofilament-H in serum as a diagnostic tool to predict injury severity in patients who have suffered mild traumatic brain injury. *Journal of Neurosurgery*, 121(5), 1232–1238.
<https://doi.org/10.3171/2014.7.JNS132474>
- Gattás, D., Neto, F. S. L., Freitas-Lima, P., Bonfim-Silva, R., Malaquias de Almeida, S., de Assis Cirino, M. L., Guimarães Tiezzi, D., Tirapelli, L. F., Velasco, T. R., Sakamoto, A. C., Matias, C. M., Carlotti, C. G. J., & Tirapelli, D. P. C. (2022). MicroRNAs miR-629-3p, miR-1202 and miR-1225-5p as potential diagnostic and surgery outcome biomarkers for mesial temporal lobe epilepsy with hippocampal sclerosis. *Neuro-Chirurgie*, 68(6), 583–588. <https://doi.org/10.1016/j.neuchi.2022.06.002>
- Geekiyana, H., Rayatpisheh, S., Wohlschlegel, J. A., Brown, R., & Ambros, V. (2020). Extracellular microRNAs in human circulation are associated with miRISC complexes that are accessible to anti-AGO2 antibody and can bind target mimic oligonucleotides. *Proceedings of the National Academy of Sciences of the United States of America*, 117(39), 24213–24223. <https://doi.org/10.1073/pnas.2008323117>
- Ghai, V., Fallen, S., Baxter, D., Scherler, K., Kim, T. K., Zhou, Y., Meabon, J. S., Logsdon, A. F., Banks, W. A., Schindler, A. G., Cook, D. G., Peskind, E. R., Lee, I., & Wang, K. (2020). Alterations in Plasma microRNA and Protein Levels in War Veterans with Chronic Mild Traumatic Brain Injury. *Journal of Neurotrauma*, 37(12), 1418–1430.
<https://doi.org/10.1089/neu.2019.6826>
- Ghaith, H. S., Nawar, A. A., Gabra, M. D., Abdelrahman, M. E., Nafady, M. H., Bahbah, E. I., Ebada, M. A., Ashraf, G. M., Negida, A., & Barreto, G. E. (2022). A Literature Review of Traumatic Brain Injury Biomarkers. *Molecular Neurobiology*, 59(7), 4141–4158.
<https://doi.org/10.1007/s12035-022-02822-6>
- Gill, J., Latour, L., Diaz-Arrastia, R., Motamedi, V., Turtzo, C., Shahim, P., Mondello, S., DeVoto, C., Veras, E., Hanlon, D., Song, L., & Jeromin, A.

- (2018). Glial fibrillary acidic protein elevations relate to neuroimaging abnormalities after mild TBI. *Neurology*, *91*(15), E1385–E1389.
<https://doi.org/10.1212/WNL.00000000000006321>
- Gill, J., Merchant-Borna, K., Jeromin, A., Livingston, W., & Bazarian, J. (2017). Acute plasma tau relates to prolonged return to play after concussion. *Neurology*, *88*(6), 595–602.
<https://doi.org/10.1212/WNL.00000000000003587>
- Giovannini, G., Bedin, R., Ferraro, D., Vaudano, A. E., Mandrioli, J., & Meletti, S. (2021). Serum neurofilament light as biomarker of seizure-related neuronal injury in status epilepticus. *Epilepsia*.
<https://doi.org/10.1111/epi.17132>
- Gledhill, J. M., Brand, E. J., Pollard, J. R., St. Clair, R. D., Wallach, T. M., & Crino, P. B. (2021). Association of Epileptic and Nonepileptic Seizures and Changes in Circulating Plasma Proteins Linked to Neuroinflammation. *Neurology*, *96*(10), E1443–E1452.
<https://doi.org/10.1212/WNL.00000000000011552>
- Golub, V. M., & Reddy, D. S. (2022). Post-Traumatic Epilepsy and Comorbidities: Advanced Models, Molecular Mechanisms, Biomarkers, and Novel Therapeutic Interventions. *Pharmacological Reviews*, *74*(2), 387–438. <https://doi.org/10.1124/pharmrev.121.000375>
- Gomes, D. E., & Witwer, K. W. (2022). L1CAM-associated extracellular vesicles: A systematic review of nomenclature, sources, separation, and characterization. *Journal of Extracellular Biology*, *1*(3).
<https://doi.org/10.1002/jex2.35>
- Gong, G.-H., An, F.-M., Wang, Y., Bian, M., Wang, D., & Wei, C.-X. (2018). MiR-153 regulates expression of hypoxia-inducible factor-1 α in refractory epilepsy. *Oncotarget*, *9*(9), 8542–8547.
<https://doi.org/10.18632/oncotarget.24012>
- Gorter, J. A., Iyer, A., White, I., Colzi, A., van Vliet, E. A., Sisodiya, S., & Aronica, E. (2014). Hippocampal subregion-specific microRNA expression during epileptogenesis in experimental temporal lobe epilepsy. *Neurobiology of Disease*, *62*, 508–520.
<https://doi.org/10.1016/j.nbd.2013.10.026>

- Guedes, V. A., Devoto, C., Leete, J., Sass, D., Acott, J. D., Mithani, S., & Gill, J. M. (2020). Extracellular Vesicle Proteins and MicroRNAs as Biomarkers for Traumatic Brain Injury. *Frontiers in Neurology, 11*, 663. <https://doi.org/10.3389/fneur.2020.00663>
- Guedes, V. A., Lai, C., Devoto, C., Edwards, K. A., Mithani, S., Sass, D., Vorn, R., Qu, B. X., Rusch, H. L., Martin, C. A., Walker, W. C., Wilde, E. A., Diaz-Arrastia, R., Gill, J. M., & Kenney, K. (2021). Extracellular Vesicle Proteins and MicroRNAs Are Linked to Chronic Post-Traumatic Stress Disorder Symptoms in Service Members and Veterans With Mild Traumatic Brain Injury. *Frontiers in Pharmacology, 12*(October), 1–14. <https://doi.org/10.3389/fphar.2021.745348>
- Guo, D., Zeng, L., Brody, D. L., & Wong, M. (2013). Rapamycin Attenuates the Development of Posttraumatic Epilepsy in a Mouse Model of Traumatic Brain Injury. *PLoS ONE, 8*(5). <https://doi.org/10.1371/journal.pone.0064078>
- Guo, J., Wang, H., Wang, Q., Chen, Y., & Chen, S. (2014). Expression of p-CREB and activity-dependent miR-132 in temporal lobe epilepsy. *International Journal of Clinical and Experimental Medicine, 7*(5), 1297–1306.
- Haenisch, S., Zhao, Y., Chhibber, A., Kaiboriboon, K., Do, L. V., Vogelgesang, S., Barbaro, N. M., Alldredge, B. K., Lowenstein, D. H., Cascorbi, I., & Kroetz, D. L. (2015). SOX11 identified by target gene evaluation of miRNAs differentially expressed in focal and non-focal brain tissue of therapy-resistant epilepsy patients. *Neurobiology of Disease, 77*, 127–140. <https://doi.org/10.1016/j.nbd.2015.02.025>
- Hall, E. D., Sullivan, P. G., Gibson, T. R., Pavel, K. M., Thompson, B. M., & Scheff, S. W. (2005). Spatial and temporal characteristics of neurodegeneration after controlled cortical impact in mice: more than a focal brain injury. *Journal of Neurotrauma, 22*(2), 252–265. <https://doi.org/10.1089/neu.2005.22.252>
- Hallal, S., Túzesi, Á., Grau, G. E., Buckland, M. E., & Alexander, K. L. (2022). Understanding the extracellular vesicle surface for clinical molecular

- biology. *Journal of Extracellular Vesicles*, 11(10).
<https://doi.org/10.1002/jev2.12260>
- Haltiner, A. M., Temkin, N. R., & Dikmen, S. S. (1997). Risk of seizure recurrence after the first late posttraumatic seizure. *Archives of Physical Medicine and Rehabilitation*, 78(8), 835–840.
[https://doi.org/10.1016/S0003-9993\(97\)90196-9](https://doi.org/10.1016/S0003-9993(97)90196-9)
- He, M., Crow, J., Roth, M., Zeng, Y., & Godwin, A. K. (2014). Integrated immunoisolation and protein analysis of circulating exosomes using microfluidic technology. *Lab on a Chip*, 14(19), 3773–3780.
<https://doi.org/10.1039/c4lc00662c>
- Heidari, K., Vafae, A., Rastekenari, A. M., Taghizadeh, M., Shad, E. G., Eley, R., Sinnott, M., & Asadollahi, S. (2015). S100B protein as a screening tool for computed tomography findings after mild traumatic brain injury: Systematic review and meta-analysis. *Brain Injury*, 29(10), 1146–1157. <https://doi.org/10.3109/02699052.2015.1037349>
- Herman, S. T. (2002). Epilepsy after brain insult. *Neurology*, 59(9 suppl 5), S21 LP-S26. https://doi.org/10.1212/WNL.59.9_suppl_5.S21
- Hong, Z., Li, W., Qu, B., Zou, X., Chen, J., Sander, J. W., & Zhou, D. (2014). Serum brain-derived neurotrophic factor levels in epilepsy. *European Journal of Neurology*, 21(1), 57–64. <https://doi.org/10.1111/ene.12232>
- Hu, K., Zhang, C., Long, L., Long, X., Feng, L., Li, Y., & Xiao, B. (2011). Expression profile of microRNAs in rat hippocampus following lithium-pilocarpine-induced status epilepticus. *Neuroscience Letters*, 488(3), 252–257. <https://doi.org/10.1016/j.neulet.2010.11.040>
- Huang, H., Cui, G., Tang, H., Kong, L., Wang, X., Cui, C., Xiao, Q., & Ji, H. (2022). Relationships between plasma expression levels of microRNA-146a and microRNA-132 in epileptic patients and their cognitive, mental and psychological disorders. *Bioengineered*, 13(1), 941–949. <https://doi.org/10.1080/21655979.2021.2015528>
- Huang, X., Yuan, T., Tschannen, M., Sun, Z., Jacob, H., Du, M., Liang, M., Dittmar, R. L., Liu, Y., Liang, M., Kohli, M., Thibodeau, S. N., Boardman, L., & Wang, L. (2013). Characterization of human plasma-derived

- exosomal RNAs by deep sequencing. *BMC Genomics*, *14*, 319.
<https://doi.org/10.1186/1471-2164-14-319>
- Huibregtse, M. E., Bazarian, J. J., Shultz, S. R., & Kawata, K. (2021). The biological significance and clinical utility of emerging blood biomarkers for traumatic brain injury. *Neuroscience and Biobehavioral Reviews*, *130*, 433–447. <https://doi.org/10.1016/j.neubiorev.2021.08.029>
- Hunt, R. F., Boychuk, J. A., & Smith, B. N. (2013). Neural circuit mechanisms of posttraumatic epilepsy. *Frontiers in Cellular Neuroscience*, *7*(MAY), 1–14. <https://doi.org/10.3389/fncel.2013.00089>
- Hunt, R. F., Scheff, S. W., & Smith, B. N. (2009). Posttraumatic epilepsy after controlled cortical impact injury in mice. *Experimental Neurology*, *215*(2), 243–252. <https://doi.org/10.1016/j.expneurol.2008.10.005>
- Hunter, M. P., Ismail, N., Zhang, X., Aguda, B. D., Lee, E. J., Yu, L., Xiao, T., Schafer, J., Lee, M. L. T., Schmittgen, T. D., Nana-Sinkam, S. P., Jarjoura, D., & Marsh, C. B. (2008). Detection of microRNA expression in human peripheral blood microvesicles. *PLoS ONE*, *3*(11).
<https://doi.org/10.1371/journal.pone.0003694>
- Huusko, N., Römer, C., Ndode-Ekane, X. E., Lukasiuk, K., & Pitkänen, A. (2015). Loss of hippocampal interneurons and epileptogenesis: a comparison of two animal models of acquired epilepsy. *Brain Structure and Function*, *220*(1), 153–191. <https://doi.org/10.1007/s00429-013-0644-1>
- Ioriatti, E. S., Cirino, M. L. A., Lizarte Neto, F. S., Velasco, T. R., Sakamoto, A. C., Freitas-Lima, P., Tirapelli, D. P. C., & Carlotti, C. G. J. (2020). Expression of circulating microRNAs as predictors of diagnosis and surgical outcome in patients with mesial temporal lobe epilepsy with hippocampal sclerosis. *Epilepsy Research*, *166*, 106373.
<https://doi.org/10.1016/j.epilepsyres.2020.106373>
- Isgrò, M. A., Bottoni, P., & Scatena, R. (2015). Neuron-Specific Enolase as a Biomarker: Biochemical and Clinical Aspects. *Advances in Experimental Medicine and Biology*, *867*, 125–143. https://doi.org/10.1007/978-94-017-7215-0_9

- Jarrahi, A., Braun, M., Ahluwalia, M., Gupta, R. V., Wilson, M., Munie, S., Ahluwalia, P., Vender, J. R., Vale, F. L., Dhandapani, K. M., & Vaibhav, K. (2020). Revisiting traumatic brain injury: From molecular mechanisms to therapeutic interventions. *Biomedicines*, 8(10), 1–42. <https://doi.org/10.3390/biomedicines8100389>
- Jeurissen, S., Vergauwen, G., Van Deun, J., Lapeire, L., Depoorter, V., Miinalainen, I., Sormunen, R., Van den Broecke, R., Braems, G., Cocquyt, V., Denys, H., & Hendrix, A. (2017). The isolation of morphologically intact and biologically active extracellular vesicles from the secretome of cancer-associated adipose tissue. *Cell Adhesion and Migration*, 11(2), 196–204. <https://doi.org/10.1080/19336918.2017.1279784>
- Ji, Q., Ji, Y., Peng, J., Zhou, X., Chen, X., Zhao, H., Xu, T., Chen, L., & Xu, Y. (2016). Increased Brain-Specific MiR-9 and MiR-124 in the Serum Exosomes of Acute Ischemic Stroke Patients. *PloS One*, 11(9), e0163645. <https://doi.org/10.1371/journal.pone.0163645>
- Jimenez-Mateos, E. M., Bray, I., Sanz-Rodriguez, A., Engel, T., McKiernan, R. C., Mouri, G., Tanaka, K., Sano, T., Saugstad, J. A., Simon, R. P., Stallings, R. L., & Henshall, D. C. (2011). miRNA Expression profile after status epilepticus and hippocampal neuroprotection by targeting miR-132. *The American Journal of Pathology*, 179(5), 2519–2532. <https://doi.org/10.1016/j.ajpath.2011.07.036>
- Jochems, D., van Rein, E., Niemeijer, M., van Heijl, M., van Es, M. A., Nijboer, T., Leenen, L. P. H., Houwert, R. M., & van Wessum, K. J. P. (2021). Incidence, causes and consequences of moderate and severe traumatic brain injury as determined by Abbreviated Injury Score in the Netherlands. *Scientific Reports*, 11(1), 1–8. <https://doi.org/10.1038/s41598-021-99484-6>
- Jonas, S., & Izaurralde, E. (2015). Towards a molecular understanding of microRNA-mediated gene silencing. *Nature Reviews Genetics*, 16(7), 421–433. <https://doi.org/10.1038/nrg3965>
- Jovičić, A., Roshan, R., Moiso, N., Pradervand, S., Moser, R., Pillai, B., & Luthi-Carter, R. (2013). Comprehensive expression analyses of neural

- cell-type-specific miRNAs identify new determinants of the specification and maintenance of neuronal phenotypes. *The Journal of Neuroscience: The Official Journal of the Society for Neuroscience*, 33(12), 5127–5137. <https://doi.org/10.1523/JNEUROSCI.0600-12.2013>
- Jung, H. J., Lee, K.-P., Milholland, B., Shin, Y. J., Kang, J. S., Kwon, K.-S., & Suh, Y. (2017). Comprehensive miRNA Profiling of Skeletal Muscle and Serum in Induced and Normal Mouse Muscle Atrophy During Aging. *The Journals of Gerontology. Series A, Biological Sciences and Medical Sciences*, 72(11), 1483–1491. <https://doi.org/10.1093/gerona/glx025>
- Jużwik, C. A., S. Drake, S., Zhang, Y., Paradis-Isler, N., Sylvester, A., Amar-Zifkin, A., Douglas, C., Morquette, B., Moore, C. S., & Fournier, A. E. (2019). microRNA dysregulation in neurodegenerative diseases: A systematic review. *Progress in Neurobiology*, 182(November 2018), 101664. <https://doi.org/10.1016/j.pneurobio.2019.101664>
- Karimi, N., Cvjetkovic, A., Jang, S. C., Crescitelli, R., Hosseinpour Feizi, M. A., Nieuwland, R., Lötvall, J., & Lässer, C. (2018). Detailed analysis of the plasma extracellular vesicle proteome after separation from lipoproteins. *Cellular and Molecular Life Sciences*, 75(15), 2873–2886. <https://doi.org/10.1007/s00018-018-2773-4>
- Kaur, P., & Sharma, S. (2018). Recent Advances in Pathophysiology of Traumatic Brain Injury. *Current Neuropharmacology*, 16(8), 1224–1238. <https://doi.org/10.2174/1570159X15666170613083606>
- Kelly, K. M., Miller, E. R., Lepsveridze, E., Kharlamov, E. A., & Mchedlishvili, Z. (2015). Posttraumatic seizures and epilepsy in adult rats after controlled cortical impact. *Epilepsy Research*, 117, 104–116. <https://doi.org/10.1016/j.eplepsyres.2015.09.009>
- Kerr, N., Lee, S. W., Perez-Barcena, J., Crespi, C., Ibañez, J., Bullock, M. R., Dietrich, W. D., Keane, R. W., & de Rivero Vaccari, J. P. (2018). Inflammasome proteins as biomarkers of traumatic brain injury. *PLoS One*, 13(12), e0210128. <https://doi.org/10.1371/journal.pone.0210128>
- Ketting, R. F., Fischer, S. E. J., Bernstein, E., Sijen, T., Hannon, G. J., & Plasterk, R. H. A. (2001). Dicer functions in RNA interference and in synthesis of small RNA involved in developmental timing in *C. elegans*.

Genes and Development, 15(20), 2654–2659.

<https://doi.org/10.1101/gad.927801>

Kharatishvili, I., Nissinen, J. P., McIntosh, T. K., & Pitkänen, A. (2006). A model of posttraumatic epilepsy induced by lateral fluid-percussion brain injury in rats. *Neuroscience*, 140(2), 685–697.

<https://doi.org/10.1016/j.neuroscience.2006.03.012>

Kharatishvili, I., & Pitkänen, A. (2010). Posttraumatic epilepsy. *Current Opinion in Neurology*, 23(2). https://journals.lww.com/co-neurology/fulltext/2010/04000/posttraumatic_epilepsy.16.aspx

Kitahara, Y., Nakamura, K., Kogure, K., & Minegishi, T. (2013). Role of microRNA-136-3p on the expression of luteinizing hormone-human chorionic gonadotropin receptor mRNA in rat ovaries. *Biology of Reproduction*, 89(5), 114.

<https://doi.org/10.1095/biolreprod.113.109207>

Klein, P., & Tyrlikova, I. (2020). No prevention or cure of epilepsy as yet. *Neuropharmacology*, 168, 107762.

<https://doi.org/10.1016/j.neuropharm.2019.107762>

Ko, J., Hemphill, M., Yang, Z., Beard, K., Sewell, E., Shallcross, J., Schweizer, M., Sandsmark, D. K., Diaz-Arrastia, R., Kim, J., Meaney, D., & Issadore, D. (2020). Multi-Dimensional Mapping of Brain-Derived Extracellular Vesicle MicroRNA Biomarker for Traumatic Brain Injury Diagnostics. *Journal of Neurotrauma*, 37(22), 2424–2434.

<https://doi.org/10.1089/neu.2018.6220>

Ko, J., Hemphill, M., Yang, Z., Sewell, E., Na, Y. J., Sandsmark, D. K., Haber, M., Fisher, S. A., Torre, E. A., Svane, K. C., Omelchenko, A., Firestein, B. L., Diaz-Arrastia, R., Kim, J., Meaney, D. F., & Issadore, D. (2018a).

Diagnosis of traumatic brain injury using miRNA signatures in nanomagnetically isolated brain-derived extracellular vesicles. *Lab on a Chip*, 18(23), 3617–3630. <https://doi.org/10.1039/c8lc00672e>

Ko, J., Hemphill, M., Yang, Z., Sewell, E., Na, Y. J., Sandsmark, D. K., Haber, M., Fisher, S. A., Torre, E. A., Svane, K. C., Omelchenko, A., Firestein, B. L., Diaz-Arrastia, R., Kim, J., Meaney, D. F., & Issadore, D. (2018b).

Diagnosis of traumatic brain injury using miRNA signatures in

- nanomagnetically isolated brain-derived extracellular vesicles. *Lab on a Chip*, 18(23), 3617–3630. <https://doi.org/10.1039/c8lc00672e>
- Kogure, T., Yan, I. K., Lin, W. L., & Patel, T. (2013). Extracellular Vesicle-Mediated Transfer of a Novel Long Noncoding RNA TUC339: A Mechanism of Intercellular Signaling in Human Hepatocellular Cancer. *Genes and Cancer*, 4(7–8), 261–272. <https://doi.org/10.1177/1947601913499020>
- Konoshenko, M. Yu., Lekchnov, E. A., Vlassov, A. V., & Laktionov, P. P. (2018). Isolation of Extracellular Vesicles: General Methodologies and Latest Trends. *BioMed Research International*, 2018, 8545347. <https://doi.org/10.1155/2018/8545347>
- Kopczynska, M., Zelek, W. M., Vespa, S., Touchard, S., Wardle, M., Loveless, S., Thomas, R. H., Hamandi, K., & Morgan, B. P. (2018). Complement system biomarkers in epilepsy. *Seizure*, 60, 1–7. <https://doi.org/10.1016/j.seizure.2018.05.016>
- Korley, F. K., Diaz-Arrastia, R., Wu, A. H. B., Yue, J. K., Manley, G. T., Sair, H. I., Van Eyk, J., Everett, A. D., Okonkwo, D. O., Valadka, A. B., Gordon, W. A., Maas, A. I. R., Mukherjee, P., Yuh, E. L., Lingsma, H. F., Puccio, A. M., & Schnyer, D. M. (2016). Circulating Brain-Derived Neurotrophic Factor Has Diagnostic and Prognostic Value in Traumatic Brain Injury. *Journal of Neurotrauma*, 33(2), 215–225. <https://doi.org/10.1089/neu.2015.3949>
- Korley, F. K., Jain, S., Sun, X., Puccio, A. M., Yue, J. K., Gardner, R. C., Wang, K. K. W., Okonkwo, D. O., Yuh, E. L., Mukherjee, P., Nelson, L. D., Taylor, S. R., Markowitz, A. J., Diaz-Arrastia, R., Manley, G. T., Adeoye, O., Badatjia, N., Duhaime, A. C., Ferguson, A., ... Zafonte, R. (2022). Prognostic value of day-of-injury plasma GFAP and UCH-L1 concentrations for predicting functional recovery after traumatic brain injury in patients from the US TRACK-TBI cohort: an observational cohort study. *The Lancet Neurology*, 21(9), 803–813. [https://doi.org/10.1016/S1474-4422\(22\)00256-3](https://doi.org/10.1016/S1474-4422(22)00256-3)
- Korotkov, A., Broekaart, D. W. M., Banhaewa, L., Pustjens, B., van Scheppingen, J., Anink, J. J., Baayen, J. C., Idema, S., Gorter, J. A., van

- Vliet, E. A., & Aronica, E. (2020a). microRNA-132 is overexpressed in glia in temporal lobe epilepsy and reduces the expression of pro-epileptogenic factors in human cultured astrocytes. *Glia*, *68*(1), 60–75. <https://doi.org/10.1002/glia.23700>
- Korotkov, A., Puhakka, N., Gupta, S. Das, Vuokila, N., Broekaart, D. W. M., Anink, J. J., Heiskanen, M., Karttunen, J., van Scheppingen, J., Huitinga, I., Mills, J. D., van Vliet, E. A., Pitkänen, A., & Aronica, E. (2020b). Increased expression of miR142 and miR155 in glial and immune cells after traumatic brain injury may contribute to neuroinflammation via astrocyte activation. *Brain Pathology (Zurich, Switzerland)*, *30*(5), 897–912. <https://doi.org/10.1111/bpa.12865>
- Kozomara, A., Birgaoanu, M., & Griffiths-Jones, S. (2019). MiRBase: From microRNA sequences to function. *Nucleic Acids Research*, *47*(D1), D155–D162. <https://doi.org/10.1093/nar/gky1141>
- Krichevsky, A. M., Sonntag, K.-C., Isacson, O., & Kosik, K. S. (2006). Specific microRNAs modulate embryonic stem cell-derived neurogenesis. *Stem Cells (Dayton, Ohio)*, *24*(4), 857–864. <https://doi.org/10.1634/stemcells.2005-0441>
- Kumar, A., & Loane, D. J. (2012). Neuroinflammation after traumatic brain injury: Opportunities for therapeutic intervention. *Brain, Behavior, and Immunity*, *26*(8), 1191–1201. <https://doi.org/10.1016/j.bbi.2012.06.008>
- Kumar, P. (2023). miRNA dysregulation in traumatic brain injury and epilepsy: a systematic review to identify putative biomarkers for post-traumatic epilepsy. *Metabolic Brain Disease*, *38*(3), 749–765. <https://doi.org/10.1007/s11011-023-01172-z>
- Kumar, R. G., Breslin, K. B., Ritter, A. C., Conley, Y. P., & Wagner, A. K. (2019). Variability with Astroglial Glutamate Transport Genetics Is Associated with Increased Risk for Post-Traumatic Seizures. *Journal of Neurotrauma*, *36*(2), 230–238. <https://doi.org/10.1089/neu.2018.5632>
- Landgraf, P., Rusu, M., Sheridan, R., Sewer, A., Iovino, N., Aravin, A., Pfeffer, S., Rice, A., Kamphorst, A. O., Landthaler, M., Lin, C., Socci, N. D., Hermida, L., Fulci, V., Chiaretti, S., Foà, R., Schliwka, J., Fuchs, U., Novosel, A., ... Tuschl, T. (2007). A mammalian microRNA expression

- atlas based on small RNA library sequencing. *Cell*, 129(7), 1401–1414.
<https://doi.org/10.1016/j.cell.2007.04.040>
- Lapinlampi, N., Andrade, P., Paananen, T., Hämäläinen, E., Ekolle Ndode-Ekane, X., Puhakka, N., & Pitkänen, A. (2020). Postinjury weight rather than cognitive or behavioral impairment predicts development of posttraumatic epilepsy after lateral fluid-percussion injury in rats. *Epilepsia*, 61(9), 2035–2052. <https://doi.org/10.1111/epi.16632>
- LaRocca, D., Barns, S., Hicks, S. D., Brindle, A., Williams, J., Uhlig, R., Johnson, P., Neville, C., & Middleton, F. A. (2019). Comparison of serum and saliva miRNAs for identification and characterization of mTBI in adult mixed martial arts fighters. *PLOS ONE*, 14(1), e0207785.
<https://doi.org/10.1371/journal.pone.0207785>
- Lee, R. C., Feinbaum, R. L., & Ambros, V. (1993). The *C. elegans* heterochronic gene *lin-4* encodes small RNAs with antisense complementarity to *lin-14*. *Cell*, 75(5), 843–854.
[https://doi.org/10.1016/0092-8674\(93\)90529-y](https://doi.org/10.1016/0092-8674(93)90529-y)
- Leontariti, M., Avgeris, M., Katsarou, M.-S., Drakoulis, N., Siatouni, A., Verentzioti, A., Alexoudi, A., Fytraki, A., Patrikelis, P., Vassilacopoulou, D., Gatzonis, S., & Sideris, D. C. (2020). Circulating miR-146a and miR-134 in predicting drug-resistant epilepsy in patients with focal impaired awareness seizures. *Epilepsia*, 61(5), 959–970.
<https://doi.org/10.1111/epi.16502>
- Lewis, B. P., Shih, I., Jones-Rhoades, M. W., Bartel, D. P., & Burge, C. B. (2003). Prediction of mammalian microRNA targets. *Cell*, 115(7), 787–798. [https://doi.org/10.1016/s0092-8674\(03\)01018-3](https://doi.org/10.1016/s0092-8674(03)01018-3)
- Li, Y., Huang, C., Feng, P., Jiang, Y., Wang, W., Zhou, D., & Chen, L. (2016). Aberrant expression of miR-153 is associated with overexpression of hypoxia-inducible factor-1 α in refractory epilepsy. *Scientific Reports*, 6, 32091. <https://doi.org/10.1038/srep32091>
- Lighthall, J. W. (1988). Controlled cortical impact: a new experimental brain injury model. *Journal of Neurotrauma*, 5(1), 1–15.
<https://doi.org/10.1089/neu.1988.5.1>

- Liliang, P.-C., Liang, C.-L., Weng, H.-C., Lu, K., Wang, K.-W., Chen, H.-J., & Chuang, J.-H. (2010). Tau proteins in serum predict outcome after severe traumatic brain injury. *The Journal of Surgical Research*, *160*(2), 302–307. <https://doi.org/10.1016/j.jss.2008.12.022>
- Lin, C.-H., Li, C.-H., Yang, K.-C., Lin, F.-J., Wu, C.-C., Chieh, J.-J., & Chiu, M.-J. (2019). Blood NfL. *Neurology*, *93*(11), e1104 LP-e1111. <https://doi.org/10.1212/WNL.00000000000008088>
- Lin, S., & Gregory, R. I. (2015). MicroRNA biogenesis pathways in cancer. *Nature Reviews Cancer*, *15*(6), 321–333. <https://doi.org/10.1038/nrc3932>
- Liu, D.-Z., Tian, Y., Ander, B. P., Xu, H., Stamova, B. S., Zhan, X., Turner, R. J., Jickling, G., & Sharp, F. R. (2010). Brain and blood microRNA expression profiling of ischemic stroke, intracerebral hemorrhage, and kainate seizures. *Journal of Cerebral Blood Flow and Metabolism : Official Journal of the International Society of Cerebral Blood Flow and Metabolism*, *30*(1), 92–101. <https://doi.org/10.1038/jcbfm.2009.186>
- Liu, H., Lei, C., He, Q., Pan, Z., Xiao, D., & Tao, Y. (2018). Nuclear functions of mammalian MicroRNAs in gene regulation, immunity and cancer. *Molecular Cancer*, *17*(1), 1–14. <https://doi.org/10.1186/s12943-018-0765-5>
- Liu, Y., Zhang, J., Han, R., Liu, H., Sun, D., & Liu, X. (2015). Downregulation of serum brain specific microRNA is associated with inflammation and infarct volume in acute ischemic stroke. *Journal of Clinical Neuroscience: Official Journal of the Neurosurgical Society of Australasia*, *22*(2), 291–295. <https://doi.org/10.1016/j.jocn.2014.05.042>
- Ljungqvist, J., Zetterberg, H., Mitsis, M., Blennow, K., & Skoglund, T. (2017). Serum Neurofilament Light Protein as a Marker for Diffuse Axonal Injury: Results from a Case Series Study. *Journal of Neurotrauma*, *34*(5), 1124–1127. <https://doi.org/10.1089/neu.2016.4496>
- Loane, D. J., & Faden, A. I. (2010). Neuroprotection for traumatic brain injury: Translational challenges and emerging therapeutic strategies. *Trends in Pharmacological Sciences*, *31*(12), 596–604. <https://doi.org/10.1016/j.tips.2010.09.005>

- Lorente, L., Martín, M. M., López, P., Ramos, L., Blanquer, J., Cáceres, J. J., Solé-Violán, J., Solera, J., Cabrera, J., Argueso, M., Ortiz, R., Mora, M. L., Lubillo, S., Jiménez, A., Borreguero-León, J. M., González, A., Orbe, J., Rodríguez, J. A., & Páramo, J. A. (2014). Association between serum tissue inhibitor of matrix metalloproteinase-1 levels and mortality in patients with severe brain trauma injury. *PloS One*, *9*(4), e94370. <https://doi.org/10.1371/journal.pone.0094370>
- Ludwig, N., Leidinger, P., Becker, K., Backes, C., Fehlmann, T., Pallasch, C., Rheinheimer, S., Meder, B., Stähler, C., Meese, E., & Keller, A. (2016). Distribution of miRNA expression across human tissues. *Nucleic Acids Research*, *44*(8), 3865–3877. <https://doi.org/10.1093/nar/gkw116>
- Luikart, B. W., Bensen, A. L., Washburn, E. K., Perederiy, J. V, Su, K. G., Li, Y., Kernie, S. G., Parada, L. F., & Westbrook, G. L. (2011). miR-132 Mediates the Integration of Newborn Neurons into the Adult Dentate Gyrus. *PLOS ONE*, *6*(5), e19077. <https://doi.org/10.1371/journal.pone.0019077>
- Lund, E., Güttinger, S., Calado, A., Dahlberg, J. E., & Kutay, U. (2004). Nuclear Export of MicroRNA Precursors. *Science*, *303*(5654), 95–98. <https://doi.org/10.1126/science.1090599>
- Ma, S.-Q., Xu, X.-X., He, Z.-Z., Li, X.-H., & Luo, J.-M. (2019). Dynamic changes in peripheral blood-targeted miRNA expression profiles in patients with severe traumatic brain injury at high altitude. *Military Medical Research*, *6*(1), 12. <https://doi.org/10.1186/s40779-019-0203-z>
- Maas, A. I. R., Menon, D. K., Manley, G. T., Abrams, M., Åkerlund, C., Andelic, N., Aries, M., Bashford, T., Bell, M. J., Bodien, Y. G., Brett, B. L., Büki, A., Chesnut, R. M., Citerio, G., Clark, D., Clasby, B., Cooper, D. J., Czeiter, E., Czosnyka, M., ... Zumbo, F. (2022). Traumatic brain injury: progress and challenges in prevention, clinical care, and research. *The Lancet Neurology*, *21*(11), 1004–1060. [https://doi.org/10.1016/S1474-4422\(22\)00309-X](https://doi.org/10.1016/S1474-4422(22)00309-X)
- Machamer, J., Temkin, N., Dikmen, S., Nelson, L. D., Barber, J., Hwang, P., Boase, K., Stein, M. B., Sun, X., Giacino, J., McCrea, M. A., Taylor, S. R., Jain, S., & Manley, G. (2022). Symptom Frequency and Persistence in the First Year after Traumatic Brain Injury: A TRACK-TBI Study. *Journal*

of Neurotrauma, 39(5–6), 358–370.

<https://doi.org/10.1089/neu.2021.0348>

Mackay, D. F., Russell, E. R., Stewart, K., MacLean, J. A., Pell, J. P., & Stewart, W. (2019). Neurodegenerative Disease Mortality among Former Professional Soccer Players. *New England Journal of Medicine*, 381(19), 1801–1808. <https://doi.org/10.1056/NEJMoa1908483>

Magill, S. T., Cambronne, X. A., Luikart, B. W., Lioy, D. T., Leighton, B. H., Westbrook, G. L., Mandel, G., & Goodman, R. H. (2010). microRNA-132 regulates dendritic growth and arborization of newborn neurons in the adult hippocampus. *Proceedings of the National Academy of Sciences of the United States of America*, 107(47), 20382–20387.

<https://doi.org/10.1073/pnas.1015691107>

Maiti, R., Mishra, B. R., Jena, M., Mishra, A., Nath, S., & Srinivasan, A. (2018). Effect of anti-seizure drugs on serum S100B in patients with focal seizure: a randomized controlled trial. *Journal of Neurology*, 265(11), 2594–2601. <https://doi.org/10.1007/s00415-018-9026-1>

Makarova, J. A., Shkurnikov, M. U., Wicklein, D., Lange, T., Samatov, T. R., Turchinovich, A. A., & Tonevitsky, A. G. (2016). Intracellular and extracellular microRNA: An update on localization and biological role. *Progress in Histochemistry and Cytochemistry*, 51(3–4), 33–49.

<https://doi.org/10.1016/j.proghi.2016.06.001>

Makarova, J., Turchinovich, A., Shkurnikov, M., & Tonevitsky, A. (2021). Extracellular miRNAs and Cell–Cell Communication: Problems and Prospects. *Trends in Biochemical Sciences*, 46(8), 640–651.

<https://doi.org/10.1016/j.tibs.2021.01.007>

Manninen, E., Chary, K., Lapinlampi, N., Andrade, P., Paananen, T., Sierra, A., Tohka, J., Gröhn, O., & Pitkänen, A. (2020). Early Increase in Cortical T(2) Relaxation Is a Prognostic Biomarker for the Evolution of Severe Cortical Damage, but Not for Epileptogenesis, after Experimental Traumatic Brain Injury. *Journal of Neurotrauma*, 37(23), 2580–2594.

<https://doi.org/10.1089/neu.2019.6796>

Manninen, E., Chary, K., Lapinlampi, N., Andrade, P., Paananen, T., Sierra, A., Tohka, J., Gröhn, O., & Pitkänen, A. (2021). Acute thalamic damage

- as a prognostic biomarker for post-traumatic epileptogenesis. *Epilepsia*, 62(8), 1852–1864. <https://doi.org/10.1111/epi.16986>
- Martins-Ferreira, R., Chaves, J., Carvalho, C., Bettencourt, A., Chorão, R., Freitas, J., Samões, R., Boleixa, D., Lopes, J., Ramalheira, J., da Silva, B. M., Martins da Silva, A., Costa, P. P., & Leal, B. (2020). Circulating microRNAs as potential biomarkers for genetic generalized epilepsies: a three microRNA panel. *European Journal of Neurology*, 27(4), 660–666. <https://doi.org/10.1111/ene.14129>
- Mattioli, F., Bellomi, F., Stampatori, C., Mariotto, S., Ferrari, S., Monaco, S., Mancinelli, C., & Capra, R. (2020). Longitudinal serum neurofilament light chain (sNfL) concentration relates to cognitive function in multiple sclerosis patients. *Journal of Neurology*, 267(8), 2245–2251. <https://doi.org/10.1007/s00415-020-09832-1>
- Mattsson, N., Andreasson, U., Zetterberg, H., Blennow, K., & Initiative, for the A. D. N. (2017). Association of Plasma Neurofilament Light With Neurodegeneration in Patients With Alzheimer Disease. *JAMA Neurology*, 74(5), 557–566. <https://doi.org/10.1001/jamaneurol.2016.6117>
- McCrea, M. A., Giacino, J. T., Barber, J., Temkin, N. R., Nelson, L. D., Levin, H. S., Dikmen, S., Stein, M., Bodien, Y. G., Boase, K., Taylor, S. R., Vassar, M., Mukherjee, P., Robertson, C., Diaz-Arrastia, R., Okonkwo, D. O., Markowitz, A. J., Manley, G. T., Adeoye, O., ... Zafonte, R. (2021). Functional Outcomes over the First Year after Moderate to Severe Traumatic Brain Injury in the Prospective, Longitudinal TRACK-TBI Study. *JAMA Neurology*, 78(8), 982–992. <https://doi.org/10.1001/jamaneurol.2021.2043>
- McCrea, M., Broglio, S. P., McAllister, T. W., Gill, J., Giza, C. C., Huber, D. L., Harezlak, J., Cameron, K. L., Houston, M. N., McGinty, G., Jackson, J. C., Guskiewicz, K., Mihalik, J., Brooks, M. A., Duma, S., Rowson, S., Nelson, L. D., Pasquina, P., Meier, T. B., & Investigators, and the C. C. (2020). Association of Blood Biomarkers With Acute Sport-Related Concussion in Collegiate Athletes: Findings From the NCAA and Department of

- Defense CARE Consortium. *JAMA Network Open*, 3(1), e1919771–e1919771. <https://doi.org/10.1001/jamanetworkopen.2019.19771>
- McInnes, K., Friesen, C. L., MacKenzie, D. E., Westwood, D. A., & Boe, S. G. (2017). Mild Traumatic Brain Injury (mTBI) and chronic cognitive impairment: A scoping review. *PLoS ONE*, 12(4). <https://doi.org/10.1371/journal.pone.0174847>
- McIntosh, T. K., Vink, R., Noble, L., Yamakami, I., Fernyak, S., Soares, H., & Faden, A. L. (1989). Traumatic brain injury in the rat: characterization of a lateral fluid-percussion model. *Neuroscience*, 28(1), 233–244. [https://doi.org/10.1016/0306-4522\(89\)90247-9](https://doi.org/10.1016/0306-4522(89)90247-9)
- McKee, A. C., Stein, T. D., Nowinski, C. J., Stern, R. A., Daneshvar, D. H., Alvarez, V. E., Lee, H. S., Hall, G., Wojtowicz, S. M., Baugh, C. M., Riley, D. O., Kubilus, C. A., Cormier, K. A., Jacobs, M. A., Martin, B. R., Abraham, C. R., Ikezu, T., Reichard, R. R., Wolozin, B. L., ... Cantu, R. C. (2013). The spectrum of disease in chronic traumatic encephalopathy. *Brain*, 136(1), 43–64. <https://doi.org/10.1093/brain/aws307>
- Meijer, H. A., Smith, E. M., & Bushell, M. (2014). Regulation of miRNA strand selection: Follow the leader? *Biochemical Society Transactions*, 42(4), 1135–1140. <https://doi.org/10.1042/BST20140142>
- Menon, D. K., Schwab, K., Wright, D. W., & Maas, A. I. (2010). Position statement: definition of traumatic brain injury. *Archives of Physical Medicine and Rehabilitation*, 91(11), 1637–1640. <https://doi.org/10.1016/j.apmr.2010.05.017>
- Metzger, R. R., Sheng, X., Niedzwecki, C. M., Bennett, K. S., Morita, D. C., Zielinski, B., & Schober, M. E. (2018). Temporal response profiles of serum ubiquitin C-terminal hydrolase-L1 and the 145-kDa alpha II-spectrin breakdown product after severe traumatic brain injury in children. *Journal of Neurosurgery: Pediatrics*, 22(4), 369–374. <https://doi.org/10.3171/2018.4.PEDS17593>
- Michetti, F., D'Ambrosi, N., Toesca, A., Puglisi, M. A., Serrano, A., Marchese, E., Corvino, V., & Geloso, M. C. (2019). The S100B story: from biomarker to active factor in neural injury. *Journal of Neurochemistry*, 148(2), 168–187. <https://doi.org/10.1111/jnc.14574>

- Minami, K., Uehara, T., Morikawa, Y., Omura, K., Kanki, M., Horinouchi, A., Ono, A., Yamada, H., Ohno, Y., & Urushidani, T. (2014). MiRNA expression atlas in male rat. *Scientific Data*, *1*, 1–9.
<https://doi.org/10.1038/sdata.2014.5>
- Miska, E. A., Alvarez-Saavedra, E., Townsend, M., Yoshii, A., Sestan, N., Rakic, P., Constantine-Paton, M., & Horvitz, H. R. (2004). Microarray analysis of microRNA expression in the developing mammalian brain. *Genome Biology*, *5*(9), R68. <https://doi.org/10.1186/gb-2004-5-9-r68>
- Mitchell, P. S., Parkin, R. K., Kroh, E. M., Fritz, B. R., Wyman, S. K., Pogosova-Agadjanian, E. L., Peterson, A., Noteboom, J., O'Briant, K. C., Allen, A., Lin, D. W., Urban, N., Drescher, C. W., Knudsen, B. S., Stirewalt, D. L., Gentleman, R., Vessella, R. L., Nelson, P. S., Martin, D. B., & Tewari, M. (2008). Circulating microRNAs as stable blood-based markers for cancer detection. *Proceedings of the National Academy of Sciences of the United States of America*, *105*(30), 10513–10518.
<https://doi.org/10.1073/pnas.0804549105>
- Mitra, B., Reyes, J., O'Brien, W. T., Surendran, N., Carter, A., Bain, J., McEntaggart, L., Sorich, E., Shultz, S. R., O'Brien, T. J., Willmott, C., Rosenfeld, J. V., & McDonald, S. J. (2022). Micro-RNA levels and symptom profile after mild traumatic brain injury: A longitudinal cohort study. *Journal of Clinical Neuroscience: Official Journal of the Neurosurgical Society of Australasia*, *95*, 81–87.
<https://doi.org/10.1016/j.jocn.2021.11.021>
- Morel, L., Regan, M., Higashimori, H., Ng, S. K., Esau, C., Vidensky, S., Rothstein, J., & Yang, Y. (2013). Neuronal exosomal mirna-dependent translational regulation of astroglial glutamate transporter glt1. *Journal of Biological Chemistry*, *288*(10), 7105–7116.
<https://doi.org/10.1074/jbc.M112.410944>
- Mori, M. A., Ludwig, R. G., Garcia-Martin, R., Brandão, B. B., & Kahn, C. R. (2019). Extracellular miRNAs: From Biomarkers to Mediators of Physiology and Disease. *Cell Metabolism*, *30*(4), 656–673.
<https://doi.org/10.1016/j.cmet.2019.07.011>

- Mustapic, M., Eitan, E., Werner, J. K., Berkowitz, S. T., Lazaropoulos, M. P., Tran, J., Goetzl, E. J., & Kapogiannis, D. (2017). Plasma extracellular vesicles enriched for neuronal origin: A potential window into brain pathologic processes. *Frontiers in Neuroscience*, *11*(MAY), 1–12. <https://doi.org/10.3389/fnins.2017.00278>
- Nass, R. D., Akgün, K., Dague, K. O., Elger, C. E., Reichmann, H., Ziemssen, T., & Surges, R. (2021a). CSF and Serum Biomarkers of Cerebral Damage in Autoimmune Epilepsy. *Frontiers in Neurology*, *12*, 647428. <https://doi.org/10.3389/fneur.2021.647428>
- Nass, R. D., Akgün, K., Elger, C., Reichmann, H., Wagner, M., Surges, R., & Ziemssen, T. (2021b). Serum biomarkers of cerebral cellular stress after self limited tonic clonic seizures: An exploratory study. *Seizure*, *85*(May 2020), 1–5. <https://doi.org/10.1016/j.seizure.2020.12.009>
- Newcombe, V. F. J., Ashton, N. J., Posti, J. P., Glocker, B., Manktelow, A., Chatfield, D. A., Winzeck, S., Needham, E., Correia, M. M., Williams, G. B., Simrén, J., Takala, R. S. K., Katila, A. J., Maanpää, H. R., Tallus, J., Frantzén, J., Blennow, K., Tenovuo, O., Zetterberg, H., & Menon, D. K. (2022). Post-acute blood biomarkers and disease progression in traumatic brain injury. *Brain: A Journal of Neurology*, *145*(6), 2064–2076. <https://doi.org/10.1093/brain/awac126>
- Newman, L. A., Muller, K., & Rowland, A. (2022). Circulating cell-specific extracellular vesicles as biomarkers for the diagnosis and monitoring of chronic liver diseases. *Cellular and Molecular Life Sciences*, *79*(5), 1–23. <https://doi.org/10.1007/s00018-022-04256-8>
- Niemeyer, M. J. S., Jochems, D., Houwert, R. M., van Es, M. A., Leenen, L. P. H., & van Wessel, K. J. P. (2022). Mortality in polytrauma patients with moderate to severe TBI on par with isolated TBI patients: TBI as last frontier in polytrauma patients. *Injury*, *53*(4), 1443–1448. <https://doi.org/10.1016/j.injury.2022.01.009>
- Norman, M., Ter-Ovanesyan, D., Trieu, W., Lazarovits, R., Kowal, E. J. K., Lee, J. H., Chen-Plotkin, A. S., Regev, A., Church, G. M., & Walt, D. R. (2021). L1CAM is not associated with extracellular vesicles in human

cerebrospinal fluid or plasma. *Nature Methods*, 18(6), 631–634.

<https://doi.org/10.1038/s41592-021-01174-8>

- Nudelman, A. S., DiRocco, D. P., Lambert, T. J., Garelick, M. G., Le, J., Nathanson, N. M., & Storm, D. R. (2010). Neuronal activity rapidly induces transcription of the CREB-regulated microRNA-132, in vivo. *Hippocampus*, 20(4), 492–498. <https://doi.org/10.1002/hipo.20646>
- O'Brien, J., Hayder, H., Zayed, Y., & Peng, C. (2018). Overview of microRNA biogenesis, mechanisms of actions, and circulation. *Frontiers in Endocrinology*, 9(AUG), 1–12. <https://doi.org/10.3389/fendo.2018.00402>
- O'Brien, W. T., Pham, L., Brady, R. D., Bain, J., Yamakawa, G. R., Sun, M., Mychasiuk, R., O'Brien, T. J., Monif, M., Shultz, S. R., & McDonald, S. J. (2021). Temporal profile and utility of serum neurofilament light in a rat model of mild traumatic brain injury. *Experimental Neurology*, 341(February). <https://doi.org/10.1016/j.expneurol.2021.113698>
- O'Carroll, D., & Schaefer, A. (2013). General principals of miRNA biogenesis and regulation in the brain. *Neuropsychopharmacology*, 38(1), 39–54. <https://doi.org/10.1038/npp.2012.87>
- O'Connell, G. C., Alder, M. L., Smothers, C. G., Still, C. H., Webel, A. R., & Moore, S. M. (2020). Use of high-sensitivity digital ELISA improves the diagnostic performance of circulating brain-specific proteins for detection of traumatic brain injury during triage. *Neurological Research*, 42(4), 346–353. <https://doi.org/10.1080/01616412.2020.1726588>
- O'Connell, G. C., Smothers, C. G., & Winkelman, C. (2020). Bioinformatic analysis of brain-specific miRNAs for identification of candidate traumatic brain injury blood biomarkers. *Brain Injury*, 34(7), 965–974. <https://doi.org/10.1080/02699052.2020.1764102>
- Okonkwo, D. O., Yue, J. K., Puccio, A. M., Panczykowski, D. M., Inoue, T., McMahon, P. J., Sorani, M. D., Yuh, E. L., Lingsma, H. F., Maas, A. I. R., Valadka, A. B., & Manley, G. T. (2013). GFAP-BDP as an acute diagnostic marker in traumatic brain injury: results from the prospective transforming research and clinical knowledge in traumatic brain injury study. *Journal of Neurotrauma*, 30(17), 1490–1497. <https://doi.org/10.1089/neu.2013.2883>

- Onódi, Z., Pelyhe, C., Nagy, C. T., Brenner, G. B., Almási, L., Kittel, Á., Manček-Keber, M., Ferdinandy, P., Buzás, E. I., & Gircz, Z. (2018). Isolation of high-purity extracellular vesicles by the combination of iodixanol density gradient ultracentrifugation and bind-elute chromatography from blood plasma. *Frontiers in Physiology*, *9*(OCT), 1–11. <https://doi.org/10.3389/fphys.2018.01479>
- Osier, N. D., & Dixon, C. E. (2016). The controlled cortical impact model: Applications, considerations for researchers, and future directions. *Frontiers in Neurology*, *7*(AUG), 1–14. <https://doi.org/10.3389/fneur.2016.00134>
- Ostergard, T., Sweet, J., Kusyk, D., Herring, E., & Miller, J. (2016). Animal models of post-traumatic epilepsy. *Journal of Neuroscience Methods*, *272*, 50–55. <https://doi.org/10.1016/j.jneumeth.2016.03.023>
- Otani, N., Morimoto, Y., Kinoshita, M., Ogata, T., Mori, K., Kobayashi, M., Maeda, T., & Yoshino, A. (2020). Serial changes in serum phosphorylated neurofilament and value for prediction of clinical outcome after traumatic brain injury. *Surgical Neurology International*, *11*, 387. https://doi.org/10.25259/SNI_696_2020
- Ouédraogo, O., Rébillard, R. M., Jamann, H., Mamane, V. H., Clénet, M. L., Daigneault, A., Lahav, B., Uphaus, T., Steffen, F., Bittner, S., Zipp, F., Bérubé, A., Lapalme-Remis, S., Cossette, P., Nguyen, D. K., Arbour, N., Keezer, M. R., & Larochelle, C. (2021). Increased frequency of proinflammatory CD4 T cells and pathological levels of serum neurofilament light chain in adult drug-resistant epilepsy. *Epilepsia*, *62*(1), 176–189. <https://doi.org/10.1111/epi.16742>
- Panina, Y. S., Timechko, E. E., Usoltseva, A. A., Yakovleva, K. D., Kantimirova, E. A., & Dmitrenko, D. V. (2023). Biomarkers of Drug Resistance in Temporal Lobe Epilepsy in Adults. *Metabolites*, *13*(1). <https://doi.org/10.3390/metabo13010083>
- Papa, L., Brophy, G. M., Welch, R. D., Lewis, L. M., Braga, C. F., Tan, C. N., Ameli, N. J., Lopez, M. A., Haeussler, C. A., Mendez Giordano, D. I., Silvestri, S., Giordano, P., Weber, K. D., Hill-Pryor, C., & Hack, D. C. (2016). Time course and diagnostic accuracy of glial and neuronal

- blood biomarkers GFAP and UCH-L1 in a large cohort of trauma patients with and without mild traumatic brain injury. *JAMA Neurology*, 73(5), 551–560. <https://doi.org/10.1001/jamaneurol.2016.0039>
- Papa, L., Lewis, L. M., Silvestri, S., Falk, J. L., Giordano, P., Brophy, G. M., Demery, J. A., Liu, M. C., Mo, J., Akinyi, L., Mondello, S., Schmid, K., Robertson, C. S., Tortella, F. C., Hayes, R. L., & Wang, K. K. W. (2012). Serum levels of ubiquitin C-terminal hydrolase distinguish mild traumatic brain injury from trauma controls and are elevated in mild and moderate traumatic brain injury patients with intracranial lesions and neurosurgical intervention. *The Journal of Trauma and Acute Care Surgery*, 72(5), 1335–1344. <https://doi.org/10.1097/TA.0b013e3182491e3d>
- Papa, L., Slobounov, S. M., Breiter, H. C., Walter, A., Bream, T., Seidenberg, P., Bailes, J. E., Bravo, S., Johnson, B., Kaufman, D., Molfese, D. L., Talavage, T. M., Zhu, D. C., Knollmann-Ritschel, B., & Bhomia, M. (2019). Elevations in MicroRNA Biomarkers in Serum Are Associated with Measures of Concussion, Neurocognitive Function, and Subconcussive Trauma over a Single National Collegiate Athletic Association Division I Season in Collegiate Football Players. *Journal of Neurotrauma*, 36(8), 1343–1351. <https://doi.org/10.1089/neu.2018.6072>
- Pardo, P. S., Hajira, A., Boriek, A. M., & Mohamed, J. S. (2017). MicroRNA-434-3p regulates age-related apoptosis through eIF5A1 in the skeletal muscle. *Aging*, 9(3), 1012–1029. <https://doi.org/10.18632/aging.101207>
- Paul, P., Chakraborty, A., Sarkar, D., Langthasa, M., Rahman, M., Bari, M., Singha, R. K. S., Malakar, A. K., & Chakraborty, S. (2018). Interplay between miRNAs and human diseases. *Journal of Cellular Physiology*, 233(3), 2007–2018. <https://doi.org/10.1002/jcp.25854>
- Pelinka, L. E., Kroepfl, A., Leixnering, M., Buchinger, W., Raabe, A., & Redl, H. (2004). GFAP versus S100B in serum after traumatic brain injury: relationship to brain damage and outcome. *Journal of Neurotrauma*, 21(11), 1553–1561. <https://doi.org/10.1089/neu.2004.21.1553>

- Peng, J., Omran, A., Ashhab, M. U., Kong, H., Gan, N., He, F., & Yin, F. (2013). Expression patterns of miR-124, miR-134, miR-132, and miR-21 in an immature rat model and children with mesial temporal lobe epilepsy. *Journal of Molecular Neuroscience: MN*, 50(2), 291–297. <https://doi.org/10.1007/s12031-013-9953-3>
- Pham, L., Wright, D. K., O'Brien, W. T., Bain, J., Huang, C., Sun, M., Casillas-Espinosa, P. M., Shah, A. D., Schittenhelm, R. B., Sobey, C. G., Brady, R. D., O'Brien, T. J., Mychasiuk, R., Shultz, S. R., & McDonald, S. J. (2021). Behavioral, axonal, and proteomic alterations following repeated mild traumatic brain injury: Novel insights using a clinically relevant rat model. *Neurobiology of Disease*, 148, 105151. <https://doi.org/10.1016/j.nbd.2020.105151>
- Pitkänen, A. (2010). Therapeutic approaches to epileptogenesis - Hope on the horizon. *Epilepsia*, 51(SUPPL. 3), 2–17. <https://doi.org/10.1111/j.1528-1167.2010.02602.x>
- Pitkänen, A., Ekolle Ndode-Ekane, X., Lapinlampi, N., & Puhakka, N. (2019). Epilepsy biomarkers - Toward etiology and pathology specificity. *Neurobiology of Disease*, 123, 42–58. <https://doi.org/10.1016/j.nbd.2018.05.007>
- Pitkänen, A., & Immonen, R. (2014). Epilepsy Related to Traumatic Brain Injury. *Neurotherapeutics*, 11(2), 286–296. <https://doi.org/10.1007/s13311-014-0260-7>
- Pitkänen, A., Immonen, R. J., Gröhn, O. H. J., & Kharatishvili, I. (2009). From traumatic brain injury to posttraumatic epilepsy: what animal models tell us about the process and treatment options. *Epilepsia*, 50 Suppl 2, 21–29. <https://doi.org/10.1111/j.1528-1167.2008.02007.x>
- Pitkänen, A., Lukasiuk, K., Dudek, F. E., & Staley, K. J. (2015). Epileptogenesis. *Cold Spring Harbor Perspectives in Medicine*, 5(10). <https://doi.org/10.1101/cshperspect.a022822>
- Pitkänen, A., & McIntosh, T. K. (2006). Animal models of post-traumatic epilepsy. *Journal of Neurotrauma*, 23(2), 241–261. <https://doi.org/10.1089/neu.2006.23.241>

- Pitkänen, A., Paananen, T., Kyyriäinen, J., Das Gupta, S., Heiskanen, M., Vuokila, N., Bañuelos-Cabrera, I., Lapinlampi, N., Kajevu, N., Andrade, P., Ciszek, R., Lara-Valderrábano, L., Ekolle Ndode-Ekane, X., & Puhakka, N. (2021). Biomarkers for posttraumatic epilepsy. *Epilepsy and Behavior*, 121(xxxx), 107080.
<https://doi.org/10.1016/j.yebeh.2020.107080>
- Polito, F., Famà, F., Oteri, R., Raffa, G., Vita, G., Conti, A., Daniele, S., Macaione, V., Passalacqua, M., Cardali, S., Di Giorgio, R. M., Gioffrè, M., Angileri, F. F., Germanò, A., & Aguenouz, M. (2020). Circulating miRNAs expression as potential biomarkers of mild traumatic brain injury. *Molecular Biology Reports*, 47(4), 2941–2949.
<https://doi.org/10.1007/s11033-020-05386-7>
- Pollard, J. R., Eidelman, O., Mueller, G. P., Dalgard, C. L., Crino, P. B., Anderson, C. T., Brand, E. J., Burakgazi, E., Ivaturi, S. K., & Pollard, H. B. (2012). The TARC/sICAM5 Ratio in Patient Plasma is a Candidate Biomarker for Drug Resistant Epilepsy. *Frontiers in Neurology*, 3, 181.
<https://doi.org/10.3389/fneur.2012.00181>
- Posti, J. P., Takala, R. S. K., Runtti, H., Newcombe, V. F., Outtrim, J., Katila, A. J., Frantzén, J., Ala-Seppälä, H., Coles, J. P., Iftakher Hossain, M., Kyllönen, A., Maanpää, H. R., Tallus, J., Hutchinson, P. J., Van Gils, M., Menon, D. K., & Tenovuo, O. (2016). The Levels of Glial Fibrillary Acidic Protein and Ubiquitin C-Terminal Hydrolase-L1 during the First Week after a Traumatic Brain Injury: Correlations with Clinical and Imaging Findings. *Neurosurgery*, 79(3), 456–463.
<https://doi.org/10.1227/NEU.0000000000001226>
- Posti, J. P., Luoto, T. M., Sipilä, J. O. T., Rautava, P., & Kytö, V. (2022). Changing epidemiology of traumatic brain injury among the working-aged in Finland: Admissions and neurosurgical operations. *Acta Neurologica Scandinavica*, 146(1), 34–41.
<https://doi.org/10.1111/ane.13607>
- Puffer, R. C., Cumba Garcia, L. M., Himes, B. T., Jung, M. Y., Meyer, F. B., Okonkwo, D. O., & Parney, I. F. (2021). Plasma extracellular vesicles as a source of biomarkers in traumatic brain injury. *Journal of*

Neurosurgery, 134(6), 1921–1928.

<https://doi.org/10.3171/2020.4.JNS20305>

Qin, X., Li, L., Lv, Q., Shu, Q., Zhang, Y., & Wang, Y. (2018). Expression profile of plasma microRNAs and their roles in diagnosis of mild to severe traumatic brain injury. *PloS One*, 13(9), e0204051.

<https://doi.org/10.1371/journal.pone.0204051>

Raheja, A., Sinha, S., Samson, N., Bhoi, S., Subramanian, A., Sharma, P., & Sharma, B. S. (2016). Serum biomarkers as predictors of long-term outcome in severe traumatic brain injury: analysis from a randomized placebo-controlled Phase II clinical trial. *Journal of Neurosurgery*, 125(3), 631–641. <https://doi.org/10.3171/2015.6.JNS15674>

Rainer, T. H., Leung, L. Y., Chan, C. P. Y., Leung, Y. K., Abrigo, J. M., Wang, D., & Graham, C. A. (2016). Plasma miR-124-3p and miR-16 concentrations as prognostic markers in acute stroke. *Clinical Biochemistry*, 49(9), 663–668. <https://doi.org/https://doi.org/10.1016/j.clinbiochem.2016.02.016>

Raj, R., Wennervirta, J. M., Tjerkaski, J., Luoto, T. M., Posti, J. P., Nelson, D. W., Takala, R., Bendel, S., Thelin, E. P., Luostarinen, T., & Korja, M. (2022). Dynamic prediction of mortality after traumatic brain injury using a machine learning algorithm. *Npj Digital Medicine*, 5(1).

<https://doi.org/10.1038/s41746-022-00652-3>

Raouf, R., Bauer, S., El Naggar, H., Connolly, N. M. C., Brennan, G. P., Brindley, E., Hill, T., McArdle, H., Spain, E., Forster, R. J., Prehn, J. H. M., Hamer, H., Delanty, N., Rosenow, F., Mooney, C., & Henshall, D. C. (2018). Dual-center, dual-platform microRNA profiling identifies potential plasma biomarkers of adult temporal lobe epilepsy.

EBioMedicine, 38, 127–141.

<https://doi.org/10.1016/j.ebiom.2018.10.068>

Raouf, R., Jimenez-Mateos, E. M., Bauer, S., Tackenberg, B., Rosenow, F., Lang, J., Onugoren, M. D., Hamer, H., Huchtemann, T., Körtvélyessy, P., Connolly, N. M. C., Pfeiffer, S., Prehn, J. H. M., Farrell, M. A., O'Brien, D. F., Henshall, D. C., & Mooney, C. (2017). Cerebrospinal fluid microRNAs are potential biomarkers of temporal lobe epilepsy and status

- epilepticus. *Scientific Reports*, 7(1), 1–17.
<https://doi.org/10.1038/s41598-017-02969-6>
- Raposo, G., Nijman, H. W., Stoorvogel, W., Liejendekker, R., Harding, C. V., Melief, C. J., & Geuze, H. J. (1996). B lymphocytes secrete antigen-presenting vesicles. *The Journal of Experimental Medicine*, 183(3), 1161–1172. <https://doi.org/10.1084/jem.183.3.1161>
- Ravanidis, S., Bougea, A., Papagiannakis, N., Maniati, M., Koros, C., Simitsi, A.-M., Bozi, M., Pachi, I., Stamelou, M., Paraskevas, G. P., Kapaki, E., Moraitou, M., Michelakakis, H., Stefanis, L., & Doxakis, E. (2020). Circulating Brain-enriched MicroRNAs for detection and discrimination of idiopathic and genetic Parkinson's disease. *Movement Disorders: Official Journal of the Movement Disorder Society*, 35(3), 457–467.
<https://doi.org/10.1002/mds.27928>
- Redell, J. B., Moore, A. N., Ward, N. H. 3rd, Hergenroeder, G. W., & Dash, P. K. (2010). Human traumatic brain injury alters plasma microRNA levels. *Journal of Neurotrauma*, 27(12), 2147–2156.
<https://doi.org/10.1089/neu.2010.1481>
- Reid, A. Y., Bragin, A., Giza, C. C., Staba, R. J., & Engel, J. J. (2016). The progression of electrophysiologic abnormalities during epileptogenesis after experimental traumatic brain injury. *Epilepsia*, 57(10), 1558–1567. <https://doi.org/10.1111/epi.13486>
- Rekker, K., Saare, M., Roost, A. M., Kubo, A.-L., Zarovni, N., Chiesi, A., Salumets, A., & Peters, M. (2014). Comparison of serum exosome isolation methods for microRNA profiling. *Clinical Biochemistry*, 47(1), 135–138.
<https://doi.org/https://doi.org/10.1016/j.clinbiochem.2013.10.020>
- Remenyi, J., van den Bosch, M. W. M., Palygin, O., Mistry, R. B., McKenzie, C., Macdonald, A., Hutvagner, G., Arthur, J. S. C., Frenguelli, B. G., & Pankratov, Y. (2013). miR-132/212 knockout mice reveal roles for these miRNAs in regulating cortical synaptic transmission and plasticity. *PLoS One*, 8(4), e62509. <https://doi.org/10.1371/journal.pone.0062509>
- Rikkert, L. G., Nieuwland, R., Terstappen, L. W. M. M., & Coumans, F. A. W. (2019). Quality of extracellular vesicle images by transmission electron

microscopy is operator and protocol dependent. *Journal of Extracellular Vesicles*, 8(1).

<https://doi.org/10.1080/20013078.2018.1555419>

Rissin, D. M., Kan, C. W., Campbell, T. G., Howes, S. C., Fournier, D. R., Song, L., Piech, T., Patel, P. P., Chang, L., Rivnak, A. J., Ferrell, E. P., Randall, J. D., Provuncher, G. K., Walt, D. R., & Duffy, D. C. (2010). Single-molecule enzyme-linked immunosorbent assay detects serum proteins at subfemtomolar concentrations. *Nature Biotechnology*, 28(6), 595–599.

<https://doi.org/10.1038/nbt.1641>

Roncon, P., Soukupová, M., Binaschi, A., Falcicchia, C., Zucchini, S., Ferracin, M., Langley, S. R., Petretto, E., Johnson, M. R., Marucci, G., Michelucci, R., Rubboli, G., & Simonato, M. (2015). MicroRNA profiles in hippocampal granule cells and plasma of rats with pilocarpine-induced epilepsy--comparison with human epileptic samples. *Scientific Reports*, 5, 14143. <https://doi.org/10.1038/srep14143>

Russell, E. R., Mackay, D. F., Stewart, K., MacLean, J. A., Pell, J. P., & Stewart, W. (2021). Association of Field Position and Career Length With Risk of Neurodegenerative Disease in Male Former Professional Soccer Players. *JAMA Neurology*, 78(9), 1057–1063.

<https://doi.org/10.1001/jamaneurol.2021.2403>

Sajja, V. S. S. S., Jablonska, A., Haughey, N., Bulte, J. W. M., Stevens, R. D., Long, J. B., Walczak, P., & Janowski, M. (2018). Sphingolipids and microRNA Changes in Blood following Blast Traumatic Brain Injury: An Exploratory Study. *Journal of Neurotrauma*, 35(2), 353–361.

<https://doi.org/10.1089/neu.2017.5009>

Sanchez-Cabrero, D., Garcia-Guede, Á., Burdiel, M., Pernía, O., Colmenarejo-Fernandez, J., Gutierrez, L., Higuera, O., Rodriguez, I. E., Rosas-Alonso, R., Rodriguez-Antolín, C., Losantos-García, I., Vera, O., De Castro-Carpeño, J., & Ibanez de Caceres, I. (2023). miR-124 as a Liquid Biopsy Prognostic Biomarker in Small Extracellular Vesicles from NSCLC Patients. *International Journal of Molecular Sciences*, 24(14). <https://doi.org/10.3390/ijms241411464>

- Santana-Gomez, C. E., Medel-Matus, J. S., & Rundle, B. K. (2021). Animal models of post-traumatic epilepsy and their neurobehavioral comorbidities. *Seizure, 90*(May), 9–16.
<https://doi.org/10.1016/j.seizure.2021.05.008>
- Santangelo, A., Imbrucè, P., Gardenghi, B., Belli, L., Agushi, R., Tamanini, A., Munari, S., Bossi, A. M., Scambi, I., Benati, D., Mariotti, R., Di Gennaro, G., Sbarbati, A., Eccher, A., Ricciardi, G. K., Ciceri, E. M., Sala, F., Pinna, G., Lippi, G., ... Dehecchi, M. C. (2018). A microRNA signature from serum exosomes of patients with glioma as complementary diagnostic biomarker. *Journal of Neuro-Oncology, 136*(1), 51–62.
<https://doi.org/10.1007/s11060-017-2639-x>
- Schindler, C. R., Woschek, M., Vollrath, J. T., Konradowitz, K., Lustenberger, T., Störmann, P., Marzi, I., & Henrich, D. (2020). miR-142-3p Expression Is Predictive for Severe Traumatic Brain Injury (TBI) in Trauma Patients. *International Journal of Molecular Sciences, 21*(15).
<https://doi.org/10.3390/ijms21155381>
- Schnatz, A., Müller, C., Brahmer, A., & Krämer-Albers, E. M. (2021). Extracellular Vesicles in neural cell interaction and CNS homeostasis. *FASEB BioAdvances, 3*(8), 577–592. <https://doi.org/10.1096/fba.2021-00035>
- Selbach, M., Schwanhäusser, B., Thierfelder, N., Fang, Z., Khanin, R., & Rajewsky, N. (2008). Widespread changes in protein synthesis induced by microRNAs. *Nature, 455*(7209), 58–63.
<https://doi.org/10.1038/nature07228>
- Senaratne, N., Hunt, A., Sotsman, E., & Grey, M. J. (2022). Biomarkers to aid the return to play decision following sports-related concussion: a systematic review. *Journal of Concussion, 6*, 205970022110707.
<https://doi.org/10.1177/20597002211070735>
- Serrano-Pertierra, E., Oliveira-Rodríguez, M., Rivas, M., Oliva, P., Villafani, J., Navarro, A., Blanco-López, M. C., & Cernuda-Morollón, E. (2019). Characterization of plasma-derived extracellular vesicles isolated by different methods: A comparison study. *Bioengineering, 6*(1), 1–13.
<https://doi.org/10.3390/bioengineering6010008>

- Shahim, P., Gren, M., Liman, V., Andreasson, U., Norgren, N., Tegner, Y., Mattsson, N., Andreasen, N., Öst, M., Zetterberg, H., Nellgård, B., & Blennow, K. (2016). Serum neurofilament light protein predicts clinical outcome in traumatic brain injury. *Scientific Reports*, 6(November), 1–9. <https://doi.org/10.1038/srep36791>
- Shahim, P., Politis, A., van der Merwe, A., Moore, B., Chou, Y. Y., Pham, D. L., Butman, J. A., Diaz-Arrastia, R., Gill, J. M., Brody, D. L., Zetterberg, H., Blennow, K., & Chan, L. (2020). Neurofilament light as a biomarker in traumatic brain injury. *Neurology*, 95(6), e610–e622. <https://doi.org/10.1212/WNL.0000000000009983>
- Shahim, P., Politis, A., van der Merwe, A., Moore, B., Ekanayake, V., Lippa, S. M., Chou, Y. Y., Pham, D. L., Butman, J. A., Diaz-Arrastia, R., Zetterberg, H., Blennow, K., Gill, J. M., Brody, D. L., & Chan, L. (2020). Time course and diagnostic utility of NfL, tau, GFAP, and UCH-L1 in subacute and chronic TBI. *Neurology*, 95(6), e623–e636. <https://doi.org/10.1212/WNL.0000000000009985>
- Shahim, P., Tegner, Y., Wilson, D. H., Randall, J., Skillbäck, T., Pazooki, D., Kallberg, B., Blennow, K., & Zetterberg, H. (2014). Blood biomarkers for brain injury in concussed professional ice hockey players. *JAMA Neurology*, 71(6), 684–692. <https://doi.org/10.1001/jamaneurol.2014.367>
- Shahim, P., Zetterberg, H., Tegner, Y., & Blennow, K. (2017). Serum neurofilament light as a biomarker for mild traumatic brain injury in contact sports. *Neurology*, 88(19), 1788–1794. <https://doi.org/10.1212/WNL.0000000000003912>
- Shang, F.-F., Xia, Q.-J., Liu, W., Xia, L., Qian, B.-J., You, L., He, M., Yang, J.-L., & Wang, T.-H. (2016). miR-434-3p and DNA hypomethylation co-regulate eIF5A1 to increase AChRs and to improve plasticity in SCT rat skeletal muscle. *Scientific Reports*, 6, 22884. <https://doi.org/10.1038/srep22884>
- Shang, R., Lee, S., Senavirathne, G., & Lai, E. C. (2023). microRNAs in action: biogenesis, function and regulation. *Nature Reviews Genetics*. <https://doi.org/10.1038/s41576-023-00611-y>

- Sharma, A., Chandran, R., Barry, E. S., Bhomia, M., Hutchison, M. A., Balakathiresan, N. S., Grunberg, N. E., & Maheshwari, R. K. (2014). Identification of serum microRNA signatures for diagnosis of mild traumatic brain injury in a closed head injury model. *PloS One*, *9*(11), e112019. <https://doi.org/10.1371/journal.pone.0112019>
- Sharma, R., & Laskowitz, D. T. (2012). Biomarkers in traumatic brain injury. *Current Neurology and Neuroscience Reports*, *12*(5), 560–569. <https://doi.org/10.1007/s11910-012-0301-8>
- Sheinerman, K. S., Tsvinsky, V. G., Abdullah, L., Crawford, F., & Umansky, S. R. (2013). Plasma microRNA biomarkers for detection of mild cognitive impairment: biomarker validation study. *Aging*, *5*(12), 925–938. <https://doi.org/10.18632/aging.100624>
- Shen, C.-H., Zhang, Y.-X., Zheng, Y., Yang, F., Hu, Y., Xu, S., Yan, S.-Q., Ding, Y., Guo, Y., & Ding, M.-P. (2019). Expression of plasma microRNA-145-5p and its correlation with clinical features in patients with refractory epilepsy. *Epilepsy Research*, *154*, 21–25. <https://doi.org/10.1016/j.eplesyres.2019.04.010>
- Shi, M., Sheng, L., Stewart, T., Zabetian, C. P., & Zhang, J. (2019). New windows into the brain: Central nervous system-derived extracellular vesicles in blood. *Progress in Neurobiology*, *175*, 96–106. <https://doi.org/10.1016/j.pneurobio.2019.01.005>
- Shibahashi, K., Doi, T., Tanaka, S., Hoda, H., Chikuda, H., Sawada, Y., Takasu, Y., Chiba, K., Nozaki, T., Hamabe, Y., & Ogata, T. (2016). The Serum Phosphorylated Neurofilament Heavy Subunit as a Predictive Marker for Outcome in Adult Patients after Traumatic Brain Injury. *Journal of Neurotrauma*, *33*(20), 1826–1833. <https://doi.org/10.1089/neu.2015.4237>
- Shultz, S. R., Taylor, C. J., Aggio-Bruce, R., O'Brien, W. T., Sun, M., Cioanca, A. V., Neocleous, G., Symons, G. F., Brady, R. D., Hardikar, A. A., Joglekar, M. V, Costello, D. M., O'Brien, T. J., Natoli, R., & McDonald, S. J. (2022). Decrease in Plasma miR-27a and miR-221 After Concussion in Australian Football Players. *Biomarker Insights*, *17*, 11772719221081318. <https://doi.org/10.1177/11772719221081318>

- Sierra, A., Laitinen, T., Gröhn, O., & Pitkänen, A. (2015). Diffusion tensor imaging of hippocampal network plasticity. *Brain Structure & Function*, 220(2), 781–801. <https://doi.org/10.1007/s00429-013-0683-7>
- Sim, S.-E., Lim, C.-S., Kim, J.-I., Seo, D., Chun, H., Yu, N.-K., Lee, J., Kang, S. J., Ko, H.-G., Choi, J.-H., Kim, T., Jang, E.-H., Han, J., Bak, M. S., Park, J.-E., Jang, D.-J., Baek, D., Lee, Y.-S., & Kaang, B.-K. (2016). The Brain-Enriched MicroRNA miR-9-3p Regulates Synaptic Plasticity and Memory. *The Journal of Neuroscience: The Official Journal of the Society for Neuroscience*, 36(33), 8641–8652. <https://doi.org/10.1523/JNEUROSCI.0630-16.2016>
- Simani, L., Elmi, M., & Asadollahi, M. (2018). Serum GFAP level: A novel adjunctive diagnostic test in differentiate epileptic seizures from psychogenic attacks. *Seizure*, 61(July), 41–44. <https://doi.org/10.1016/j.seizure.2018.07.010>
- Simani, L., Sadeghi, M., Ryan, F., Dehghani, M., & Niknazar, S. (2020). Elevated Blood-Based Brain Biomarker Levels in Patients with Epileptic Seizures: A Systematic Review and Meta-analysis. *ACS Chemical Neuroscience*, 11(24), 4048–4059. <https://doi.org/10.1021/acscchemneuro.0c00492>
- Smith, D. H., Soares, H. D., Pierce, J. S., Perlman, K. G., Saatman, K. E., Meaney, D. F., Dixon, C. E., & McIntosh, T. K. (1995). A model of parasagittal controlled cortical impact in the mouse: cognitive and histopathologic effects. *Journal of Neurotrauma*, 12(2), 169–178. <https://doi.org/10.1089/neu.1995.12.169>
- Sohn, W., Kim, J., Kang, S. H., Yang, S. R., Cho, J. Y., Cho, H. C., Shim, S. G., & Paik, Y. H. (2015). Serum exosomal microRNAs as novel biomarkers for hepatocellular carcinoma. *Experimental and Molecular Medicine*, 47(9), e184-8. <https://doi.org/10.1038/emm.2015.68>
- Stein, D. M., Lindell, A., Murdock, K. R., Kufera, J. A., Menaker, J., Keledjian, K., Bochicchio, G. V, Aarabi, B., & Scalea, T. M. (2011). Relationship of serum and cerebrospinal fluid biomarkers with intracranial hypertension and cerebral hypoperfusion after severe traumatic brain

- injury. *The Journal of Trauma*, 70(5), 1096–1103.
<https://doi.org/10.1097/TA.0b013e318216930d>
- Sun, B., Dalvi, P., Abadjian, L., Tang, N., & Pulliam, L. (2017). Blood neuron-derived exosomes as biomarkers of cognitive impairment in HIV. *Aids*, 31(14), F9–F17. <https://doi.org/10.1097/QAD.0000000000001595>
- Sun, L., Liu, A., Zhang, J., Ji, W., Li, Y., Yang, X., Wu, Z., & Guo, J. (2018). miR-23b improves cognitive impairments in traumatic brain injury by targeting ATG12-mediated neuronal autophagy. *Behavioural Brain Research*, 340, 126–136. <https://doi.org/10.1016/j.bbr.2016.09.020>
- Sun, Y., Wang, X., Wang, Z., Zhang, Y., Che, N., Luo, X., Tan, Z., Sun, X., Li, X., Yang, K., Wang, G., Luan, L., Liu, Y., Zheng, X., Wei, M., Cheng, H., & Yin, J. (2016). Expression of microRNA-129-2-3p and microRNA-935 in plasma and brain tissue of human refractory epilepsy. *Epilepsy Research*, 127, 276–283.
<https://doi.org/10.1016/j.epilepsyres.2016.09.016>
- Surges, R., Kretschmann, A., Abnaof, K., van Rikxoort, M., Ridder, K., Fröhlich, H., Danis, B., Kaminski, R. M., Foerch, P., Elger, C. E., Weinsberg, F., & Pfeifer, A. (2016). Changes in serum miRNAs following generalized convulsive seizures in human mesial temporal lobe epilepsy. *Biochemical and Biophysical Research Communications*, 481(1–2), 13–18. <https://doi.org/10.1016/j.bbrc.2016.11.029>
- Svingos, A. M., Asken, B. M., Bauer, R. M., DeKosky, S. T., Hromas, G. A., Jaffee, M. S., Hayes, R. L., & Clugston, J. R. (2019). Exploratory study of sport-related concussion effects on peripheral micro-RNA expression. *Brain Injury*, 33(4), 1–7.
<https://doi.org/10.1080/02699052.2019.1573379>
- Takala, R. S. K., Posti, J. P., Runtti, H., Newcombe, V. F., Outtrim, J., Katila, A. J., Frantzén, J., Ala-Seppälä, H., Kyllönen, A., Maanpää, H. R., Tallus, J., Hossain, M. I., Coles, J. P., Hutchinson, P., Van Gils, M., Menon, D. K., & Tenovuo, O. (2016). Glial Fibrillary Acidic Protein and Ubiquitin C-Terminal Hydrolase-L1 as Outcome Predictors in Traumatic Brain Injury. *World Neurosurgery*, 87, 8–20.
<https://doi.org/10.1016/j.wneu.2015.10.066>

- Tang, Y.-T., Huang, Y.-Y., Zheng, L., Qin, S.-H., Xu, X.-P., An, T.-X., Xu, Y., Wu, Y.-S., Hu, X.-M., Ping, B.-H., & Wang, Q. (2017). Comparison of isolation methods of exosomes and exosomal RNA from cell culture medium and serum. *International Journal of Molecular Medicine*, *40*(3), 834–844. <https://doi.org/10.3892/ijmm.2017.3080>
- Teasdale, G., Maas, A., Lecky, F., Manley, G., Stocchetti, N., & Murray, G. (2014). The Glasgow Coma Scale at 40 years: standing the test of time. *The Lancet. Neurology*, *13*(8), 844–854. [https://doi.org/10.1016/S1474-4422\(14\)70120-6](https://doi.org/10.1016/S1474-4422(14)70120-6)
- Thelin, E., Al Nimer, F., Frostell, A., Zetterberg, H., Blennow, K., Nyström, H., Svensson, M., Bellander, B. M., Piehl, F., & Nelson, D. W. (2019). A Serum protein biomarker panel improves outcome prediction in human traumatic brain injury. *Journal of Neurotrauma*, *36*(20), 2850–2862. <https://doi.org/10.1089/neu.2019.6375>
- Théry, C., Witwer, K. W., Aikawa, E., Alcaraz, M. J., Anderson, J. D., Andriantsitohaina, R., Antoniou, A., Arab, T., Archer, F., Atkin-Smith, G. K., Ayre, D. C., Bach, J. M., Bachurski, D., Baharvand, H., Balaj, L., Baldacchino, S., Bauer, N. N., Baxter, A. A., Bebawy, M., ... Zuba-Surma, E. K. (2018). Minimal information for studies of extracellular vesicles 2018 (MISEV2018): a position statement of the International Society for Extracellular Vesicles and update of the MISEV2014 guidelines. *Journal of Extracellular Vesicles*, *7*(1). <https://doi.org/10.1080/20013078.2018.1535750>
- Thompson, A. G., Gray, E., Heman-Ackah, S. M., Mäger, I., Talbot, K., Andaloussi, S. El, Wood, M. J., & Turner, M. R. (2016). Extracellular vesicles in neurodegenerative disease - pathogenesis to biomarkers. *Nature Reviews. Neurology*, *12*(6), 346–357. <https://doi.org/10.1038/nrneurol.2016.68>
- Thompson, H. J., LeBold, D. G., Marklund, N., Morales, D. M., Hagner, A. P., & McIntosh, T. K. (2006). Cognitive evaluation of traumatically brain-injured rats using serial testing in the Morris water maze. *Restorative Neurology and Neuroscience*, *24*(2), 109–114.

- Toffolo, K., Osei, J., Kelly, W., Poulsen, A., Donahue, K., Wang, J., Hunter, M., Bard, J., Wang, J., & Poulsen, D. (2019). Circulating microRNAs as biomarkers in traumatic brain injury. *Neuropharmacology*, *145*, 199–208. <https://doi.org/https://doi.org/10.1016/j.neuropharm.2018.08.028>
- Turchinovich, A., Weiz, L., & Burwinkel, B. (2012). Extracellular miRNAs: the mystery of their origin and function. *Trends in Biochemical Sciences*, *37*(11), 460–465. <https://doi.org/10.1016/j.tibs.2012.08.003>
- Turchinovich, A., Weiz, L., Langheinz, A., & Burwinkel, B. (2011). Characterization of extracellular circulating microRNA. *Nucleic Acids Research*, *39*(16), 7223–7233. <https://doi.org/10.1093/nar/gkr254>
- Undén, J., Ingebrigtsen, T., & Romner, B. (2013). Scandinavian guidelines for initial management of minimal, mild and moderate head injuries in adults: an evidence and consensus-based update. *BMC Medicine*, *11*, 50. <https://doi.org/10.1186/1741-7015-11-50>
- Upadhyaya, R., Zingg, W., Shetty, S., & Shetty, A. K. (2020). Astrocyte-derived extracellular vesicles: Neuroreparative properties and role in the pathogenesis of neurodegenerative disorders. *Journal of Controlled Release*, *323*, 225–239. <https://doi.org/10.1016/j.jconrel.2020.04.017>
- Valadi, H., Ekström, K., Bossios, A., Sjöstrand, M., Lee, J. J., & Lötvall, J. O. (2007). Exosome-mediated transfer of mRNAs and microRNAs is a novel mechanism of genetic exchange between cells. *Nature Cell Biology*, *9*(6), 654–659. <https://doi.org/10.1038/ncb1596>
- van der Pol, E., Böing, A. N., Harrison, P., Sturk, A., & Nieuwland, R. (2012). Classification, functions, and clinical relevance of extracellular vesicles. *Pharmacological Reviews*, *64*(3), 676–705. <https://doi.org/10.1124/pr.112.005983>
- Van Deun, J., Mestdagh, P., Sormunen, R., Cocquyt, V., Vermaelen, K., Vandesompele, J., Bracke, M., De Wever, O., & Hendrix, A. (2014). The impact of disparate isolation methods for extracellular vesicles on downstream RNA profiling. *Journal of Extracellular Vesicles*, *3*(1). <https://doi.org/10.3402/jev.v3.24858>
- Venø, M. T., Reschke, C. R., Morris, G., Connolly, N. M. C., Su, J., Yan, Y., Engel, T., Jimenez-Mateos, E. M., Harder, L. M., Pultz, D., Haunsberger,

- S. J., Pal, A., Heller, J. P., Campbell, A., Langa, E., Brennan, G. P., Conboy, K., Richardson, A., Norwood, B. A., ... Henshall, D. C. (2020). A systems approach delivers a functional microRNA catalog and expanded targets for seizure suppression in temporal lobe epilepsy. *Proceedings of the National Academy of Sciences of the United States of America*, 117(27), 15977–15988. <https://doi.org/10.1073/pnas.1919313117>
- Vergauwen, G., Tulkens, J., Pinheiro, C., Avila Cobos, F., Dedeyne, S., De Scheerder, M. A., Vandekerckhove, L., Impens, F., Miinalainen, I., Braems, G., Gevaert, K., Mestdagh, P., Vandesompele, J., Denys, H., De Wever, O., & Hendrix, A. (2021). Robust sequential biophysical fractionation of blood plasma to study variations in the biomolecular landscape of systemically circulating extracellular vesicles across clinical conditions. *Journal of Extracellular Vesicles*, 10(10). <https://doi.org/10.1002/jev2.12122>
- Vezzani, A., Aronica, E., Mazarati, A., & Pittman, Q. J. (2013). Epilepsy and brain inflammation. *Experimental Neurology*, 244, 11–21. <https://doi.org/10.1016/j.expneurol.2011.09.033>
- Vezzani, A., French, J., Bartfai, T., & Baram, T. Z. (2011). The role of inflammation in epilepsy. *Nature Reviews. Neurology*, 7(1), 31–40. <https://doi.org/10.1038/nrneurol.2010.178>
- Vickers, K. C., Palmisano, B. T., Shoucri, B. M., Shamburek, R. D., & Remaley, A. T. (2011). MicroRNAs are transported in plasma and delivered to recipient cells by high-density lipoproteins. *Nature Cell Biology*, 13(4), 423–433. <https://doi.org/10.1038/ncb2210>
- Vidal, M. (2019). Exosomes: Revisiting their role as “garbage bags.” *Traffic*, 20(11), 815–828. <https://doi.org/10.1111/tra.12687>
- Visser, K., Koggel, M., Blaauw, J., van der Horn, H. J., Jacobs, B., & van der Naalt, J. (2022). Blood-based biomarkers of inflammation in mild traumatic brain injury: A systematic review. *Neuroscience and Biobehavioral Reviews*, 132(November 2021), 154–168. <https://doi.org/10.1016/j.neubiorev.2021.11.036>
- Vo, N., Klein, M. E., Varlamova, O., Keller, D. M., Yamamoto, T., Goodman, R. H., & Impey, S. (2005). A cAMP-response element binding protein-

- induced microRNA regulates neuronal morphogenesis. *Proceedings of the National Academy of Sciences of the United States of America*, 102(45), 16426–16431. <https://doi.org/10.1073/pnas.0508448102>
- von Räden, E.-L., Janssen-Peters, H., Reiber, M., van Dijk, R. M., Xiao, K., Seiffert, I., Koska, I., Hubl, C., Thum, T., & Potschka, H. (2023). An exploratory approach to identify microRNAs as circulatory biomarker candidates for epilepsy-associated psychiatric comorbidities in an electrical post-status epilepticus model. *Scientific Reports*, 13(1), 4552. <https://doi.org/10.1038/s41598-023-31017-9>
- Vorn, R., Suarez, M., White, J. C., Martin, C. A., Kim, H.-S., Lai, C., Yun, S.-J., Gill, J. M., & Lee, H. (2021). Exosomal microRNA Differential Expression in Plasma of Young Adults with Chronic Mild Traumatic Brain Injury and Healthy Control. *Biomedicines*, 10(1). <https://doi.org/10.3390/biomedicines10010036>
- Vuokila, N., Das Gupta, S., Huusko, R., Tohka, J., Puhakka, N., & Pitkänen, A. (2020). Elevated Acute Plasma miR-124-3p Level Relates to Evolution of Larger Cortical Lesion Area after Traumatic Brain Injury. *Neuroscience*, 433, 21–35. <https://doi.org/10.1016/j.neuroscience.2020.02.045>
- Vuokila, N., Lukasiuk, K., Bot, A. M., van Vliet, E. A., Aronica, E., Pitkänen, A., & Puhakka, N. (2018). miR-124-3p is a chronic regulator of gene expression after brain injury. *Cellular and Molecular Life Sciences : CMLS*, 75(24), 4557–4581. <https://doi.org/10.1007/s00018-018-2911-z>
- Wagner, J., Riwanto, M., Besler, C., Knau, A., Fichtlscherer, S., Röxe, T., Zeiher, A. M., Landmesser, U., & Dimmeler, S. (2013). Characterization of levels and cellular transfer of circulating lipoprotein-bound microRNAs. *Arteriosclerosis, Thrombosis, and Vascular Biology*, 33(6), 1392–1400. <https://doi.org/10.1161/ATVBAHA.112.300741>
- Wanet, A., Tacheny, A., Arnould, T., & Renard, P. (2012). miR-212/132 expression and functions: within and beyond the neuronal compartment. *Nucleic Acids Research*, 40(11), 4742–4753. <https://doi.org/10.1093/nar/gks151>
- Wang, J., Tan, L., Tan, L., Tian, Y., Ma, J., Tan, C.-C., Wang, H.-F., Liu, Y., Tan, M.-S., Jiang, T., & Yu, J.-T. (2015). Circulating microRNAs are promising

- novel biomarkers for drug-resistant epilepsy. *Scientific Reports*, 5, 10201. <https://doi.org/10.1038/srep10201>
- Wang, J., Yu, J.-T., Tan, L., Tian, Y., Ma, J., Tan, C.-C., Wang, H.-F., Liu, Y., Tan, M.-S., Jiang, T., & Tan, L. (2015). Genome-wide circulating microRNA expression profiling indicates biomarkers for epilepsy. *Scientific Reports*, 5, 9522. <https://doi.org/10.1038/srep09522>
- Wang, K. K., Yang, Z., Zhu, T., Shi, Y., Rubenstein, R., Tyndall, J. A., & Manley, G. T. (2018). An update on diagnostic and prognostic biomarkers for traumatic brain injury. *Expert Review of Molecular Diagnostics*, 18(2), 165–180. <https://doi.org/10.1080/14737159.2018.1428089>
- Wang, P., Ma, H., Zhang, Y., Zeng, R., Yu, J., Liu, R., Jin, X., & Zhao, Y. (2020). Plasma Exosome-derived MicroRNAs as Novel Biomarkers of Traumatic Brain Injury in Rats. *International Journal of Medical Sciences*, 17(4), 437–448. <https://doi.org/10.7150/ijms.39667>
- Wang, R., Zeng, G. Q., Liu, X., Tong, R. Z., Zhou, D., & Hong, Z. (2016). Evaluation of serum matrix metalloproteinase-3 as a biomarker for diagnosis of epilepsy. *Journal of the Neurological Sciences*, 367, 291–297. <https://doi.org/10.1016/j.jns.2016.06.031>
- Wang, X., Luo, Y., Liu, S., Tan, L., Wang, S., & Man, R. (2017). MicroRNA-134 plasma levels before and after treatment with valproic acid for epilepsy patients. *Oncotarget*, 8(42), 72748–72754. <https://doi.org/10.18632/oncotarget.20292>
- Wang, X., Sun, Y., Tan, Z., Che, N., Ji, A., Luo, X., Sun, X., Li, X., Yang, K., Wang, G., Luan, L., Liu, Y., Wei, M., & Yin, J. (2016). Serum MicroRNA-4521 is a Potential Biomarker for Focal Cortical Dysplasia with Refractory Epilepsy. *Neurochemical Research*, 41(4), 905–912. <https://doi.org/10.1007/s11064-015-1773-0>
- Wang, Y., Wang, Y., Chen, Y., Hua, Y., Xu, L., Zhu, M., Zhao, C., Zhang, W., Sheng, G., Liu, L., Jiang, P., Yuan, Z., Zhao, Z., & Gao, F. (2022). Circulating MicroRNAs From Plasma Small Extracellular Vesicles as Potential Diagnostic Biomarkers in Pediatric Epilepsy and Drug-Resistant Epilepsy. *Frontiers in Molecular Neuroscience*, 15, 823802. <https://doi.org/10.3389/fnmol.2022.823802>

- Washington, P. M., Forcelli, P. A., Wilkins, T., Zapple, D. N., Parsadanian, M., & Burns, M. P. (2012). The effect of injury severity on behavior: A phenotypic study of cognitive and emotional deficits after mild, moderate, and severe controlled cortical impact injury in mice. *Journal of Neurotrauma*, *29*(13), 2283–2296.
<https://doi.org/10.1089/neu.2012.2456>
- Wayman, G. A., Davare, M., Ando, H., Fortin, D., Varlamova, O., Cheng, H.-Y. M., Marks, D., Obrietan, K., Soderling, T. R., Goodman, R. H., & Impey, S. (2008). An activity-regulated microRNA controls dendritic plasticity by down-regulating p250GAP. *Proceedings of the National Academy of Sciences of the United States of America*, *105*(26), 9093–9098.
<https://doi.org/10.1073/pnas.0803072105>
- Webster, K. M., Sun, M., Crack, P., O'Brien, T. J., Shultz, S. R., & Semple, B. D. (2017). Inflammation in epileptogenesis after traumatic brain injury. *Journal of Neuroinflammation*, *14*(1), 10.
<https://doi.org/10.1186/s12974-016-0786-1>
- Weissberg, I., Wood, L., Kamintsky, L., Vazquez, O., Milikovsky, D. Z., Alexander, A., Oppenheim, H., Ardizzone, C., Becker, A., Frigerio, F., Vezzani, A., Buckwalter, M. S., Huguenard, J. R., Friedman, A., & Kaufer, D. (2015). Albumin induces excitatory synaptogenesis through astrocytic TGF- β /ALK5 signaling in a model of acquired epilepsy following blood-brain barrier dysfunction. *Neurobiology of Disease*, *78*, 115–125. <https://doi.org/10.1016/j.nbd.2015.02.029>
- Weisz, H. A., Kennedy, D., Widen, S., Spratt, H., Sell, S. L., Bailey, C., Sheffield-Moore, M., DeWitt, D. S., Prough, D. S., Levin, H., Robertson, C., & Hellmich, H. L. (2020). MicroRNA sequencing of rat hippocampus and human biofluids identifies acute, chronic, focal and diffuse traumatic brain injuries. *Scientific Reports*, *10*(1), 3341.
<https://doi.org/10.1038/s41598-020-60133-z>
- Welch, R. D., Ayaz, S. I., Lewis, L. M., Unden, J., Chen, J. Y., Mika, V. H., Saville, B., Tyndall, J. A., Nash, M., Buki, A., Barzo, P., Hack, D., Tortella, F. C., Schmid, K., Hayes, R. L., Vossough, A., Sweriduk, S. T., & Bazarian, J. J. (2016). Ability of Serum Glial Fibrillary Acidic Protein, Ubiquitin C-

- Terminal Hydrolase-L1, and S100B To Differentiate Normal and Abnormal Head Computed Tomography Findings in Patients with Suspected Mild or Moderate Traumatic Brain Injury. *Journal of Neurotrauma*, 33(2), 203–214. <https://doi.org/10.1089/neu.2015.4149>
- Welch, R. D., Ellis, M., Lewis, L. M., Ayaz, S. I., Mika, V. H., Millis, S., & Papa, L. (2017). Modeling the Kinetics of Serum Glial Fibrillary Acidic Protein, Ubiquitin Carboxyl-Terminal Hydrolase-L1, and S100B Concentrations in Patients with Traumatic Brain Injury. *Journal of Neurotrauma*, 34(11), 1957–1971. <https://doi.org/10.1089/neu.2016.4772>
- Whitnall, L., McMillan, T. M., Murray, G. D., & Teasdale, G. M. (2006). Disability in young people and adults after head injury: 5-7 Year follow up of a prospective cohort study. *Journal of Neurology, Neurosurgery and Psychiatry*, 77(5), 640–645. <https://doi.org/10.1136/jnnp.2005.078246>
- Wightman, B., Ha, I., & Ruvkun, G. (1993). Posttranscriptional regulation of the heterochronic gene lin-14 by lin-4 mediates temporal pattern formation in *C. elegans*. *Cell*, 75(5), 855–862. [https://doi.org/10.1016/0092-8674\(93\)90530-4](https://doi.org/10.1016/0092-8674(93)90530-4)
- Wilson, L., Stewart, W., Dams-O'Connor, K., Diaz-Arrastia, R., Horton, L., Menon, D. K., & Polinder, S. (2017). The chronic and evolving neurological consequences of traumatic brain injury. *The Lancet Neurology*, 16(10), 813–825. [https://doi.org/10.1016/S1474-4422\(17\)30279-X](https://doi.org/10.1016/S1474-4422(17)30279-X)
- Wong, K. R., O'Brien, W. T., Sun, M., Yamakawa, G., O'Brien, T. J., Mychasiuk, R., Shultz, S. R., McDonald, S. J., & Brady, R. D. (2021). Serum Neurofilament Light as a Biomarker of Traumatic Brain Injury in the Presence of Concomitant Peripheral Injury. *Biomarker Insights*, 16, 15–18. <https://doi.org/10.1177/11772719211053449>
- Woodcock, T., & Morganti-Kossmann, M. C. (2013). The role of markers of inflammation in traumatic brain injury. *Frontiers in Neurology*, 4, 18. <https://doi.org/10.3389/fneur.2013.00018>

- Xiong, Y., Mahmood, A., & Chopp, M. (2013). Animal models of traumatic brain injury. *Nature Reviews. Neuroscience*, *14*(2), 128–142.
<https://doi.org/10.1038/nrn3407>
- Yan, J., Bu, X., Li, Z., Wu, J., Wang, C., Li, D., Song, J., & Wang, J. (2019). Screening the expression of several miRNAs from TaqMan Low Density Array in traumatic brain injury: miR-219a-5p regulates neuronal apoptosis by modulating CCNA2 and CACUL1. *Journal of Neurochemistry*, *150*(2), 202–217. <https://doi.org/10.1111/jnc.14717>
- Yáñez-Mó, M., Siljander, P. R. M., Andreu, Z., Zavec, A. B., Borràs, F. E., Buzas, E. I., Buzas, K., Casal, E., Cappello, F., Carvalho, J., Colás, E., Cordeiro-Da Silva, A., Fais, S., Falcon-Perez, J. M., Ghobrial, I. M., Giebel, B., Gimona, M., Graner, M., Gursel, I., ... De Wever, O. (2015). Biological properties of extracellular vesicles and their physiological functions. *Journal of Extracellular Vesicles*, *4*(2015), 1–60.
<https://doi.org/10.3402/jev.v4.27066>
- Yang, T., Song, J., Bu, X., Wang, C., Wu, J., Cai, J., Wan, S., Fan, C., Zhang, C., & Wang, J. (2016). Elevated serum miR-93, miR-191, and miR-499 are noninvasive biomarkers for the presence and progression of traumatic brain injury. *Journal of Neurochemistry*, *137*(1), 122–129.
<https://doi.org/10.1111/jnc.13534>
- Yang, V. K., Loughran, K. A., Meola, D. M., Juhr, C. M., Thane, K. E., Davis, A. M., & Hoffman, A. M. (2017). Circulating exosome microRNA associated with heart failure secondary to myxomatous mitral valve disease in a naturally occurring canine model. *Journal of Extracellular Vesicles*, *6*(1). <https://doi.org/10.1080/20013078.2017.1350088>
- Yang, Z., & Wang, K. K. W. (2015). Glial fibrillary acidic protein: From intermediate filament assembly and gliosis to neurobiomarker. *Trends in Neurosciences*, *38*(6), 364–374.
<https://doi.org/10.1016/j.tins.2015.04.003>
- Younus, I., & Reddy, D. S. (2017). Epigenetic interventions for epileptogenesis: A new frontier for curing epilepsy. *Pharmacology & Therapeutics*, *177*, 108–122.
<https://doi.org/10.1016/j.pharmthera.2017.03.002>

- Yu, T., Liu, X., Sun, L., Wu, J., & Wang, Q. (2021). Clinical characteristics of post-traumatic epilepsy and the factors affecting the latency of PTE. *BMC Neurology*, 21(1), 1–11. <https://doi.org/10.1186/s12883-021-02273-x>
- Yuana, Y., Levels, J., Grootemaat, A., Sturk, A., & Nieuwland, R. (2014). Co-isolation of extracellular vesicles and high-density lipoproteins using density gradient ultracentrifugation. *Journal of Extracellular Vesicles*, 3(1). <https://doi.org/10.3402/jev.v3.23262>
- Yue, J. K., Kobeissy, F. H., Jain, S., Sun, X., Phelps, R. R. L., Korley, F. K., Gardner, R. C., Ferguson, A. R., Huie, J. R., Schneider, A. L. C., Yang, Z., Xu, H., Lynch, C. E., Deng, H., Rabinowitz, M., Vassar, M. J., Taylor, S. R., Mukherjee, P., Yuh, E. L., ... Wang, K. K. W. (2023). Neuroinflammatory Biomarkers for Traumatic Brain Injury Diagnosis and Prognosis: A TRACK-TBI Pilot Study. *Neurotrauma Reports*, 4(1), 171–183. <https://doi.org/10.1089/neur.2022.0060>
- Zhu, M., Chen, J., Guo, H., Ding, L., Zhang, Y., & Xu, Y. (2018). High Mobility Group Protein B1 (HMGB1) and Interleukin-1 β as Prognostic Biomarkers of Epilepsy in Children. *Journal of Child Neurology*, 33(14), 909–917. <https://doi.org/10.1177/0883073818801654>
- Zhu, Y., Yang, B., Wang, F., Liu, B., Li, K., Yin, K., Yin, W. F., Zhou, C., Tian, S., Ren, H., Pang, A., & Yang, X. (2021). Association between plasma neurofilament light chain levels and cognitive function in patients with Parkinson's disease. *Journal of Neuroimmunology*, 358(March), 577662. <https://doi.org/10.1016/j.jneuroim.2021.577662>

ORIGINAL PUBLICATIONS (I – III)


I

Precipitation-based extracellular vesicle isolation from rat plasma co-precipitate vesicle-free miRNAs

Karttunen J, Heiskanen M, Navarro-Ferrandis V, Das Gupta S, Lipponen A, Puhakka N, Rilla K, Koistinen A and Pitkänen A

Journal of Extracellular Vesicles 8(1): 1555410, 2018

Precipitation-based extracellular vesicle isolation from rat plasma co-precipitate vesicle-free microRNAs

Jenni Karttunen^a, Mette Heiskanen^a, Vicente Navarro-Ferrandis^a, Shalini Das Gupta^a, Anssi Lipponen^a, Noora Puhakka^a, Kirsi Rilla ^b, Arto Koistinen^c and Asla Pitkänen^a

^aA. I. Virtanen Institute for Molecular Sciences, University of Eastern Finland, Kuopio, Finland; ^bInstitute of Biomedicine, University of Eastern Finland, Kuopio, Finland; ^cSIB Labs, University of Eastern Finland, Kuopio, Finland

ABSTRACT

The microRNA (miRNA) cargo contained in plasma extracellular vesicles (EVs) offers a relatively little explored source of biomarkers for brain diseases that can be obtained noninvasively. Methods to isolate EVs from plasma, however, are still being developed. For EV isolation, it is important to ensure the removal of vesicle-free miRNAs, which account for approximately two-thirds of plasma miRNAs. Membrane particle precipitation-based EV isolation is an appealing method because of the simple protocol and high yield. Here, we evaluated the performance of a precipitation-based method to obtain enriched EV-specific miRNAs from a small volume of rat plasma. We performed size-exclusion chromatography (SEC) on precipitation-isolated EV pellets and whole plasma. The SEC fractions were analysed using Nanoparticle Tracking Analysis (NTA), protein and miRNA concentration assays, and droplet digital polymerase chain reaction for four miRNAs (miR-142-3p, miR-124-3p, miR-23a, miR-122). Precipitation-isolated EVs and selected SEC fractions from the plasma were also analysed with transmission electron microscopy (TEM). Precipitation-based EV isolation co-precipitated 9% to 15% of plasma proteins and 21% to 99% of vesicle-free miRNAs, depending on the individual miRNAs. In addition, the amount of miR-142-3p, found mainly in EV fractions, was decreased in the EV fractions, indicating that part of it was lost during precipitation-based isolation. Western blot and TEM revealed both protein and lipoprotein contamination in the precipitation-isolated EV-pellets. Our findings indicate that a precipitation-based method is not sufficient for purifying plasma EV-contained miRNA cargo. The particle number measured by NTA is high, but this is mostly due to the contaminating lipoproteins. Although a part of the vesicle-free miRNA is removed, vesicle-free miRNA still dominates in plasma EV pellets isolated by the precipitation-based method.

ARTICLE HISTORY

Received 10 April 2018
Revised 21 November 2018
Accepted 23 November 2018

KEYWORDS

Extracellular vesicle; extracellular vesicle isolation; plasma; precipitation; miRNA; ddPCR; size-exclusion chromatography

Introduction



Extracellular vesicles (EVs), lipid particles found in all body fluids, are secreted by many cell types and used in inter-cellular communication [1]. Both the surface proteins and the cargo, especially in plasma EVs, represent emerging targets for biomarker and treatment discovery for various diseases [2].


Currently, there are several methods for isolating plasma EVs. Each method has its advantages and disadvantages [3]. Several commercial EV isolation kits, such as the miRCURY™ Exosome Isolation Kit, ExoQuick and Invitrogen Total Exosome isolation reagent, are based on the precipitation of membrane particles. According to a worldwide survey performed in 2015 by the International society for extracellular vesicles (ISEV), precipitation-based methods are used especially for biologic samples with a small starting

volume. In addition, 84% of researchers using precipitation techniques perform RNA analysis of the EV fraction [4].

In addition to EVs, plasma contains a high number of lipoproteins, including high-density lipoproteins (HDL), low-density lipoproteins, very low-density lipoproteins and chylomicrons [5]. Some of these lipoproteins are within the size-range or density of EVs, which makes it difficult to isolate EVs from plasma [6,7].

MicroRNAs are small non-coding RNAs that regulate protein synthesis at the post-transcriptional level. Circulating miRNAs are considered potential biomarkers, such as for cancer, infections, and neurologic diseases [8–10]. Circulating miRNAs are not intrinsically resistant to endogenous RNases and therefore, require protection against degrading enzymes [11]. In plasma, miRNAs are found in EVs [1,11], lipoproteins

CONTACT Asla Pitkänen  asla.pitkanen@uef.fi  Department of Neurobiology, A. I. Virtanen Institute for Molecular Sciences, University of Eastern Finland, PO Box 1627, Kuopio FI-70211, Finland

 Supplemental data for this article can be accessed [here](#).

© 2018 The Author(s). Published by Informa UK Limited, trading as Taylor & Francis Group on behalf of The International Society for Extracellular Vesicles. This is an Open Access article distributed under the terms of the Creative Commons Attribution-NonCommercial License (<http://creativecommons.org/licenses/by-nc/4.0/>), which permits unrestricted non-commercial use, distribution, and reproduction in any medium, provided the original work is properly cited.

like HDL and low-density lipoproteins [12,13], and protein complexes [11,14]. All these carriers appear to have an individual miRNA profile [13]. A study using size exclusion chromatography (SEC) estimated that approximately 15% of circulating miRNAs in humans are enriched in EV fractions and 66% are enriched in lipoprotein/protein fractions [11]. In addition, a notable amount of protein-bound miRNA appears to be bound specifically to Argonaute-2, a protein in the intracellular miRNA-silencing complex [11,14]. A recent position paper by the ISEV listed the opportunities and limitations of EV-related RNA studies emphasising that the methods are still developing, and that isolation techniques, especially regarding RNA, must be critically evaluated [3].

Several studies have compared the miRNA yield in EVs obtained from plasma or serum using different EV isolation methods, including precipitation-based methods [15–21]. Based on microarray or next generation sequencing studies it is evident that the EV isolation method influences the captured miRNome [20–22]. The presence of lipoproteins, of contaminating miRNAs or miRNA-binding proteins is less studied [15]. In studies of EV miRNA cargo, it is critical to ensure that protein- and lipoprotein-bound miRNAs are removed during the EV isolation process. The present study aimed to test the efficiency of the precipitation-based miRCURY™ Exosome Isolation Kit – Serum and Plasma, combined with filtration, for removing non-EV-related miRNAs, and thereby enriching the EV miRNA cargo from rat plasma.

Materials and methods

Animals and plasma collection

Naïve male Sprague-Dawley rats ($n = 5$, body weight 327–403 g at the time of decapitation) were used. Water and pellet food were freely available and provided ad libitum. All animal procedures were approved by the Animal Ethics Committee of the Provincial Government of Southern Finland and carried out in accordance with the guidelines of the European Community Council Directives 2010/63/EU.

Rats were anaesthetised with isoflurane and decapitated. The trunk blood was collected into K2-EDTA-tubes (di-potassium ethylenediaminetetraacetic acid, Vacutainer, BD Biosciences, Franklin Lakes, NJ, USA). The tubes were immediately placed into ice. For plasma isolation, blood samples were centrifuged at 1300g for 10 min (+4°C) within 1 h after collection and stored in 200 µl aliquots at –70°C until further processed.

EV isolation using a precipitation-based method

EVs for various experiments were isolated from 250–800 µl of trunk plasma. A 10 µl aliquot of pooled plasma was stored at –70°C for sodium dodecyl sulfate-polyacrylamide gel electrophoresis (SDS-PAGE) and Western blot analysis. The remaining plasma was used for EV isolation with the miRCURY™ Exosome Isolation Kit—Serum and Plasma (#300112, Exiqon A/S, Denmark). Briefly, after thrombin treatment, the plasma was filtered through a 0.22 µm polyvinylidene difluoride filter (#SLGV013SL, Millex-GV, Merck Millipore) to eliminate larger vesicles. Next, the filtered plasma was combined with 0.4 volumes of precipitation buffer, incubated for 1 h at 4°C and then the EVs were pelleted by centrifugation (500 g, 5 min, RT). The pelleted EVs were resuspended in 270 µl resuspension buffer from the kit and stored at –70°C and the supernatant was collected and stored at –70°C.

EV isolation with SEC and RNA isolation

From each of the four rats, eight 200 µl aliquots (total volume 1 600 µl) were pooled and used for analysis. After centrifugation (5 min, 10,000 g), the supernatant was divided into two 800 µl aliquots.

Plasma SEC analysis (plasma-SEC). The first 800 µl aliquot was filled to 1 ml with filtered (0.22 µm) PBS containing 0.32% trisodium citrate and loaded into a 10 ml Sepharose CL-2B column as described by Böing et al. [23]. After loading, 25 fractions of filtrates (500 µl each) were collected.

EV pellet SEC analysis (EV-SEC). EVs from the second 800 µl plasma aliquot was isolated using the miRCURY™ Exosome Isolation Kit—Serum and Plasma as described above. The resuspended precipitation-isolated EV pellet (270 µl) was combined with 730 µl of 0.22 µm filtered phosphate-buffered saline (PBS, VWRVE404-200TABS, VWR) including 0.32% trisodium citrate, and then loaded into the SEC column. After loading, 25 fractions of filtrates (500 µl each) were collected.

RNA isolation. RNA was isolated from the SEC fractions (plasma-SEC and EV-SEC) obtained from two individual rats. For RNA isolation, 400 µl portions of each of the two consecutive 500 µl SEC fractions were combined, starting from fraction 4. This resulted in 11 800 µl fractions per SEC for RNA isolation. Each 800 µl fraction was combined with five volumes of Qiazol lysis reagent (#79306, Qiagen), vortexed for 10 s, and incubated at room temperature for 5 min. The mixture was then frozen in dry ice and stored at –80°C. After thawing on ice, chloroform (0.2 volumes) was added to the Qiazol-

mixture. The phases were separated by centrifugation (15 min, 4°C, 12,000g) and then ethanol (1.5 volumes) was added to the collected aqueous phase. The mixture was loaded into a single affinity column from miRNeasy Mini Kit (Qiagen, #217004) and washed according to the kit's instructions. Finally, the RNA was eluted with 30 µl of nuclease-free water. The miRNA concentration of the purified RNA was measured using a Qubit® microRNA Assay Kit (#Q32880, Thermo Fisher Scientific) and a DeNovix DS-11 FX fluorometer. The remaining fractions were saved for nanoparticle tracking analysis (NTA) and protein concentration analyses. Protein concentration was measured using a Pierce BCA protein assay kit according to manufacturer instructions (#23225, Thermo Fisher Scientific).

Nanoparticle tracking analysis

NTA was used to measure the relative concentration and size distribution of the particles. Measurements were obtained using NS300 NanoSight (Malvern, Worcestershire, UK). Polystyrene latex beads (91 nm; Bal-Tec, Balzers, Lichtenstein) were used as a positive control and PBS (VWRVE404-200TABS, VWR) was used as a negative control. For recordings, the camera level was adjusted to 13 (range: 1–16) and the remaining settings were set to automatic. The sample was injected to the sample chamber at a constant flow rate using the Malvern NanoSight syringe pump system. Three 30 s captures per sample were recorded. For analysis of the recordings, the settings were set to automatic, except for the detection threshold, which was set to 5. Each sample was diluted to reach a concentration between 5×10^7 and 2×10^9 particles/ml, expect for SEC fractions 1–7 whose particle counts were too low to reach the detectable concentration range.

SDS-PAGE and western blot

Protein concentrations in the plasma, EVs, and supernatant samples were determined using the Pierce BCA protein assay kit. First, samples were mixed with 2x RIPA lysis buffer and incubated at 4°C for 15 min. The samples were mixed with 4x Laemmli sample buffer (#161-0747, Bio-Rad, Hercules, CA, USA) including 2-mercaptoethanol and denatured at 95°C for 10 min. For Western blot analysis, 5 µg (albumin) or 25 µg (Tsg-101 and ApoA1) protein was separated by 12% SDS-PAGE (TGX Stain-Free™ FastCast™ Acrylamide kit, Bio-Rad, 161-0185) and transferred to Amersham Hybond-P polyvinylidene difluoride membranes (P 0.45, GE Healthcare) using a Thermo Scientific™ Pierce™ Power Blotter. Protein

bands on the gels and membranes were visualised after separation and transfer using a Bio-Rad ChemiDoc™ TM MP System.

Primary antibodies against ApoA1 (rabbit, dilution 1:400, Abcam, Cambridge, MA, USA, ab33470), albumin (goat, dilution 1:2000, Santa Cruz Biotechnology, Dalas, TX, USA, sc-46,293) and Tsg-101 (rabbit, dilution 1:5000, Abcam, Cambridge, MA, USA, ab125011) were used for the Western blot analysis. After primary and secondary antibody incubations (mouse anti-rabbit horseradish peroxidase [HRP; dilution 1:10,000 or 1:5000, Abcam ab99697] or rabbit anti-goat HRP [dilution 1:10,000, Santa Cruz Biotechnology, sc-2922]), the membranes were subjected to HRP chemiluminescent substrate (#34080, SuperSignal™ West Pico Chemiluminescent Substrate, Thermo Fisher Scientific). Protein bands were visualised using the signal accumulation mode in Bio-Rad ChemiDoc™ MP System. Image Lab™ (version 6.0, Bio-Rad) was used to measure the adjusted intensity of the albumin bands after SDS-PAGE.

Scanning electron microscopy

For scanning electron microscopy (SEM), EVs were isolated from 350 µl rat plasma using the miRCURY™ Exosome Isolation Kit—Serum and Plasma as described above. SEM of the EVs was performed as previously described [24]. Briefly, precipitation-isolated EV preparations were diluted 1:10 in PBS and left to settle onto poly-D-lysine-coated coverslips overnight at 4°C. They were then washed in 0.1 M sodium cacodylate and 0.1 M sucrose (pH 7.4) and fixed in sodium cacodylate-buffered 2% (v/v) glutaraldehyde for 30 min. After washing with 0.1 M sodium cacodylate the samples were postfixated in 1% osmium tetroxide and 0.1 M Na-cacodylate for 1 h followed by washing with sodium cacodylate and distilled water. Thereafter, the samples were dehydrated through a graded series of ethanol. Samples were chemically dried with hexamethyldisilazane, air-dried, coated with chrome and imaged with a Zeiss Sigma HD|VP (Carl Zeiss Microscopy GmbH, Oberkochen, Germany) scanning electron microscope at 3 kV. A negative control was prepared using PBS as the starting material. Solution containing 91-nm polystyrene latex beads (Bal-Tec) served as a positive control.

Transmission electron microscopy

For transmission electron microscopy (TEM), EVs were isolated from 250 µl of rat plasma using the miRCURY™ Exosome Isolation Kit—Serum and Plasma as described above. In addition, SEC was performed with 250 µl of plasma as described above. TEM of EVs was performed

according to Thery et al. [25]. Before preparing the TEM samples, SEC fractions 6–7 were concentrated to ~100 µl using an Amicon Ultra-4 10 K concentrator column. Next, SEC fractions 8–10 and 12–13 were concentrated to 390 µl and 260 µl, respectively, using Pierce 3K concentrator columns. Then, 8 µl of sample was mixed with 8 µl of 4% paraformaldehyde. Five microliters of sample-paraformaldehyde suspension was deposited on each of two Formvar-carbon coated and glow-discharged electron microscopy grids, and the membranes were covered for 20 min. For washing, 100 µl drops of PBS were placed on a sheet of parafilm, and the grids were transferred to the drops for 2 min with the sample membrane side facing down. The grids were transferred to a 50 µl drop of 1% glutaraldehyde for 5 min. The grids were then washed by transferring them to a 100 µl drop of distilled water for 2 min. The washing step was repeated seven times for a total of eight washes. For the contrast, the grids were transferred to a 50 µl drop of uranyl-oxalate solution, pH 7, for 5 min. The grids were then transferred to a 50 µl drop of methyl cellulose-UA for 10 min on ice. The grids were removed with stainless steel loops and the excess fluid was blotted on Whatman no. 1 filter paper. Finally, the grids were air-dried on the loop for 5–10 min and stored in grid storage boxes. Imaging was performed using a JEOL JEM-2100F electron microscope (Jeol Ltd, Tokyo, Japan) at 200 kV.

Droplet digital PCR

Four miRNAs were selected for individual miRNA analysis based on previously reported data. Brain enriched miR-124-3p was found from serum EVs when ExoQuick precipitation-based isolation method was used [26]. Other miRNAs were selected based on the previous knowledge about their co-precipitation with EVs (miR-142-3p) or proteins (miR-23a and miR-122) in SEC [11].

cDNA synthesis was conducted using a TaqMan miRNA Reverse Transcription kit (#4366596, Applied Biosystems™) according to the manufacturer's instructions. Five microliters of extracted RNA (mmu-miR-124a: assay ref 001182, Thermo Fisher Scientific) or a 1:3 dilution of extracted RNA (hsa-miR-122: 002245, has-miR-23a: 000399 and has-miR-142-3p: 000464, Thermo Fisher Scientific) was used as a template. The cDNA synthesis was conducted with a Bio-Rad T100 Thermal Cycler (30 min at 16°C; 30 min at 42°C; and 5 min at 85°C). TaqMan™ MicroRNA Assays were used in both cDNA synthesis and droplet digital PCR (ddPCR).

For the ddPCR reaction, 1.3 µl of cDNA was combined with 10 µl of 2x ddPCR™ Supermix for Probes (#1863027, Bio-Rad), 1 µl of microRNA Assay and 7.7 µl of nuclease-free water. Samples and 70 µl of droplet generator oil for

probes (#1863005, Bio-Rad) were loaded into the wells of the droplet generator cartridge (#1864008, Bio-Rad). Droplets were generated using a QX200 Droplet Generator (Bio-Rad). Droplets were applied to a 96-well plate (#Z651443-25EA, Sigma Millipore, St. Louis, MO, USA), and the plate was sealed with foil (#1814040, Bio-Rad) using a PX1 PCR Plate Sealer (Bio-Rad). The PCR reaction was conducted with a BIO-RAD T100 Thermal Cycler (10 min at 95°C; 40 cycles of 15 s at 95°C and 60s at 60°C; 10 min at 98°C). The fluorescence of each droplet was measured using a QX200 Droplet Reader (Bio-Rad). Data were analysed with QuantaSoft software v1.7 (Bio-Rad) to determine the copy number of the measured miRNA. Each sample was run in duplicate and the mean of positive droplets per 20 µl of reaction mix was used in further calculations. A no-template (nuclease-free water) control was included in each run.

Results

Characterisation of plasma EVs isolated by the precipitation method

To assess the overall quality of the EVs (i.e. EV pellet) that were isolated from rat trunk plasma using a precipitation-based EV isolation method, we applied several techniques recommended by the ISEV, including NTA, SEM, SDS-PAGE, and Western blot [27].

NTA indicated a peak in the EV pellet particle size within the range of 60–120 nm (Figure 1(b)). In the positive control (91-nm polystyrene latex beads), NTA detected a constant peak at 83 nm using several settings (data not shown).

SEM images of the EV pellets revealed spherical particles that were within the same size range as the particles measured with NTA from the same EV isolation (Figure 1(a)). In addition, we found a large number of smaller particles in the background. In the positive control (91-nm polystyrene latex beads), SEM showed 90-nm round particles (data not shown). In the negative control (PBS), we detected small asymmetrical particles in the background (data not shown).

SDS-PAGE of total proteins in plasma, EV pellet and supernatant revealed different protein band patterns (Figure 1(c)). The albumin band (66 kDa, the most abundant protein in plasma) accounted for 25% of the total intensity of the protein bands in the plasma, 16% in the EV pellet and 32% in the supernatant.

Western blot did not reveal EV-specific marker tsg-101 in the EV pellet, plasma, or supernatant (Figure 1(d)). Instead, HDL marker ApoA1 was enriched in the EV pellet (Figure 1(d)). Western blot analysis confirmed the presence of albumin in both the EV pellet

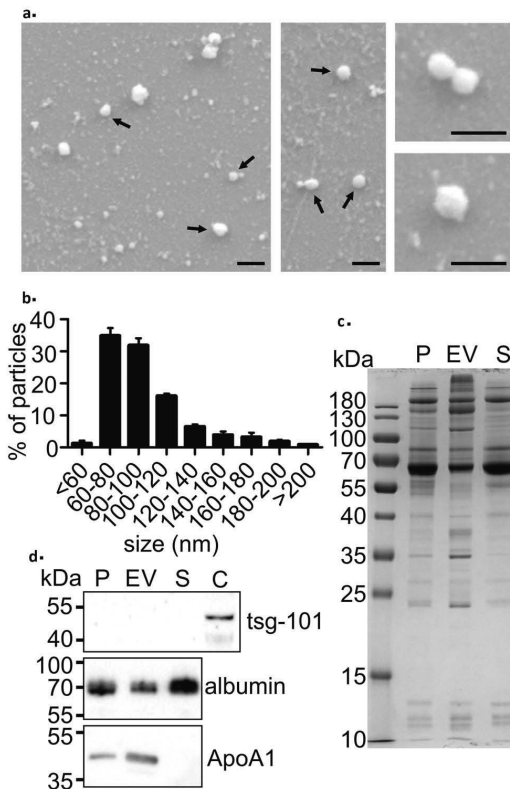


Figure 1. Characterisation of EVs isolated using the precipitation method. (a) Scanning electron microscopy (SEM) images of the isolated EV fraction show round vesicle-like particles (black arrows) and smaller background particles. Scale bar: 200 nm in all panels. (b) Nanoparticle tracking analysis (NTA) showed that the size of most particles ranged from 60–120 nm, which is comparable to that measured with SEM. Data are expressed as the mean \pm standard error of the mean. (c) SDS-PAGE of proteins in trunk plasma (P), EV pellet (EV), and the remaining supernatant (S). Each lane was loaded with 5 μ g protein. Note that almost all protein bands present in plasma were also observed in the EV-pellet. (d) Western blot analysis showed no signal on EV-marker tsg-101, reduced signal in the albumin and enrichment of the HDL marker ApoA1 in the EV pellet. Rat cortex lysate (C) was used as a positive control for tsg-101.

and supernatant (Figure 1(d)). The TGX Stain-free images for all Western blots are presented in Supplementary figure 1.

TEM analysis of precipitation and SEC-isolated EVs

To study the precipitation-isolated EV pellet in more detail, we imaged it with TEM and compared it to results of the SEC EV-isolation from plasma. TEM imaging of the precipitation-isolated EV pellet showed several round

particles, some of which were cup-shaped, which is consistent with EVs [23,28,29]. Most of the round particles, however, had a morphology comparable to that of lipoproteins [23,30]. In addition, the TEM images showed a “dense background smudge”, consistent with the presence of protein aggregates [6] (Figure 2(a)). In negative control (precipitation purification performed to PBS), no particles or background were visible (Supplementary Figure 2).

TEM imaging of plasma-SEC revealed a few cup-shaped EVs in the SEC fractions 6–7 (Figure 2(c)). As in the TEM images of the precipitation-isolated EV pellet, most of the round vesicles in plasma-SEC fractions 6–7, 8–10 and 12–13 had a diameter ranging from 20 nm to 200 nm, and a morphology consistent with that of lipoproteins (Figure 2(c-e)). The plasma-SEC fractions were devoid of the “dense background smudge”. TEM imaging confirmed the particle size distribution measured with NTA, indicating a progressive decrease in the particle diameter from earlier to later SEC fractions (Figure 2(f-h)). In addition, Western blot analysis with ApoA1-antibody from plasma-SEC fractions revealed an intensity profile similar to NTA particle profile. The highest intensity was detected in fractions 15–16 (Supplementary figure 3).

SEC analysis of EVs isolated using the precipitation method

Next, we further purified the precipitation-isolated EV pellet with SEC (EV-SEC) and compared the protein and particle concentrations in the various fractions to that in the corresponding fractions collected from SEC-purified plasma (plasma-SEC) (Figure 3(a)). NTA and the protein concentration were measured separately for each SEC fraction.

Proteins. The highest protein concentrations were detected in fractions 17–20 in both EV-SEC and plasma-SEC preparations (Figure 3(b)). The protein concentration in the presumed EV-rich fractions 7–10 was under the detection limit in both preparations. Interestingly, the total amount of protein in the EV-SEC samples (all protein-containing fractions combined) was only 9% to 15% that in plasma-SEC samples.

NTA. The highest total particle concentration was in fractions 13–18 in both preparations and tended to be higher in later fractions of the EV-SEC preparations (Figure 3(c)). The total number of particles in EV-SEC samples (all fractions combined) was 54% to 138% of that in the plasma-SEC samples.

To further analyse the miRNA content of EV-pellet, we combined two adjacent fractions from plasma-SEC and EV-SEC for RNA isolation.

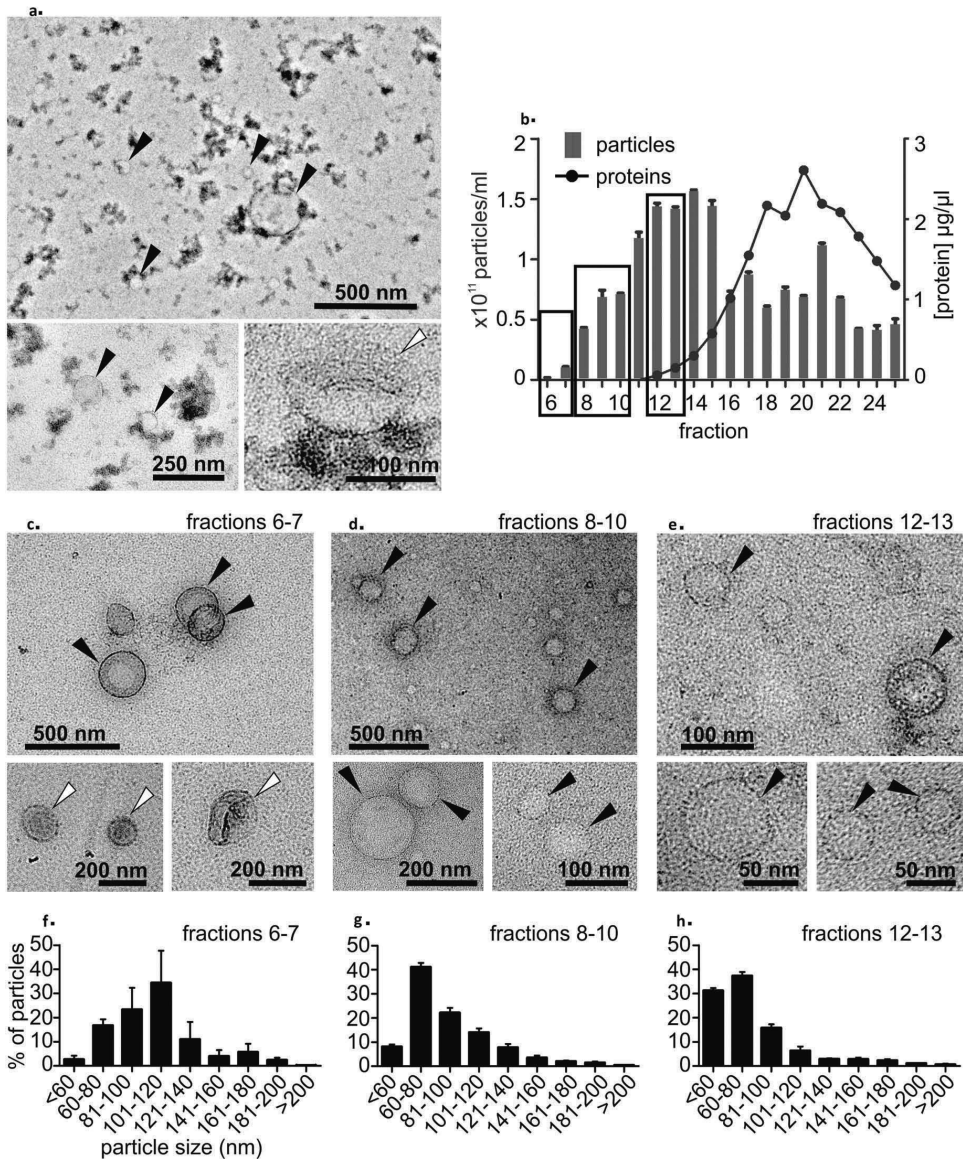


Figure 2. (a) Transmission electron microscopy (TEM) analysis of the precipitation-isolated EV pellet showed round particles, presumably lipoproteins (marked with black arrows), and a few cup-shaped particles (marked with white arrows). The “dense smudge” background indicates protein contamination. (b) Plasma size-exclusion chromatography (SEC). The relative number of particles measured with nanoparticle tracking analysis indicated the highest particle count in fractions 12–15 and the highest protein concentration in fractions 18–22. Fractions marked with black boxes were pooled and concentrated for TEM imaging. Data are from one series of SEC fractions. Three 30-sec videos were recorded by NTA for each fraction. Data are expressed as the mean \pm standard error of the mean. (c) TEM analysis of SEC fractions 6–7 showed a few cup-shaped vesicles (white arrows) and round lipoprotein-like particles (black arrows). In fractions 8–10 (d) and 12–13 (e) cup-shaped EVs were not found, but lipoprotein-like particles were observed (black arrows). Particle size distribution from SEC fractions (f) 6–7, (g) 8–10 and (h) 12–13 measured with nanoparticle tracking analysis showed that the proportion of larger particles (>100 nm) was higher in earlier fractions and that of <60 nm particles increased in the later fractions. Fractions are the same as in Figure 2 B. Data from three 30-second videos recorded by NTA are expressed as the mean \pm standard error of the mean.

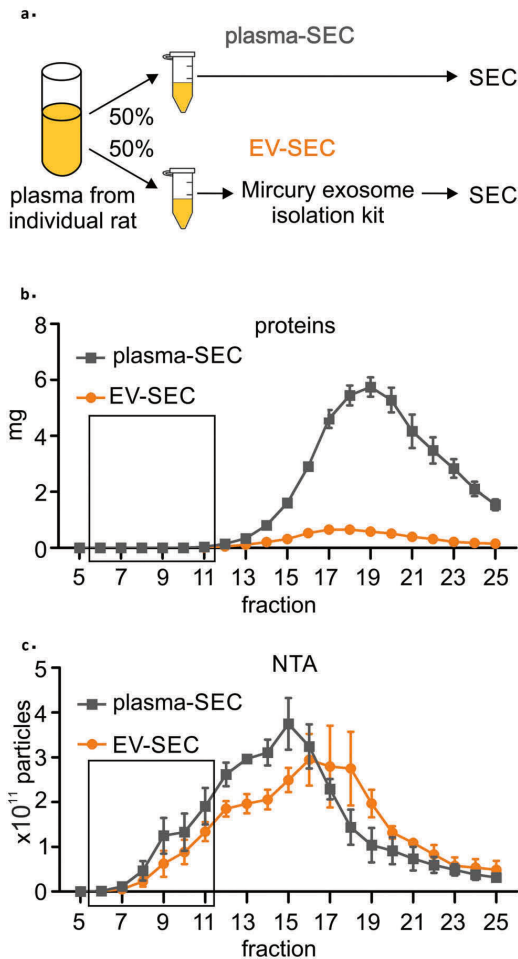


Figure 3. (a) A precipitation-based isolation method was evaluated using size-exclusion chromatography (SEC). Plasma from individual rat was divided in two 800 µl aliquots and the first aliquot was analysed with SEC (plasma-SEC). EVs from the second aliquot was first isolated using precipitation-based kit and the EV pellet was further analysed with SEC (EV-SEC). (b) Measurement of the protein concentration in each fraction showed that precipitation isolation removed 85% to 91% of the total plasma proteins. (c) Nanoparticle tracking analysis (NTA) indicated that the total number of particles was comparable in the plasma-SEC and EV-SEC, but the main peak moved towards later fractions in EV-SEC. The figures present four individual rats (biological replicates). Data are expressed as the mean \pm standard error of the mean. Black box indicates the EV-rich fractions.

miRNAs. In the EV-SEC samples, the miRNAs were evenly distributed among the fractions. In plasma-SEC preparations, the highest amount of miRNA was detected in the protein-rich fractions, rather than in

the fractions with the highest particle number (i.e. NTA peak, Figure 4(a)) or in EV-rich fractions 7–10. The total amount of miRNA in the protein-enriched fractions 16–21 in the EV-SEC samples was 51% to 70% of that in the plasma-SEC samples.

miR-142-3p, miR-124-3p, miR-23a, and miR-122. ddPCR analysis indicated that in both the EV-SEC and plasma-SEC samples, the EV-related miR-142-3p [11] formed two main peaks: fractions 6–11 (presumed EVs) and fractions 16–23 (proteins) (Figure 4(b)). Its concentration was lowest in the mid-fractions, which contained the highest particle concentration in the NTA. The total amount of miR-142-3p in the SEC-fractions 6–11 of the EV-SEC samples was 14% to 23% that in the plasma-SEC samples. The precipitation-based method did not enrich miR-142-3p.

The highest amounts of miR-124-3p, miR-23a, and miR-122 were in the protein-rich fractions in both the EV-SEC and plasma-SEC preparations (Figure 4(c-e)). In the EV-SEC preparations, the total amount of miR-124-3p was 41% to 51%, miR-23a 56% to 99% and miR-122 21% to 37% that in the plasma-SEC preparations.

Discussion

The present study evaluated the ability of a precipitation-based EV isolation method to remove vesicle-free miRNAs to provide enriched EV cargo-related miRNAs. We had two major findings. First, lipoproteins precipitated with the EV pellet during precipitation isolation. Second, vesicle-free miRNAs were also present in the EV pellet.

Precipitation-based EV-isolation co-precipitates plasma lipoproteins

SEM, TEM and NTA revealed the presence of particles within the EV size range in the precipitation-isolated EV pellet from plasma. SDS-PAGE, however, showed that the precipitation-isolated EV pellet was contaminated with albumin, and Western blot analysis revealed contamination with HDLs.

In plasma, lipoproteins are major contaminating particles that interfere with various EV isolation methodologies [5–7]. HDLs have a density comparable to that of EVs, whereas very low-density lipoproteins and chylomicrons fall into the same size-range as EVs [6,7]. In a recent “Viewpoints” article, Simonsen estimated that one milliliter of plasma contains 10^7 – 10^9 EV particles and up to 10^{16} lipoprotein particles [7]. Our TEM images of the precipitation-isolated EV pellet revealed particles with a mainly round shape, consistent with

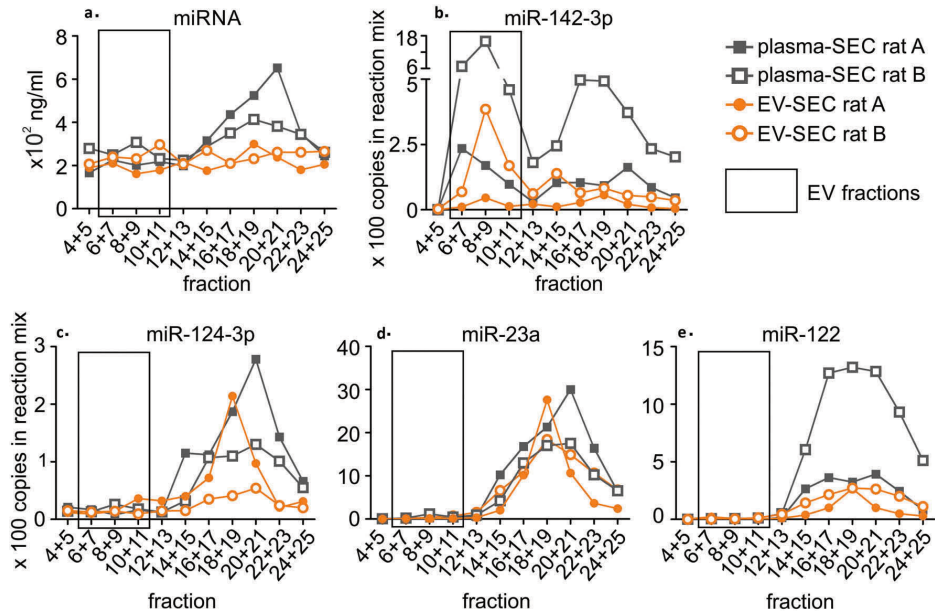


Figure 4. A precipitation-based isolation method was evaluated using size-exclusion chromatography (SEC). Plasma was divided in two 800 μ l aliquots, and the first aliquot was analysed with SEC (plasma-SEC). EVs from the second aliquot was first isolated using precipitation-based kit and the EV pellet was further analysed with SEC (EV-SEC). RNA was isolated from combined adjacent fractions. The analysis was made for two individual rats (rat A and B). (a) The miRNA concentration peaked in the protein fractions in plasma-SEC, whereas no clear peak was in the EV-SEC. (b) Droplet digital PCR analysis of miR-142-3p showed the highest peaks in the EV fractions (6–11). The total amount of miR-142-3p appeared lower in the EV-SEC fractions. (c) miR-124-3p, (d) miR-23a and (e) miR-122 were found in protein-rich fractions in both plasma-SEC and EV-SEC.

a lipoprotein morphology [23,30], and only very few EVs with a distinct cup-shaped morphology [23,28,29], suggesting that the plasma lipoproteins were not removed during precipitation-based EV isolation.

Earlier studies revealed that lipoproteins and larger protein complexes affect particle counts in human plasma samples in NTA [31,32]. Accordingly, our TEM images from SEC fractions with the highest NTA particle concentration showed round lipoprotein-like particles instead of cup-shaped EVs. These data together with the observations of Mork and coworkers, that the NTA particle concentration in platelet-free plasma is reduced by 32% to 72% when lipoproteins are removed by immunoprecipitation, indicate that lipoproteins also contribute to the particle counts measured with NTA.

Finally, we used SEC followed by NTA to compare the particle counts in the precipitation-isolated plasma EV-pellet to that in the original plasma sample. Importantly, the total number of particles was comparable in both samples, providing further evidence that lipoproteins co-precipitate with the EV pellet during precipitation isolation.

Precipitation-based EV isolation co-precipitates plasma miRNAs

Arroyo et al. estimated that 66% of miRNAs elute in the same fractions as proteins in SEC [11]. Further, Turchinovich et al. showed that a majority of plasma miRNA is independent of EVs, and possibly bound to Argonaute-2 protein complexes [14]. Our miRNA profile from plasma-SEC confirmed the finding of Arroyo et al., as the highest amount of total miRNA was detected in the protein-rich fractions, instead of fractions with EVs [11].

Droplet digital PCR detected EV-enriched miR-142-3p in both the EV-rich and protein-rich SEC fractions of rat plasma, comparable to that in human plasma [11]. Interestingly, the amount of miR-142-3p in EVs contained in the EV-SEC fractions was only 14% to 23% compared with that in the EV-containing fractions of whole plasma-SEC, indicating that the precipitation method did not enrich miR-142-3p in the EV pellet.

The other three miRNAs (miR-124-3p, miR-122 and miR-23a) eluted mainly in the protein-rich fractions in both EV-SEC and plasma-SEC derived samples. Thus,

the precipitation-based method was not able to remove the protein-co-precipitating miRNAs, i.e. miR-124-3p, miR-122 miR-23a. Interestingly, earlier study used ExoQuick precipitation-based method for isolation of EVs and found increased amount of miR-124 in serum EVs after acute ischemic stroke [26].

Taken together, our data show that a precipitation-based EV isolation method removes only part of the vesicle-free miRNAs, which has implications for interpreting previously published data. For example, a recent comparison of the miRNA contents of plasma and precipitation-isolated EV pellets using a miRNA array indicated that the miRNA profile was comparable between the two preparations [33]. On the other hand, another report showed that EVs carry only a minor proportion of the plasma miRNAs [11]. The data inconsistencies obtained can be explained by poor performance of a precipitation-based method of purifying the EVs and removing vesicle-free miRNAs. Buschmann et al. [22] performed miRNA-sequencing and compared several serum EV-isolation methods, including miRCURY Exosome isolation kit and SEC. MicroRNA content of EVs purified with SEC failed to separate sepsis patients from healthy volunteers, but significant changes were found between the groups with the precipitation method. One discussed explanation to the difference was co-precipitation of non-vesicular miRNA with the precipitation method, which is supported by our data. Further, Van Deun et al. detected Argonaute-2, a protein known to bind miRNAs, in the EV pellet when using precipitation-based ExoQuick method [17]. The presence of Argonaute-bound miRNAs in precipitation-isolated EVs remains to be studied.

Future directions

Precipitation-based EV isolation is appealing in cases with a limited sample volume, such as when analysing EV-related biomarkers in small amounts of rat tail vein plasma. As demonstrated here, however, the precipitated EV fractions also contain lipoproteins and vesicle-free miRNAs. Further analysis with SEC more specifically revealed EV-specific miRNA cargo, but the EV pellet was not completely free from co-precipitated lipoproteins and vesicle-free miRNAs. Therefore, further development of EV isolation methodologies and the identification of markers that reliably indicate the isolation quality are needed. One approach in this direction was recently published by Karimi et al., who combined density-based isolation with SEC and demonstrated improved enrichment of cup-shaped EVs in human plasma samples with

a proteomics profile matching that in EVs isolated from cell culture media [6]. Scaling the analysis to a small sample volume, however, remains to be accomplished.

Acknowledgments

We thank Joonas Malinen for excellent technical assistance. This study was supported by the Academy of Finland, the Sigrid Juselius Foundation, the European Union's Seventh Framework Programme (FP7/2007-2013) under grant agreement n°602102 (EPITARGET) and by EATRIS, the European Infrastructure for Translational Medicine, University of Eastern Finland (Biocenter Kuopio) and Biocenter Finland.

Disclosure statement

No potential conflict of interest was reported by the authors.

Funding

This work was supported by the Academy of Finland [273909]; Academy of Finland [272249]; Sigrid Juselius Foundation; the European Union's Seventh Framework Programme (FP7/2007-2013) under grant agreement [602102 EPITARGET]; EATRIS, the European Infrastructure for Translational Medicine, University of Eastern Finland (Biocenter Kuopio) and Biocenter Finland.

ORCID

Kirsi Rilla  <http://orcid.org/0000-0002-7862-5727>

References

- [1] Yanez-Mo M, Siljander PR, Andreu Z, et al. Biological properties of extracellular vesicles and their physiological functions. *J Extracell Vesicles*. 2015;4:27066.
- [2] Whiteside TL. The potential of tumor-derived exosomes for noninvasive cancer monitoring. *Expert Rev Mol Diagn*. 2015;15(10):1293–1310.
- [3] Mateescu B, Kowal EJ, van Balkom BW, et al. Obstacles and opportunities in the functional analysis of extracellular vesicle RNA - an ISEV position paper. *J Extracell Vesicles*. 2017;6(1):1286095.
- [4] Gardiner C, Di Vizio D, Sahoo S, et al. Techniques used for the isolation and characterization of extracellular vesicles: results of a worldwide survey. *J Extracell Vesicles*. 2016;5:32945.
- [5] Yuana Y, Koning RI, Kuil ME, et al. Cryo-Electron microscopy of extracellular vesicles in fresh plasma. *J Extracell Vesicles*. 2013;2. eCollection 2013 Dec 31. DOI:10.3402/jev.v2i0.21494
- [6] Karimi N, Cvjetkovic A, Jang SC, et al. Detailed analysis of the plasma extracellular vesicle proteome after separation from lipoproteins. *Cell Mol Life Sci*. 2018;75:2873–2886.

- [7] Simonsen JB. What are we looking at? Extracellular vesicles, lipoproteins, or both? *Circ Res.* **2017**;121(8):920–922.
- [8] Armand-Labit V, Pradines A. Circulating cell-free microRNAs as clinical cancer biomarkers. *Biomol Concepts.* **2017**;8(2):61–81.
- [9] Correia CN, Nalpas NC, McLoughlin KE, et al. Circulating microRNAs as potential biomarkers of infectious disease. *Front Immunol.* **2017**;8:118.
- [10] Sheinerman KS, Umansky SR. Circulating cell-free microRNA as biomarkers for screening, diagnosis and monitoring of neurodegenerative diseases and other neurologic pathologies. *Front Cell Neurosci.* **2013**;7:150.
- [11] Arroyo JD, Chevillet JR, Kroh EM, et al. Argonaute2 complexes carry a population of circulating microRNAs independent of vesicles in human plasma. *Proc Natl Acad Sci USA.* **2011**;108(12):5003–5008.
- [12] Vickers KC, Palmisano BT, Shoucri BM, et al. MicroRNAs are transported in plasma and delivered to recipient cells by high-density lipoproteins. *Nat Cell Biol.* **2011**;13(4):423–433.
- [13] Wagner J, Riwanto M, Besler C, et al. Characterization of levels and cellular transfer of circulating lipoprotein-bound microRNAs. *Arterioscler Thromb Vasc Biol.* **2013**;33(6):1392–1400.
- [14] Turchinovich A, Weiz L, Langheinz A, et al. Characterization of extracellular circulating microRNA. *Nucleic Acids Res.* **2011**;39(16):7223–7233.
- [15] Stranska R, Gysbrechts L, Wouters J, et al. Comparison of membrane affinity-based method with size-exclusion chromatography for isolation of exosome-like vesicles from human plasma. *J Transl Med.* **2018**;16(1):1–017–1374–6.
- [16] Helwa I, Cai J, Drewry MD, et al. A comparative study of serum exosome isolation using differential ultracentrifugation and three commercial reagents. *PLoS One.* **2017**;12(1):e0170628.
- [17] Van Deun J, Mestdagh P, Sormunen R, et al. The impact of disparate isolation methods for extracellular vesicles on downstream RNA profiling. *J Extracell Vesicles.* **2014**;3. eCollection 2014. DOI:10.3402/jev.v3.24858
- [18] Crossland RE, Norden J, Bibby LA, et al. Evaluation of optimal extracellular vesicle small RNA isolation and qRT-PCR normalisation for serum and urine. *J Immunol Methods.* **2016**;429:39–49.
- [19] Ding M, Wang C, Lu X, et al. Comparison of commercial exosome isolation kits for circulating exosomal microRNA profiling. *Anal Bioanal Chem.* **2018**;410(16):3805–3814.
- [20] Tang YT, Huang YY, Zheng L, et al. Comparison of isolation methods of exosomes and exosomal RNA from cell culture medium and serum. *Int J Mol Med.* **2017**;40(3):834–844.
- [21] Rekker K, Saare M, Roost AM, et al. Comparison of serum exosome isolation methods for microRNA profiling. *Clin Biochem.* **2014**;47(1–2):135–138.
- [22] Buschmann D, Kirchner B, Hermann S, et al. Evaluation of serum extracellular vesicle isolation methods for profiling miRNAs by next-generation sequencing. *J Extracell Vesicles.* **2018**;7(1):1481321.
- [23] Boing AN, van der Pol E, Grootemaat AE, et al. Single-step isolation of extracellular vesicles by size-exclusion chromatography. *J Extracell Vesicles.* **2014**;3. eCollection 2014. DOI:10.3402/jev.v3.23430
- [24] Latham SL, Chaponnier C, Dugina V, et al. Cooperation between beta- and gamma-cytoplasmic actins in the mechanical regulation of endothelial microparticle formation. *FASEB J.* **2013**;27(2):672–683.
- [25] Thery C, Amigorena S, Raposo G, et al. Isolation and characterization of exosomes from cell culture supernatants and biological fluids. *Curr Protoc Cell Biol.* **2006**;30:3.22.1–3.22.29. Chapter 3Unit 3.22.
- [26] Ji Q, Ji Y, Peng J, et al. Increased brain-specific MiR-9 and MiR-124 in the serum exosomes of acute ischemic stroke patients. *PLoS One.* **2016**;11(9):e0163645.
- [27] Lotvall J, Hill AF, Hochberg F, et al. Minimal experimental requirements for definition of extracellular vesicles and their functions: a position statement from the international society for extracellular vesicles. *J Extracell Vesicles.* **2014**;3:26913.
- [28] Lobb RJ, Becker M, Wen SW, et al. Optimized exosome isolation protocol for cell culture supernatant and human plasma. *J Extracell Vesicles.* **2015**;4:27031.
- [29] Jeurissen S, Vergauwen G, Van Deun J, et al. The isolation of morphologically intact and biologically active extracellular vesicles from the secretome of cancer-associated adipose tissue. *Cell Adh Migr.* **2017**;11(2):196–204.
- [30] Yuana Y, Levels J, Grootemaat A, et al. Co-isolation of extracellular vesicles and high-density lipoproteins using density gradient ultracentrifugation. *J Extracell Vesicles.* **2014**;3. eCollection 2014. DOI:10.3402/jev.v3.23262
- [31] Gardiner C, Ferreira YJ, Dragovic RA, et al. Extracellular vesicle sizing and enumeration by nanoparticle tracking analysis. *J Extracell Vesicles.* **2013**;2. eCollection 2013. DOI:10.3402/jev.v2i0.19671
- [32] Mork M, Handberg A, Pedersen S, et al. Prospects and limitations of antibody-mediated clearing of lipoproteins from blood plasma prior to nanoparticle tracking analysis of extracellular vesicles. *J Extracell Vesicles.* **2017**;6(1):1308779.
- [33] Tian F, Shen Y, Chen Z, et al. No significant difference between plasma miRNAs and plasma-derived exosomal miRNAs from healthy people. *Biomed Res Int.* **2017**;2017:1304816.

II

Discovery and Validation of Circulating microRNAs as Biomarkers for Epileptogenesis after Experimental Traumatic Brain injury - The EPITARGET Cohort

Heiskanen M, Das Gupta S, Mills J D, van Vliet E A, Manninen E, Ciszek R, Andrade P, Puhakka N, Aronica E and Pitkänen A

International Journal of Molecular Sciences 24(3): 2823, 2023



Article

Discovery and Validation of Circulating microRNAs as Biomarkers for Epileptogenesis after Experimental Traumatic Brain Injury—The EPITARGET Cohort

Mette Heiskanen ¹ , Shalini Das Gupta ¹, James D. Mills ^{2,3,4}, Erwin A. van Vliet ^{2,5} , Eppu Manninen ¹ , Robert Cizek ¹, Pedro Andrade ¹ , Noora Puhakka ¹, Eleonora Aronica ^{2,6} and Asla Pitkänen ^{1,*}

- ¹ A.I. Virtanen Institute for Molecular Sciences, University of Eastern Finland, 70211 Kuopio, Finland
 - ² Department of (Neuro)Pathology, Amsterdam UMC, University of Amsterdam, 1105 AZ Amsterdam, The Netherlands
 - ³ Department of Clinical and Experimental Epilepsy, UCL Queen Square Institute of Neurology, London WC1N 3BG, UK
 - ⁴ Chalfont Centre for Epilepsy, Buckinghamshire SL9 0RJ, UK
 - ⁵ Swammerdam Institute for Life Sciences, Center for Neuroscience, University of Amsterdam, 1098 XH Amsterdam, The Netherlands
 - ⁶ Stichting Epilepsie Instellingen Nederland, 2103 SW Heemstede, The Netherlands
- * Correspondence: asla.pitkanen@uef.fi



Citation: Heiskanen, M.; Das Gupta, S.; Mills, J.D.; van Vliet, E.A.; Manninen, E.; Cizek, R.; Andrade, P.; Puhakka, N.; Aronica, E.; Pitkänen, A. Discovery and Validation of Circulating microRNAs as Biomarkers for Epileptogenesis after Experimental Traumatic Brain Injury—The EPITARGET Cohort. *Int. J. Mol. Sci.* **2023**, *24*, 2823. <https://doi.org/10.3390/ijms24032823>

Academic Editor: Jarogniew J. Luszczki

Received: 27 December 2022
Revised: 18 January 2023
Accepted: 26 January 2023
Published: 1 February 2023



Copyright: © 2023 by the authors. Licensee MDPI, Basel, Switzerland. This article is an open access article distributed under the terms and conditions of the Creative Commons Attribution (CC BY) license (<https://creativecommons.org/licenses/by/4.0/>).

Abstract: Traumatic brain injury (TBI) causes 10–20% of structural epilepsies and 5% of all epilepsies. The lack of prognostic biomarkers for post-traumatic epilepsy (PTE) is a major obstacle to the development of anti-epileptogenic treatments. Previous studies revealed TBI-induced alterations in blood microRNA (miRNA) levels, and patients with epilepsy exhibit dysregulation of blood miRNAs. We hypothesized that acutely altered plasma miRNAs could serve as prognostic biomarkers for brain damage severity and the development of PTE. To investigate this, epileptogenesis was induced in adult male Sprague Dawley rats by lateral fluid-percussion-induced TBI. Epilepsy was defined as the occurrence of at least one unprovoked seizure during continuous 1-month video-electroencephalography monitoring in the sixth post-TBI month. Cortical pathology was analyzed by magnetic resonance imaging on day 2 (D2), D7, and D21, and by histology 6 months post-TBI. Small RNA sequencing was performed from tail-vein plasma samples on D2 and D9 after TBI ($n = 16$, 7 with and 9 without epilepsy) or sham operation ($n = 4$). The most promising miRNA biomarker candidates were validated by droplet digital polymerase chain reaction in a validation cohort of 115 rats (8 naïve, 17 sham, and 90 TBI rats [21 with epilepsy]). These included 7 brain-enriched plasma miRNAs (miR-434-3p, miR-9a-3p, miR-136-3p, miR-323-3p, miR-124-3p, miR-212-3p, and miR-132-3p) that were upregulated on D2 post-TBI ($p < 0.001$ for all compared with naïve rats). The acute post-TBI plasma miRNA profile did not predict the subsequent development of PTE or PTE severity. Plasma miRNA levels, however, predicted the cortical pathology severity on D2 (Spearman $\rho = 0.345\text{--}0.582$, $p < 0.001$), D9 ($\rho = 0.287\text{--}0.522$, $p < 0.001\text{--}0.01$), D21 ($\rho = 0.269\text{--}0.581$, $p < 0.001\text{--}0.05$) and at 6 months post-TBI ($\rho = 0.230\text{--}0.433$, $p < 0.001\text{--}0.05$). We found that the levels of 6 of 7 miRNAs also reflected mild brain injury caused by the craniotomy during sham operation (ROC AUC 0.76–0.96, $p < 0.001\text{--}0.05$). In conclusion, our findings revealed that increased levels of neuronally enriched miRNAs in the blood circulation after TBI reflect the extent of cortical injury in the brain but do not predict PTE development.

Keywords: fluid-percussion injury; post-traumatic epilepsy; rat; plasma

1. Introduction

Worldwide, it is estimated that >50 million people have epilepsy and 5 million people are diagnosed with epilepsy each year, meaning that a new epilepsy diagnosis is made every

6 s (WHO, <https://www.who.int/publications/i/item/who-information-kit-on-epilepsy>, accessed on 14 November 2022). Traumatic brain injury (TBI) causes 10–20% of structural epilepsies and 5% of all epilepsies [1]. TBI is defined as an alteration in brain function or other brain pathology caused by an external force [2]. The risk of post-traumatic epilepsy (PTE) increases with TBI severity: the 30-year cumulative incidence rate for PTE is 2% for mild, 4% for moderate, and 17% for severe TBI [3]. The latency period from the initial injury to the appearance of the first seizures can vary from months to years [3]. Currently, there are no available treatments for stopping or preventing the epileptogenic process [4,5]. The major obstacle in developing anti-epileptogenic treatments is the lack of prognostic biomarkers, hindering the stratification of subjects with the highest risk into preclinical and clinical studies. Therefore, testing of candidate anti-epileptogenic treatments remains laborious and expensive [6]. Identifying prognostic biomarkers for the development of PTE after TBI is a major unmet medical need.

The major modalities investigated to date as a source of prognostic biomarkers for PTE include brain imaging, electroencephalography (EEG), and blood or cerebrospinal fluid (CSF) [5]. Blood sampling is minimally invasive, making circulating molecules such as microRNAs (miRNAs) an appealing source of disease biomarkers. MiRNAs are short (~22 nucleotides) non-coding RNAs that regulate gene expression at the post-transcriptional level by binding to the 3' untranslated region of their target mRNAs [7,8]. MiRNAs are estimated to regulate more than 60% of all human proteins [9], and many miRNAs are specifically expressed in the brain [10–12]. Thus, circulating brain-enriched miRNAs provide an attractive source, not only for diagnosis but also for longitudinally monitoring brain pathology progression.

Accumulating evidence indicates dysregulation of miRNAs in the brain tissue of patients with epilepsy [13,14]. The dysregulated miRNAs are proposed to be involved in many epileptogenesis-related brain pathologies, such as neuroinflammation and synaptic plasticity [14]. Consistent with miRNA dysregulation in the brain, circulating miRNAs are altered in patients with epilepsy [15]. These data provide a promising scenario that alterations in brain-enriched miRNAs in the blood circulation after TBI could reflect ongoing epileptogenic processes before the onset of PTE. Importantly, preclinical and clinical studies revealed TBI-induced alterations in circulating miRNAs [15,16]. It remains to be explored, however, whether the post-TBI alterations in circulating miRNA profiles provide information on the risk of developing PTE.

We hypothesized that plasma miRNAs at the acute post-TBI time-point will present prognostic biomarkers for brain damage severity and the development of PTE. The data presented derive from a uniquely large and well-characterized animal cohort (EPITARGET, [17]) in which TBI was induced by lateral fluid-percussion injury (LFPI) and epilepsy phenotyping was conducted by 1-month video-electroencephalography (vEEG) monitoring during the sixth month after TBI. The three main objectives were to: (a) discover differentially expressed plasma miRNA profiles after TBI; (b) investigate associations between plasma miRNA levels and the cortical damage severity; and (c) determine whether the plasma miRNA profile at an acute post-TBI time-point could be used as a biomarker to predict epileptogenesis or epilepsy severity after TBI.

2. Results

2.1. MiRNA Sequencing

2.1.1. MiRNA Quantification

Read counts. MicroRNA sequencing was performed on D2 and D9 plasma samples of the discovery cohort, including 4 sham-operated controls and 16 rats with TBI (7 with epilepsy [TBI+], 9 without epilepsy [TBI−]). MicroRNA sequencing detected a total of 565 miRNAs in at least one D2 sample and 541 miRNAs in at least one D9 sample (Figure 1A,B). In D2 samples, the number of mapped reads did not differ between the groups. In the D9 samples, the number of mapped reads in the sham-operated group was only 17% of that in the TBI animals (Mann–Whitney U test, $p < 0.001$) (Supplementary Figure S1).

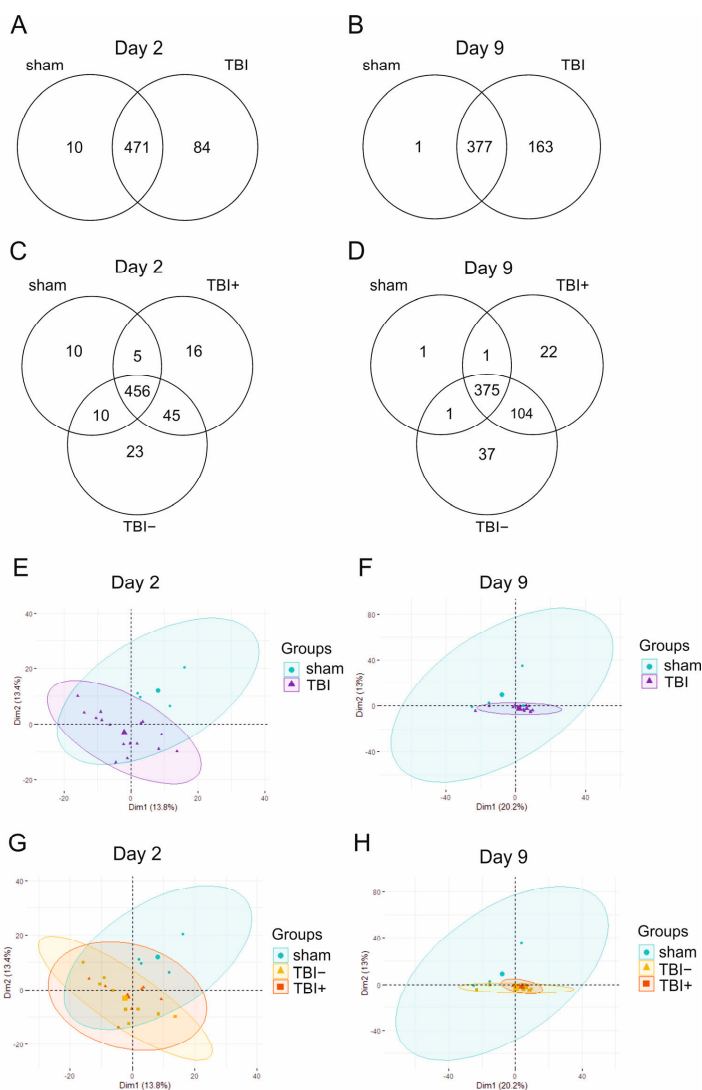


Figure 1. Venn diagrams and principal component analysis (PCA) plots of miRNAs detected in rat plasma by small RNA sequencing. (A) A total of 565 miRNAs were detected in rat plasma on day 2 (D2), 471 of which were common between sham and TBI rats. There were 84 miRNAs detected only in the TBI group. (B) A total of 541 miRNAs were detected in rat plasma on D9, 377 of which were common between sham and TBI rats. There were 163 miRNAs detected only in the TBI group. (C) On D2, 16 miRNAs were detected in the TBI animals with epilepsy (TBI+) but not in the sham group or in TBI animals without epilepsy (TBI−). These miRNAs, however, were typically found in only 1 sample in the TBI+ group, and the number of reads was very low (<3). (D) On D9, 22 miRNAs were detected in the TBI+ group but not in the sham and TBI− groups. As on D2, these miRNAs were typically found in only 1 sample in the TBI+ group and had a very low read number. (E–H) According to PCA, the first and second principal components explained 27% of the variance in the data on D2 and 33% on D9. Plasma miRNA expression profile separated sham and TBI rats into different clusters on D2 but not on D9. The miRNA expression profile did not separate TBI+ and TBI− rats at either time-point.

Principal component analysis (PCA). On D2, the PCA of normalized read counts (counts/million) revealed that the first (14%) and second (13%) principal components explained only 27% of the variance in the data (Figure 1E,G). The plasma miRNA expression profile on D2 separated sham and TBI rats into different clusters (Figure 1E). On D9, the first (20%) and second (13%) components explained 33% of the data variance (Figure 1F,H). The plasma miRNA expression profile on D9 did not separate sham and TBI rats (Figure 1F). The miRNA expression profile did not separate TBI+ and TBI− at either time-point (Figure 1G,H).

Spearman correlation analysis yielded a high positive correlation between miRNA expression profiles across all samples on both D2 and D9 (Supplementary Figure S2).

Heatmaps. On D2, heatmap analysis of miRNA expression profiles in all samples showed a separation between sham and TBI animals (Supplementary Figure S3). Pairwise comparisons revealed a clear separation between sham and TBI, sham and TBI+, and sham and TBI− groups (Supplementary Figure S4). No separation, however, was detected between the TBI+ and TBI− animals.

On D9, heatmap analysis of miRNA expression profiles in all samples revealed no clear separation between sham and TBI samples (Supplementary Figure S3). In addition, pairwise comparisons revealed no clear separation between groups (Supplementary Figure S5). As on D2, no separation was detected between the TBI+ and TBI− animals on D9.

2.1.2. Differential Expression Analysis

Differentially expressed miRNAs are presented in the Supplementary Materials (Tables S1–S6).

D2 samples. DESeq2 analysis detected 45 differentially expressed miRNAs between the TBI and sham groups (28 upregulated, 17 downregulated), 34 between the TBI+ and sham groups (27 upregulated, 7 downregulated), and 37 between the TBI− and sham groups (21 upregulated, 16 downregulated). No differentially expressed miRNAs were detected between the TBI+ and TBI− groups on D2.

D9 samples. DESeq2 analysis detected 17 differentially expressed miRNAs between the TBI and sham groups, (6 upregulated, 11 downregulated), 11 between the TBI+ and sham groups (2 upregulated, 9 downregulated), and 22 between the TBI− and sham groups (8 upregulated, 14 downregulated). No differentially expressed miRNAs were detected between the TBI+ and TBI− groups on D9.

2.1.3. Expression Pattern Differences from Machine Learning Analysis

The feature importance from logistic regression analysis for the miRNA candidates differentiating the groups is presented in Supplementary Figure S6.

D2 samples. On D2, logistic regression analysis differentiated between TBI and sham groups with the cross-validated area under the curve (CV AUC) 0.94. Among these miRNAs, 23/30 were also identified by differential expression analysis. Logistic regression analysis did not differentiate TBI+ and TBI− on D2 (CV AUC 0.50).

D9 samples. On D9, logistic regression analysis differentiated between TBI and sham groups with a cross-validated AUC 0.94. None of the 29 miRNAs from the logistic regression analysis were identified by the differential expression analysis. Logistic regression analysis did not differentiate TBI+ and TBI− on D9 (CV AUC 0.31).

2.2. Technical Validation with RT-qPCR–Discovery Cohort

As the heatmap analysis of miRNA expression profiles from miRNA sequencing indicated poor separation of the TBI and sham groups on D9, the subsequent technical validation (TBI vs. sham) focused on D2 sequencing data in samples available from the discovery cohort.

2.2.1. Selection of Differentially Expressed miRNAs for PCR Validation in D2 Samples

Of the 28 upregulated miRNAs (TBI vs. sham) in the miRNA-sequencing analysis, we selected 3 miRNAs (miR-136-3p, miR-323-3p, and miR-129-5p) for technical validation by

RT-qPCR. The selection was based on $\log_2FC \geq 1.0$, a low adjusted p-value, and a mean CPM ≥ 30 . In addition, we validated two other miRNAs (miR-434-3p and miR-9a-3p), which we earlier identified as strongly upregulated on D2 after TBI [18], to assess the consistency of findings between the studies and their potential as biomarkers for epileptogenesis.

2.2.2. Quantitative Reverse Transcription PCR

TBI vs. sham. Quantitative reverse transcription PCR (RT-qPCR) results are summarized in Figure 2. Technical validation of the 3 miRNAs (miR-139-3p, miR-323-3p, miR-129-5p) included different aliquots of plasma samples collected from the same 16 TBI rats and 4 sham-operated controls that were used for small RNA sequencing. Although miR-434-3p and miR-9a-3p were not detected in small RNA sequencing, both were detected by RT-qPCR. **miR-434-3p.** The miR-434-3p levels were 4.2-fold higher in the TBI group than in the sham group (2.20 ± 1.41 vs. 0.52 ± 0.31 , $p < 0.01$). **miR-9a-3p.** The miR-9a-3p levels were 9.3-fold higher in the TBI group than in the sham group (0.79 ± 0.45 vs. 0.09 ± 0.05 , $p < 0.001$). **miR-136-3p.** The miR-136-3p levels were 4.4-fold higher in the TBI group than in the sham group (1.37 ± 1.26 vs. 0.31 ± 0.24 , $p < 0.05$). **miR-323-3p.** The miR-323-3p levels were 4.5-fold higher in the TBI group than in the sham group (2.08 ± 1.61 vs. 0.47 ± 0.24 , $p < 0.05$). **miR-129-5p.** The miR-129-5p levels were 1.9-fold higher in the TBI group than in the sham group (0.17 ± 0.16 vs. 0.05 ± 0.05), but the difference was not statistically significant ($p > 0.05$). Because the miR-129-5p expression levels were very low and did not differ between the sham and TBI groups, miR-129-5p was excluded from the subsequent ddPCR-based analysis in the validation cohort.

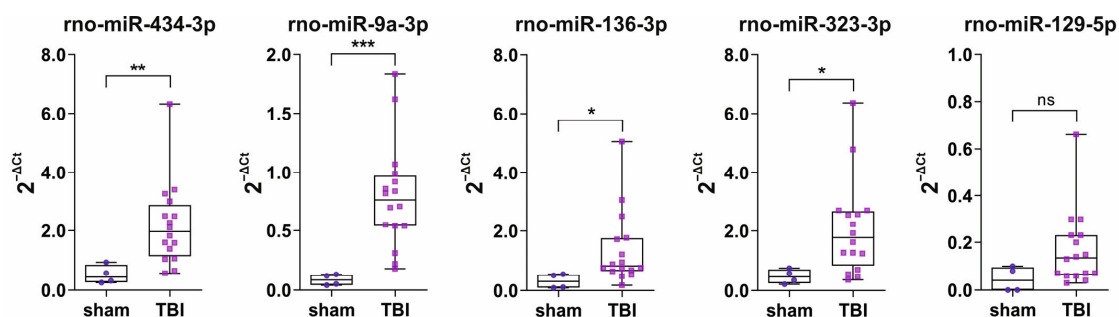


Figure 2. Technical validation of 5 plasma miRNA levels by RT-qPCR. Box and whisker plots (whiskers: minimum and maximum; box: interquartile range; line: median) showing the levels of 5 miRNAs (miR-434-3p, miR-9a-3p, miR-136-3p, miR-323-3p, and miR-129-5p) in rat plasma on D2 (48 h) after TBI or sham-operation. All of the miRNAs except miR-129-5p were upregulated in the TBI group ($n = 16$) compared with the sham group ($n = 4$). Expression levels were normalized to the endogenous control miR-28-3p with the $2^{-\Delta Ct}$ method. Statistical significance: *, $p < 0.05$; **, $p < 0.01$; ***, $p < 0.001$ (Mann–Whitney U test). Abbreviations: ns, not significant; TBI, traumatic brain injury.

TBI+ vs. TBI−. No differences were detected in any of the five miRNAs assessed with RT-qPCR ($p > 0.05$) between the TBI+ ($n = 7$) and TBI− ($n = 9$) groups.

2.3. D2 Plasma Levels of miRNAs in the Validation Cohort

2.3.1. Selection of miRNAs for ddPCR Analysis

Upregulated miRNAs. Based on the miRNA sequencing, we made a list of brain-specific or brain-enriched miRNAs with $\log_2FC \geq 1.0$ and a low p-value [PubMed search, Human miRNA tissue atlas [12]; RATEmiRs database [19]. Preliminary experiments revealed that miRNAs on that list with a CPM < 30 were difficult to validate with ddPCR. Therefore, we focused on miRNAs with a CPM ≥ 30 in the TBI group. Consequently, miR-434-3p, miR-9a-3p, miR-136-3p, and miR-323-3p were included in the final analysis

based on the miRNA-sequencing and technical validation. The list was complemented by three additional miRNAs, including miR-124-3p (log₂FC 7.4, CPM 31), miR-212-3p (log₂FC 1.3, CPM 39), and miR-132-3p (log₂FC 1.4, CPM 67), which we anticipated being able to quantify by ddPCR.

Downregulated miRNAs. We also performed preliminary experiments using ddPCR of three miRNAs that were downregulated in miRNA sequencing and showed the lowest adjusted *p*-value (miR-455-5p [log₂FC −1.5, CPM 107 in the TBI group], miR-140-3p [log₂FC −1.1, CPM 5930 in the TBI group], and miR-149-5p [log₂FC −1.3, CPM 248 in the TBI group]) (Supplementary Table S1). **miR-455-5p.** On D2, normalized plasma levels of miR-455-5p in the TBI group were only 40% of that in naïve rats (0.92 ± 0.21 vs. 2.32 ± 0.88 , $p < 0.01$) (Supplementary Figure S7A). In addition, miR-455-5p levels showed a decreasing trend in the sham group compared with naïve animals (1.04 ± 0.48 vs. 2.32 ± 0.88 , 55% decrease; $p > 0.05$). No difference was detected, however, between the TBI and sham groups (11% decrease, $p > 0.05$). **miR-140-3p** or **miR-149-5p** levels did not differ between the experimental groups (Kruskal–Wallis test, $p > 0.05$), although there was a decreasing trend in the order of naïve>sham or TBI (Supplementary Figure S7B,C).

Based on these data, we focused our search of plasma miRNA biomarkers on the list of the seven upregulated miRNAs.

2.3.2. Sample Quality

Plasma quality–hemolysis measurement by NanoDrop. Altogether, 115 of the 150 plasma samples (77%) available on D2 from the epilepsy-phenotyped rats qualified for ddPCR analysis (sufficient volume of plasma and A414 < 0.25). The mean A414 in the 115 pooled plasma samples was 0.13 ± 0.04 (range 0.05–0.24, median 0.14) (Supplementary Figure S8A). Animals with TBI ($n = 90$) had a slightly lower A414 than naïve animals ($n = 8$; 0.130 vs. 0.162 , $p < 0.05$) (Supplementary Figure S8B).

Small RNA concentration by Qubit assay. In plasma samples collected from the validation cohort, the mean small RNA concentration after RNA extraction was $419 \text{ ng/mL} \pm 288 \text{ ng/mL}$ ($n = 111$; range: 4.9 ng/mL – 1471 ng/mL , median: 343 ng/mL). Four samples (two naïve, one TBI−, one TBI+) had miRNA concentrations below the Qubit detection limit, but they could still be analyzed by ddPCR and were included in the analysis. We detected no differences in small RNA concentration between naïve, sham, and TBI groups (Kruskal–Wallis test, $p > 0.05$) (Supplementary Figure S6C).

Correlation between hemolysis and small RNA concentration. A weak positive correlation was detected between the A414 values and small RNA concentration measured by Qubit ($n = 111$, Spearman $r = 0.327$, $p < 0.001$), that is, the higher the A414 value, the greater the small RNA concentration (Supplementary Figure S8D). We detected no correlation, however, between the plasma A414 value and unnormalized miRNA expression levels of any of the analyzed miRNAs ($n = 115$, Spearman correlation, $p > 0.05$ for all), indicating that hemolysis did not affect miRNA expression levels.

2.4. D2 Plasma miRNA Levels in Different Treatment Groups

2.4.1. Naïve vs. Sham vs. TBI

The plasma concentrations of the seven miRNAs in the validation cohort are summarized in Figure 3. The validation cohort included 8 naïve, 17 sham, and 90 TBI rats (21 TBI+, 69 TBI−). As the samples had variable small RNA concentrations after RNA extraction, the target miRNA expression levels in each sample were normalized to the endogenous control miR-28-3p (target miRNA copy number/miR-28-3p copy number). The mean copy number of miR-28-3p was similar between the different experimental groups (Kruskal–Wallis test, $p > 0.05$).

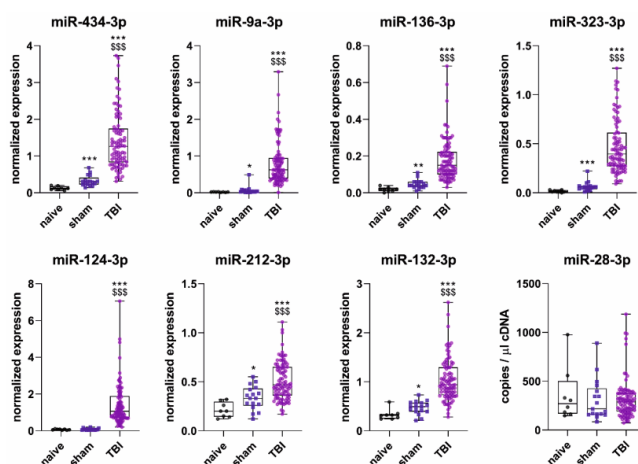


Figure 3. D2 plasma miRNA levels in different animal groups. Box and whisker plots (whiskers: minimum and maximum; box: interquartile range; line: median) showing the normalized expression levels of 7 validated miRNAs (miR-434-3p, miR-9a-3p, miR-136-3p, miR-323-3p, miR-124-3p, miR-212-3p, and miR-132-3p) measured by droplet digital PCR (ddPCR). MiR-28-3p was used as endogenous reference for normalization (target concentration/reference concentration). All 7 miRNAs were upregulated in the TBI group ($n = 90$) compared with naïve ($n = 8$) or sham-operated ($n = 17$) rats. Of 7 miRNAs, 6 (all except miR-124-3p) were upregulated in the sham group compared with the naïve group. The levels of the endogenous control miR-28-3p did not differ between the animal groups. Statistical significance: *, $p < 0.05$; **, $p < 0.01$; ***, $p < 0.001$ (compared with naïve); \$\$\$, $p < 0.001$ (compared with sham; Mann–Whitney U test). Abbreviations: TBI, traumatic brain injury.

miR-434-3p. The average normalized plasma levels of miR-434-3p in the sham-operated controls were 2.3-fold higher than in naïve rats (0.33 ± 0.15 vs. 0.13 ± 0.05 , $p < 0.001$). TBI rats had 11.2-fold higher normalized miR-434-3p levels than naïve rats (1.41 ± 0.77 vs. 0.13 , $p < 0.001$) and 4.3-fold higher levels than sham-operated controls (1.41 vs. 0.33 , $p < 0.001$).

miR-9a-3p. Sham-operated controls had 3.4-fold higher normalized levels of plasma miR-9a-3p than naïve rats (0.07 ± 0.11 vs. 0.02 ± 0.008 , $p < 0.05$). TBI rats had 41.1-fold higher miR-9a-3p levels than naïve rats (0.81 ± 0.59 vs. 0.02 , $p < 0.001$) and 22.4-fold higher levels than sham-operated controls (0.81 vs. 0.07 , $p < 0.001$).

miR-136-3p. The sham group had 2.9-fold higher normalized levels of plasma miR-136-3p than the naïve group (0.05 ± 0.02 vs. 0.02 ± 0.01 , $p < 0.01$). TBI rats had 10.6-fold higher miR-136-3p levels than naïve rats (0.18 ± 0.11 vs. 0.02 , $p < 0.001$) and 3.7-fold higher levels than sham-operated controls (0.18 vs. 0.05 , $p < 0.001$).

miR-323-3p. Sham-operated controls had 4.2-fold higher normalized levels of plasma miR-323-3p levels than naïve rats (0.06 ± 0.05 vs. 0.02 ± 0.01 , $p < 0.001$). TBI rats had 30.6-fold higher miR-323-3p levels than naïve rats (0.47 ± 0.28 vs. 0.02 , $p < 0.001$) and 7.3-fold higher levels than sham-operated controls (0.47 vs. 0.06 , $p < 0.001$).

miR-124-3p. Sham-operated controls and naïve rats had similar normalized levels of plasma miR-124-3p (0.08 ± 0.05 vs. 0.07 ± 0.03 , $p > 0.05$). TBI rats had 20.8-fold higher miR-124-3p levels than naïve rats (1.41 ± 1.11 vs. 0.07 , $p < 0.001$) and 18.2-fold higher levels than sham-operated controls (1.41 vs. 0.08 , $p < 0.001$).

miR-212-3p. Sham-operated controls had 1.6-fold higher normalized levels of plasma miR-212-3p than naïve rats (0.34 ± 0.12 vs. 0.21 ± 0.08 , $p < 0.05$). TBI rats had 2.4-fold higher miR-212-3p levels than naïve rats (0.51 ± 0.19 vs. 0.21 , $p < 0.001$) and 1.5-fold higher levels than sham-operated controls (0.51 vs. 0.34 , $p < 0.001$).

miR-132-3p. Sham-operated controls had 1.4-fold higher normalized levels of plasma miR-132-3p than naïve rats (0.47 ± 0.14 vs. 0.33 ± 0.11 , $p < 0.05$). TBI rats had 3.1-fold higher miR-132-3p levels than naïve rats (1.04 ± 0.43 vs. 0.33 , $p < 0.001$) and 2.2-fold higher levels than sham-operated controls (1.04 vs. 0.47 , $p < 0.001$).

2.4.2. ROC Analysis

The ROC curves for miR-434-3p, miR-9a-3p, miR-136-3p, miR-323-3p, miR-124-3p, miR-212-3p, and miR-132-3p are presented in Figure 4. The AUC and optimal cut-off values for the normalized miRNA levels measured by ddPCR are summarized in Supplementary Table S7.

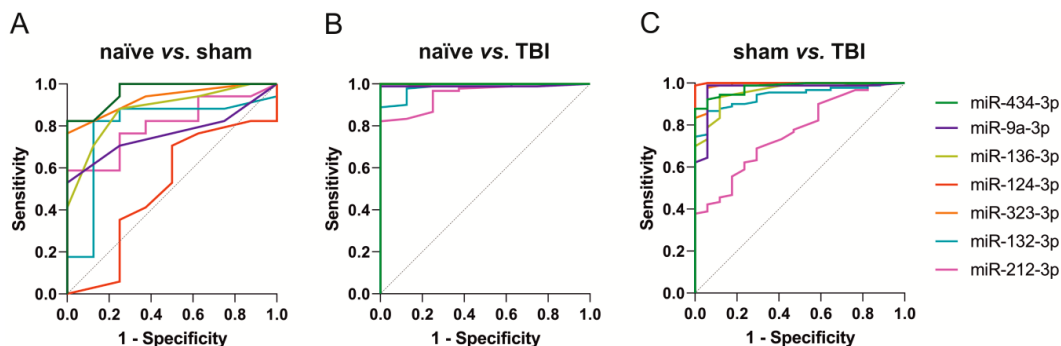


Figure 4. ROC analysis of plasma miRNA levels measured on D2 after TBI or sham operation. (A) Naïve vs. sham. Of 7 miRNAs, 6 (miR-434-3p, miR-9a-3p, miR-136-3p, miR-323-3p, miR-132-3p, and miR-212-3p) separated sham-operated controls ($n = 17$) from naïve rats ($n = 8$; $p < 0.05$). MiR-124-3p did not separate sham-operated controls from naïve animals (AUC 0.59, $p > 0.05$). See results for details. (B) TBI vs. naïve. All analyzed miRNAs separated rats with TBI ($n = 90$) from naïve animals ($n = 8$) with an AUC ≥ 0.90 ($p < 0.001$), indicating a very good performance as diagnostic TBI biomarkers. (C) TBI vs. sham operation. All analyzed miRNAs separated rats with TBI ($n = 90$) from sham-operated controls ($n = 17$). MiR-434-3p, miR-9a-3p, miR-136-3p, miR-323-3p, and miR-132-3p had AUC ≥ 0.90 ($p < 0.001$), whereas miR-212-3p had an AUC of 0.76 ($p < 0.001$). See results for details. Abbreviations: TBI, traumatic brain injury.

miR-434-3p. The miR-434-3p levels separated sham-operated controls from naïve rats (AUC 0.96, $p < 0.001$) with 82% sensitivity and 100% specificity (cut-off 0.22). TBI rats were separated from naïve rats (AUC 1.00, $p < 0.001$) with 100% sensitivity and 100% specificity (cut-off 0.31) and from sham-operated controls (AUC 0.98, $p < 0.001$) with 88% sensitivity and 100% specificity (cut-off 0.69).

miR-9a-3p. The miR-9a-3p levels separated sham-operated controls from naïve rats (AUC 0.76, $p < 0.05$) with 53% sensitivity and 100% specificity (cut-off 0.04). TBI rats were separated from naïve rats (AUC 0.99, $p < 0.001$) with 99% sensitivity and 100% specificity (cut-off 0.18) and from sham-operated controls (AUC 0.97, $p < 0.001$) with 99% sensitivity and 94% specificity (cut-off 0.18).

miR-136-3p. The miR-136-3p levels separated sham-operated controls from naïve rats (AUC 0.88, $p < 0.01$) with 88% sensitivity and 75% specificity (cut-off 0.03). TBI rats were separated from naïve rats (AUC 1.00, $p < 0.001$) with 99% sensitivity and 100% specificity (cut-off 0.05) and from sham-operated controls (AUC 0.96, $p < 0.001$) with 93% sensitivity and 88% specificity (cut-off 0.07).

miR-323-3p. The miR-323-3p levels separated sham-operated controls from naïve rats (AUC 0.93, $p < 0.001$) with 76% sensitivity and 100% specificity (cut-off 0.04). TBI rats were separated from naïve rats (AUC 1.00, $p < 0.001$) with 100% sensitivity and 100% specificity (cut-off 0.09) and from sham-operated controls (AUC 0.99, $p < 0.001$) with 98% sensitivity and 94% specificity (cut-off 0.12).

miR-124-3p. The miR-124-3p levels did not separate sham-operated controls from naïve rats (AUC 0.49, $p > 0.05$). The miR-124-3p levels separated TBI rats from naïve rats (AUC 1.00, $p < 0.001$, 100% sensitivity and 100% specificity, cut-off 0.20) and sham-operated controls (AUC 1.00, $p < 0.001$, 99% sensitivity and 100% specificity, cut-off 0.26).

miR-212-3p. The miR-212-3p levels separated sham-operated controls from naïve rats (AUC 0.81, $p < 0.05$) with 59% sensitivity and 100% specificity (cut-off 0.33). TBI rats were separated from naïve rats (AUC 0.95, $p < 0.001$) with 82% sensitivity and 100% specificity (cut-off 0.33) and from sham-operated controls (AUC 0.76, $p < 0.001$) with 69% sensitivity and 71% specificity (cut-off 0.39).

miR-132-3p. The miR-132-3p levels separated sham-operated controls from naïve rats (AUC 0.79, $p < 0.05$) with 82% sensitivity and 88% specificity (cut-off 0.39). TBI rats were separated from naïve animals (AUC 0.98, $p < 0.001$) with 89% sensitivity and 100% specificity (cut-off 0.60) and from sham-operated (AUC 0.94, $p < 0.001$) with 87% sensitivity and 94% specificity (cut-off 0.65).

2.5. Epilepsy Outcome

2.5.1. D2 Plasma miRNA Levels

Next, we investigated whether plasma miRNA levels on D2 differentiated TBI rats with (TBI+) or without epilepsy (TBI−) or different epilepsy severities.

Epilepsy vs. no epilepsy. Of the 90 TBI rats included in the miRNA analysis, 21 had epilepsy (TBI+) and 69 did not (TBI−). We detected no differences in the miRNA levels between the TBI+ and TBI− groups ($p > 0.05$ for all miRNAs) (Figure 5).

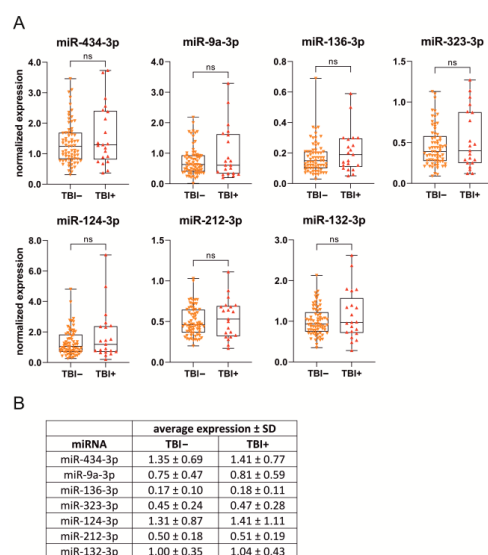


Figure 5. Normalized plasma miRNA levels on D2 and epilepsy outcome. (A) Box and whisker plots (whiskers: minimum and maximum; box: interquartile range; line: median) showing comparable plasma miRNA levels in the injured rats with (TBI+) and without (TBI−) epilepsy (Mann–Whitney U test, $p > 0.05$ for all miRNAs). (B) A table summarizing normalized miRNA expression levels (mean \pm SD) in the TBI− and TBI+ groups. Abbreviations: ns, not significant; SD, standard deviation; TBI, traumatic brain injury.

Epilepsy severity–seizure frequency. To investigate possible differences in plasma miRNA levels within the TBI+ group depending on the severity of epilepsy, we categorized the 21 TBI+ animals based on two criteria: seizure frequency and occurrence of seizure clusters.

First, rats with epilepsy were divided according to whether the total number of seizures was ≥ 3 ($n = 15$) vs. < 3 seizures ($n = 6$) during the 1-month vEEG monitoring. We detected no differences in the miRNA levels between the rats with ≥ 3 seizures or < 3 seizures ($p > 0.05$ for all miRNAs) (Figure 6A). The total number of seizures did not correlate with any of the miRNAs ($p > 0.05$).

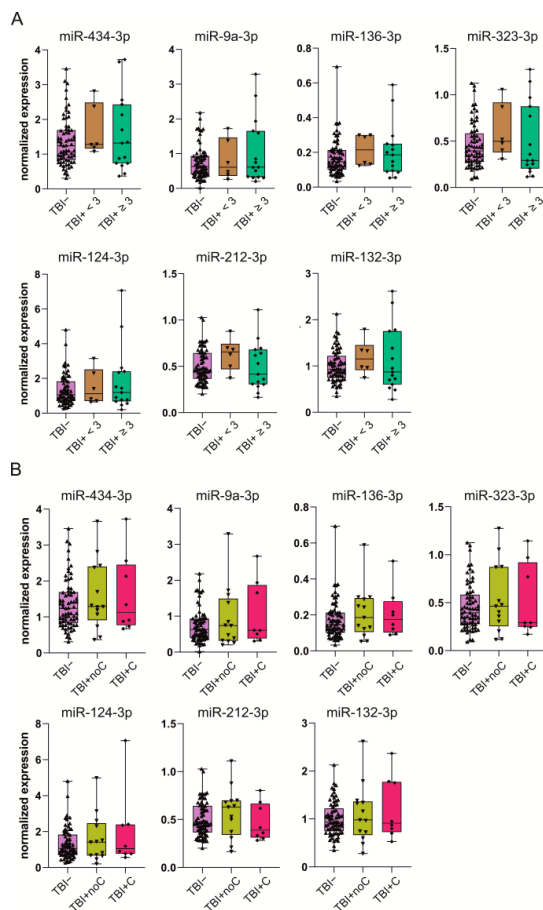


Figure 6. Normalized plasma miRNA levels on D2 and severity of epilepsy. **(A)** Rats with frequent (i.e., ≥ 3 late seizures per month) vs. less frequent seizures (< 3 seizures per month). Box and whisker plots (whiskers: minimum and maximum; box: interquartile range; line: median) show that plasma miRNA levels on D2 in TBI+ animals with frequent (15/21) or less frequent late seizures (6/21) were comparable (Mann–Whitney U test, $p > 0.05$). In addition, the average miRNA levels were comparable when the TBI+ rats with frequent seizures were compared with TBI– animals or with all remaining TBI rats (TBI+ > 3 seizures vs. TBI– and TBI+ < 3 seizures; $p > 0.05$). **(B)** Rats with or without seizure clusters (i.e., ≥ 3 seizures within 24 h). Box and whisker plots summarize the levels of miRNAs in rats with epilepsy (TBI+) with seizure clusters (TBI+ C, 8/21) or without seizure clusters (TBI+ noC, 13/21). Plasma miRNAs on D2 did not differ between the rats with or without seizure clusters (Mann–Whitney U test, $p > 0.05$ for all miRNAs). In addition, plasma miRNA levels were comparable when the TBI+ rats with seizure clusters (severe epilepsy) were compared with TBI– rats or with all remaining TBI rats (TBI+ C vs. TBI– and TBI+ noC, TBI–, $n = 69$, $p > 0.05$). Abbreviations: TBI, traumatic brain injury; TBI–, TBI rats without epilepsy.

Epilepsy severity–seizure clusters. For the analysis, rats with epilepsy were divided into two categories according to whether the animal had seizure clusters (8 yes, 13 no). A seizure cluster was defined as ≥ 3 seizures within 24 h. We detected no differences in different miRNA levels between the rats with or without seizure clusters ($p > 0.05$ for all miRNAs) (Figure 6B).

2.5.2. ROC Analysis

The AUC and optimal cut-off values for the normalized miRNA levels measured by ddPCR are summarized in Supplementary Table S8.

Epilepsy vs. no epilepsy. None of the seven miRNAs distinguished TBI+ from TBI– rats on D2 (Figure 7A).

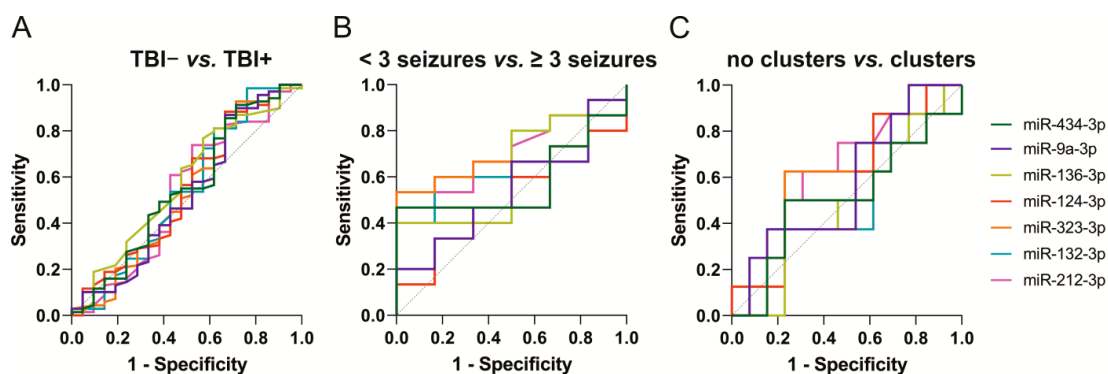


Figure 7. ROC analysis of plasma miRNA levels measured on D2 between epilepsy severity groups. None of the plasma miRNAs measured on D2 after traumatic brain injury (TBI) differentiated: (A) TBI rats with epilepsy (TBI+, $n = 21$) from rats without epilepsy (TBI–, $n = 69$); (B) TBI+ rats with ≥ 3 seizures ($n = 15$) from TBI+ rats with < 3 seizures ($n = 6$); and (C) TBI+ rats with seizure clusters ($n = 8$) from TBI+ rats without seizure clusters ($n = 13$).

Epilepsy severity–seizure frequency. None of the seven miRNAs distinguished rats with ≥ 3 or < 3 seizures (Figure 7B).

Epilepsy severity–seizure clusters. None of the seven miRNAs distinguished rats with or without clusters (Figure 7C).

2.5.3. Glmnet Analysis

We then used elastic net regularized logistic regression (glmnet) to determine the optimal set of explanatory variables (i.e., miRNAs) to use in the logistic regression analysis to distinguish between TBI+ and TBI– animals, as well as to distinguish between the epilepsy severity groups.

TBI+ vs. TBI–. Glmnet analysis did not identify any combination of miRNAs (all coefficients zero in the majority of the cross-validation folds) that differentiated TBI+ rats ($n = 21$) from TBI– rats ($n = 69$).

≥ 3 seizures vs. < 3 seizures. Glmnet analysis identified a combination of five miRNAs (miR-9a-3p, miR-323-3p, miR-124-3p, miR-212-3p, and miR-132-3p) as the optimal combination for differentiating TBI+ rats with ≥ 3 seizures ($n = 15$) from TBI+ rats with < 3 seizures ($n = 6$). Logistic regression analysis using these predictors produced a cross-validated AUC of 0.76 (95% CI: 0.51–0.93, $p = 0.056$) (Figure 8A).

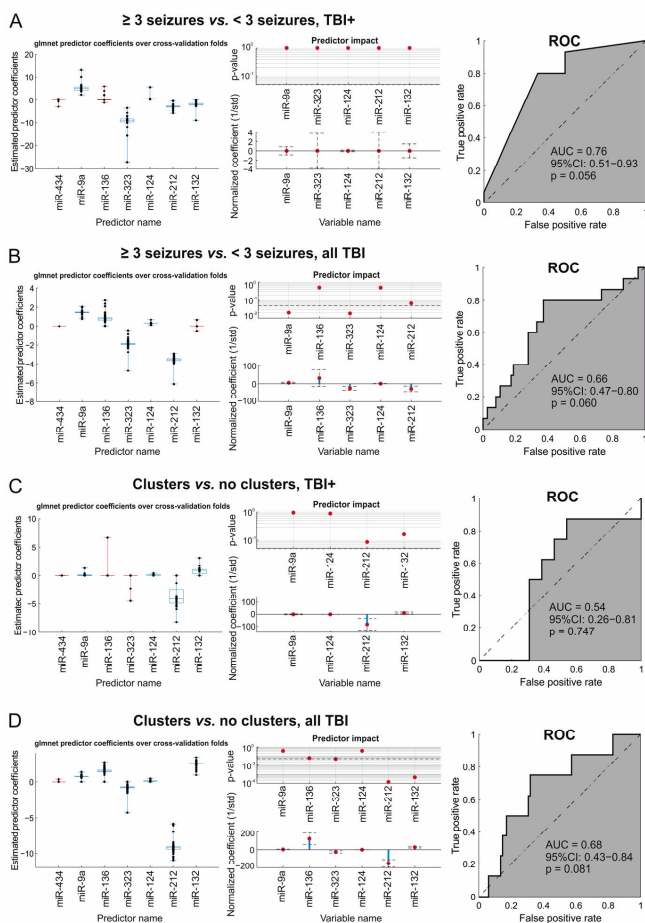


Figure 8. Elastic net regularized logistic regression (glmnet) analysis of plasma miRNA profile in epilepsy severity groups. **(A) Left panel:** Boxplots of predictor coefficients over cross-validation folds. The analysis defined miR-9a-3p, miR-323-3p, miR-124-3p, miR-212-3p, and miR-132-3p (blue boxplots) as the optimal set of miRNAs to separate TBI+ rats with ≥ 3 seizures/month ($n = 15$) from TBI+ rats with < 3 seizures/month ($n = 6$). Due to having a coefficient of zero in most cross-validation folds, miR-434-3p and miR-136-3p were excluded (red boxplot). Center panel: p -value and normalized coefficient of each predictor in the standard logistic regression analysis. **Right panel:** Cross-validated ROC AUC was only 0.76 with a large confidence interval and $p > 0.05$. **(B)** The analysis defined miR-9a-3p, miR-136-3p, miR-323-3p, miR-124-3p, and miR-212-3p as the optimal set of miRNAs to separate TBI+ rats with ≥ 3 seizures/month ($n = 15$) from all remaining TBI rats ($n = 75$), but the ROC AUC was 0.66 with a large confidence interval and $p > 0.05$. **(C)** The analysis defined miR-9a-3p, miR-124-3p, miR-212-3p, and miR-132-3p as the optimal set of miRNAs to separate TBI+ rats with ($n = 8$) or without ($n = 13$) seizure clusters. The ROC AUC, however, was only 0.54 with a large confidence interval and a nonsignificant p -value ($p > 0.05$). **(D)** The analysis defined miR-9a-3p, miR-136-3p, miR-323-3p, miR-124-3p, miR-212-3p, and miR-132-3p as the optimal set of miRNAs to separate TBI+ rats with seizure clusters ($n = 8$) from all remaining TBI rats ($n = 82$). The ROC AUC was 0.68, however, with a larger confidence interval and $p > 0.05$. Abbreviations: AUC, area under the curve; CI, confidence interval; ROC, receiver operating characteristics; TBI, traumatic brain injury; TBI+, rats with epilepsy; TBI−, rats without epilepsy.

Next, we investigated the optimal combination for differentiating TBI+ rats with ≥ 3 seizures ($n = 15$) from all TBI rats (TBI+ with < 3 seizures and TBI- rats combined, $n = 75$). Glmnet analysis identified a combination of five miRNAs (miR-9a-3p, miR-136-3p, miR-323-3p, miR-124-3p, and miR-212-3p) as the optimal set of miRNAs for differentiating the groups (AUC 0.66, 95% CI: 0.47–0.80, $p = 0.060$) (Figure 8B).

Clusters vs. no clusters. Glmnet analysis identified miR-9a, miR-124-3p, miR-212-3p, and miR-132-3p as the optimal combination for differentiating TBI+ rats with seizure clusters ($n = 8$) from TBI+ rats without seizure clusters ($n = 13$) (Figure 8C). The AUC was low (0.54), however, and the confidence interval range large (95% CI: 0.26–0.81, $p = 0.747$).

Next, we investigated the optimal miRNA combination for differentiating TBI+ rats with seizure clusters ($n = 8$) from all TBI rats (TBI+ with no clusters and TBI- rats combined, $n = 82$). Glmnet analysis identified a combination of six miRNAs (miR-9a-3p, miR-136-3p, miR-323-3p, miR-124-3p, miR-212-3p, and miR-132-3p) as the optimal miRNA set for differentiating the groups (AUC 0.68, 95% CI: 0.43–0.84, $p = 0.081$) (Figure 8D).

2.6. Correlation of Acute Post-Injury Plasma miRNA Levels with Structural Outcome

To address whether the elevated plasma miRNAs report on the severity of cortical injury after TBI, we correlated the D2 miRNA levels with the severity of the lateral FPI-induced cortical lesion at acute and chronic time-points. For that, we measured: (a) the volume of abnormal cortical T₂ in MRI on D2, D7, and D21 post-injury, and (b) the cortical lesion area in unfolded cortical maps on D182 post-injury.

2.6.1. Correlation of miRNA Levels with Cortical Lesion Volume in MRI

The T₂ MRI analysis for the whole EPITARGET cohort was previously presented by [20]. Quantitative T₂ MRI data were available for all 90 TBI rats included in the plasma miRNA analysis, except for one animal missing D2 MRI data. Consequently, the animal numbers were 89 for D2, 90 for D7, and 90 for D21. Correlation plots for normalized miRNA levels and T₂ MRI data are summarized in Figure 9.

miR-434-3p. The higher the plasma levels of miR-434-3p on D2, the larger the volume of the ipsilateral cortical T₂ abnormality on D2 ($\rho = 0.411$, $p < 0.001$), on D7 ($\rho = 0.342$, $p < 0.001$), and on D21 ($\rho = 0.438$, $p < 0.001$).

miR-9a-3p. The higher the plasma levels of miR-9a-3p on D2, the larger the volume of the ipsilateral cortical T₂ abnormality on D2 ($\rho = 0.566$, $p < 0.001$), on D7 ($\rho = 0.507$, $p < 0.001$), and on D21 ($\rho = 0.571$, $p < 0.001$).

miR-136-3p. The higher the plasma levels of miR-136-3p on D2, the larger the volume of the ipsilateral cortical T₂ abnormality on D2 ($\rho = 0.345$, $p < 0.001$), on D7 ($\rho = 0.287$, $p < 0.01$), and on D21 ($\rho = 0.394$, $p < 0.001$).

miR-323-3p. The higher the plasma levels of miR-323-3p on D2, the larger the volume of the ipsilateral cortical T₂ abnormality on D2 ($\rho = 0.468$, $p < 0.001$), on D7 ($\rho = 0.418$, $p < 0.001$), and on D21 ($\rho = 0.489$, $p < 0.001$).

miR-124-3p. The higher the plasma levels of miR-124-3p on D2, the larger the volume of the ipsilateral cortical T₂ abnormality on D2 ($\rho = 0.582$, $p < 0.001$), on D7 ($\rho = 0.522$, $p < 0.001$), and on D21 ($\rho = 0.581$, $p < 0.001$).

miR-212-3p. The higher the plasma levels of miR-212-3p on D2, the larger the volume of the ipsilateral cortical T₂ abnormality on D21 ($\rho = 0.269$, $p < 0.05$) but not on D2 or D7 ($p > 0.05$).

miR-132-3p. The higher the plasma levels of miR-132-3p on D2, the larger the volume of the ipsilateral cortical T₂ abnormality on D2 ($\rho = 0.460$, $p < 0.001$), on D7 ($\rho = 0.433$, $p < 0.001$), and on D21 ($\rho = 0.463$, $p < 0.001$).

miR-28-3p. We detected no correlation between the plasma miR-28-3p levels and the volume of the ipsilateral cortical T₂ abnormality at any time-point ($p > 0.05$).

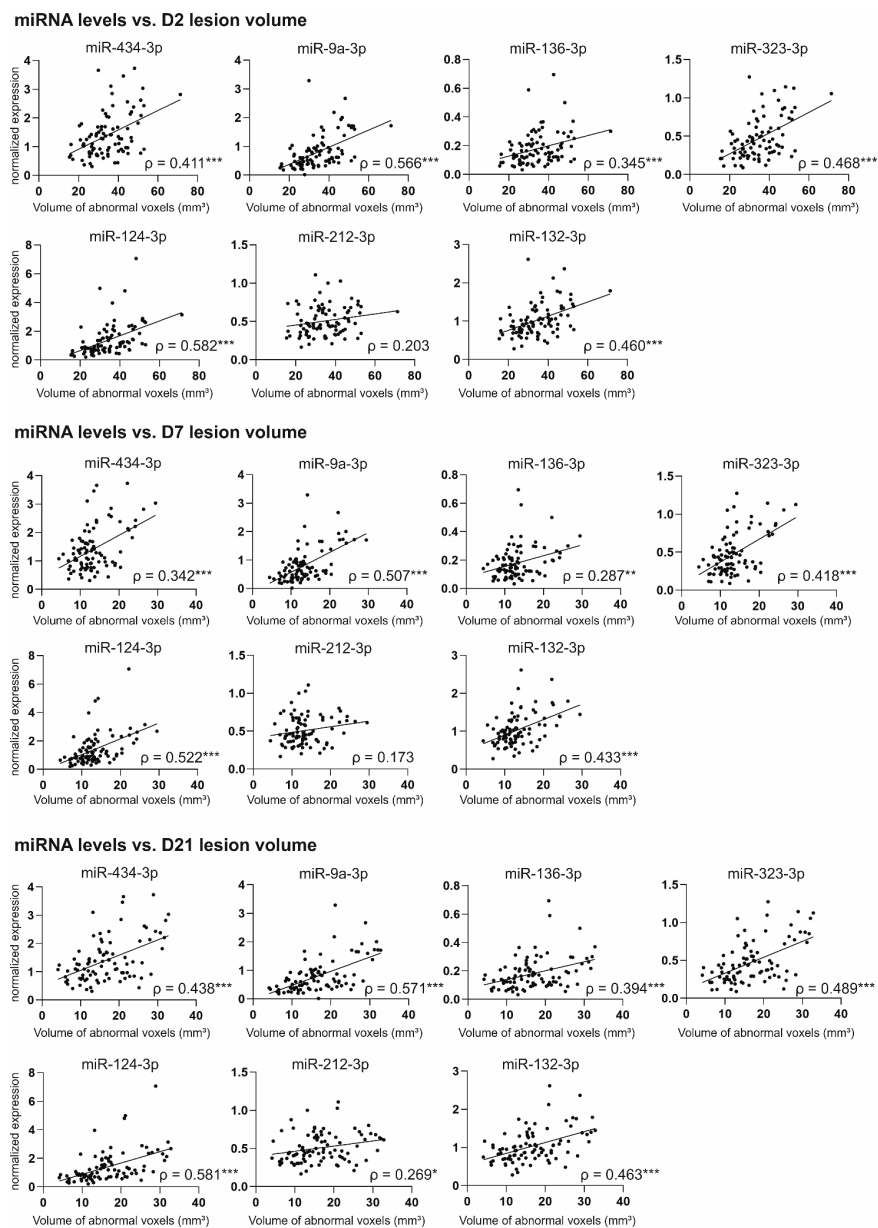


Figure 9. Spearman correlations (ρ) between normalized plasma miRNA levels on D2 and cortical lesion severity in quantitative T2 MRI on D2, D7, and D21 after TBI. Each dot represents 1 TBI animal ($n = 89$ for D2, $n = 90$ for D7 and D21). The higher the plasma miRNA levels on D2, the larger the lesion volume in MRI. The total volume of abnormal cortical T2 is shown on the x-axis and the normalized plasma miRNA level is shown on the y-axis. Note that the correlation coefficients were highest on D2 and D21. Statistical significance: *, $p < 0.05$; **, $p < 0.01$; ***, $p < 0.001$ (Spearman correlation). Abbreviations: D2, day 2 after TBI; D7, day 7 after TBI; D21, day 21 after TBI; TBI, traumatic brain injury.

2.6.2. Correlation of miRNA Levels with Cortical Lesion Area in Unfolded Maps

Unfolded cortical maps were created for all 90 TBI rats included in the miRNA analysis. Correlation plots for normalized miRNA levels on D2 and cortical lesion area on D182 are presented in Figure 10.

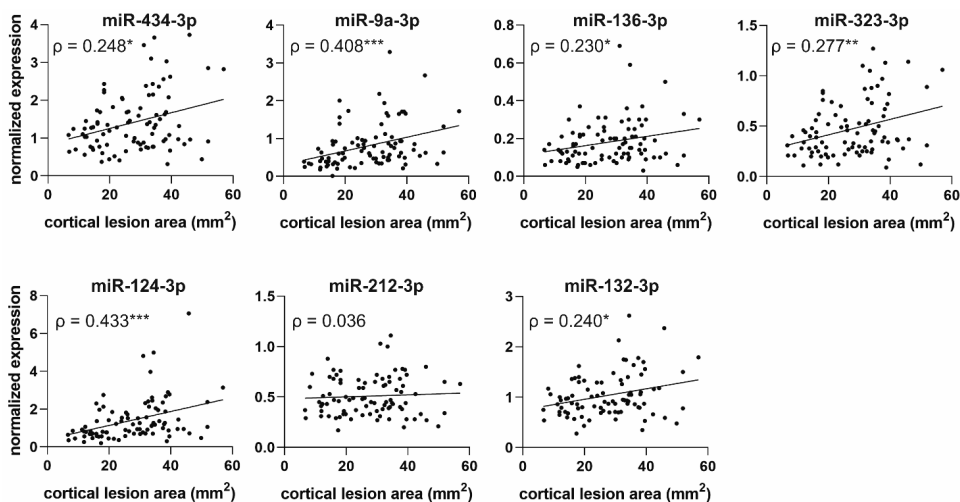


Figure 10. Spearman correlations (ρ) between normalized plasma miRNA levels on D2 and cortical lesion area in unfolded cortical maps on D182 after TBI. The greater the normalized plasma levels of miR-9a-3p and miR-124-3p on D2 after TBI ($n = 90$), the greater the cortical lesion area on D182 ($\rho > 0.4$). In addition, elevated normalized plasma miR-434-3p, miR-136-3p, miR-323-3p, and miR-132-3p levels were associated with a greater cortical lesion area 6 months later ($\rho > 0.2$). No correlation was detected between miR-212-3p level and cortical lesion area ($\rho = 0.036$, $p > 0.05$). Statistical significance: *, $p < 0.05$; **, $p < 0.01$; ***, $p < 0.001$ (Spearman correlation).

Correlation analysis showed that the greater the normalized plasma levels of all miRNAs on D2, the larger the cortical lesion area on D182. The only exception was miR-212-3p ($p > 0.05$). The miRNAs most strongly associated with the extent of cortical lesion area were miR-124-3p ($\rho = 0.433$, $p < 0.001$) and miR-9a-3p ($\rho = 0.408$, $p < 0.001$), followed by miR-323-3p ($\rho = 0.277$, $p < 0.01$), miR-434-3p ($\rho = 0.248$, $p < 0.05$), miR-132-3p ($\rho = 0.240$, $p < 0.05$), and miR-136-3p ($\rho = 0.230$, $p < 0.05$). We detected no correlation between the endogenous control miR-28-3p levels and cortical lesion area ($p > 0.05$).

2.7. MiRNA Target Analysis

Ingenuity pathway analysis (IPA) was used to search for the predicted mRNA targets of the validated miRNAs. We also conducted a pathway analysis to investigate the canonical pathways associated with the target genes.

IPA found 1 target for miR-434-3p, 89 targets for miR-9a-3p, 27 targets for miR-136-3p, 29 targets for miR-323-3p, 460 targets for miR-124-3p, and 91 targets for miR-132-3p/miR-212-3p. The targets are visualized in Supplementary Figure S9A. Canonical pathway analysis of the predicted target genes revealed different top canonical pathways for each miRNA, except for miR-434-3p for which no data was available (Supplementary Figure S9B). The top canonical pathways included pathways associated with cancer, inflammation, and immune cell function.

3. Discussion

The present study investigated whether acute alterations in the circulating plasma miRNA expression levels after experimental TBI can be used as prognostic biomarkers

for the evolution of cortical damage and epileptogenesis after TBI. Four major findings were revealed. First, small RNA sequencing revealed 45 differentially expressed miRNAs between the TBI and sham-operated controls on D2 after injury. Second, craniotomy without TBI induction resulted in miRNA upregulation compared with naïve rats. Third, the higher the plasma miRNA levels at the acute post-TBI time-point, the larger the cortical lesion within both the first 3 weeks and 6 months after injury. Fourth, D2 plasma miRNA levels did not predict post-traumatic epileptogenesis or epilepsy severity.

3.1. Acute Post-Injury Regulation of Circulating Neuron-Enriched miRNAs Is Clear but Short-Lasting

We investigated TBI-induced alterations in plasma miRNA expression at acute (D2) and subacute (D9) time-points after TBI. Small RNA sequencing revealed that the plasma miRNA expression profile separated TBI from sham rats on D2 but not on D9. The two time-points had no common upregulated miRNAs and shared only three downregulated miRNAs, suggesting that most of the miRNAs with altered expression on D2 returned to baseline levels by D9 after injury. Consequently, we focused our analysis on validating differentially expressed miRNAs found on D2 after TBI. The miRNAs selected for validation were brain-enriched and had at least a 2-fold ($\log_2FC \geq 1$) difference between the TBI and sham groups and a CPM value ≥ 30 .

Using ddPCR, we showed increased expression of seven miRNAs (miR-434-3p, miR-9a-3p, miR-136-3p, miR-323-3p, miR-124-3p, miR-212-3p, and miR-132-3p) in the rat plasma on D2 after TBI compared with sham-operated (craniotomy) controls. All analyzed miRNAs are primarily expressed in neurons [10,21–28]. The greatest fold changes were observed for miR-9a-3p (22-fold) and miR-124-3p (18-fold). The dysregulation of miR-323-3p (7-fold) as well as miR-136-3p and miR-434-3p (around 4-fold for both) was also clear. Upregulation of miR-132-3p and miR-212-3p was approximately 2-fold and 1.5-fold, respectively, after TBI.

Our study also included naïve controls that did not undergo any surgery. Interestingly, the fold changes in the plasma miRNA expression were greater when TBI rats were compared with naïve rats than when they were compared with sham-operated controls. The largest fold change was observed for miR-9a-3p (41-fold), followed by miR-323-3p (31-fold) and miR-124-3p (21-fold). Upregulation of miR-434-3p and miR-136-3p was approximately 11-fold, and upregulation of miR-132-3p and miR-212-3p was approximately 3-fold and 2-fold, respectively.

We previously reported upregulation of miR-434-3p, miR-9a-3p, miR-136-3p [18], and miR-124-3p [29] in the plasma on D2 after LFPI-induced TBI. The fold changes of miR-9a-3p, miR-434-3p, and miR-136-3p levels after TBI in the present study were comparable to our previous data [18]. The 18-fold increase in miR-124-3p levels on D2 in TBI rats compared with sham-operated controls, however, was clearly higher than the 1.4-fold increase reported by [29]. This may relate to slight differences in the ddPCR analysis methods. In the present study, we used ddPCR with EvaGreen chemistry, whereas the study by Vuokila et al. [29] used ddPCR with TaqMan chemistry. Interestingly, Wang et al. [30] reported a >2-fold increase in exosomal miR-124-3p levels in the rat plasma at 24 h after weight-drop-induced TBI, indicating that miR-124-3p levels report on brain injury induced by different mechanisms. To the best of our knowledge, the levels of miR-323-3p, miR-132-3p, and miR-212-3p in blood circulation have not been previously investigated in TBI models.

We used ROC analysis to assess the performance of the seven validated miRNAs as diagnostic biomarkers for TBI. We found that acutely increased levels of all seven miRNAs distinguished TBI rats from naïve rats with an ROC AUC ≥ 0.90 . All seven miRNAs also distinguished TBI from sham controls and 6 of 7 had an ROC AUC ≥ 0.90 . Taken together, the validated circulating miRNAs demonstrate excellent performance as diagnostic biomarkers for brain injury.

We next investigated whether the miRNAs detected in preclinical models are also dysregulated after human TBI. Some of the miRNAs analyzed in our study were previously

investigated in blood samples collected from TBI patients [18,31–33]. O’Connell et al. reported a 4-fold increase in the serum miR-9-3p levels and a 3-fold increase in the serum miR-124-3p levels in TBI patients at hospital admission (≤ 24 h after injury) [31]. The patients included in the study had variable injury severities with a mean Glasgow Coma Score (GSC) of 10.8 ± 2.5 . Schindler et al. [33] detected miR-124-3p in the blood of patients with severe TBI within 6 h after injury; the fold change compared with controls, however, was < 2 . In our previous study [18], we detected a 9-fold increase in miR-9-3p levels in plasma collected from severe TBI patients (≤ 48 h after injury). In addition, we detected elevated plasma levels of miR-9-3p and miR-136-3p in a subpopulation of mild TBI patients with high plasma S100B levels.

To the best of our knowledge, there is only one study on blood miR-132-3p levels in TBI patients [32]. That study used a microarray and reported a 2-fold increase in serum miR-132-3p levels at 12 h and 48 h post-injury compared with the 2-h post-injury time-point. Interestingly, they did not detect an increase in miR-132-3p levels at 24 h post-injury.

Taken together, we report the upregulation of seven neuronally enriched plasma miRNAs on D2 in a clinically relevant experimental model of closed head injury. Of these, miR-434-3p is rodent-specific and not detected in humans [18]. Two of the miRNAs, however, miR-323-3p and miR-212-3p, have not yet been analyzed in humans, and thus present novel upregulated candidate plasma biomarkers to be validated in TBI patients.

3.2. Plasma miRNA Levels Detect Mild Injury Caused by Craniotomy during Sham Operation

Craniotomy can induce structural and functional damage to the underlying brain [34]. In addition, craniotomy results in mild T_2 relaxation abnormalities in MRI and increased levels of circulating neurofilament light, a protein marker of axonal injury [35].

In the present study, we detected an increase in 6 of 7 miRNAs (all except miR-124-3p) in sham-operated controls on D2 after surgery compared with naïve rats. The six upregulated miRNAs distinguished the sham-operated rats from naïve rats in the ROC analysis. In contrast to the other miRNAs, the plasma levels of miR-124-3p were unaltered in the sham-operated control group compared with naïve rats, and miR-124-3p levels did not separate sham from naïve animals in the ROC analysis. This suggests that the release of miR-124-3p into blood circulation requires an impact stronger than craniotomy, whereas miR-434-3p, miR-9a-3p, miR-323-3p, miR-136-3p, miR-212-3p, and miR-132-3p appear to be sensitive indicators of injury induced by craniotomy. All of the investigated miRNAs are neuronally enriched, suggesting that their release into the plasma results from neuronal injury rather than injury to other tissues, such as bone or skin. As there are limited data available on the expression of these miRNAs in other tissues, or on the impact of TBI on miRNA expression in organs other than the brain, a peripheral contribution cannot be completely excluded.

The ability to distinguish sham-operated controls from naïve rats makes miR-434-3p, miR-9a-3p, miR-323-3p, miR-136-3p, miR-212-3p, and miR-132-3p potential biomarkers of mild brain injury. In our earlier study with a low number of TBI patients [18], miR-9-3p and miR-136-3p did not differentiate mild TBI patients from controls in the ROC analysis, and the rodent-specific miR-434-3p was not detected in humans. On the other hand, the remaining three miRNAs, miR-323-3p, miR-212-3p, and miR-132-3p, have not been previously investigated after mild TBI.

Taken together, our results indicate that craniotomy can cause injury to the brain, leading to a detectable increase of neuron-enriched miRNAs in plasma. Of the analyzed miRNAs, miR-323-3p, miR-212-3p, and miR-132-3p in particular have potential as sensitive markers of mild brain injury and warrant further preclinical and clinical studies.

3.3. Functions of the Analyzed miRNAs

The cellular and molecular aftermath after TBI is proposed to include multiple sequentially progressing pathologies, such as apoptosis, neurodegeneration, astrogliosis, axonal injury, and demyelination [36]. We hypothesized that the function of the upregulated

miRNAs will report on some of these ongoing pathologies on D2 after injury. Consequently, we performed a literature search to obtain an overview of the functions of the analyzed miRNAs in healthy brain and the impact of neurodegenerative diseases on their expression in the blood and brain.

On D2 after TBI, the most prominent upregulation was observed for miR-9a-3p (22-fold increase compared with sham). MiR-9 is highly enriched in the vertebrate developing and mature nervous system [37]. It functions in embryonic neurogenesis and regulates neural progenitor proliferation [23,37]. Inhibition of miR-9-3p in mature neurons impairs hippocampal long-term potentiation in mice, supporting its role in regulating synaptic plasticity and memory [38]. As noted earlier, a TBI-induced increase in miR-9-3p levels in the blood is reported in both TBI animal models and patients [18]. The release of miR-9 from the brain to the blood or CSF, however, is not specific to TBI. Several studies report elevated blood or CSF miR-9 levels in stroke patients [39–41]. In addition, increased plasma miR-9 levels are reported to associate with an unfavorable neurologic outcome after cardiac arrest [42]. Taken together, these studies indicate that miR-9 is a general marker of brain injury.

The second largest increase after TBI was observed for miR-124-3p (18-fold increase compared with sham). MiR-124 is specifically expressed in the brain of both rodents and humans [10,22,25], and it is the most abundant miRNA in the brain. MiR-124 functions in embryonic neurogenesis [23] and plays an important role in differentiating progenitor cells to mature neurons [24]. Brain injury induces an increase in circulating miR-124 levels at an acute post-TBI time-point in both animal models [29,30] and TBI patients [31]. Similar to miR-9, miR-124 appears to be a general marker of brain injury. In addition to TBI, alterations in circulating miR-124 are reported at an acute time-point in ischemic and hemorrhagic stroke patients [39,41,43,44].

The third largest increase after TBI was observed for miR-323-3p (7-fold increase compared with sham). MiR-323 is neuronally enriched [21,28]. To the best of our knowledge, the expression of miR-323 in the blood or brain has not been previously investigated in TBI models or TBI patients. Instead, miR-323 expression in plasma is reported to differentiate human subjects with mild cognitive impairment from age-matched controls [45]. One study reported increased plasma miR-323 expression in genetic Parkinson's disease [46], but the results were not validated in a subsequent study [47].

Plasma miR-136-3p levels showed a 4.4-fold increase after lateral FPI. MiR-136 is specifically enriched in neurons [21,28]. Expression outside of the central nervous system is also reported. For example, Chen et al. [48] measured miR-136-3p in cultured human umbilical vein endothelial cells and bone mesenchymal stem cells. Kitahara et al. [49] detected upregulation of miR-136-3p in rat ovaries together with miR-434 and miR-132 following the administration of human chorionic gonadotropin. Because our study included only male rats, the possible expression of these miRNAs in the rat ovaries does not affect our results. As mentioned above, we previously reported increased plasma miR-136-3p levels on D2 after injury in a rat model of TBI [18]. In addition, increased miR-136-3p levels are detected in the plasma [46,47] and in CSF exosomes [50] of patients with Parkinson's disease compared with healthy controls.

Plasma miR-434-3p showed a 4.2-fold increase on D2 after TBI. MiR-434 is a rodent-specific miRNA (miRBase, accessed on 9 September 2022). Although Jovičić et al. [28] showed that miR-434 is specifically expressed in rat cortical neurons, a few studies have also detected miR-434-3p in the skeletal muscle of rats and mice [51–53]. In neurons, miR-434-3p is suggested to be involved in regulating stress-induced transcripts [54]. A study with weight-drop-induced mild TBI detected upregulation of miR-434-3p in mouse plasma at 3 h post-injury [55]. As mentioned above, we previously reported increased miR-434-3p levels in rat plasma on D2 after mild TBI [18].

MiR-212 and miR-132 are closely related and located in the same miRNA cluster [56]. They are highly conserved among vertebrates. MiR-212 and miR-132 are enriched in neurons [21,28,57] but are also detected in other cells, such as immune cells [58,59], rat vas-

cular smooth muscle cells [60], insulin-secreting β -cells [61], and several cancer types [56]. Importantly, miR-132 is detected in astrocytes and microglia in both experimental (rat) and human temporal lobe epilepsy (TLE) [62]. In the rat brain, miR-212 and miR-132 are reported to be especially enriched in the neurons of forebrain regions and less abundantly in the cerebellum [26]. Within the normal mouse cerebrum, miR-132 and miR-212 are most abundantly expressed in the frontal cortex compared with the hippocampus [27]. In neurons, miR-212 and miR-132 have important roles in regulating neurite outgrowth, dendrite maturation, and synaptic plasticity [57,63–66]. Knock-out of miR-132 and/or miR-212 in mice is linked to cognitive deficits [67,68]. MiR-132 is also involved in circadian clock function [69].

Studies on miR-212 and miR-132 in TBI are scarce. As mentioned above, there is only one study on blood miR-132-3p levels in TBI patients [32]. There are, however, a couple of studies on miR-212 and miR-132 in Alzheimer's disease. One study reported downregulation of miR-212 and miR-132 in the temporal cortex of Alzheimer's disease patients [70]. Another study found that reduced plasma exosomal miR-212 and miR-132 levels differentiated patients with Alzheimer's disease from cognitively non-impaired controls [71].

In addition to a literature search, we used ingenuity pathway analysis (IPA) to determine the mRNA targets of the validated injury effect miRNAs, particularly whether there were any shared targets between the different miRNAs included in our analysis. In addition, we investigated the canonical pathways involving the target genes. The analysis revealed only a few common targets between the investigated miRNAs, and none of them were shared by more than two miRNAs, suggesting that the plasma-upregulated miRNAs report on the regulation of different pathways. There was also a large variation in the number of predicted targets. More than 400 targets were found for miR-124-3p, whereas only one target was found for miR-434-3p. As we noticed while conducting the literature search, the amount of data available on different miRNAs varies remarkably. This results in a large disparity in the amount of available miRNA target data in IPA, which can cause bias in the target and pathway analyses.

Taken together, all of the miRNAs validated in our study are brain-enriched, and alterations in their expression were previously detected in brain injury or in neurodegenerative diseases. Some of the miRNAs, such as miR-124 and miR-212/miR-132, have been studied more extensively than others, whereas the functions of, for example, miR-323, miR-136, and miR-434 in the brain remain unclear.

3.4. Acute Elevation of Plasma miRNA Levels Does Not Predict the Development of PTE

Several previous studies reported alterations in circulating miRNA expression levels in experimental models of epileptogenesis induced by electrical stimulation or chemoconvulsants and in epilepsy patients [15,72,73]. To the best of our knowledge, there are no prior studies on circulating miRNA expression in PTE models or in patients with TBI. The present study is the first to investigate plasma miRNAs in a model of PTE.

During the 6-month follow-up of the EPITARGET study, 25% of the TBI rats developed PTE. We searched for differentially expressed circulating miRNAs at an acute post-TBI time-point between rats that did (TBI+) or did not (TBI-) develop epilepsy, but differential expression analysis of the small RNA-seq data yielded no differentially expressed miRNAs between the groups on D2 or D9 after TBI. As shown in the Venn diagrams, on both D2 and D9, small RNA sequencing revealed 16 (D2) and 22 (D9) miRNAs detected in TBI+ but not in TBI- or sham animals. These miRNAs, however, typically had only 1–3 raw reads in one sample and no reads in the others. Therefore, they were not considered for further analysis.

Because previous studies demonstrated that the risk of PTE increases with injury severity [1], we investigated whether the acute post-TBI increase in plasma miRNAs predicted the development of epilepsy. We compared the levels of miR-434-3p, miR-9a-3p,

miR-136-3p, miR-323-3p, miR-124-3p, miR-212-3p, and miR-132-3p on D2 between the TBI+ and TBI− rats. Disappointingly, no differences were detected.

We further investigated whether the miRNA levels on D2 differed between TBI+ rats with different epilepsy severities, using the total number of seizures and the presence of seizure clusters as markers of epilepsy severity. No differences were detected, however, between the rats with milder or severe PTE.

Finally, we used elastic net regularized logistic regression (glmnet) to investigate whether a combination of miRNAs rather than a single miRNA could differentiate the TBI+/TBI− and epilepsy severity groups. Our analysis revealed no miRNA sets for TBI+/TBI− differentiation. For the epilepsy severity groups, the analysis did identify optimal sets of miRNAs to differentiate rats with milder or severe PTE but the findings were not statistically significant. It should be noted that the analyses included only 21 TBI+ rats and, consequently, the number of animals in the different epilepsy severity groups was small.

From the seven miRNAs investigated in our study, miR-132 and miR-212 are the most extensively studied in the context of epilepsy. Several studies report increased levels of miR-132 and/or miR-212 in the brain tissue of animal models of epileptogenesis induced with status epilepticus (SE). Nudelman et al. [74] observed a 50% increase in miR-132 levels in RT-qPCR analysis of mouse hippocampus at 8 h after pilocarpine injection. Bot et al. [75] reported a 2-fold upregulation of miR-132-3p and miR-212-3p in a miRNA array analysis of the rat dentate gyrus at 7 d after electrical amygdala stimulation-induced SE. Gorter et al. [76] also used a miRNA array and detected upregulation of miR-132 and miR-212 in the rat dentate gyrus at 1 day, 1 week, and 3 months after SE induced by electrical stimulation of the hippocampus by a stimulation electrode implanted in the angular bundle. Guo et al. [77] found a ~2-fold increase in brain miR-132 expression in the RT-qPCR analysis at 24 h and 7 d after lithium-pilocarpine-induced SE in rats. Similarly, Korotkov et al. [62] observed a 2-fold increase in miR-132 expression in the rat dentate gyrus at 1 d after SE induced by tetanic stimulation of the hippocampus. In contrast to other studies, however, they detected no differences in miR-132 expression at 1 week after SE. A recent study by Bencurova et al. [78] reported a 2-fold upregulation of miR-132-3p and a 3-fold upregulation of miR-212-3p in next-generation sequencing of rat hippocampal tissue 24 h after pilocarpine-induced SE. In addition, Venø et al. [79] reported upregulation of miR-132-3p and miR-212-3p in next-generation sequencing of hippocampal tissue in three different models of TLE, including SE induced by intra-amygdala kainic acid, systemic pilocarpine, or perforant path stimulation. They also reported that treatment with an miR-212-3p antagomir did not reduce seizure burden or neuronal damage after SE in the intra-amygdala kainic acid model. Treatment with an miR-132-3p antagomir was not tested. In contrast, Jimenez-Mateos et al. [80] observed a 5-fold increase in miR-132 levels in the CA3 region of the mouse hippocampus at 24 h after SE induction and reported that treatment with an miR-132 antagomir led to less apoptotic cells and more surviving neurons. There are also several studies on miR-132 and/or miR-212 in epilepsy patients, that is, at later stages of epileptogenesis, after the diagnosis of epilepsy and the occurrence of unprovoked seizures. A study by Peng et al. [81] found a 2-fold upregulation of miR-132 in hippocampal tissues of children with mesial TLE. Korotkov et al. [62] observed a ~3-fold higher expression of miR-132 in patients with TLE and hippocampal sclerosis compared with controls. In contrast to other studies, Guo et al. [77] reported a ~50% reduction in miR-132 expression in the temporal neocortex of TLE patients compared with controls, which could relate to neuronal loss and glial cell proliferation due to long-term effects of epilepsy. Recently, one study reported post-ictal elevation in plasma miR-132 levels at 2 h after seizure onset in patients with epilepsy [82]. Most of the patients (75%) had generalized tonic-clonic seizures, whereas the rest had simple or complex partial seizures. The study reported that the longer the disease course and the longer duration of seizures, the greater the increase in plasma miR-132 levels. Interestingly, opposite to miR-132, studies reported the downregulation of miR-212 in epilepsy patients. Haenisch et al. [83]

found a 33% decrease in miR-212-3p expression in the hippocampus compared with the temporal neocortex in patients with mesial TLE. Another study reported a 50% decrease in miR-212 levels in both the serum and hippocampus of TLE patients [84]. In the present study, miR-124-3p was one of the miRNAs with the largest increase in the plasma after TBI, and miR-124 is a general marker of brain injury. Several studies on animal models report alterations in miR-124 expression in the brain tissue following the induction of SE. Vuokila et al. [85] observed a slight downregulation of miR-124 in the rat dentate gyrus at 7 d after SE in the electrical amygdala stimulation model. Ambrogini et al. [86] observed a trend toward decreased miR-124 levels in hippocampal homogenates and serum of rats 15 d after kainic-acid-induced SE, but the difference was not statistically significant compared with non-epileptic controls. Brennan et al. [87] observed a sharp decrease in miR-124 levels in rat hippocampus at 1.5–48 h after kainic acid-induced SE. The miR-124 levels were lowest 48 h after SE, ~10% of that in controls. The study also found that treatment of rats with miR-124 agomirs promoted inflammation and therefore suggested that reduction of miR-124 levels in the brain after SE may be an adaptive response to control excess inflammation. Interestingly, in contrast to other SE induction methods, SE induction by pilocarpine appears to have the opposite effect on miR-124 levels in the brain. Hu et al. [88] observed upregulation of miR-124 in rat hippocampus 24 h after lithium-pilocarpine-induced SE. Peng et al. [81] reported upregulation of miR-124 in the hippocampus of immature mesial TLE model rats 2 h and 8 weeks after pilocarpine-induced SE. For the remaining miRNAs analyzed in the present study (miR-9, miR-323, miR-434, and miR-136), only a few studies exist on their expression in the context of epilepsy. Brennan et al. [87] found no difference in rat hippocampal miR-9 levels following kainic-acid-induced SE. Jimenez-Mateos et al. [80] observed a 22-fold increase in miR-323 levels in the miRNA screening of mouse hippocampus at 24 h after intra-amygdalar kainic-acid-induced SE, but they did not validate the observation by PCR. Chen et al. [89] reported a 4-fold upregulation of miR-434-3p in the blood of mice 24 h after pilocarpine-induced SE. A recent study reported the reduced expression of miR-136 in the hippocampus of rats with pilocarpine-induced TLE at 7 d after SE induction [90]. They also showed that overexpression of miR-136 reduced the number and duration of seizures and the levels of pro-inflammatory cytokines and increased the number of neurons in the hippocampus, suggesting that miR-136 has neuroprotective effects. Taken together, our results showed that elevated plasma levels of the seven neuronally enriched miRNAs at an acute post-TBI time-point did not reach statistical power as prognostic biomarkers for post-traumatic epileptogenesis or epilepsy severity. This was unexpected as elevated brain levels of miR-132 and miR-212, in particular, within the acute time window assessed in the present study, are linked to epileptogenesis in chemoconvulsant and electrical-stimulation-induced epileptogenesis models. The most apparent explanation is the etiology specificity of the spatiotemporal evolution of brain pathology after epileptogenic insults and associated miRNA expression.

3.5. Increased Plasma miRNA Levels at an Acute Post-TBI Time-Point Correlate with a Larger Cortical Lesion Area at Acute, Subacute, and Chronic Time-Points

One of our aims was to investigate whether circulating miRNA levels at an acute post-TBI time-point reflect injury severity in the brain and could be used to predict progression of the cortical pathology at later time-points.

During the first 3 weeks after TBI, we assessed the cortical pathology of the rats with T₂ relaxation MRI on D2, D7, and D21 after the injury. The method detects edema as increased T₂ and post-impact hemorrhage as decreased T₂ [20]. We determined the cortical lesion volume from the total volume of imaging voxels with abnormal T₂ values. We demonstrated that with 6 of 7 validated miRNAs, increased plasma miRNA levels on D2 after TBI correlated with a larger lesion volume in MRI at all three time-points. In addition to T₂ MRI conducted at acute and subacute time-points, we assessed the cortical lesion area 6 months after TBI with histologic analysis. The analysis revealed a correlation between elevated acute plasma miRNA levels and a larger lesion area at the chronic time-

point, although the correlations were slightly weaker than in the MRI analysis at earlier time-points.

In both MRI and histologic analysis, neuronally enriched miR-124 and miR-9 exhibited the strongest correlation with cortical pathology. We previously demonstrated that TBI causes the downregulation of miR-124-3p in the perilesional cortex in both rats and humans [29]. In the same study, we demonstrated that elevated plasma miR-124 levels correlate with a larger lesion area in MRI 2 months after LFPI-induced TBI [29].

The correlation of circulating miR-124 or miR-9 levels with cortical pathology is not limited to TBI. Several studies investigated blood miR-124 levels in stroke patients. Leung et al. [43] observed higher plasma miR-124 levels within <24 h after onset of symptoms in hemorrhagic stroke patients than in ischemic stroke patients or controls. Rainer et al. [91] reported that the higher the plasma miR-124-3p concentrations measured <24 h from stroke onset, the larger the lesion volume and the worse the stroke outcome. Ji et al. [39] detected increased miR-124 and miR-9 levels in exosomes isolated from the serum of acute ischemic stroke patients (average 16.5 h after stroke), and they reported that higher exosomal miR-124 and miR-9 levels correlated with larger infarct volume and worse outcome. Increased exosomal miR-124 and miR-9 levels in the serum of ischemic stroke patients at 11–72 h after admission to the hospital were also reported by Zhou et al. [41]. In addition to blood levels, CSF miR-9 levels are reported to be elevated on D3 after acute ischemic stroke and are associated with a larger infarct size [40]. In contrast to other studies, Liu et al. [44] observed decreased miR-124 and miR-9 levels in the serum of acute ischemic stroke patients (<24 h from stroke onset), and they reported that patients with larger infarct volume had lower miRNA levels.

Interestingly, miR-212 and miR-132, two very closely related miRNAs, yielded different results from each other when their correlation with the structural outcome was investigated. Acute plasma miR-132 levels correlated with larger lesion volume in MRI at all time-points, whereas for miR-212, a correlation was detected only on D21. This suggests that unlike the other investigated miRNAs, increased miR-212 levels in the plasma after TBI may indicate the initiation of pathologic processes becoming evident at later time-points. In addition, miR-212 was the only miRNA in our analysis that did not correlate with the extent of the lesion area at a chronic time-point after TBI.

To the best of our knowledge, this is the first study assessing the relation between circulating miRNA levels and cortical lesion severity and progression from an acute time-point to a chronic time-point in rats with severe TBI. Taken together, our results indicate that increased levels of neuronally enriched miRNAs in the blood circulation after TBI reflect the extent of cortical injury in the brain. Use of circulating miRNAs as a new tool to evaluate TBI severity and predict disease progression in patients remains to be validated in a clinical setting.

4. Materials and Methods

4.1. Animals

The study design is summarized in Figure 11. The EPITARGET animal cohort included 257 adult male Sprague Dawley rats (Envigo Laboratories S.r.l, Udine, Italy). The mean weight of rats in the EPITARGET cohort was 356 ± 13 g (median 356 g, range 326–419 g) at the time of injury or sham operation. Rats were housed in individual cages in a controlled environment (temperature 22 ± 1 °C, humidity 50–60%, lights on 07:00–19:00) and had ad libitum access to food and water.

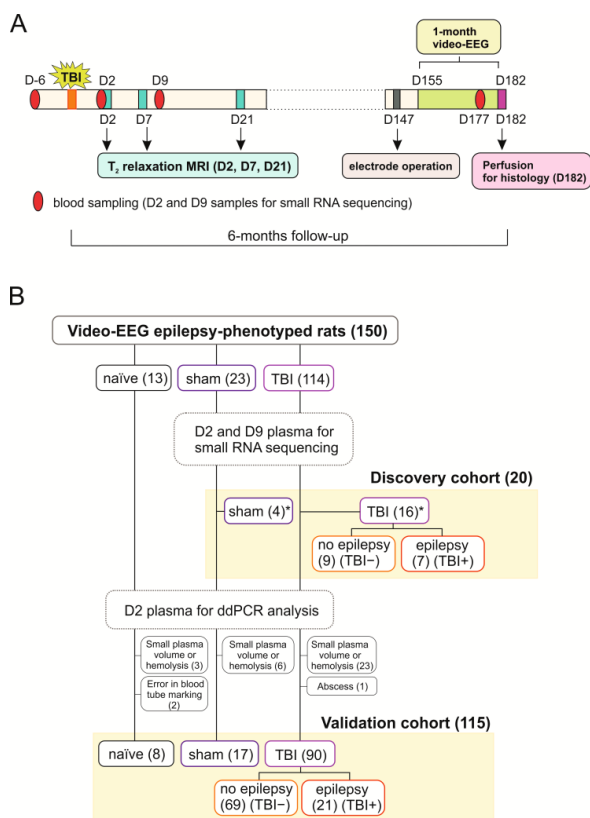


Figure 11. Study design and animal numbers. **(A)** Traumatic brain injury (TBI) was induced in rats by lateral fluid percussion injury. Sham-operated experimental controls underwent the same surgery, including craniotomy without TBI induction. Blood was collected from the tail vein 6 d before (D-6) the injury or sham operation, and then on D2, D9, and D177 after injury. Animals underwent T2 magnetic resonance imaging (MRI) on D2, D7, and D21 to measure cortical lesion volume. To monitor the occurrence of spontaneous seizures (i.e., to diagnose PTE), rats were continuously monitored with vEEG (24/7) for 1 month during the sixth post-injury month. **(B)** A total of 150 animals (13 naïve, 23 sham, 114 TBI) of the EPITARGET cohort were epilepsy-phenotyped using vEEG. Then, D2 and D9 plasma of 20/150 rats, including 4 sham and 16 TBI animals (7 with epilepsy [TBI+], 9 without epilepsy [TBI-]) were used for small RNA sequencing (discovery cohort). The discovery cohort included samples from the first 20 epilepsy-phenotyped rats with acceptable sample quality and sample volume sufficient for small RNA sequencing (see Methods). Validation of miRNA-sequencing data using ddPCR was performed in the plasma of 115 rats [validation cohort; 8 naïve, 17 sham, and 90 TBI animals (21 TBI+, 69 TBI-)]. Abbreviations: D, day; vEEG, video-electroencephalography; *, 2 samples from sham-operated and 5 samples from injured animals (3 TBI-, 2 TBI+) that were used for small RNA sequencing in the discovery cohort were also included in the ddPCR analysis in the validation cohort.

The 257 rats were randomized into naïve animals ($n = 16$), sham-operated experimental controls ($n = 27$), and rats with TBI ($n = 214$). From these, a total of 150 rats (13 naïve, 23 sham, 114 TBI [31 rats with epilepsy and 83 rats without epilepsy]) completed the 6-month follow-up, including vEEG monitoring.

The 150 rats included in the plasma miRNA analysis were divided into a discovery cohort and a validation cohort. Samples from the *discovery cohort* were used for the small

RNA sequencing experiment and contained 4 sham-operated experimental controls and 16 rats with TBI (7 with epilepsy [TBI+] and 9 without epilepsy [TBI−]). The *validation cohort* used for digital drop polymerase chain reaction (ddPCR) analysis comprised a total of 115 rats, including 8 naïve, 17 sham, and 90 TBI rats (21 TBI+, 69 TBI−).

A detailed description of the procedures was reported previously [17,20]. All experiments were approved by the Animal Ethics Committee of the Provincial Government of Southern Finland and performed in accordance with the guidelines of the European Community Council Directives 2010/63/EU.

4.2. Induction of TBI by LFPI

TBI was induced by LFPI as described previously [17]. The impact pressure was adjusted to produce severe TBI with an expected acute post-impact mortality of 20–30% within the first 48 h. The mean impact pressure in the EPITARGET cohort was 3.25 ± 0.10 atm ($n = 212$, median 3.3 atm, range 2.5–3.6 atm). Time in apnea and the occurrence and duration of impact-related seizure-like behaviors were monitored and documented using project-tailored common data elements (<https://epitarget.eu/>, accessed on 14 November 2022).

4.3. Blood Collection

Blood was sampled 7 days (D) before injury (baseline), and thereafter on D2 (48 h after impact), D9, and 6 months after injury (day of injury referred as D0). Blood sampling from the tail vein and plasma sample preparation were performed according to [92]. Briefly, rats were anesthetized by isoflurane inhalation (5% induction, 1–2% maintenance). A 24G butterfly needle was used to draw blood from the lateral tail vein into 2 BD Microtainer K₂ EDTA-tubes (#365975, di-potassium ethylenediaminetetraacetic acid, BD Biosciences, Franklin Lakes, NJ, USA; 500 µL/tube). To obtain plasma, tubes were centrifuged at $1300 \times g$ for 10 min at 4 °C (5417R Eppendorf, Hamburg, Germany) within 1 h after blood sampling. Plasma aliquots of 50 µL were carefully collected and pipetted into 0.5 mL Protein LoBind tubes (#022431064, Eppendorf, Hamburg, Germany) and stored at −70 °C.

4.4. Video-EEG Monitoring

At 5 months after TBI (D147), rats were anesthetized and implanted with 3 skull electrodes. Starting on D154 (1 week after electrode implantation), rats underwent continuous (24 h/day; 7 days/week) vEEG monitoring for 4 weeks to diagnose PTE (for details, see [17]). Seizure occurrence was detected both by visual screening and a seizure detection algorithm. An electroencephalographic seizure was defined as a high-amplitude rhythmic discharge that clearly represented an atypical EEG pattern (i.e., repetitive spikes, spike-and-wave discharges, poly-spike-and-wave, or slow-waves; frequency, and amplitude modulation) lasting >10 s [93]. Rats were defined as having epilepsy if at least 1 unprovoked electrographic seizure was detected. In the EPITARGET cohort of 114 TBI animals, the prevalence of PTE was 25% (29/114).

4.5. Analysis of Structural Outcome

4.5.1. Magnetic Resonance Imaging and Lesion Analysis

Rats were imaged on D2, D7, and D21 using quantitative T₂ magnetic resonance imaging (MRI), as described previously [20]. Imaging voxels within the cortex were classified as normal or abnormal based on their T₂ values. The range for normal T₂ was defined as $45 \text{ ms} \leq T_2 \leq 55 \text{ ms}$, with the lower limit corresponding to the 2.5th percentile and the upper limit corresponding to the 97.5th percentile of all imaging voxels of all sham-operated controls across all time-points. Values below the lower limit or above the upper limit were classified as abnormal. To estimate the cortical lesion volume for each animal, the number of abnormal voxels was counted and multiplied by voxel size.

4.5.2. Histology and Preparation of Unfolded Maps

Details of the histology and preparation of cortical unfolded maps were previously described [35] and are only briefly summarized here.

Perfusion. Deeply anesthetized rats were intracardially perfused with 0.9% NaCl followed by 4% paraformaldehyde in 0.1 M sodium phosphate buffer (PB) after completing the vEEG monitoring (D182). The brain was removed from the skull and fixed in 4% paraformaldehyde for 4 h, cryoprotected in 20% glycerol in 0.02 M potassium phosphate-buffered saline (KPBS, pH 7.4) for 24 h, frozen in dry ice, and stored in -70°C for further processing. Frozen coronal sections of the brain were cut (25- μm thick, 1-in-12 series) using a sliding microtome. The first series of sections was stored in 10% formalin at room temperature and used for thionin staining. Other series of sections were collected into tissue collection solution (30% ethylene glycol, 25% glycerol in 0.05 M PB) and stored at -20°C until processed.

Nissl staining. The first series of sections was stained with thionin, cleared in xylene, and cover-slipped using Depex[®] (BDH Chemical, Poole, UK) as a mounting medium.

Preparation of cortical unfolded maps. To assess the cortical lesion area and the damage to different cytoarchitectonic cortical areas after TBI, thionin-stained sections were digitized (40 \times , Hamamatsu Photonics, Hamamatsu, Japan; NanoZoomer-XR, NDP.scan 3.2]. Unfolded cortical maps were then prepared from the digitized histologic sections as described in detail by [94] and by applying in-house software from <https://unfoldedmap.org> (accessed on 14 November 2022) adapted to the rat brain [95].

4.6. Small RNA Sequencing from Plasma

4.6.1. Library Preparation and Sequencing

Sequencing was performed for D2 and D9 plasma samples collected from 4 sham-operated controls and 16 TBI rats (7 with epilepsy [TBI+] and 9 without epilepsy [TBI-]). For each animal, 5 frozen 50- μL aliquots (total 250 μL) were pooled for RNA extraction at each time-point. Any visible hemolysis in the plasma samples was visually inspected by an experienced researcher before pooling the aliquots and further confirmed by measurement of hemoglobin absorbance at 414 nm using a spectrophotometer (NanoDrop 2000, Thermo Fisher Scientific, Wilmington, DE, USA). Samples were considered hemolyzed if the A414 value was ≥ 0.25 (see [92]).

RNA was extracted from 200 μL plasma using an miRNeasy Mini Kit (#217004, QIAGEN, Hilden, Germany). Small RNA sequencing was conducted by GenomeScan (Leiden, the Netherlands). Small RNA library preparation was performed using the Illumina TruSeq Small RNA Sample Prep Kit (Illumina, San Diego, CA, USA). Briefly, small RNA was isolated from purified RNA by size selection after adapter ligation. The excised product was used for PCR amplification of the resulting product. The quality and yield after sample preparation were measured with a Fragment Analyzer. The size of the resulting products was consistent with the expected size of approximately 150 bp. Single-end sequencing with a read length of 51 nucleotides was performed on the Illumina HiSeq 4000. To increase read depth each sample was sequenced on two flow-cells giving two replicates for each sample.

4.6.2. Quantification of miRNAs and Differential Expression Analysis

Read quality of the raw data was assessed using FastQC v11.8 software produced by the Babraham Institute (Babraham, Cambridgeshire, UK) and the Trimmomatic v0.36 was used to filter low-quality base calls and any adapter contamination [96]. Low-quality leading and trailing bases were removed from each read, and a sliding window trimming using a window of 4 and a phred33 score threshold of 15 was used to assess the quality of the read body. Any reads <17 nucleotides were discarded. After quality control, the replicates for each sample were merged and aligned to the rat reference genome (Rno6) using Bowtie2 with the—very-sensitive-local settings. Using the featureCounts program from the Subread package, the number of reads aligned with the known rat miRNAs in accordance with miRBase22 was calculated [97,98].

Following the primary quantification, differential expression analysis was performed with DESeq2 (v. 1.30.1) in RStudio (v. 1.1.463) using R (v. 4.0.2). D2 samples and D9 samples were analyzed separately. First, the raw read table was filtered to exclude miRNAs with no reads in any of the samples. Next, DESeq2 analysis was run to compare TBI vs. sham, TBI+ vs. sham, TBI– vs. sham, and TBI+ vs. TBI– groups. MicroRNAs with an adjusted *p*-value < 0.05 were considered differentially expressed.

4.6.3. Identification of Expression Pattern Differences with Machine Learning

We applied logistic regression with feature selection, utilizing nested leave-1-out cross-validation to identify miRNAs (“features”) that contributed the most to the group differences between sham and TBI, and between TBI– and TBI+. The logistic regression model was optimized on raw counts from miRNAs with counts ≥ 1 in at least 80% of the samples to maximize separation between groups in terms of the area under the curve (AUC) of the receiver operating characteristic (ROC) curve. The miRNA counts were standardized to 0 mean and unit variance. In the inner cross-validation loop, miRNAs with 0 variance were filtered and feature selection was performed using recursive feature elimination and filtering by F-score. Model hyperparameters and feature selection configurations were optimized with a grid search over combinations of regularization factor levels, feature selection methods, number of selected features, and choices between L1 (LASSO) and L2 (Ridge) regularization. Feature importance was calculated by averaging the absolute values of logistic regression model covariates over the outer fold of nested cross-validation. The averaged values were normalized to sum to 1 and organized in descending order to identify miRNAs that contributed the most to group separability. Analyses were performed using Python (3.7.0) and the sklearn package (20.2) on Centos 7.

4.6.4. Visualization of Sequencing Data

Shared miRNAs between the experimental groups in small RNA sequencing were visualized using Venn diagrams (<https://bioinfogp.cnb.csic.es/tools/venny/>, accessed on 6 October 2022).

Normalization of the raw read counts to counts per million (CPM) was performed using the Equation (1):

$$CPM = \frac{\text{read count per gene}}{\text{total read count per sample}} \times 1,000,000 \quad (1)$$

Normalized data were visualized using principal component analysis (PCA), Spearman correlation matrices, and heatmaps with a complete linkage clustering method and Spearman correlation as the distance measurement. PCA plots, correlation plots, and heatmaps were prepared using RStudio (v. 1.1.463) by R (v. 4.0.2).

4.7. Technical Validation of miRNA-Sequencing Data by RT-qPCR

4.7.1. MiRNA Extraction from Plasma

MicroRNA was extracted from 50- μ L plasma samples of 20 rats (4 sham, 16 TBI) using an miRNeasy Mini Kit (#217004, QIAGEN) with a final elution volume of 30 μ L. These plasma samples came from the same rats used for sequencing, but the aliquots were different from those used for sequencing.

4.7.2. Reverse Transcription

Reverse transcription (cDNA synthesis) was conducted using a miRCURY LNA RT Kit (#339340, QIAGEN). In each reaction, 2 μ L of template miRNA was used. The following temperature cycling protocol was used: incubation for 60 min at 42 °C followed by incubation for 5 min at 95 °C to heat activate the reverse transcriptase, and immediate cooling to 4 °C.

4.7.3. RT-qPCR

Quantitative PCR was conducted using miRCURY LNA SYBR Green PCR Kit (#339345, QIAGEN) and miRCURY LNA miRNA PCR assays (hsa-miR-9-3p, #YP00204620; mmu-miR-434-3p, #YP00205190; hsa-miR-323a-3p, #YP00204278; hsa-miR-136-3p, #YP00205503; hsa-miR-129-5p, #YP00204534; hsa-miR-28-3p, #YP00204119, QIAGEN). We selected miR-28-3p as an endogenous control based on geNorm analysis (<https://genorm.cmgg.be/>, accessed on 10 September 2019) of the sequencing data. The analysis identified miR-28-3p as the most stable miRNA across the sequencing samples on D2 and D9.

Template cDNA was diluted 1:30 (miR-9a-3p, miR-434-3p, and miR-28-3p) or 1:10 (miR-136-3p, miR-129-5p, and miR-323-3p) in nuclease-free water. The following PCR cycling conditions were used: 2 min heat activation at 95 °C, 40 cycles of 10 s denaturation at 95 °C, and annealing/extension for 60 s at 56 °C. Quantitative PCR was performed using a LightCycler 96 Instrument (Roche, Basel, Switzerland) and LightCycler 96 v. 1.1 software (Roche).

Data were normalized to miR-28-3p using the formula $2^{-\Delta Ct}$. Results were analyzed by GraphPad Prism 8 software (GraphPad Software, San Diego, CA, USA).

4.8. ddPCR Analysis

4.8.1. Plasma Quality Control

For the ddPCR analysis, plasma quality was controlled by measuring hemolysis (absorbance at wavelength 414 nm) by a NanoDrop ND-1000 spectrophotometer (Thermo Fisher Scientific, Waltham, MA, USA). Samples were considered hemolyzed if the A414 value was ≥ 0.25 [92].

First, A414 was measured from one 50 μ L plasma aliquot (3rd of the 4 aliquots). If A414 was < 0.25 , another 3 aliquots (50 μ L each) were thawed. The four aliquots were pooled to obtain a total of 200 μ L plasma, and A414 was measured again from the pooled plasma sample.

4.8.2. MiRNA Extraction from Plasma

MicroRNA was extracted from the pooled 200 μ L plasma samples using an miRNeasy Mini Kit following the protocol from the miRNeasy Serum/Plasma kit. The elution volume was 30 μ L. Extracted miRNA samples were stored at -70 °C. The small RNA concentration in each sample was determined using the Qubit microRNA Assay Kit (#Q32880, Thermo Fisher Scientific) with a DeNovix DS-11 FX Fluorometer (DeNovix Inc., Wilmington, DE, USA) from a separate 1 μ L sample aliquot.

4.8.3. ddPCR Validation of miRNAs

Total RNA was transcribed to cDNA with the miRCURY LNA RT kit as described in the preceding text. The total reaction volume was 30 μ L (6 μ L template RNA in each reaction). The cDNA was stored at -20 °C until ddPCR analysis.

For ddPCR analysis, cDNA was diluted 1:10 in nuclease-free water. The master mix for 1 reaction (reaction volume 20 μ L) contained 10 μ L of 2 X QX200 ddPCR EvaGreen SuperMix (#1864034, BIO-RAD, Hercules, CA, USA), 1.0 μ L nuclease-free water, and 1.0 μ L miRCURY LNA PCR assay (QIAGEN). Each reaction contained 8 μ L of the diluted cDNA template. Droplets were generated using the QX200 AutoDG Droplet Digital PCR System (BIO-RAD) with Automated Droplet Generation Oil for EvaGreen (#1864112, BIO-RAD). Seven target miRNAs (hsa-miR-9-3p, #YP00204620; mmu-miR-434-3p, #YP00205190; hsa-miR-136-3p, #YP00205503; hsa-miR-323a-3p, #YP00204278; hsa-miR-124-3p, #YP00206026; hsa-miR-132-3p, #YP00206035; mmu-miR-212-3p, #YP00206022, QIAGEN) and the endogenous control (miR-28-3p) were all analyzed on the same ddPCR plate, 5 samples per plate. The plate contained 2 replicate wells for each sample. Each plate contained a control sample to monitor possible differences between the ddPCR runs. PCR was conducted using a C1000 Touch™ Thermal Cycler (#1851196, BIO-RAD) with the following program: 95 °C 5 min, 95 °C 30 s, 56 °C 1 min, repeat total 40 cycles, 4 °C 5 min, 90 °C 5 min, 4 °C hold. Droplets

were quantified by the QX200 Droplet Reader (#1864003, BIO-RAD). The ddPCR results were analyzed by QuantaSoft software (version 1.7.4.0917). Target miRNA concentrations were normalized to the miR-28-3p concentration (target/reference) to acquire normalized expression values for each sample. Results were visualized by GraphPad Prism (v. 9.0.1, GraphPad software, San Diego, CA, USA).

4.9. DdPCR Validation of Downregulated miRNAs

From the list of differentially expressed miRNAs between the TBI and sham groups on D2, we selected 3 downregulated miRNAs for further validation: miR-140-3p, miR-149-5p, and miR-455-5p. These 3 miRNAs were selected as they had a low adjusted p-value, $\log_2FC \leq -1.00$, with a mean CPM ≥ 100 in both the TBI and sham samples.

To save the valuable plasma from the EPITARGET cohort, we used D2 plasma from 5 sham and 5 TBI rats available from another animal cohort in our laboratory for ddPCR validation. In addition, baseline samples (D-7) from 1 sham and 4 TBI rats were used as naïve samples ($n = 5$). The mean weight of these rats was 357 ± 14 g ($n = 34$, median: 356 g, range 334–389 g) at the time of TBI or sham operation. TBI was induced as described above. Mean impact pressure was 3.36 ± 0.09 atm ($n = 25$, median: 3.4 atm, range 3.2–3.5 atm). Plasma was collected on D2 after TBI or sham operation.

RNA was extracted from 188 μ L of plasma using the miRNeasy Mini Kit (30 μ L elution volume). The ddPCR analysis was conducted using miRCURY LNA miRNA PCR assays (hsa-miR-140-3p, #YP00204304; hsa-miR-455-5p, #YP00204363; hsa-miR-149-5p, #YP00204321). For ddPCR analysis, cDNA was diluted in nuclease-free water as follows: 1:200 dilution for miR-140-3p analysis, 1:10 dilution for miR-455-5p and miR-149-5p analyses. The ddPCR analysis was conducted similarly as described above.

4.10. Glmnet Logistic Regression Analysis

We investigated the optimal combination of analyzed plasma miRNAs as a biomarker panel for predicting epileptogenesis and epilepsy severity by conducting an elastic-net-based analysis using glmnet (https://hastie.su.domains/glmnet_matlab/, accessed on 14 November 2022) [99,100] for MATLAB (R2017a, the MathWorks Inc., Natick, MA, USA). Elastic net uses least absolute shrinkage selector operator (LASSO) and Ridge regularization to reduce overfitting of the models, and we selected equal weighting for the 2 [101]. Nested (externally validated) leave-1-out cross-validation was used to avoid overfitting the regularization parameter [102,103]. Observations were weighted to compensate for class imbalance, and the fitting was performed by minimizing binomial deviance. Normalized expression levels of 7 miRNAs in the plasma on D2 after TBI were used as predictor variables (miR-434, miR-9, miR-136, miR-323, miR-124, miR-212, and miR-132). The predictor variables that had a coefficient of zero in the majority of the outer cross-validation folds after the glmnet fit were excluded [104]. The remaining predictors were used in a standard (non-regularized) logistic regression analysis (MATLAB function “fitglm”). For the TBI+ vs. TBI– analysis, the response variable was epilepsy (yes/no) determined by the vEEG analysis. For the epilepsy severity analyses, the response variable was seizure clusters (yes/no) or at least 3 seizures during the follow-up (yes/no). Cross-validated ROC AUC was computed as a measure of goodness of fit for the logistic regression models using the pooling method [105] ROC AUC and its 95% confidence interval were estimated with Brian Lau’s MatlabAUC codes (<https://github.com/brian-lau/MatlabAUC>, accessed on 14 November 2022). The confidence interval was estimated as a bias-corrected and accelerated bootstrap using 10,000 samples.

4.11. Ingenuity Pathway Analysis

Ingenuity pathway analysis (IPA, QIAGEN, version 76765844) was used to investigate miRNA target genes and their function. Because miR-132-3p and miR-212-3p are closely related and share the same seed sequence, IPA only used miR-132-3p for target prediction in the microRNA Target Filter. The resulting target genes were further analyzed by Ex-

pression Analysis in IPA to reveal the canonical pathways associated with the target genes. “Experimentally observed” and “High (predicted)” confidence settings were applied in both the microRNA Target Filter and Expression Analysis.

4.12. Statistics

Differential miRNA expression analysis was performed with DESeq2. Differential expression was considered at a level of FDR < 0.05. Other statistical analyses were performed using GraphPad Prism 9 and RStudio (v. 1.1.463) by R (v. 4.0.2). Comparisons of 3 or more groups were performed using the Kruskal–Wallis test, followed by *post hoc* analysis using the Mann–Whitney U test. Correlations were analyzed by the Spearman correlation test (ρ). The ROC analysis was performed for each ddPCR-validated miRNA to assess its sensitivity and specificity in differentiating the animal groups. Statistical significance of the AUC was assessed by Mann–Whitney U test. The optimal cut-off in ROC analysis was determined using the cutpoint package (v. 1.1.1) in R by maximizing the sum of sensitivity and specificity. Results are presented as mean \pm standard deviation. A *p*-value < 0.05 was considered statistically significant.

5. Conclusions

We validated the upregulation of seven brain-enriched miRNAs in the plasma on D2 after LFPI-induced TBI in the EPITARGET study cohort. The plasma miRNA expression profile on D2 after TBI did not predict the subsequent development of PTE or the PTE severity. Our data did, however, reveal that acute post-TBI plasma miRNA levels predicted the severity of the cortical pathology at acute, subacute, and chronic time-points. Moreover, we found that six miRNAs, including miR-434-3p, miR-9a-3p, miR-136-3p, miR-323-3p, miR-212-3p, and miR-132-3p, differentiated naive rats from sham-operated rats, demonstrating the capability to detect mild brain injury caused by the craniotomy.

Supplementary Materials: The following supporting information can be downloaded at <https://www.mdpi.com/article/10.3390/ijms24032823/s1>.

Author Contributions: Conceptualization, M.H., S.D.G., E.A.v.V., N.P., E.A. and A.P.; data curation, M.H. and P.A.; formal analysis, M.H., J.D.M. and E.M.; funding acquisition, E.A.v.V., E.A. and A.P.; investigation, M.H., E.M. and R.C.; methodology, M.H., S.D.G., E.M. and R.C.; project administration, N.P., E.A.v.V. and A.P.; resources, E.A.v.V., E.A. and A.P.; software, P.A. and R.C.; supervision: N.P. and A.P.; writing—original draft, M.H.; writing—review and editing, M.H., A.P., M.H. and A.P. wrote the manuscript with input from all authors. All authors have read and agreed to the published version of the manuscript.

Funding: This research was funded by The Medical Research Council of the Academy of Finland (Grants 272249, 273909, 2285733-9), The Sigrid Jusélius Foundation, and the European Union’s Seventh Framework Programme (FP7/2007-2013) under grant agreement n°602102 (EPITARGET).

Institutional Review Board Statement: All animal experiments were approved by the Animal Ethics Committee of the Provincial Government of Southern Finland (ESAVI/5744/04.10.07/2017) and performed in accordance with the guidelines of the European Community Council Directives 2010/63/EU.

Informed Consent Statement: Not applicable.

Data Availability Statement: The small RNA sequencing data has been deposited to the Gene Expression Omnibus (GEO) under accession No. GSE222801. Further data are available on request from the corresponding author.

Acknowledgments: We thank Jarmo Hartikainen and Merja Lukkari for their excellent technical assistance and Niina Lapinlampi for her help in setting up the RedCap database for data collection.

Conflicts of Interest: The authors declare no conflict of interest.

References

1. Pitkänen, A.; Immonen, R. Epilepsy Related to Traumatic Brain Injury. *Neurotherapeutics* **2014**, *11*, 286–296. [[CrossRef](#)] [[PubMed](#)]
2. Menon, D.K.; Schwab, K.; Wright, D.W.; Maas, A.I. Position Statement: Definition of Traumatic Brain Injury. *Arch. Phys. Med. Rehabil.* **2010**, *91*, 1637–1640. [[CrossRef](#)] [[PubMed](#)]
3. Annegers, J.F.; Hauser, W.A.; Coan, S.P.; Rocca, W.A. A Population-Based Study of Seizures after Traumatic Brain Injuries. *N. Engl. J. Med.* **1998**, *338*, 20–24. [[CrossRef](#)]
4. Klein, P.; Tyrlikova, I. No Prevention or Cure of Epilepsy as Yet. *Neuropharmacology* **2020**, *168*, 107762. [[CrossRef](#)] [[PubMed](#)]
5. Dulla, C.G.; Pitkänen, A. Novel Approaches to Prevent Epileptogenesis After Traumatic Brain Injury. *Neurotherapeutics* **2021**, *18*, 1582–1601. [[CrossRef](#)] [[PubMed](#)]
6. Engel, J.; Pitkänen, A.; Loeb, J.A.; Dudek, F.E.; Bertram, E.H.; Cole, A.J.; Moshé, S.L.; Wiebe, S.; Jensen, F.E.; Mody, I.; et al. Epilepsy Biomarkers. *Epilepsia* **2013**, *54*, 61–69. [[CrossRef](#)] [[PubMed](#)]
7. Lee, R.C.; Feinbaum, R.L.; Ambros, V. The C. Elegans Heterochronic Gene Lin-4 Encodes Small RNAs with Antisense Complementarity to Lin-14. *Cell* **1993**, *75*, 843–854. [[CrossRef](#)]
8. Bartel, D.P. MicroRNAs: Genomics, Biogenesis, Mechanism, and Function. *Cell* **2004**, *116*, 281–297. [[CrossRef](#)]
9. Friedman, R.C.; Farh, K.K.-H.; Burge, C.B.; Bartel, D.P. Most Mammalian MRNAs Are Conserved Targets of MicroRNAs. *Genome Res.* **2009**, *19*, 92–105. [[CrossRef](#)]
10. Lagos-Quintana, M.; Rauhut, R.; Yalcin, A.; Meyer, J.; Lendeckel, W.; Tuschl, T. Identification of Tissue-Specific MicroRNAs from Mouse. *Curr. Biol.* **2002**, *12*, 735–739. [[CrossRef](#)]
11. Landgraf, P.; Rusu, M.; Sheridan, R.; Sewer, A.; Iovino, N.; Aravin, A.; Pfeffer, S.; Rice, A.; Kamphorst, A.O.; Landthaler, M.; et al. A Mammalian MicroRNA Expression Atlas Based on Small RNA Library Sequencing. *Cell* **2007**, *129*, 1401–1414. [[CrossRef](#)] [[PubMed](#)]
12. Ludwig, N.; Leidinger, P.; Becker, K.; Backes, C.; Fehlmann, T.; Pallasch, C.; Rheinheimer, S.; Meder, B.; Stähler, C.; Meese, E.; et al. Distribution of MiRNA Expression across Human Tissues. *Nucleic Acids Res.* **2016**, *44*, 3865–3877. [[CrossRef](#)] [[PubMed](#)]
13. Dogini, D.B.; Avansini, S.H.; Vieira, A.S.; Lopes-Cendes, I. MicroRNA Regulation and Dysregulation in Epilepsy. *Front. Cell Neurosci.* **2013**, *7*, 172. [[CrossRef](#)] [[PubMed](#)]
14. Henshall, D.C.; Hamer, H.M.; Pasterkamp, R.J.; Goldstein, D.B.; Kjems, J.; Prehn, J.H.M.; Schorge, S.; Lamottke, K.; Rosenow, F. MicroRNAs in Epilepsy: Pathophysiology and Clinical Utility. *Lancet Neurol.* **2016**, *15*, 1368–1376. [[CrossRef](#)]
15. Pitkänen, A.; Paananen, T.; Kyyriäinen, J.; Das Gupta, S.; Heiskanen, M.; Vuokila, N.; Bañuelos-Cabrera, I.; Lapinlampi, N.; Kajevu, N.; Andrade, P.; et al. Biomarkers for Posttraumatic Epilepsy. *Epilepsy Behav.* **2021**, *121*, 107080. [[CrossRef](#)]
16. Toffolo, K.; Osei, J.; Kelly, W.; Poulsen, A.; Donahue, K.; Wang, J.; Hunter, M.; Bard, J.; Wang, J.; Poulsen, D. Circulating MicroRNAs as Biomarkers in Traumatic Brain Injury. *Neuropharmacology* **2019**, *145*, 199–208. [[CrossRef](#)]
17. Lapinlampi, N.; Andrade, P.; Paananen, T.; Hämäläinen, E.; Ekolle Ndode-Ekane, X.; Puhakka, N.; Pitkänen, A. Postinjury Weight Rather than Cognitive or Behavioral Impairment Predicts Development of Posttraumatic Epilepsy after Lateral Fluid-Perfusion Injury in Rats. *Epilepsia* **2020**, *61*, 2035–2052. [[CrossRef](#)]
18. Das Gupta, S.; Ciszek, R.; Heiskanen, M.; Lapinlampi, N.; Kukkonen, J.; Leinonen, V.; Puhakka, N.; Pitkänen, A. Plasma MiR-9-3p and MiR-136-3p as Potential Novel Diagnostic Biomarkers for Experimental and Human Mild Traumatic Brain Injury. *Int. J. Mol. Sci.* **2021**, *22*, 1563. [[CrossRef](#)]
19. Bushel, P.R.; Caiment, F.; Wu, H.; O’Lone, R.; Day, F.; Calley, J.; Smith, A.; Li, J. RATEmiRs: The Rat Atlas of Tissue-Specific and Enriched MiRNAs Database. *BMC Genomics* **2018**, *19*, 825. [[CrossRef](#)]
20. Manninen, E.; Chary, K.; Lapinlampi, N.; Andrade, P.; Paananen, T.; Sierra, A.; Tohka, J.; Gröhn, O.; Pitkänen, A. Early Increase in Cortical T(2) Relaxation Is a Prognostic Biomarker for the Evolution of Severe Cortical Damage, but Not for Epileptogenesis, after Experimental Traumatic Brain Injury. *J. Neurotrauma* **2020**, *37*, 2580–2594. [[CrossRef](#)]
21. Miska, E.A.; Alvarez-Saavedra, E.; Townsend, M.; Yoshii, A.; Sestan, N.; Rakic, P.; Constantine-Paton, M.; Horvitz, H.R. Microarray Analysis of MicroRNA Expression in the Developing Mammalian Brain. *Genome Biol.* **2004**, *5*, R68. [[CrossRef](#)] [[PubMed](#)]
22. Sempere, L.F.; Freemantle, S.; Pitha-Rowe, I.; Moss, E.; Dmitrovsky, E.; Ambros, V. Expression Profiling of Mammalian MicroRNAs Uncovers a Subset of Brain-Expressed MicroRNAs with Possible Roles in Murine and Human Neuronal Differentiation. *Genome Biol.* **2004**, *5*, R13. [[CrossRef](#)] [[PubMed](#)]
23. Krichevsky, A.M.; Sonntag, K.-C.; Isacson, O.; Kosik, K.S. Specific MicroRNAs Modulate Embryonic Stem Cell-Derived Neurogenesis. *Stem Cells* **2006**, *24*, 857–864. [[CrossRef](#)] [[PubMed](#)]
24. Makeyev, E.V.; Zhang, J.; Carrasco, M.A.; Maniatis, T. The MicroRNA MiR-124 Promotes Neuronal Differentiation by Triggering Brain-Specific Alternative Pre-mRNA Splicing. *Mol. Cell* **2007**, *27*, 435–448. [[CrossRef](#)]
25. Mishima, T.; Mizuguchi, Y.; Kawahigashi, Y.; Takizawa, T.; Takizawa, T. RT-PCR-Based Analysis of MicroRNA (MiR-1 and -124) Expression in Mouse CNS. *Brain Res.* **2007**, *1131*, 37–43. [[CrossRef](#)]
26. Olsen, L.; Klausen, M.; Helboe, L.; Nielsen, F.C.; Werge, T. MicroRNAs Show Mutually Exclusive Expression Patterns in the Brain of Adult Male Rats. *PLoS ONE* **2009**, *4*, e2725. [[CrossRef](#)]
27. Juhila, J.; Sipilä, T.; Ica, K.; Nicorici, D.; Ellonen, P.; Kallio, A.; Korpelainen, E.; Greco, D.; Hovatta, I. MicroRNA Expression Profiling Reveals MiRNA Families Regulating Specific Biological Pathways in Mouse Frontal Cortex and Hippocampus. *PLoS ONE* **2011**, *6*, e21495. [[CrossRef](#)]

28. Jovičić, A.; Roshan, R.; Moiso, N.; Pradervand, S.; Moser, R.; Pillai, B.; Luthi-Carter, R. Comprehensive Expression Analyses of Neural Cell-Type-Specific miRNAs Identify New Determinants of the Specification and Maintenance of Neuronal Phenotypes. *J. Neurosci.* **2013**, *33*, 5127–5137. [[CrossRef](#)]
29. Vuokila, N.; Das Gupta, S.; Huusko, R.; Tohka, J.; Puhakka, N.; Pitkänen, A. Elevated Acute Plasma miR-124-3p Level Relates to Evolution of Larger Cortical Lesion Area after Traumatic Brain Injury. *Neuroscience* **2020**, *433*, 21–35. [[CrossRef](#)]
30. Wang, P.; Ma, H.; Zhang, Y.; Zeng, R.; Yu, J.; Liu, R.; Jin, X.; Zhao, Y. Plasma Exosome-Derived MicroRNAs as Novel Biomarkers of Traumatic Brain Injury in Rats. *Int. J. Mol. Sci.* **2020**, *17*, 437–448. [[CrossRef](#)]
31. O'Connell, G.C.; Smothers, C.G.; Winkelman, C. Bioinformatic Analysis of Brain-Specific miRNAs for Identification of Candidate Traumatic Brain Injury Blood Biomarkers. *Brain Inj.* **2020**, *34*, 965–974. [[CrossRef](#)] [[PubMed](#)]
32. Ma, S.-Q.; Xu, X.-X.; He, Z.-Z.; Li, X.-H.; Luo, J.-M. Dynamic Changes in Peripheral Blood-Targeted miRNA Expression Profiles in Patients with Severe Traumatic Brain Injury at High Altitude. *Mil. Med. Res.* **2019**, *6*, 12. [[CrossRef](#)] [[PubMed](#)]
33. Schindler, C.R.; Woschek, M.; Vollrath, J.T.; Konradowitz, K.; Lustenberger, T.; Störmann, P.; Marzi, I.; Henrich, D. miR-142-3p Expression Is Predictive for Severe Traumatic Brain Injury (TBI) in Trauma Patients. *Int. J. Mol. Sci.* **2020**, *21*, 5381. [[CrossRef](#)] [[PubMed](#)]
34. Cole, J.T.; Yarnell, A.; Kean, W.S.; Gold, E.; Lewis, B.; Ren, M.; McMullen, D.C.; Jacobowitz, D.M.; Pollard, H.B.; O'Neill, J.T.; et al. Craniotomy: True Sham for Traumatic Brain Injury, or a Sham of a Sham? *J. Neurotrauma* **2011**, *28*, 359–369. [[CrossRef](#)] [[PubMed](#)]
35. Heiskanen, M.; Jääskeläinen, O.; Manninen, E.; Das Gupta, S.; Andrade, P.; Ciszek, R.; Gröhn, O.; Herukka, S.-K.; Puhakka, N.; Pitkänen, A. Plasma Neurofilament Light Chain (NF-L) Is a Prognostic Biomarker for Cortical Damage Evolution but Not for Cognitive Impairment or Epileptogenesis Following Experimental TBI. *Int. J. Mol. Sci.* **2022**, *23*, 5208. [[CrossRef](#)]
36. Zhang, Y.; Liao, Y.; Wang, D.; He, Y.; Cao, D.; Zhang, F.; Dou, K. Altered Expression Levels of miRNAs in Serum as Sensitive Biomarkers for Early Diagnosis of Traumatic Injury. *J. Cell Biochem.* **2011**, *112*, 2435–2442. [[CrossRef](#)]
37. Coolen, M.; Katz, S.; Bally-Cuif, L. miR-9: A Versatile Regulator of Neurogenesis. *Front. Cell Neurosci.* **2013**, *7*, 220. [[CrossRef](#)]
38. Sim, S.-E.; Lim, C.-S.; Kim, J.-I.; Seo, D.; Chun, H.; Yu, N.-K.; Lee, J.; Kang, S.J.; Ko, H.-G.; Choi, J.-H.; et al. The Brain-Enriched MicroRNA miR-9-3p Regulates Synaptic Plasticity and Memory. *J. Neurosci.* **2016**, *36*, 8641–8652. [[CrossRef](#)]
39. Ji, Q.; Ji, Y.; Peng, J.; Zhou, X.; Chen, X.; Zhao, H.; Xu, T.; Chen, L.; Xu, Y. Increased Brain-Specific miR-9 and miR-124 in the Serum Exosomes of Acute Ischemic Stroke Patients. *PLoS ONE* **2016**, *11*, e0163645. [[CrossRef](#)]
40. Sørensen, S.S.; Nygaard, A.-B.; Carlsen, A.L.; Heegaard, N.H.H.; Bak, M.; Christensen, T. Elevation of Brain-Enriched miRNAs in Cerebrospinal Fluid of Patients with Acute Ischemic Stroke. *Biomark Res.* **2017**, *5*, 24. [[CrossRef](#)]
41. Zhou, X.; Xu, C.; Chao, D.; Chen, Z.; Li, S.; Shi, M.; Pei, Y.; Dai, Y.; Ji, J.; Ji, Y.; et al. Acute Cerebral Ischemia Increases a Set of Brain-Specific miRNAs in Serum Small Extracellular Vesicles. *Front. Mol. Neurosci.* **2022**, *15*, 874903. [[CrossRef](#)] [[PubMed](#)]
42. Beske, R.P.; Bache, S.; Abild Stengaard Meyer, M.; Kjærgaard, J.; Bro-Jeppesen, J.; Obilling, L.; Olsen, M.H.; Rossing, M.; Nielsen, F.C.; Møller, K.; et al. MicroRNA-9-3p: A Novel Predictor of Neurological Outcome after Cardiac Arrest. *Eur. Heart J. Acute Cardiovasc. Care.* **2022**, *11*, 609–616. [[CrossRef](#)] [[PubMed](#)]
43. Leung, L.Y.; Chan, C.P.Y.; Leung, Y.K.; Jiang, H.L.; Abrigo, J.M.; Wang, D.F.; Chung, J.S.H.; Rainer, T.H.; Graham, C.A. Comparison of miR-124-3p and miR-16 for Early Diagnosis of Hemorrhagic and Ischemic Stroke. *Clin. Chim. Acta* **2014**, *433*, 139–144. [[CrossRef](#)]
44. Liu, Y.; Zhang, J.; Han, R.; Liu, H.; Sun, D.; Liu, X. Downregulation of Serum Brain Specific MicroRNA Is Associated with Inflammation and Infarct Volume in Acute Ischemic Stroke. *J. Clin. Neurosci.* **2015**, *22*, 291–295. [[CrossRef](#)] [[PubMed](#)]
45. Sheinerman, K.S.; Tsvinsky, V.G.; Abdullah, L.; Crawford, F.; Umansky, S.R. Plasma MicroRNA Biomarkers for Detection of Mild Cognitive Impairment: Biomarker Validation Study. *Aging* **2013**, *5*, 925–938. [[CrossRef](#)]
46. Ravanidis, S.; Bougea, A.; Papagiannakis, N.; Maniati, M.; Koros, C.; Simitsi, A.-M.; Bozi, M.; Pachi, I.; Stamelou, M.; Paraskevas, G.P.; et al. Circulating Brain-Enriched MicroRNAs for Detection and Discrimination of Idiopathic and Genetic Parkinson's Disease. *Mov. Disord.* **2020**, *35*, 457–467. [[CrossRef](#)]
47. Ravanidis, S.; Bougea, A.; Papagiannakis, N.; Koros, C.; Simitsi, A.M.; Pachi, I.; Breza, M.; Stefanis, L.; Doxakis, E. Validation of Differentially Expressed Brain-Enriched MicroRNAs in the Plasma of PD Patients. *Ann. Clin. Transl. Neurol.* **2020**, *7*, 1594–1607. [[CrossRef](#)]
48. Chen, Y.; Yu, H.; Zhu, D.; Liu, P.; Yin, J.; Liu, D.; Zheng, M.; Gao, J.; Zhang, C.; Gao, Y. miR-136-3p Targets PTEN to Regulate Vascularization and Bone Formation and Ameliorates Alcohol-Induced Osteopenia. *FASEB J.* **2020**, *34*, 5348–5362. [[CrossRef](#)]
49. Kitahara, Y.; Nakamura, K.; Kogure, K.; Minegishi, T. Role of MicroRNA-136-3p on the Expression of Luteinizing Hormone-Human Chorionic Gonadotropin Receptor mRNA in Rat Ovaries. *Biol. Reprod.* **2013**, *89*, 114. [[CrossRef](#)]
50. Gui, Y.; Liu, H.; Zhang, L.; Lv, W.; Hu, X. Altered MicroRNA Profiles in Cerebrospinal Fluid Exosome in Parkinson Disease and Alzheimer Disease. *Oncotarget* **2015**, *6*, 37043–37053. [[CrossRef](#)]
51. Shang, F.-F.; Xia, Q.-J.; Liu, W.; Xia, L.; Qian, B.-J.; You, L.; He, M.; Yang, J.-L.; Wang, T.-H. miR-434-3p and DNA Hypomethylation Co-Regulate EIF5A1 to Increase AChRs and to Improve Plasticity in SCT Rat Skeletal Muscle. *Sci. Rep.* **2016**, *6*, 22884. [[CrossRef](#)]
52. Jung, H.J.; Lee, K.-P.; Milholland, B.; Shin, Y.J.; Kang, J.S.; Kwon, K.-S.; Suh, Y. Comprehensive miRNA Profiling of Skeletal Muscle and Serum in Induced and Normal Mouse Muscle Atrophy During Aging. *J. Gerontol. A Biol. Sci. Med. Sci.* **2017**, *72*, 1483–1491. [[CrossRef](#)]
53. Pardo, P.S.; Hajira, A.; Boriek, A.M.; Mohamed, J.S. MicroRNA-434-3p Regulates Age-Related Apoptosis through EIF5A1 in the Skeletal Muscle. *Aging* **2017**, *9*, 1012–1029. [[CrossRef](#)] [[PubMed](#)]

54. Manakov, S.A.; Morton, A.; Enright, A.J.; Grant, S.G.N. A Neuronal Transcriptome Response Involving Stress Pathways Is Buffered by Neuronal MicroRNAs. *Front. Neurosci.* **2012**, *6*, 156. [[CrossRef](#)] [[PubMed](#)]
55. Sharma, A.; Chandran, R.; Barry, E.S.; Bhomia, M.; Hutchison, M.A.; Balakathiresan, N.S.; Grunberg, N.E.; Maheshwari, R.K. Identification of Serum MicroRNA Signatures for Diagnosis of Mild Traumatic Brain Injury in a Closed Head Injury Model. *PLoS ONE* **2014**, *9*, e112019. [[CrossRef](#)] [[PubMed](#)]
56. Wanet, A.; Tacheny, A.; Arnould, T.; Renard, P. MiR-212/132 Expression and Functions: Within and beyond the Neuronal Compartment. *Nucleic Acids Res.* **2012**, *40*, 4742–4753. [[CrossRef](#)] [[PubMed](#)]
57. Vo, N.; Klein, M.E.; Varlamova, O.; Keller, D.M.; Yamamoto, T.; Goodman, R.H.; Impey, S. A CAMP-Response Element Binding Protein-Induced MicroRNA Regulates Neuronal Morphogenesis. *Proc. Natl. Acad. Sci. USA* **2005**, *102*, 16426–16431. [[CrossRef](#)]
58. Pauley, K.M.; Satoh, M.; Chan, A.L.; Bubb, M.R.; Reeves, W.H.; Chan, E.K. Upregulated MiR-146a Expression in Peripheral Blood Mononuclear Cells from Rheumatoid Arthritis Patients. *Arthritis Res. Ther.* **2008**, *10*, R101. [[CrossRef](#)]
59. Mehta, A.; Mann, M.; Zhao, J.L.; Marinov, G.K.; Majumdar, D.; Garcia-Flores, Y.; Du, X.; Erikci, E.; Chowdhury, K.; Baltimore, D. The MicroRNA-212/132 Cluster Regulates B Cell Development by Targeting Sox4. *J. Exp. Med.* **2015**, *212*, 1679–1692. [[CrossRef](#)]
60. Jin, W.; Reddy, M.A.; Chen, Z.; Putta, S.; Lanting, L.; Kato, M.; Park, J.T.; Chandra, M.; Wang, C.; Tangirala, R.K.; et al. Small RNA Sequencing Reveals MicroRNAs That Modulate Angiotensin II Effects in Vascular Smooth Muscle Cells. *J. Biol. Chem.* **2012**, *287*, 15672–15683. [[CrossRef](#)]
61. Malm, H.A.; Mollet, I.G.; Berggreen, C.; Orho-Melander, M.; Esguerra, J.L.S.; Göransson, O.; Eliasson, L. Transcriptional Regulation of the MiR-212/MiR-132 Cluster in Insulin-Secreting β -Cells by CAMP-Regulated Transcriptional Co-Activator 1 and Salt-Inducible Kinases. *Mol. Cell Endocrinol.* **2016**, *424*, 23–33. [[CrossRef](#)]
62. Korotkov, A.; Broekaart, D.W.M.; Banchaewa, L.; Pustjens, B.; van Scheppingen, J.; Anink, J.J.; Baayen, J.C.; Idema, S.; Gorter, J.A.; van Vliet, E.A.; et al. MicroRNA-132 Is Overexpressed in Glia in Temporal Lobe Epilepsy and Reduces the Expression of pro-Epileptogenic Factors in Human Cultured Astrocytes. *Glia* **2020**, *68*, 60–75. [[CrossRef](#)] [[PubMed](#)]
63. Wayman, G.A.; Davare, M.; Ando, H.; Fortin, D.; Varlamova, O.; Cheng, H.-Y.M.; Marks, D.; Obrietan, K.; Soderling, T.R.; Goodman, R.H.; et al. An Activity-Regulated MicroRNA Controls Dendritic Plasticity by down-Regulating P250GAP. *Proc. Natl. Acad. Sci. USA* **2008**, *105*, 9093–9098. [[CrossRef](#)]
64. Magill, S.T.; Cambronne, X.A.; Luikart, B.W.; Lioy, D.T.; Leighton, B.H.; Westbrook, G.L.; Mandel, G.; Goodman, R.H. MicroRNA-132 Regulates Dendritic Growth and Arborization of Newborn Neurons in the Adult Hippocampus. *Proc. Natl. Acad. Sci. USA* **2010**, *107*, 20382–20387. [[CrossRef](#)] [[PubMed](#)]
65. Luikart, B.W.; Bensen, A.L.; Washburn, E.K.; Perederiy, J.V.; Su, K.G.; Li, Y.; Kernie, S.G.; Parada, L.F.; Westbrook, G.L. MiR-132 Mediates the Integration of Newborn Neurons into the Adult Dentate Gyrus. *PLoS ONE* **2011**, *6*, e19077. [[CrossRef](#)] [[PubMed](#)]
66. Remenyi, J.; van den Bosch, M.W.M.; Palygin, O.; Mistry, R.B.; McKenzie, C.; Macdonald, A.; Hutvagner, G.; Arthur, J.S.C.; Frenguelli, B.G.; Pankratov, Y. MiR-132/212 Knockout Mice Reveal Roles for These MiRNAs in Regulating Cortical Synaptic Transmission and Plasticity. *PLoS ONE* **2013**, *8*, e62509. [[CrossRef](#)] [[PubMed](#)]
67. Hernandez-Rapp, J.; Smith, P.Y.; Filali, M.; Goupil, C.; Planel, E.; Magill, S.T.; Goodman, R.H.; Hébert, S.S. Memory Formation and Retention Are Affected in Adult MiR-132/212 Knockout Mice. *Behav. Brain Res.* **2015**, *287*, 15–26. [[CrossRef](#)] [[PubMed](#)]
68. Hansen, K.F.; Sakamoto, K.; Aten, S.; Price, K.H.; Loeser, J.; Hesse, A.M.; Page, C.E.; Pelz, C.; Arthur, J.S.C.; Impey, S.; et al. Targeted Deletion of MiR-132/-212 Impairs Memory and Alters the Hippocampal Transcriptome. *Learn. Mem.* **2016**, *23*, 61–71. [[CrossRef](#)]
69. Cheng, H.-Y.M.; Papp, J.W.; Varlamova, O.; Dziema, H.; Russell, B.; Curfman, J.P.; Nakazawa, T.; Shimizu, K.; Okamura, H.; Impey, S.; et al. MicroRNA Modulation of Circadian-Clock Period and Entrainment. *Neuron* **2007**, *54*, 813–829. [[CrossRef](#)]
70. Pichler, S.; Gu, W.; Hartl, D.; Gasparoni, G.; Leidinger, P.; Keller, A.; Meese, E.; Mayhaus, M.; Hampel, H.; Riemenschneider, M. The MiRNome of Alzheimer's Disease: Consistent Downregulation of the MiR-132/212 Cluster. *Neurobiol. Aging* **2017**, *50*, e1–e167. [[CrossRef](#)]
71. Cha, D.J.; Mengel, D.; Mustapic, M.; Liu, W.; Selkoe, D.J.; Kapogiannis, D.; Galasko, D.; Rissman, R.A.; Bennett, D.A.; Walsh, D.M. MiR-212 and MiR-132 Are Downregulated in Neurally Derived Plasma Exosomes of Alzheimer's Patients. *Front. Neurosci.* **2019**, *13*, 1208. [[CrossRef](#)] [[PubMed](#)]
72. Enright, N.; Simonato, M.; Henshall, D.C. Discovery and Validation of Blood MicroRNAs as Molecular Biomarkers of Epilepsy: Ways to Close Current Knowledge Gaps. *Epilepsia Open* **2018**, *3*, 427–436. [[CrossRef](#)] [[PubMed](#)]
73. Simonato, M.; Agoston, D.V.; Brooks-Kayal, A.; Dulla, C.; Fureman, B.; Henshall, D.C.; Pitkänen, A.; Theodore, W.H.; Twyman, R.E.; Kobeissy, F.H.; et al. Identification of Clinically Relevant Biomarkers of Epileptogenesis—A Strategic Roadmap. *Nat. Rev. Neurol.* **2021**, *17*, 231–242. [[CrossRef](#)] [[PubMed](#)]
74. Nudelman, A.S.; DiRocco, D.P.; Lambert, T.J.; Garelick, M.G.; Le, J.; Nathanson, N.M.; Storm, D.R. Neuronal Activity Rapidly Induces Transcription of the CREB-Regulated MicroRNA-132, In Vivo. *Hippocampus* **2010**, *20*, 492–498. [[CrossRef](#)] [[PubMed](#)]
75. Bot, A.M.; Dębski, K.J.; Lukasiuk, K. Alterations in MiRNA Levels in the Dentate Gyrus in Epileptic Rats. *PLoS ONE* **2013**, *8*, e76051. [[CrossRef](#)]
76. Gorter, J.A.; Iyer, A.; White, I.; Colzi, A.; van Vliet, E.A.; Sisodiya, S.; Aronica, E. Hippocampal Subregion-Specific MicroRNA Expression during Epileptogenesis in Experimental Temporal Lobe Epilepsy. *Neurobiol. Dis.* **2014**, *62*, 508–520. [[CrossRef](#)]
77. Guo, J.; Wang, H.; Wang, Q.; Chen, Y.; Chen, S. Expression of P-CREB and Activity-Dependent MiR-132 in Temporal Lobe Epilepsy. *Int. J. Clin. Exp. Med.* **2014**, *7*, 1297–1306.

78. Bencurova, P.; Baloun, J.; Hynst, J.; Oppelt, J.; Kubova, H.; Pospisilova, S.; Brazdil, M. Dynamic miRNA Changes during the Process of Epileptogenesis in an Infantile and Adult-Onset Model. *Sci. Rep.* **2021**, *11*, 9649. [[CrossRef](#)]
79. Venø, M.T.; Reschke, C.R.; Morris, G.; Connolly, N.M.C.; Su, J.; Yan, Y.; Engel, T.; Jimenez-Mateos, E.M.; Harder, L.M.; Pultz, D.; et al. A Systems Approach Delivers a Functional MicroRNA Catalog and Expanded Targets for Seizure Suppression in Temporal Lobe Epilepsy. *Proc. Natl. Acad. Sci. USA* **2020**, *117*, 15977–15988. [[CrossRef](#)]
80. Jimenez-Mateos, E.M.; Bray, I.; Sanz-Rodriguez, A.; Engel, T.; McKiernan, R.C.; Mouri, G.; Tanaka, K.; Sano, T.; Saugstad, J.A.; Simon, R.P.; et al. miRNA Expression Profile after Status Epilepticus and Hippocampal Neuroprotection by Targeting miR-132. *Am. J. Pathol.* **2011**, *179*, 2519–2532. [[CrossRef](#)]
81. Peng, J.; Omran, A.; Ashhab, M.U.; Kong, H.; Gan, N.; He, F.; Yin, F. Expression Patterns of miR-124, miR-134, miR-132, and miR-21 in an Immature Rat Model and Children with Mesial Temporal Lobe Epilepsy. *J. Mol. Neurosci.* **2013**, *50*, 291–297. [[CrossRef](#)] [[PubMed](#)]
82. Huang, H.; Cui, G.; Tang, H.; Kong, L.; Wang, X.; Cui, C.; Xiao, Q.; Ji, H. Relationships between Plasma Expression Levels of MicroRNA-146a and MicroRNA-132 in Epileptic Patients and Their Cognitive, Mental and Psychological Disorders. *Bioengineered* **2022**, *13*, 941–949. [[CrossRef](#)] [[PubMed](#)]
83. Haenisch, S.; Zhao, Y.; Chhibber, A.; Kaiboriboon, K.; Do, L.V.; Vogelgesang, S.; Barbaro, N.M.; Alldredge, B.K.; Lowenstein, D.H.; Cascorbi, I.; et al. SOX11 Identified by Target Gene Evaluation of miRNAs Differentially Expressed in Focal and Non-Focal Brain Tissue of Therapy-Resistant Epilepsy Patients. *Neurobiol. Dis.* **2015**, *77*, 127–140. [[CrossRef](#)] [[PubMed](#)]
84. Cai, X.; Long, L.; Zeng, C.; Ni, G.; Meng, Y.; Guo, Q.; Chen, Z.; Li, Z. lncRNA ILF3-AS1 Mediated the Occurrence of Epilepsy through Suppressing Hippocampal miR-212 Expression. *Aging* **2020**, *12*, 8413–8422. [[CrossRef](#)]
85. Vuokila, N.; Lukasiuk, K.; Bot, A.M.; van Vliet, E.A.; Aronica, E.; Pitkänen, A.; Puhakka, N. miR-124-3p Is a Chronic Regulator of Gene Expression after Brain Injury. *Cell Mol. Life Sci.* **2018**, *75*, 4557–4581. [[CrossRef](#)]
86. Ambrogini, P.; Albertini, M.C.; Betti, M.; Galati, C.; Lattanzi, D.; Savelli, D.; di Palma, M.; Saccomanno, S.; Bartolini, D.; Torquato, P.; et al. Neurobiological Correlates of Alpha-Tocopherol Antiepileptogenic Effects and MicroRNA Expression Modulation in a Rat Model of Kainate-Induced Seizures. *Mol. Neurobiol.* **2018**, *55*, 7822–7838. [[CrossRef](#)]
87. Brennan, G.P.; Dey, D.; Chen, Y.; Patterson, K.P.; Magnetta, E.J.; Hall, A.M.; Dube, C.M.; Mei, Y.-T.; Baram, T.Z. Dual and Opposing Roles of MicroRNA-124 in Epilepsy Are Mediated through Inflammatory and NRSF-Dependent Gene Networks. *Cell Rep.* **2016**, *14*, 2402–2412. [[CrossRef](#)]
88. Hu, K.; Zhang, C.; Long, L.; Long, X.; Feng, L.; Li, Y.; Xiao, B. Expression Profile of MicroRNAs in Rat Hippocampus Following Lithium-Pilocarpine-Induced Status Epilepticus. *Neurosci. Lett.* **2011**, *488*, 252–257. [[CrossRef](#)]
89. Chen, M.; Zhao, Q.-Y.; Edson, J.; Zhang, Z.H.; Li, X.; Wei, W.; Bredy, T.; Reutens, D.C. Genome-Wide MicroRNA Profiling in Brain and Blood Samples in a Mouse Model of Epileptogenesis. *Epilepsy Res.* **2020**, *166*, 106400. [[CrossRef](#)]
90. Cui, H.; Zhang, W. The Neuroprotective Effect of miR-136 on Pilocarpine-Induced Temporal Lobe Epilepsy Rats by Inhibiting Wnt/ β -Catenin Signaling Pathway. *Comput. Math Methods Med.* **2022**, *2022*, 1938205. [[CrossRef](#)]
91. Rainer, T.H.; Leung, L.Y.; Chan, C.P.Y.; Leung, Y.K.; Abrigo, J.M.; Wang, D.; Graham, C.A. Plasma miR-124-3p and miR-16 Concentrations as Prognostic Markers in Acute Stroke. *Clin. Biochem.* **2016**, *49*, 663–668. [[CrossRef](#)]
92. van Vliet, E.A.; Puhakka, N.; Mills, J.D.; Srivastava, P.K.; Johnson, M.R.; Roncon, P.; Das Gupta, S.; Karttunen, J.; Simonato, M.; Lukasiuk, K.; et al. Standardization Procedure for Plasma Biomarker Analysis in Rat Models of Epileptogenesis: Focus on Circulating MicroRNAs. *Epilepsia* **2017**, *58*, 2013–2024. [[CrossRef](#)]
93. Kharatishvili, I.; Nissinen, J.P.; McIntosh, T.K.; Pitkänen, A. A Model of Posttraumatic Epilepsy Induced by Lateral Fluid-Perfusion Brain Injury in Rats. *Neuroscience* **2006**, *140*, 685–697. [[CrossRef](#)] [[PubMed](#)]
94. Ekolle Ndode-Ekane, X.; Kharatishvili, I.; Pitkänen, A. Unfolded Maps for Quantitative Analysis of Cortical Lesion Location and Extent after Traumatic Brain Injury. *J. Neurotrauma* **2017**, *34*, 459–474. [[CrossRef](#)] [[PubMed](#)]
95. Andrade, P.; Ciszek, R.; Pitkänen, A.; Ndode-Ekane, X.E. A Web-Based Application for Generating 2D-Unfolded Cortical Maps to Analyze the Location and Extent of Cortical Lesions Following Traumatic Brain Injury in Adult Rats. *J. Neurosci. Methods* **2018**, *308*, 330–336. [[CrossRef](#)] [[PubMed](#)]
96. Bolger, A.M.; Lohse, M.; Usadel, B. Trimmomatic: A Flexible Trimmer for Illumina Sequence Data. *Bioinformatics* **2014**, *30*, 2114–2120. [[CrossRef](#)]
97. Kozomara, A.; Griffiths-Jones, S. miRBase: Annotating High Confidence MicroRNAs Using Deep Sequencing Data. *Nucleic Acids Res.* **2014**, *42*, D68–D73. [[CrossRef](#)]
98. Liao, Y.; Smyth, G.K.; Shi, W. FeatureCounts: An Efficient General Purpose Program for Assigning Sequence Reads to Genomic Features. *Bioinformatics* **2014**, *30*, 923–930. [[CrossRef](#)]
99. Zou, H.; Hastie, T. Regularization and Variable Selection via the Elastic Net. *J. R. Stat. Soc. Ser. B Stat. Methodol.* **2005**, *67*, 301–320. [[CrossRef](#)]
100. Friedman, J.H.; Hastie, T.; Tibshirani, R. Regularization Paths for Generalized Linear Models via Coordinate Descent. *J. Stat. Softw.* **2010**, *33*, 1–22. [[CrossRef](#)]
101. Tohka, J.; Moradi, E.; Huttunen, H.; Initiative, A.D.N. Comparison of Feature Selection Techniques in Machine Learning for Anatomical Brain MRI in Dementia. *Neuroinformatics* **2016**, *14*, 279–296. [[CrossRef](#)] [[PubMed](#)]
102. Ambrose, C.; McLachlan, G.J. Selection Bias in Gene Extraction on the Basis of Microarray Gene-Expression Data. *Proc. Natl. Acad. Sci. USA* **2002**, *99*, 6562–6566. [[CrossRef](#)] [[PubMed](#)]

103. Tohka, J.; van Gils, M. Evaluation of Machine Learning Algorithms for Health and Wellness Applications: A Tutorial. *Comput. Biol. Med.* **2021**, *132*, 104324. [[CrossRef](#)] [[PubMed](#)]
104. Lewis, J.D.; Evans, A.C.; Tohka, J. T1 White/Gray Contrast as a Predictor of Chronological Age, and an Index of Cognitive Performance. *Neuroimage* **2018**, *173*, 341–350. [[CrossRef](#)] [[PubMed](#)]
105. Bradley, A.P. The Use of the Area under the ROC Curve in the Evaluation of Machine Learning Algorithms. *Pattern Recognit.* **1997**, *30*, 1145–1159. [[CrossRef](#)]

Disclaimer/Publisher’s Note: The statements, opinions and data contained in all publications are solely those of the individual author(s) and contributor(s) and not of MDPI and/or the editor(s). MDPI and/or the editor(s) disclaim responsibility for any injury to people or property resulting from any ideas, methods, instructions or products referred to in the content.

III

Neurofilament Light Chain (NF-L) Is a Prognostic Biomarker for Cortical Damage Evolution but Not for Cognitive Impairment or Epileptogenesis Following Experimental TBI

Heiskanen M, Jääskeläinen O, Manninen E, Das Gupta S, Andrade P, Ciszek R, Gröhn O, Herukka S-K, Puhakka N and Pitkänen A

International Journal of Molecular Sciences 23(23): 15208, 2022



Article

Plasma Neurofilament Light Chain (NF-L) Is a Prognostic Biomarker for Cortical Damage Evolution but Not for Cognitive Impairment or Epileptogenesis Following Experimental TBI

Mette Heiskanen ¹, Olli Jääskeläinen ², Eppu Manninen ¹, Shalini Das Gupta ¹, Pedro Andrade ¹, Robert Cizek ¹, Olli Gröhn ¹, Sanna-Kaisa Herukka ^{2,3}, Noora Puhakka ¹ and Asla Pitkänen ^{1,*}

¹ A.I. Virtanen Institute for Molecular Sciences, University of Eastern Finland, P.O. Box 1627, 70211 Kuopio, Finland

² Institute of Clinical Medicine/Neurology, University of Eastern Finland, P.O. Box 1627, 70211 Kuopio, Finland

³ Department of Neurology, Kuopio University Hospital, P.O. Box 1777, 70211 Kuopio, Finland

* Correspondence: asla.pitkanen@uef.fi



Citation: Heiskanen, M.; Jääskeläinen, O.; Manninen, E.; Das Gupta, S.; Andrade, P.; Cizek, R.; Gröhn, O.; Herukka, S.-K.; Puhakka, N.; Pitkänen, A. Plasma Neurofilament Light Chain (NF-L) Is a Prognostic Biomarker for Cortical Damage Evolution but Not for Cognitive Impairment or Epileptogenesis Following Experimental TBI. *Int. J. Mol. Sci.* **2022**, *23*, 15208. <https://doi.org/10.3390/ijms232315208>

Academic Editor: Marwa Zafarullah

Received: 5 October 2022

Accepted: 29 November 2022

Published: 2 December 2022

Publisher's Note: MDPI stays neutral with regard to jurisdictional claims in published maps and institutional affiliations.



Copyright: © 2022 by the authors. Licensee MDPI, Basel, Switzerland. This article is an open access article distributed under the terms and conditions of the Creative Commons Attribution (CC BY) license (<https://creativecommons.org/licenses/by/4.0/>).

Abstract: Plasma neurofilament light chain (NF-L) levels were assessed as a diagnostic biomarker for traumatic brain injury (TBI) and as a prognostic biomarker for somatomotor recovery, cognitive decline, and epileptogenesis. Rats with severe TBI induced by lateral fluid-percussion injury (n = 26, 13 with and 13 without epilepsy) or sham-operation (n = 8) were studied. During a 6-month follow-up, rats underwent magnetic resonance imaging (MRI) (day (D) 2, D7, and D21), composite neuroscore (D2, D6, and D14), Morris-water maze (D35–D39), and a 1-month-long video-electroencephalogram to detect unprovoked seizures during the 6th month. Plasma NF-L levels were assessed using a single-molecule assay at baseline (i.e., naïve animals) and on D2, D9, and D178 after TBI or a sham operation. Plasma NF-L levels were 483-fold higher on D2 (5072.0 ± 2007.0 pg/mL), 89-fold higher on D9 (930.3 ± 306.4 pg/mL), and 3-fold higher on D178 (32.2 ± 8.9 pg/mL) after TBI compared with baseline (10.5 ± 2.6 pg/mL; all $p < 0.001$). Plasma NF-L levels distinguished TBI rats from naïve animals at all time-points examined (area under the curve [AUC] 1.0, $p < 0.001$), and from sham-operated controls on D2 (AUC 1.0, $p < 0.001$). Plasma NF-L increases on D2 were associated with somatomotor impairment severity ($\rho = -0.480$, $p < 0.05$) and the cortical lesion extent in MRI ($\rho = 0.401$, $p < 0.05$). Plasma NF-L increases on D2 or D9 were associated with the cortical lesion extent in histologic sections at 6 months post-injury ($\rho = 0.437$ for D2; $\rho = 0.393$ for D9, $p < 0.05$). Plasma NF-L levels, however, did not predict somatomotor recovery, cognitive decline, or epileptogenesis ($p > 0.05$). Plasma NF-L levels represent a promising noninvasive translational diagnostic biomarker for acute TBI and a prognostic biomarker for post-injury somatomotor impairment and long-term structural brain damage.

Keywords: fluid-percussion injury; post-traumatic epilepsy; rat; ROC analysis; single molecule array (SIMOA)

1. Introduction

Every year, approximately 2.5 million people suffer traumatic brain injury (TBI) in Europe (<https://www.center-tbi.eu/>, accessed on 4 October 2022) and the United States (<https://www.cdc.gov/traumaticbraininjury/>, accessed on 4 October 2022), with over 60 million affected globally [1]. Despite the demonstrated efficacy of a large number of interventions in preclinical proof-of-concept trials for mitigating the secondary damage and consequent functional deficits of TBI, including cognitive decline and epileptogenesis, none of these interventions have advanced to clinical application [2–4]. The development of treatments for TBI and its consequent morbidities remains a major unmet medical need [5]. One major obstacle to efficient therapy development is the lack of preclinical and clinical

biomarkers that could be used to stratify subjects for therapy trials and monitor treatment effects [5,6].

Blood-derived biomarkers are proposed as minimally invasive tools for the stratification of study subjects as well as for monitoring therapy responses, for example, in Alzheimer's disease [7]. In patients with TBI, biofluid biomarkers, including glial fibrillary acidic protein (GFAP), ubiquitin C-terminal hydrolase-L1 (UCH-L1), s100 β , and neurofilaments, show some promise for diagnosing injury severity, monitoring disease progression, and predicting the structural and functional outcome and therapy response [3,8,9]. Compared with humans, blood and cerebrospinal fluid (CSF) biomarker studies in animal models of TBI remain sparse [8]. This is a major knowledge gap, as the use of biomarkers could speed up laborious in vivo experimental studies, allowing for more rigorous, controlled, and cost-effective therapy discovery [5,10].

Neurofilament light chain (NF-L) is a neuron-specific cytoskeletal protein that provides structural support to axons and dendrites, but it is also found in synapses, where it is thought to influence the distribution of NMDA GluN1 receptors [11,12]. NF-L is one of the five subunits that form the full neurofilament, the other four being neurofilament heavy and medium chains, α -internexin, and peripherin [12]. Neurofilaments are exclusively expressed in neurons, which makes them specific indicators of neuroaxonal damage [11]. Accordingly, acute and chronic neuro-axonal damage due to TBI or other brain diseases triggers the release of a large quantity of NF-L from neurons to the interstitial fluid, from which it enters the cerebrospinal fluid (CSF) and blood [12–14]. Importantly, recent studies have demonstrated that NF-L levels in the blood and CSF at acute post-injury time-points are associated with TBI severity and predict clinical outcome, including progression of structural brain damage, functional recovery, and death [15–19].

Animal models can recapitulate various long-term clinically relevant structural and functional abnormalities of TBI, including cognitive impairment and post-traumatic epilepsy (PTE) [20,21]. In the present study, we aimed (a) to determine the temporal profile of circulating NF-L, (b) to assess associations between plasma NF-L levels and the evolution of cortical damage, and (c) to determine whether NF-L could be used as a sensitive and specific prognostic biomarker to predict the functional outcome after TBI, focusing on somatomotor recovery, cognitive decline, and epileptogenesis.

2. Results

2.1. Sample Quality and Lack of a Hemolysis Effect on Plasma NF-L Levels

Absorbance at 414 nm measured from plasma samples with NanoDrop varied from 0.08 to 0.65 ($n = 120$, mean 0.23 ± 0.10 , median 0.21). Of the 120 samples, 39 (33%) had an absorbance ≥ 0.25 and were considered to be hemolyzed. No correlation, however, was detected between absorbance at 414 nm and plasma NF-L levels at any time-point (Spearman correlation, $p > 0.05$ for all). Consequently, no samples were excluded due to hemolysis.

2.2. Post-TBI Increase in Plasma NF-L Levels Is Time-Dependent

Baseline (Naïve). Plasma NF-L levels at different post-TBI time points are summarized in Figure 1A. At baseline, the plasma NF-L levels varied from 4.2 pg/mL to 16.0 pg/mL ($n = 34$; mean 10.3 ± 2.9 pg/mL; median 10.3 pg/mL).

Sham. On D2 (48 h after sham-operation), the plasma NF-L levels were increased in craniotomized sham-operated experimental controls compared with the baseline levels of the same animals (244.3 ± 245.6 pg/mL vs. 9.6 ± 2.9 pg/mL, $p < 0.01$) (Figure 1A).

TBI. On D2, injured animals showed a 483-fold increase in the mean plasma NF-L levels compared with the baseline levels of the same rats (5072.0 ± 2007.0 pg/mL vs. 10.5 ± 2.6 pg/mL, $p < 0.001$) and a 21-fold increase compared with the sham-operated group (5072.0 ± 2007.0 pg/mL vs. 244.3 ± 245.6 pg/mL, $p < 0.001$) (Figure 1A).

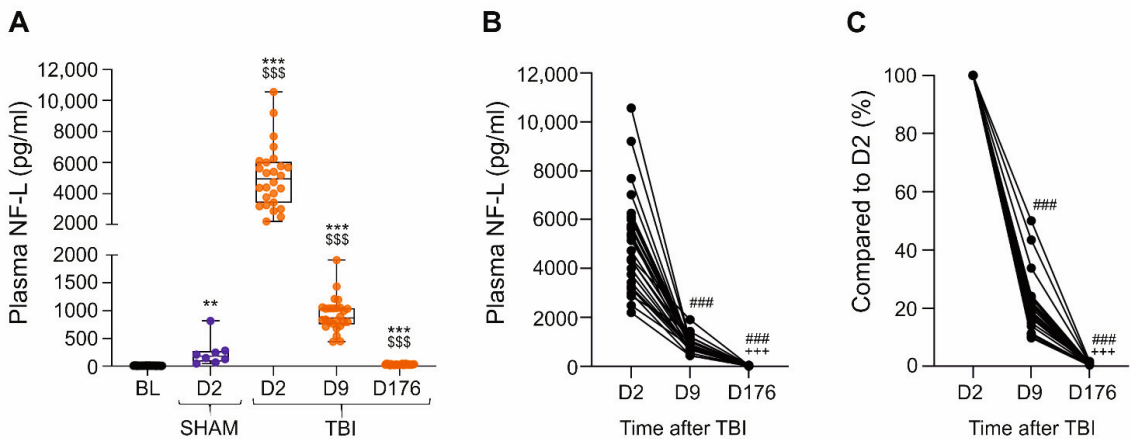


Figure 1. Plasma NF-L concentrations at different time-points after a sham operation or TBI. **(A)** Box and whisker plots (whiskers: minimum and maximum; box: interquartile range; line: median) showing plasma NF-L levels (y-axis) in different groups (x-axis). Samples collected at baseline (n = 34) before any operation (BL on D-6) were considered comparable to naïve samples. In the sham group (n = 8, blue), plasma NF-L levels were analyzed on D2 post-operation only. In the TBI group (n = 26, orange), plasma NF-L levels were assessed on D2, D9, and D176 after TBI. Each dot represents 1 animal. Note the slightly elevated plasma NF-L levels in the sham-operated animals on D2 compared with their baseline values (** $p < 0.01$, Wilcoxon). In the TBI group, the NF-L levels were elevated on all testing days as compared to their baseline values [Friedman test ($p < 0.001$) followed by *post hoc* analysis with Wilcoxon: ***, $p < 0.001$]. On D2 and D9, the average NF-L levels were higher in the TBI group than in the sham group (\$\$\$, $p < 0.001$, Mann-Whitney U test). **(B)** Dynamics of NF-L concentrations in individual TBI animals over time [Friedman test ($p < 0.001$) followed by *post hoc* analysis with Wilcoxon: ###, $p < 0.001$ compared with D2; +++, $p < 0.001$ compared with D9]. **(C)** Change in plasma NF-L levels as a percentage over time (D2 marked as 100%) [Friedman test ($p < 0.001$) followed by *post hoc* analysis with Wilcoxon: ###, $p < 0.001$ compared with D2; +++, $p < 0.001$ compared with D9]. Abbreviations: BL, baseline; D2, day 2 after TBI; D9, day 9; D176, day 176 (6 months); NF-L, neurofilament light chain; TBI, traumatic brain injury.

On D9, the plasma NF-L levels in the TBI group decreased to 930.3 ± 306.4 pg/mL. The levels remained elevated when compared to the same rats' baseline levels (930.3 ± 306.4 pg/mL vs. 10.5 ± 2.6 pg/mL, $p < 0.001$) or to the sham-operated controls on D2 (930.3 ± 306.4 pg/mL vs. 244.3 ± 245.6 pg/mL, $p < 0.001$) (Figure 1A).

On D176 (6 months post-TBI), NF-L levels remained approximately 3-fold higher than the baseline levels of the same animals (32.2 ± 8.9 pg/mL vs. 10.5 ± 2.6 pg/mL, $p < 0.001$), but only 13% of that in the sham group on D2 (32.2 ± 8.9 pg/mL vs. 244.3 ± 245.6 pg/mL, $p < 0.001$) (Figure 1A).

The temporal dynamics of the plasma NF-L concentration in each TBI rat are summarized in Figure 1B. The percent change in plasma NF-L levels from D2 to D9 is summarized in Figure 1C. On average, the plasma NF-L concentration on D9 was $20.4 \pm 9.5\%$ (range 9.80–50.1%) of that on D2. That is, the plasma NF-L concentration decreased by approximately 80% from D2 to D9. On D176, plasma NF-L levels were only $0.7 \pm 0.4\%$ (range 0.3–1.7%) of the levels on D2.

2.3. Plasma NF-L Levels Correlated with the Severity of Acute and Chronic Cortical Damage

To assess whether plasma NF-L levels correlated with the severity of the lateral fluid-percussion injury (FPI)-induced cortical lesion at acute and chronic time-points, we measured (a) the volume of abnormal cortical T_2 in MRI on D2, D7, and D21 post-injury and (b) the cortical lesion area in unfolded cortical maps on D182 post-injury.

2.3.1. Plasma NF-L and Volume of Abnormal Cortical T₂ in MRI

Quantitative T₂ MRI was available for all rats included in the NF-L analysis.

Sham. On D2, the cortical volume of the abnormal T₂ area was small ($5.4 \pm 1.2 \text{ mm}^3$, range 3.8 mm^3 – 7.0 mm^3 , median 5.7 mm^3). On D7, the volume of the T₂ change was $3.3 \pm 1.5 \text{ mm}^3$ and on D21, $3.1 \pm 1.0 \text{ mm}^3$ (Figure 2A). The ipsilateral signal increase on D2, D7, and D21 was located in areas close to the rhinal fissure at the rostrocaudal level—3.5 mm from the bregma—as the median of the ipsilateral T₂ area was higher than that contralaterally. A parasagittal signal decrease was observed on D7.

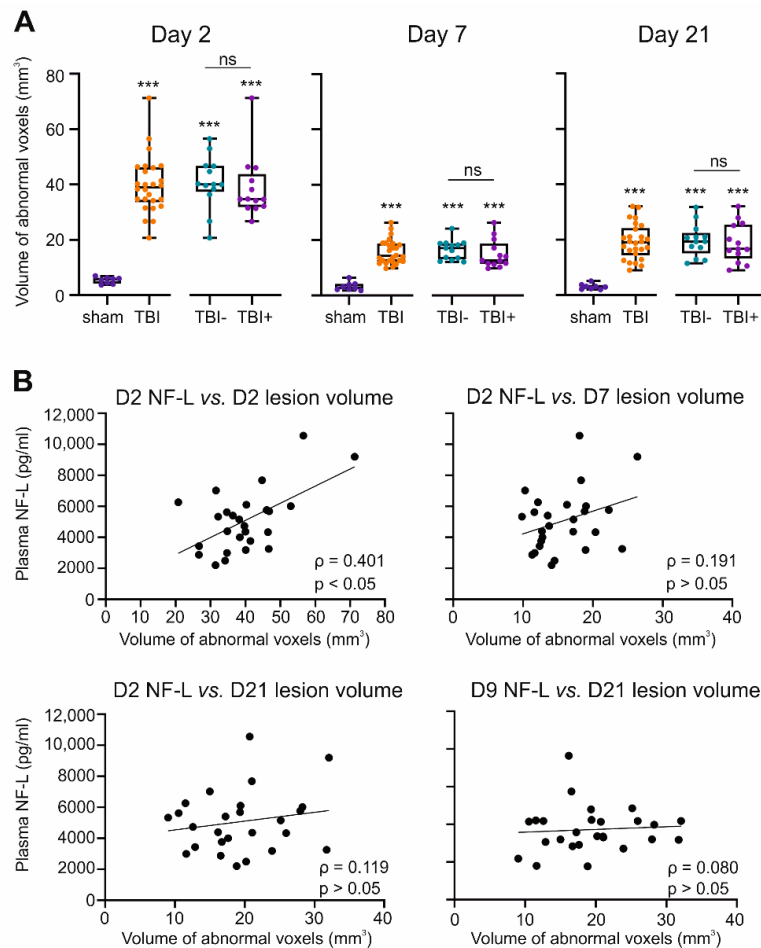


Figure 2. Plasma NF-L and cortical lesion severity in quantitative T₂ magnetic resonance imaging (MRI). **(A)** Box and whisker plots (whiskers: minimum and maximum; box: interquartile range; line: median) showing the total volume of abnormal pixels (cortical T₂ signal, y-axis) in rat brain MRI on D2, D7, and D21 after TBI (n = 26) or sham operation (n = 8). The TBI group included 13 rats without epilepsy (TBI⁻) and 13 rats with epilepsy (TBI⁺). Each dot represents 1 animal. **(B)** Spearman correlation between the plasma levels of NF-L (y-axis) and volume of abnormal T₂ area (x-axis) in MRI (TBI group only) on D2, D7, and D21. Note that on D2, the higher the NF-L level, the greater the volume of the abnormal T₂ area. No correlations were detected at later time-points. Statistical significance: ***, $p < 0.001$ as compared with the sham group (Mann-Whitney U test). Abbreviations: D2, day 2 after TBI; D9, day 9; D21, day 21; NF-L, neurofilament light chain; ns, not significant; TBI, traumatic brain injury.

On D2, plasma NF-L levels did not correlate with the volume of abnormal T₂ in the sham group ($n = 8$, $\rho = 0.095$, $p > 0.05$).

TBI. On D2, the mean volume of the abnormal cortical T₂ area was $39.8 \pm 10.4 \text{ mm}^3$ (Figure 2A). By D7, the volume of the abnormal T₂ area had decreased to $15.8 \pm 4.4 \text{ mm}^3$ ($p < 0.001$ compared with D2). On D21, the volume of the abnormal cortical T₂ area was $19.4 \pm 6.4 \text{ mm}^3$ ($p < 0.001$ compared with D2 or D7).

On D2, the higher the plasma NF-L concentration, the greater the volume of the abnormal cortical T₂ area ($\rho = 0.401$, $p < 0.05$) (Figure 2B). No correlation was detected between the D2 plasma NF-L levels and lesion volumes on D7 or D21 ($p > 0.05$). Also, no correlation was detected between the plasma NF-L levels on D9 and the volume of the abnormal T₂ area on D7 or D21 (D7 $\rho = 0.127$, $p > 0.05$; D21 $\rho = 0.080$, $p > 0.05$) (Figure 2B).

2.3.2. Plasma NF-L and Cortical Lesion Area in Histologic Sections

None of the SIMOA cohort rats had abscesses or other non-TBI-related lesions. The cortical lesion area in unfolded maps prepared from histologic section D182 post-TBI ranged between 14.0 – 56.9 mm^2 (median 33.4 mm^2) (Supplementary Figure S1). There was no difference in the cortical lesion area between the TBI+ ($31.5 \pm 13.3 \text{ mm}^2$) and TBI– ($37.7 \pm 10.6 \text{ mm}^2$) groups ($p > 0.05$).

A correlation analysis revealed that the higher the plasma NF-L level on D2 or D9, the larger the cortical lesion area on D182 ($\rho = 0.437$ for D2 and $\rho = 0.393$ for D9, $p < 0.05$ for both). In contrast, no correlation was detected between plasma NF-L levels on D176 and the cortical lesion area on D182 ($p > 0.05$).

2.4. Plasma NF-L as a Diagnostic Biomarker for Sham-Operation and TBI

Next, we assessed whether plasma NF-L levels on D2, D9, or D176 after TBI differentiated rats with TBI from naïve animals and/or sham-operated controls.

Sham-operated experimental controls vs. naïve (baseline) samples. On D2, ROC analysis revealed that plasma NF-L levels differentiated sham-operated experimental controls from naïve animals with 100% sensitivity and 100% specificity (AUC 1.0, $p < 0.001$; cut-off 49.1 pg/mL) (Figure 3A).

TBI vs. naïve (baseline) samples. On D2, NF-L levels differentiated TBI animals from naïve rats with 100% sensitivity and 100% specificity (AUC = 1.0, $p < 0.001$; cut-off: 2201 pg/mL) (Figure 3B). On D9, plasma NF-L levels differentiated TBI animals from naïve rats with 100% sensitivity and 100% specificity (AUC = 1.0, $p < 0.001$; cut-off 442 pg/mL). Even on D176, plasma NF-L levels differentiated TBI animals from naïve rats with 100% sensitivity and 97% specificity (AUC = 0.999, $p < 0.001$; cut-off 15.8 pg/mL).

TBI vs. sham-operated controls. On D2, plasma NF-L levels differentiated the TBI and sham-operated animals with 100% sensitivity and 100% specificity (AUC 1.0, $p < 0.001$; cut-off 2201 pg/mL) (Figure 3C).

2.5. Plasma NF-L as a Prognostic Biomarker for Somatomotor Recovery

Plasma NF-L and neuroscore. In sham-operated experimental controls ($n = 8$), the composite neuroscore differed between testing days over the 14-day follow-up (average neuroscore: D2 26.5, D6 27.4, D14 27.5, Friedman test, $p < 0.01$). *Post hoc* analysis with the Wilcoxon test revealed improvement in the neuroscore from D2 to D6 ($p < 0.05$), but no difference between D6 and D14 ($p > 0.05$).

In the TBI group, the evolution of the composite neuroscore over the 14-day testing period is shown in Figure 4A (Friedman test, $p < 0.001$, followed by Wilcoxon test). On D2, the average neuroscore was 7.9 (range 3.0–13.0, median 7.8), on D6 12.0 (range 7.0–19.7, median 11.5; $p < 0.001$ compared with D2), and on D14 14.2 (range 9.7–22.7, median 15.0; $p < 0.001$ compared with D2 and D6).

On D2, the higher the plasma NF-L concentration, the lower the neuroscore ($\rho = -0.480$, $p < 0.05$) (Figure 4C). Interestingly, plasma NF-L levels on D2 did not correlate with the neuroscore at later time-points ($p > 0.05$).

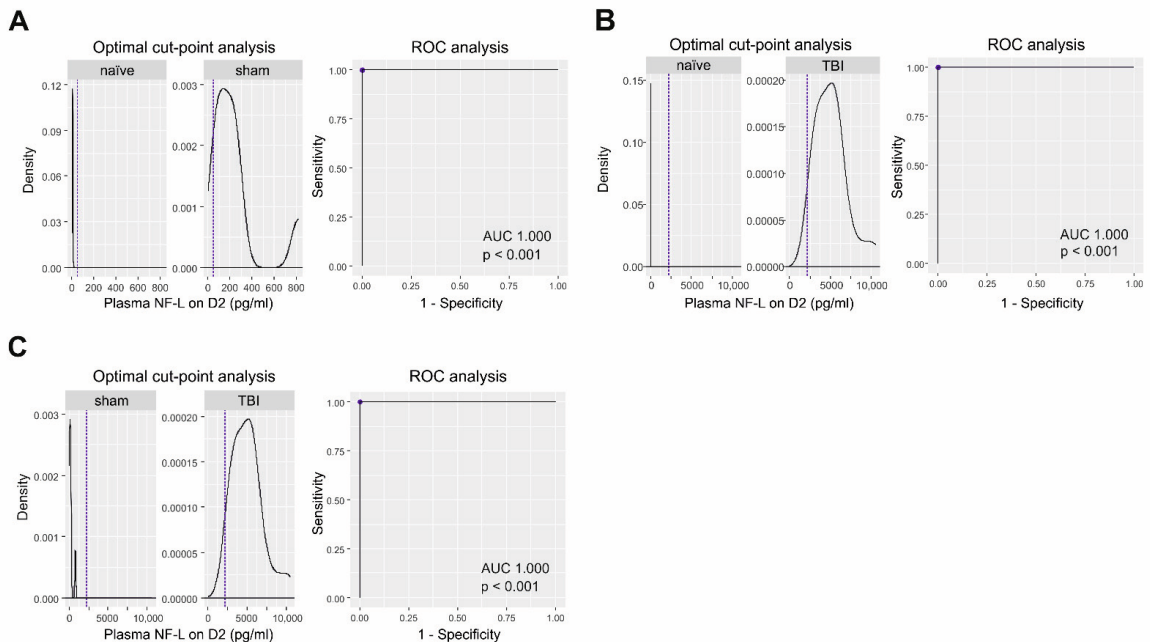


Figure 3. Plasma NF-L as a diagnostic biomarker for sham operation and TBI. (A) ROC analysis indicated that NF-L levels on D2 distinguished sham-operated rats ($n = 8$) from the naïve condition (baseline samples, $n = 34$) with 100% sensitivity and 100% specificity (AUC 1.0, $p < 0.001$, cut-off 49 pg/mL (dashed line)]. (B) NF-L levels on D2 distinguished TBI rats ($n = 26$) from the naïve condition ($n = 34$) with 100% sensitivity and 100% specificity (AUC 1.0, $p < 0.001$, cut-off: 2201 pg/mL). (C) NF-L levels on D2 distinguished TBI ($n = 13$) and sham-operated rats ($n = 13$) with 100% sensitivity and 100% specificity (AUC 1.0, $p < 0.001$, cut-off: 2201 pg/mL). Abbreviations: AUC, area under the curve; BL, baseline; D2, day 2 post-TBI, NF-L, neurofilament light chain; ROC, receiver operating characteristics; TBI, traumatic brain injury.

Plasma NF-L and recovery index. To assess whether plasma NF-L levels differed between rats with poor or good recovery, we next calculated the recovery index for each animal. The mean D14/D2 neuroscore recovery index in the TBI group was $193\% \pm 71\%$ (range 107–400%). Of the 26 rats with TBI, 9 had a D14/D2 recovery index greater than 200% (good long-term recovery), and 17 had an index $\leq 200\%$ (poor long-term recovery). The mean D6/D2 recovery index was $161\% \pm 53\%$ (range 88–281%, Figure 4D). Of the 26 rats, 12 had a D6/D2 recovery index greater than 150% (early recovery) and 14 had an index $\leq 150\%$ (no early recovery). The mean D14/D6 recovery index was $121\% \pm 24\%$ (range 82–180%). Of the 26 rats, 21 had D14/D6 recovery index greater than 100% (late recovery), and 5 had an index $\leq 100\%$ (no late recovery).

The plasma NF-L levels did not differ significantly on D2, D9, or D176 between rats with good or poor overall recovery ($p > 0.05$ in all). Similarly, no differences in plasma NF-L levels were detected between rats with or without early recovery or between rats with or without late recovery (all $p > 0.05$).

No correlation was detected between the plasma NF-L levels on D2, D9, or D176 and any of the recovery indices ($p > 0.05$ for all).

ROC analysis indicated that the D2, D9, or D176 plasma NF-L levels did not distinguish the good from the poor overall recovery groups, the early recovery groups from the non-early recovery groups, or the late recovery groups from the non-late recovery groups ($p > 0.05$).

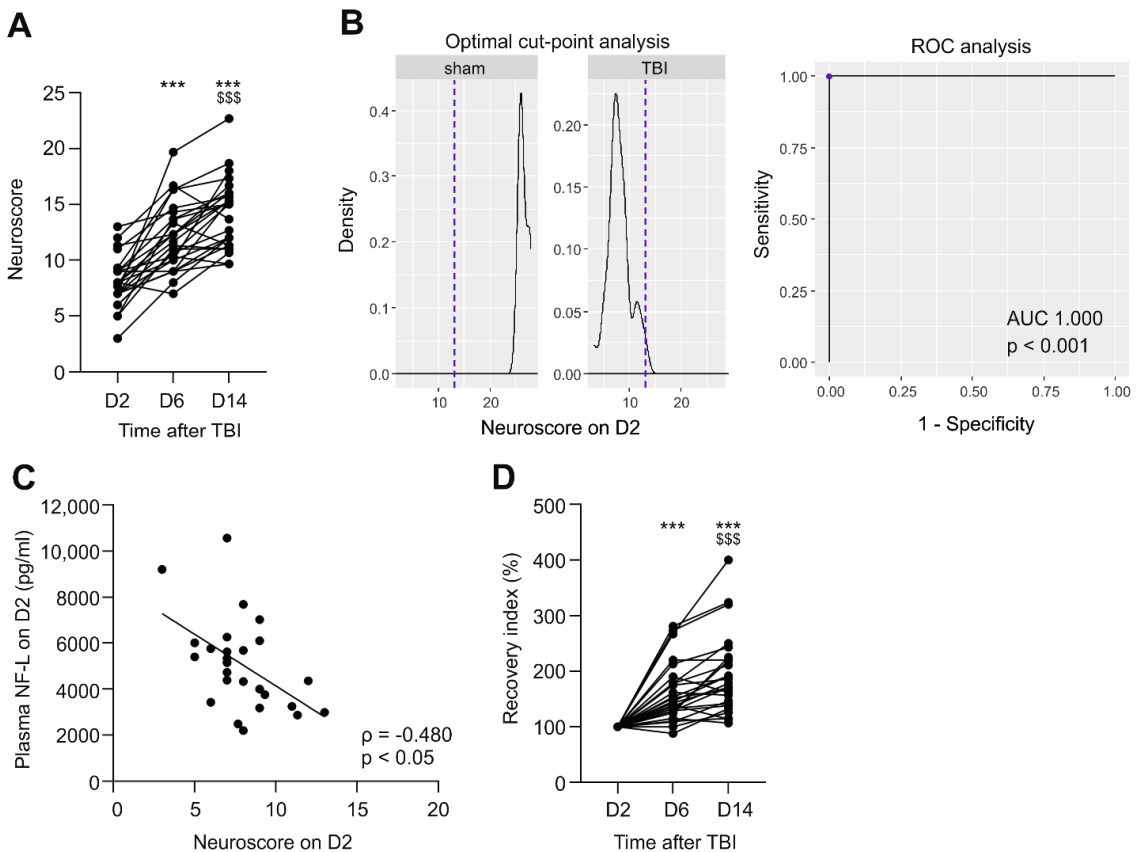


Figure 4. Plasma NF-L and somatomotor performance after TBI. **(A)** Evolution of the neuroscore in each TBI rat ($n = 26$) over the 14-day follow-up (D2, D6, and D14) after TBI. Note that in the sham-group, the average neuroscore was 26.5 on D2, 27.4 on D6, and 27.5 on D14. **(B)** The optimal cut-off and ROC analysis indicated that the D2 neuroscore differentiated TBI ($n = 26$) and sham-operated rats ($n = 8$) with 100% sensitivity and 100% specificity [AUC 1.0, $p < 0.001$, cut-off 13.0 (dashed line)]. **(C)** Spearman's correlation revealed that the higher the plasma NF-L levels on D2, the lower the neuroscore on D2 post-TBI ($\rho = -0.480$, $p < 0.05$). **(D)** Improvement of the neuroscore (recovery index) for each TBI rat ($n = 26$), compared with the neuroscore on D2. Statistical significances: ***, $p < 0.001$ compared to D2; \$\$\$, $p < 0.001$ compared to D6 (Wilcoxon matched pairs signed rank test). Abbreviations: AUC, area under the curve; D2, day 2 post-TBI; D6, day 6, D14, day 14; NF-L, neurofilament light chain; ROC, receiver operating characteristics; TBI, traumatic brain injury.

2.6. Plasma NF-L as a Prognostic Biomarker for Memory Impairment

Cut-point analysis. Next, we assessed whether plasma NF-L levels in the early post-injury phase would predict cognitive impairment (CI). Therefore, we performed a cut-point analysis of Morris water-maze data of the entire EPITARGET animal cohort, including 23 sham-operated and 118 rats with TBI, to identify the best parameter that could be used to differentiate cognitively impaired (CI+) from non-impaired (CI-) animals [22]. The analysis revealed that a latency cut-off value of 19.2 s to reach the platform on the third testing day (D37 post-TBI) separated TBI animals from sham-operated experimental controls with an AUC of 0.94 (84% sensitivity, 100% specificity, $p < 0.001$) (Figure 5A). Latencies for rats included in the NF-L analysis are presented in Supplementary Figure S2.

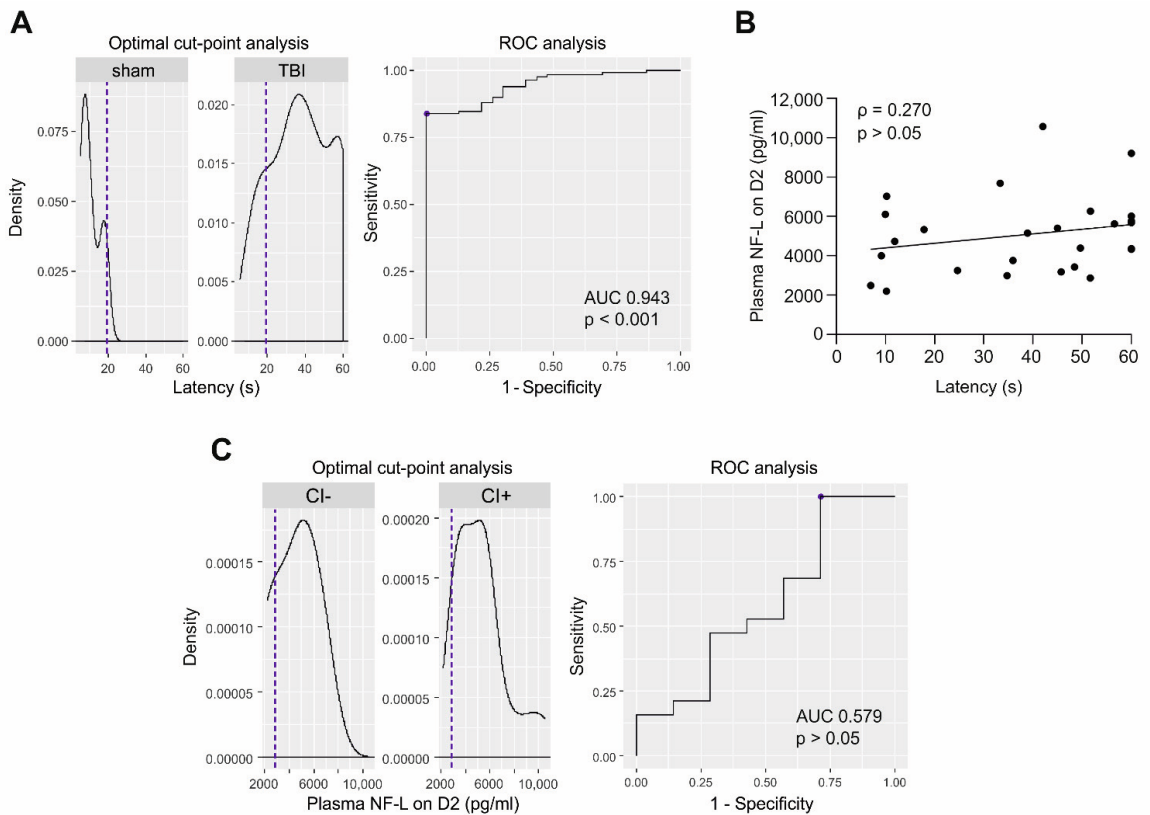


Figure 5. Plasma NF-L and cognitive impairment after TBI. (A) Optimal cut-point analysis was performed in the EPITARGET animal cohort to identify parameters that differentiate cognitively impaired (CI+) and non-impaired (CI−) rats. The cut-point latency of 19.2 s (i.e., latency to reach the platform in the Morris water maze (MWM) on the 3rd day of testing, i.e., on D37, dashed line) differentiated TBI ($n = 118$) and sham-operated rats ($n = 23$) with AUC 0.94 ($p < 0.001$) and was set as a limit for cognitive impairment. (B) No correlation was detected between plasma NF-L levels on D2 and MWM latency on D37 (Spearman correlation ρ (p) = 0.270, $p > 0.05$, $n = 26$). (C) Accordingly, ROC analysis indicated that plasma NF-L levels did not distinguish CI+ (latency > 19.2 s) from CI− (<19.2 s) rats (AUC 0.58, $p > 0.05$, Mann-Whitney U test). Abbreviations: AUC, area under the curve; D2, day 2 post-TBI; ROC, receiver operating characteristics; TBI, traumatic brain injury.

In the entire EPITARGET cohort, 70% (98/141) of the rats with TBI were categorized into the “cognitively impaired” (CI+) and 30% (20/141) were categorized into the “cognitively non-impaired” (CI−) group. The percentages in the NF-L cohort were comparable, as 73% (19/26) of the TBI animals were classified into the CI+ group (latency > 19.2 s) and 27% (7/26) into the CI− group (latency < 19.2 s, performing closer to the control level) (Supplementary Figure S3A).

Plasma NF-L levels and CI. Plasma NF-L levels did not differ significantly between CI− and CI+ rats at any time-point ($p > 0.05$) (Supplementary Figure S3B).

No correlation was detected between D2 plasma NF-L levels and latency on D37 in the TBI group ($\rho = 0.270$, $p > 0.05$) (Figure 5B).

ROC analysis indicated that plasma NF-L concentrations on D2 did not separate CI+ from CI− animals (AUC 0.579, $p > 0.05$) (Figure 5C).

2.7. Plasma NF-L as a Prognostic Biomarker for Post-Traumatic Epileptogenesis

Finally, we assessed whether, within the TBI group, plasma NF-L levels differentiated the epileptic (TBI+) from non-epileptic (TBI−) animals.

Plasma NF-L levels. Of the 26 rats with TBI, 13 had epilepsy (TBI+), and 13 did not (TBI−). Plasma NF-L levels did not differ between the TBI+ and TBI− groups at any time-point (Figure 6A). Also, the D2 to D9 change in the plasma NF-L concentrations did not differ between the TBI+ (mean decrease 3761 ± 1966 pg/mL, range 1434–8164 pg/mL) and TBI− (mean decrease 4523 ± 1966 pg/mL, range 2457–9527 pg/mL, $p > 0.05$) groups. Similarly, the D9–D176 change did not differ between TBI+ and TBI− (TBI+ mean decrease 911 ± 407 pg/mL, range 408–1863 pg/mL vs. TBI− mean decrease 885 ± 162 pg/mL, range 646–1166 pg/mL, $p > 0.05$). Within the TBI+ group, 3 of the 13 rats had a seizure on the day preceding the blood sampling; their NF-L levels, however, did not differ from those in other TBI+ rats ($p > 0.05$).

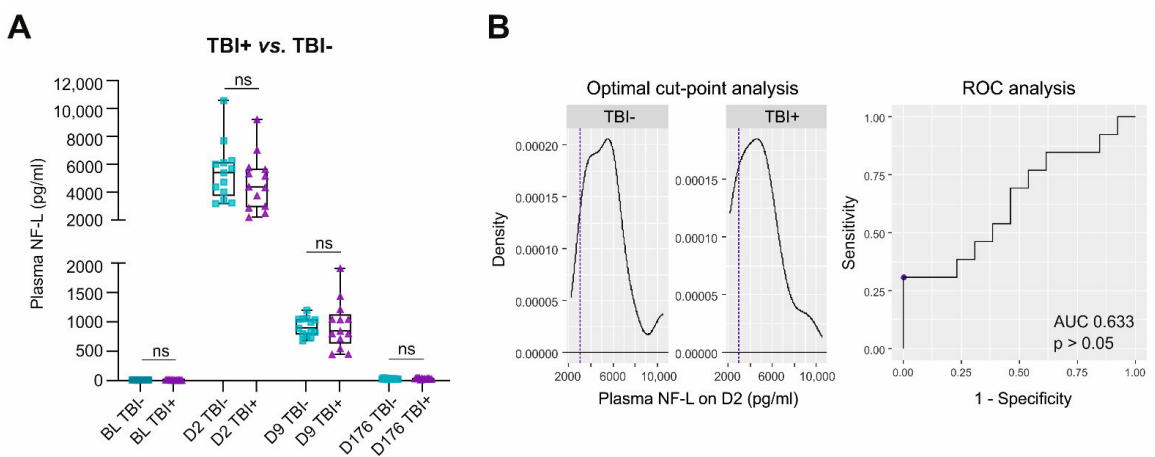


Figure 6. Plasma NF-L and epileptogenesis after TBI. (A) Box and whisker plots (whiskers: minimum and maximum; box: interquartile range; line: median) showing plasma NF-L levels (y -axis) in different groups and time-points (x -axis). Plasma NF-L levels on D2, D9, or D176 did not differ between rats that did (TBI+, $n = 13$) or did not develop epilepsy (TBI−, $n = 13$, $p > 0.05$). (B) Plasma NF-L levels on D2, D9, or D176 did not distinguish TBI+ and TBI− rats in the ROC analysis ($p > 0.05$, results for D2 shown in the figure). Statistical significance: ns, not significant (Mann-Whitney U test). Abbreviations: AUC, area under the curve; BL, baseline; D2, day 2 post-TBI; D9, day 9; D176, day 176; NF-L, neurofilament light chain; ROC, receiver operating characteristics.

Severity of epilepsy (clusters vs. no clusters). The total number of seizures did not correlate with plasma NF-L levels at any time point ($p > 0.05$). Of the 13 TBI+ rats, 4 had seizure clusters (≥ 3 seizures within 24 h). The plasma NF-L levels did not differ significantly between TBI+ rats with or without seizure clusters at any time-point ($p > 0.05$).

ROC analysis. The plasma NF-L concentration did not distinguish TBI+ from TBI− animals on D2 (AUC 0.633, $p > 0.05$), D9 (AUC 0.521, $p > 0.05$), or D176 (AUC 0.479, $p > 0.05$) (ROC for D2 shown in Figure 6B).

3. Discussion

The present study investigated whether rat plasma NF-L levels predict structural and behavioral outcomes and post-traumatic epileptogenesis after lateral FPI-induced TBI. Our findings revealed that the higher the acute plasma NF-L levels, the larger the cortical lesion in acute MRI and chronically in histology. Also, the higher the acute plasma NF-L levels, the poorer the performance in the neuroscore test. In contrast, we found no

association between plasma NF-L levels and somatomotor recovery, the development of chronic cognitive impairment, or epileptogenesis.

3.1. Presence and Temporal Profile of NF-L in the Plasma after TBI

Animal models of TBI enable detailed longitudinal studies on the temporal expression of potential plasma molecular biomarkers and how their levels relate to disease severity and progression [10]. Several studies have assessed circulating NF-L levels in rodent TBI models, including those induced by lateral FPI, single or repeated mild awake closed-head injury, and Marmarou's weight-drop injury in rats [23–26], and a closed-head impact model of engineered rotational acceleration (CHIMERA) in mice [27]. All but one of these reports, however, focused on mild or mild-to-moderate TBI [25]. To the best of our knowledge, the present study is the first to assess circulating NF-L concentrations over time and their value as a preclinical prognostic biomarker for chronic functional outcomes after severe TBI induced by lateral FPI.

Plasma NF-L concentrations peaked on D2 after lateral FPI-induced TBI, reaching approximately 5000 pg/mL, or a 483-fold increase compared with the pre-injury levels. Although comparisons of injury severities and NF-L analyses between laboratories are challenging, plasma NF-L levels in our rats on D2 were comparable to those reported by Wong et al. [25]. Wong and co-workers also used SIMOA technology, assessed serum NF-L levels on D2 post-injury, and induced TBI in Sprague-Dawley rats with lateral FPI using a 2.6–3.0 atm impact force, comparable to the present study. Similar to our observations in the lateral FPI model, plasma NF-L concentrations in an awake closed-head injury model of mild TBI or Marmarou's weight-drop model peaked on D1–2 post-injury [23,26]. As expected, however, the levels after severe TBI (5000 pg/mL) were substantially higher than those after a single mild TBI (~6 pg/mL) or mild-to-moderate weight drop (~60 pg/mL).

After a massive 483-fold increase on D2, the plasma NF-L levels declined rapidly to almost 89-fold on D9 compared with the baseline. Interestingly, even though the increase in the NF-L concentrations was substantially lower after mild than severe TBI, the temporal profile of the serum NF-L levels was comparable [23]. Similar to that after severe TBI, concentrations decreased from approximately 50 pg/mL on D1–2 to approximately 40 pg/mL on D7, and to 30 pg/mL on D14 after a single mild TBI [23].

Interestingly, even at 6 months post-injury, we detected an approximately 3-fold increase in NF-L levels. The average concentration was 32 pg/mL, which is close to the level observed after single or repeated mild TBI in rats [23,24]. Previous studies reported an approximately 3-week half-life of the NF-L protein in mouse brain tissue [28]. However, information is needed on the biological half-life of circulating NF-L in normal and/or injured rats.

Recent human data suggests that NF-L fragments are secreted by the kidney, and the filtration rate can affect the blood NF-L levels [29,30]. Although the clearance time of NF-L protein released into the blood in the rat lateral FPI model remains to be determined, it is likely to be less than 6 months, and therefore, the chronically increased levels suggest ongoing chronic release of NF-L from the brain tissue into the blood [19,31,32]. Our observations support previous histologic and diffusion tensor imaging studies reporting chronic ongoing axonal injury after severe lateral FPI-induced TBI [33,34]. Recently, a prolonged increase in post-injury serum NF-L levels was reported in 50% of rats exposed to a blast overpressure model at 4 months post-injury, supporting the idea that a chronic increase in post-injury plasma NF-L levels is not model-specific [35]. Importantly, studies in human TBI have also reported increased serum NF-L levels up to 5 years after injury [19].

Studies of patients with different types of TBI indicate an injury severity-dependent increase in serum levels of NF-L up to 100–200 pg/mL when sampled within 24 to 48 h post-admission [16,36]. Interestingly, the D2 serum NF-L levels were substantially lower in humans than in rats after severe TBI, approximately 200 pg/mL vs. 5000 pg/mL in rats [16]. In rats, we observed a large reduction in NF-L levels from the D2 value of 5000 pg/mL down to 900 pg/mL on D9. Instead, in humans, the serum NF-L levels continue to increase

during the 2nd post-injury week, reaching a level of approximately 2000 pg/mL on days 10–12 after admission [15,16]. Shahim and co-workers recently reported that at 30 days after TBI, the median serum NF-L levels were approximately 13 pg/mL—almost 2-fold higher than those of controls [19]. These studies suggest a different temporal evolution in the post-injury levels of circulating NF-L in rats and humans.

Taken together, while the magnitude of the plasma/serum NF-L concentrations after TBI is greater and the timescale of expression is shorter in rat models than in humans, the response to injury severity appears similar in rats and humans with TBI. In both rats and humans, however, the levels remain higher for a prolonged period of time, suggesting ongoing axonal injury.

3.2. Acute Plasma NF-L Levels Report on Cortical Lesion Severity in Structural MRI and Histology

Despite the heterogeneity of the clinical population, timing of blood sampling, and MRI analysis, recent clinical studies demonstrated an association between increased serum NF-L levels and the severity of brain damage as well as the progression of brain pathology [17,19]. Our correlation analysis revealed that the higher the plasma NF-L levels on D2, the greater the cortical lesion volume when imaged within hours after the blood sampling on the same day. The D2 NF-L levels, however, did not predict lesion volume on D7 or D21. This was expected, as we previously reported that the volume of the abnormal cortical T₂ area undergoes dynamic changes during the first post-injury weeks in rats with lateral FPI, becoming significantly reduced from D2 to D7 and increasing thereafter [37]. Importantly, a correlation was detected between the acute D2 NF-L levels and the cortical lesion area at 6 months post-TBI. To the best of our knowledge, this is the first study assessing the relation between circulating NF-L levels and cortical lesion severity and progression in rats with severe TBI.

The results suggest that, similar to humans, plasma NF-L levels report on the severity of acute TBI and its chronic progression in the lateral FPI model.

3.3. Elevated Plasma NF-L as a Diagnostic Biomarker for TBI and Craniotomy in the Rat Lateral FPI Model

Circulating NF-L is considered a diagnostic biomarker for mild and severe TBI in clinical studies [16,19,38]. Next, we analyzed the sensitivity and specificity of post-TBI plasma NF-L levels as diagnostic biomarkers for TBI after lateral FPI-induced severe TBI. We found that plasma NF-L differentiated TBI rats from naïve controls both at the acute (D2 and D9) and chronic (6-month) time points. Our study expands the previous results by Wong et al. [25] who reported comparable results at the D2 post-TBI time-point. Increased circulating NF-L levels were also reported after a single or repeated mild TBI in animal models, but the sensitivity and specificity of plasma/serum NF-L as a diagnostic biomarker for mild TBI remain to be assessed [23,24].

Unexpectedly, we observed that the plasma NF-L levels increased from 9.6 pg/mL at baseline to 244 pg/mL on D2 after craniotomy in sham-operated animals. Moreover, plasma NF-L levels separated sham controls from naïve rats on D2 with an AUC of 1.0 and a cut-off concentration of 49 pg/mL. Previous studies demonstrated that craniotomy can induce an inflammatory reaction in the underlying cortex [39]. Our MRI analysis suggested mild T₂ relaxation abnormalities in sham-operated controls with a craniotomy. Interestingly, however, the greatest T₂ area increase was located rostral to the craniotomy center and close to the rhinal fissure rather than under the craniotomy. We also found a parasagittal signal decrease on D7 in a region corresponding to the medial aspect of the craniotomy. Plasma NF-L levels, however, were not associated with the severity of the T₂ abnormality. We assume that the increased plasma NF-L levels are related to craniotomy-induced meningeal irritation and submeningeal inflammation and subtle intracortical axonal injury rather than to the cortical cellular pathology suggested by T₂ MRI.

Taken together, not only TBI of different severities, but also a mere craniotomy, typically used as a sham procedure, can lead to an increase in the plasma NF-L levels. This

observation emphasizes the importance of using naïve animals as “controls” in biomarker discovery studies, especially when one examines low-expressing biomarkers or milder injury severities with lower biomarker expression.

3.4. Increased Plasma NF-L Levels Correlate with Acute Somatomotor Impairment but Not with Recovery after TBI

Previous studies demonstrated that the greater the severity of the brain injury, the greater the somatomotor impairment [40]. Here, we used the composite neuroscore test to assess the severity of the somatomotor impairment and recovery during the first 2 weeks after lateral FPI. We found that the higher the plasma NF-L concentration on D2, the greater the impairment in the neuroscore test on D2. The D2 plasma NF-L levels, however, did not predict the performance on later follow-up points (D6 and D14). Consistent with our findings, previous studies of rats with single or repeated mild TBI indicated that the higher the acute serum NF-L levels, the greater the impairment in the beam-walking test [23,24].

Like the severity of impairment on the D2 neuroscore test, the trajectory of recovery also varied between animals. We were unable to find any association between the D2 plasma NF-L levels and early recovery, however, which was measured as a change in the neuroscore from D2 to D6. The NF-L levels also did not differ between the late-recovering and non-recovering animals.

Taken together, increases in the plasma/serum NF-L levels indicate not only the severity of brain damage, but also the severity of the acute somatomotor impairment. The correlation between the D2 somatomotor impairment and elevation in plasma NF-L levels may relate to axonal injury in pathways required for proper somatomotor performance.

3.5. Increased Plasma NF-L Levels Do Not Differentiate Animals with or without Chronic Hippocampus-Dependent Memory Impairment after TBI

In chronic neurodegenerative disease and multiple sclerosis, high NF-L levels are associated with cognitive impairment [41–44]. Rats with severe lateral FPI-induced TBI show hippocampus-dependent memory deficits already on D2 after TBI and remain impaired for months [45]. Moreover, animals show both hippocampal principal cell and interneuron death, with remarkable atrophy in hippocampal afferent and efferent myelinated axonal pathways after lateral FPI that progresses over weeks to months post-injury [46–48]. Therefore, we anticipated that acutely increased plasma NF-L levels would differentiate rats that will develop chronic memory impairment from those who will not. Our cut-point analysis of the entire EPITARGET animal cohort indicated that 70% of rats with severe TBI had poor memory on D37. In the sub-cohort, the percentage was 73%, indicating no animal selection bias. In contrast to our expectations, we detected no difference in the plasma NF-L levels between rats with or without cognitive impairment.

Further studies are needed to explore the cerebral origin of elevated post-TBI NF-L plasma levels to determine whether plasma NF-L has any localizing specificity, such as to lesions in selective myelinated axonal pathways, rather than being a nonspecific marker of axonal injury.

3.6. Elevated Plasma NF-L Levels Do Not Predict Post-Traumatic Epileptogenesis

Previous studies reported that the risk of PTE relates to injury severity [49] and that the epileptogenic focus develops at the perilesional cortex [50]. As circulating NF-L levels reflect the extent of cortical injury, we investigated whether an acute NF-L increase predicted which animals developed PTE during the 6-month follow-up. We failed to detect any differences in plasma NF-L levels at any investigated time point between the rats that developed PTE and those that did not.

Previous studies demonstrated that the average interictal NF-L levels in patients with drug-refractory epilepsy due to structural and other etiologies, genetic epilepsy, or temporal lobe epilepsy with hippocampal sclerosis are comparable to those in controls, although they can be slightly increased in some subpopulations of patients when using a cut-off level of 10 pg/mL [51–53]. Other studies, however, reported that patients with post-stroke

epilepsy or epilepsy related to auto-immune encephalitis have chronically increased serum NF-L levels, even though the levels remain below 100 pg/mL [52,54].

In addition to etiology, prior seizure occurrence could also influence the NF-L levels. Nass et al. [55] reported a non-significant increase (<1 pg/mL) in serum NF-L levels caused by a single tonic-clonic seizure when assessed right after the seizure that remained quite stable over the next 24 h. Also, no change in NF-L levels was detected in children with simple or complex febrile seizures or epileptic seizures when serum was analyzed within 2 h after seizure onset [56]. In our NF-L animal cohort, 50% of the rats in the TBI group experienced 1-17 seizures over the 1-month video-EEG monitoring period in the 6th post-injury month and were diagnosed with PTE. Consistent with clinical studies, the NF-L levels at 6 months post-TBI did not differ between rats with or without epilepsy. Also, there was no correlation between the NF-L levels and seizure frequency. Nor did we find a difference in NF-L levels between epileptic rats with or without seizure clusters (i.e., ≥ 3 seizures/24 h). Of the 13 rats with epilepsy, 3 had experienced an unprovoked seizure on the day preceding the plasma sampling. Their NF-L concentrations, however, did not differ from those of the other animals. These findings suggest that the epilepsy- and seizure-related increases in plasma NF-L are meager in the lateral FPI model compared with the TBI-induced increase in circulating NF-L levels, thereby reproducing the data available on structural epilepsies in humans to date.

A recent study reported increased serum NF-L levels in patients with status epilepticus (SE) when assessed within 48 h after the beginning of seizure activity [51]. In addition, elevated NF-L levels are associated with the development of treatment refractoriness and 30-day clinical worsening or death. We previously reported that 90% of rats with lateral FPI develop SE after TBI, lasting 3 to 4 days [57]. Thus, the ongoing epileptiform activity could have affected the D2 plasma NF-L levels in our study cohort. Unfortunately, we did not perform acute vEEG recordings in these animals. We consider it unlikely, however, that the occurrence of SE was a major contributor to the NF-L levels on D2. In humans, the SE-induced increase measured within 48 h after the start of SE, corresponding to the timeline of D2 plasma sampling in the present study, ranged from 13 pg/mL to 101 pg/mL [51]. In our animal cohort, the NF-L levels increased from 11 pg/mL to 5072 pg/mL, supporting the view that TBI rather than SE was the major contributor to the robust NF-L increase. Considering the slower kinetics of the brain injury-induced increase in serum NF-L in humans compared with that in rats, further clinical studies with more chronic sampling time-points are needed for more accurate comparisons between the clinical and experimental studies.

Taken together, acute post-TBI plasma NF-L levels did not predict the development of PTE or correlate with the severity of PTE after lateral FPI.

3.7. Methodologic Considerations

Human studies suggest a mild, 3% average age-related increase in circulating NF-L levels, which is proposed to relate to subclinical co-morbidities [58]. In our study cohort, the first sampling, which included naive and control samples, was performed in animals at the age of 3 months, whereas the last sampling point (D176) was at the age of 9 months. Although we cannot completely rule out that some of the 20 pg/mL concentration difference between the 3 and 9 months samples in the TBI group relate to aging rather than continuing axonal damage, we consider an aging effect unlikely as it had required an almost 20% monthly age-related increase in NF-L levels. Also, as all samples were assessed in the same batch, the assay-related variability does not explain the finding.

The average peak post-TBI concentration of plasma NF-L in rats was approximately 5000 pg/mL, whereas in humans with severe TBI, the median concentrations were approximately 2000 pg/mL, with some subjects showing levels up to 10,000 pg/mL or even higher [15,16]. It remains to be explored whether the ~2.5-fold higher average circulating NF-L concentrations reflect a greater proportion of brain damage in rodents than in humans, differences in the volume distribution or NF-L metabolism, or other factors. Finally,

the kinetics of released NF-L flow to cerebrospinal fluid and blood compartments and its relation to the breakdown of blood-CSF and blood brain barriers in a given subject need to be further explored [59].

Finally, the study was powered to differentiate the TBI+ and TBI− groups, if the AUC of the biomarker was 0.800 or greater. However, the data presented for the smaller subgroups should be interpreted as preliminary observations due to the small sample size.

4. Materials and Methods

4.1. Animals

The study design is summarized in Figure 7. The study cohort included the first 34 rats (8 sham, 26 TBI) of a total of 137 animals (23 sham-operated experimental controls, 114 TBI) that completed the 6-month-long EPITARGET project (<https://epitarget.eu>, accessed on 4 October 2022). Detailed descriptions of the project and procedures were previously reported [22,37].

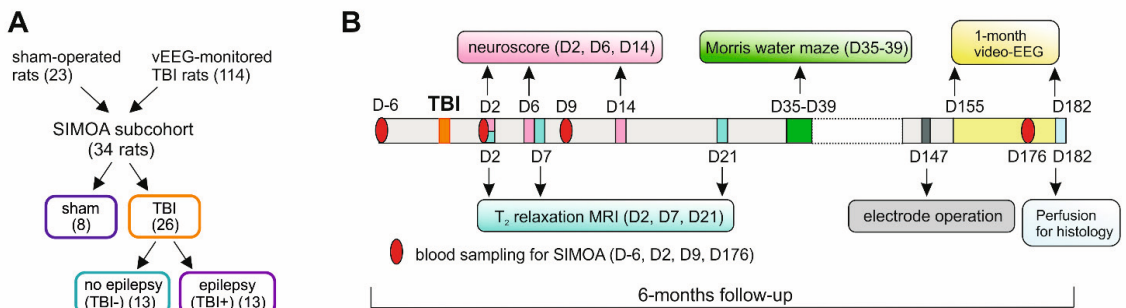


Figure 7. Study design. **(A)** The first 34 rats [8 sham-operated experimental controls, and 26 with traumatic brain injury (TBI)] completing the 6-month follow-up in the EPITARGET animal cohort of 137 animals (23 sham, and 114 TBI) were included in the present analysis [22,37]. Within the TBI group, 13 rats exhibited no unprovoked seizures in video-encephalogram (vEEG) (TBI−). In 13 rats, we found at least 1 unprovoked seizure during the 6th month vEEG (TBI+). The number of animals was based on a power calculation. That is, we expected the plasma NF-L to separate the TBI− and TBI+ groups with AUC 0.800 (MedCalc software). **(B)** Timing of the tests included in the present analysis (for a complete study design, see [22]). During the 6-month follow-up, rats underwent blood sampling via the tail vein, behavioral tests (neuroscore and Morris water maze), in vivo quantitative T₂ magnetic resonance imaging (MRI), and 1-month continuous vEEG monitoring. Plasma levels of neurofilament light chain were assessed using a single molecule array (SIMOA). Abbreviations: D, day.

The cohort size for the NF-L analysis was calculated based on an expected area under the curve (AUC) of 0.800 (power 0.8, $p < 0.05$, epilepsy vs. no-epilepsy ratio of 1:1, MedCalc software). Consequently, plasma NF-L was analyzed from 34 adult male Sprague-Dawley rats (Envigo Laboratories S.r.l, Udine, Italy), 8 of which were sham-operated controls (to assess the direction and magnitude of the changes after TBI), and the remaining 26 were exposed to lateral fluid-percussion (FPI)-induced TBI [including 13 rats that developed epilepsy (TBI+) and 13 that did not develop epilepsy (TBI−)].

At the time of injury or sham operation, average body weight was $364 \text{ g} \pm 13 \text{ g}$ (median 364 g, range 337–396 g). Rats were housed in individual cages in a controlled environment (temperature $22 \pm 1 \text{ }^\circ\text{C}$, humidity 50–60%, lights on 07:00–19:00), and had free access to food and water. All experiments were approved by the Animal Ethics Committee of the Provincial Government of Southern Finland and performed in accordance with the guidelines of the European Community Council Directives 2010/63/EU.

4.2. Lateral Fluid-Percussion-Induced Traumatic Brain Injury

TBI was induced by lateral FPI (as described in detail in [22]). Impact pressure in the EPITARGET cohort was adjusted to produce severe TBI with an expected post-impact mortality of 20–30% within the first 48 h. The mean impact pressure in the NF-L cohort was 3.27 ± 0.07 atm ($n = 26$, median 3.26 atm, range 3.13–3.41 atm). Time spent in apnea and the occurrence and duration of impact-related seizure-like behaviors were monitored and documented. The sham-operated experimental controls underwent the same anesthesia and surgical procedures without the induction of lateral FPI.

4.3. Analysis of Plasma NF-L Levels

Plasma sampling. NF-L was analyzed in plasma samples collected at baseline (7 days before injury [range D-8 to D-5, mean D-6]), D2 (48 h), D9, and at 6 months (D174 to D178, mean D176) after injury or sham operation. Sampling of tail vein blood and preparation of plasma samples were performed according to van Vliet et al. [60]. Briefly, rats were placed in an anesthesia chamber and anesthetized with 5% isoflurane. Anesthesia was maintained with 1–2% isoflurane through a nose mask. Blood was drawn from the lateral tail vein into 2 Microtainer K₂ EDTA-tubes (#365975, di-potassium ethylenediaminetetraacetic acid, BD Microtainer, BD Biosciences, Franklin Lakes, NJ, USA), 500 μ L of blood per tube, using a 24G butterfly needle. Within 1 h after blood sampling, blood tubes were centrifuged at $1300 \times g$ for 10 min at 4 °C (5417R Eppendorf Biotools). Plasma aliquots of 50 μ L were carefully collected, pipetted into 0.5-mL Protein LoBind tubes (#022431064, Eppendorf AG, Hamburg, Germany), and stored at -70 °C.

Single molecule array of NF-L. Plasma NF-L levels from 26 TBI rats [13 that developed epilepsy (TBI+) and 13 that did not develop epilepsy (TBI–)] were analyzed at baseline, and on D2, D9, and D176. In sham-operated experimental controls, we analyzed the plasma collected at baseline and on D2. The baseline plasma of both sham-operated and TBI rats was considered to represent the plasma of naïve animals.

Plasma NF-L levels were measured using a Single Molecule Array (SIMOA) digital immunoassay (NF-light Advantage assay, #103186, Quanterix, Lexington, MA, USA) [61]. Prior to SIMOA, the plasma samples were diluted 1:16 in NF-light sample diluent buffer (Quanterix). All samples were analyzed using the same batch of reagents and the same SIMOA HD-1 instrument (Quanterix). The average intra-assay coefficient of variability for duplicate sample measurements was 4.5%. Three D2 samples had an average enzyme per bead (AEB) value beyond the range of the calibration curve (>7200 pg/mL), and their concentrations were determined by extrapolation [62]. To assess the possible effect of hemolysis on NF-L levels, absorbance at 414 nm was measured in each sample using a NanoDrop spectrophotometer (NanoDrop 1000, Thermo Fisher Scientific, Waltham, MA, USA).

4.4. Behavioral Tests

4.4.1. Composite Neuromotor Score (Neuroscore)

The composite neuroscore test was used to measure the severity of somatomotor and vestibular deficits [40]. The tests were performed at D-6, D2, D6, and D14 (for details, see [22]). Briefly, the test included 7 parameters: (1) left and right forelimb flexion (2 parameters), (2) left and right hindlimb flexion (2 parameters), (3) left and right lateral pulsion resistance test (2 parameters), and (4) angle board standing test (1 parameter). The animals were scored from 0 (severely impaired) to 4 (normal) on an ordinal scale for each parameter, resulting in a composite neuroscore of 0 to 28 (the maximum score).

To evaluate the rate of early (D2 to D6), late (D6 to D14), and overall (D2 to D14) somatomotor recovery, the recovery index was calculated for each TBI rat as a percentage difference in the neuroscore between time-points. Rats with a D6/D2 recovery index $> 150\%$ were classified into the “good early recovery” group, and those with an index $\leq 150\%$ were classified into the “poor early recovery” group. Rats with a D14/D6 recovery index $> 100\%$ were classified into the “late recovery” group, and those with an index of $\leq 100\%$ were

classified into the “poor late recovery” group. Rats with a D14/D2 recovery index $> 200\%$ were classified into the “good overall recovery” group, and those with an index $\leq 200\%$ were classified into the “poor overall recovery” group.

4.4.2. Morris Water Maze

The Morris water-maze test was used to assess spatial learning and memory. The tests, including a probe trial, were performed on D35–D39 after injury (for details, see [22]).

Cognitive performance of rats with TBI varied substantially on D35–D39, with some exhibiting severe impairment and others performing at control level [22]. Therefore, we next categorized the TBI rats ($n = 118$) into those that showed or did not show memory impairment compared with the sham-operated controls ($n = 23$) by performing a cut-point analysis. To maximize the statistical power, the data used in the cut-point analysis was derived from the entire EPITARGET cohort. Based on the cut-off value of the latency to find the hidden platform on the 3rd testing day, we categorized each rat into either the “cognitively impaired” (CI+) or the “cognitively not impaired” (CI−) group.

4.5. Magnetic Resonance Imaging (MRI) and Lesion Analysis

Details of the quantitative T_2 MRI performed in the EPITARGET cohort, including the rats analyzed here, were previously provided [37]. Rats were imaged on D2, D7, and D21 after injury (Figure 7B).

Cortical lesion volume. Analysis of cortical lesion volumes from MRI was previously described [37]. Briefly, T_2 relaxation time maps were estimated from multi-slice-multi-echo spin-echo images acquired with a 7-Tesla Bruker PharmaScan magnet (Bruker BioSpin MRI GmbH). The imaging time-points were 2, 7, and 21 days after TBI. The slice thickness was $500 \mu\text{m}$, in-plane resolution $201 \times 201 \mu\text{m}^2$, repetition time 3016 ms, and echo times 14.6, 29.2, 43.8, 58.4, 73.0, and 87.6 ms. As a result of the challenges in the image registration accuracy caused by cortical lesions, the injured cortex was manually outlined for each animal at each time-point. Based on their T_2 values, imaging voxels within the cortex were classified as normal or abnormal. The range for normal T_2 values was defined as $45 \text{ ms} \leq T_2 \leq 55 \text{ ms}$, with the lower limit corresponding to the 2.5th percentile and the upper limit corresponding to the 97.5th percentile of all imaging voxels of all sham-operated controls across all time-points. Values below the lower limit or above the upper limit were classified as abnormal. The number of abnormal voxels was counted and multiplied by voxel size to obtain an estimate of the cortical lesion volume for each animal.

Gridded unfolded cortical map. As we unexpectedly found increased NF-L levels in the D2 plasma of sham-operated animals (see results), we analyzed their D2 T_2 MRI in further detail to identify the locations of possible structural abnormalities. No major cortical lesions were detected, and we were able to accurately register the images to a template brain (see [63]). First, the ipsilateral and contralateral cortex were manually outlined in each 0.5-mm-thick imaging slice in the template brain. Then, unfolded cortical maps were generated from the registered images as described previously [37]. The cortical profile of T_2 was measured in each slice, starting at the rhinal fissure and continuing toward the brain midline (Figure 8A). The T_2 profiles of different slices were joined to form a 2-dimensional mapping of T_2 relaxation times over the cortical surface. The resulting 2-dimensional cortical maps were filtered using an isotropic spatial Gaussian filter (standard deviation 0.5 mm), followed by an interpolation of the maps on a grid with a $0.5 \times 0.5 \text{ mm}^2$ resolution. The Mann-Whitney U-test along with the Benjamini-Hochberg procedure (average false discovery rate of 0.05) [64] were used to correct for multiple comparisons and to test for differences between the ipsilateral and contralateral cortical T_2 values at each grid point.

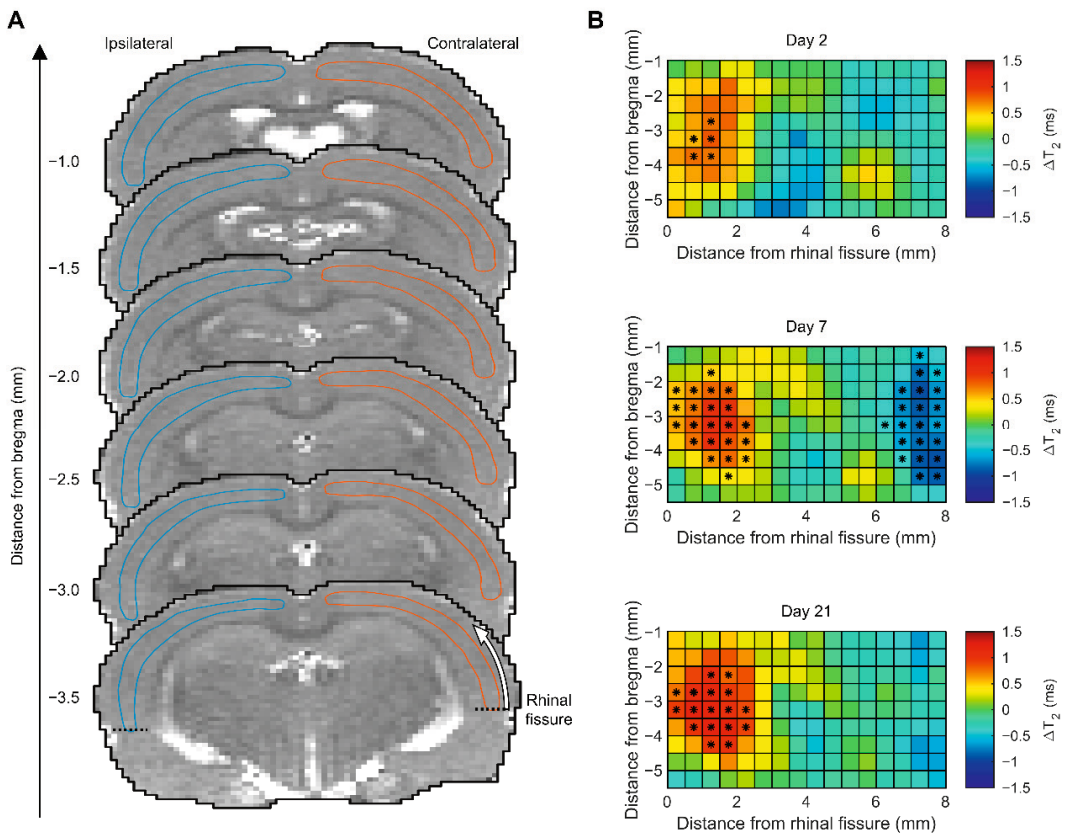


Figure 8. Cortical T_2 magnetic resonance imaging (MRI) analysis in the sham-operated experimental control group. (A) T_2 images of the sham animals were registered to a template brain. Then, the ipsilateral (left, blue outline) and the contralateral (right, orange outline) cortex was manually outlined in each image slice (thickness 0.5 mm). In each slice, a cortical profile of the T_2 relaxation time was measured, starting at the rhinal fissure and continuing dorsally towards the brain midline as indicated by the white arrow (bottom slice). (B) The cortical T_2 profiles of different slices were combined, filtered using a 2-dimensional isotropic Gaussian filter with a standard deviation of 0.5 mm, and interpolated on a grid with a $0.5 \times 0.5 \text{ mm}^2$ resolution. We found an ipsilateral signal increase on D2, D7, and D21 in areas close to the rhinal fissure at the rostrocaudal level (-3.5 mm from the bregma) as the median of the ipsilateral T_2 area was increased compared with that contralaterally. We also found a parasagittal signal decrease on D7. Color coding of the heatmap: red indicates a positive ipsilateral vs. contralateral difference in T_2 (higher T_2 ipsilaterally), and blue indicates a negative difference (higher T_2 contralaterally). An asterisk (*) at a given grid point indicates a statistically significant difference for the median T_2 (Mann-Whitney U-test, after correcting for multiple comparisons using the Benjamini-Hochberg procedure with an average false discovery rate of 0.05).

4.6. Video-EEG Monitoring

At 5 months post-TBI (D147), rats were anesthetized and implanted with 3 skull electrodes. Starting on D154 (1 week after electrode implantation), rats underwent continuous (24/7) video-EEG (vEEG) monitoring for 4 weeks to diagnose PTE [22]. Rats were defined as having epilepsy if at least one unprovoked electrographic seizure was detected (Supplementary Figure S4). The electroencephalographic seizure was defined as a high-amplitude rhythmic discharge that clearly represented an atypical EEG pattern (i.e., repetitive spikes, spike-and-wave discharges, poly-spike-and-wave discharges, or slow-

waves with frequency and amplitude modulation) that lasted >10 s [65]. The prevalence of epilepsy in the EPITARGET cohort was 27% (31/114).

4.7. Histology and Preparation of Cortical Unfolded Maps

Perfusion. To assess the location and extent of the FPI and exclude non-TBI related epileptogenic lesions (e.g., abscess), rats were intracardially perfused for histology after completing the vEEG (D182). Briefly, rats were deeply anesthetized with pentobarbital (60 mg/kg, i.p.) and perfused transcardially with 0.9% NaCl followed by 4% paraformaldehyde in 0.1 M sodium phosphate buffer (PB), pH 7.4. The brain was removed from the skull, fixed in 4% paraformaldehyde for 4 h, cryoprotected in 20% glycerol in 0.02 M potassium phosphate-buffered saline (KPBS, pH 7.4) for 24 h, frozen in dry ice, and stored at -70°C for further processing.

Frozen coronal sections of the brain were cut (25- μm thick, 1-in-12 series) using a sliding microtome. The first series of sections was stored in 10% formalin at room temperature and used for thionin staining. Other series of sections were collected into a tissue collection solution (30% ethylene glycol and 25% glycerol in 0.05 M PB) and stored at -20°C until processed.

Nissl staining. The first series of sections was stained with thionin, cleared in xylene, and cover-slipped using Depex[®] (BDH Chemical, Poole, UK) as a mounting medium.

Preparation of cortical unfolded maps. To assess the cortical lesion area and the damage to different cytoarchitectonic cortical areas after TBI, thionin-stained sections were digitized (40 \times , Hamamatsu Photonics, NanoZoomer-XR, NDP.scan 3.2). Unfolded cortical maps were then prepared from the digitized histologic sections as described in detail by [66] and by applying in-house software from <https://unfoldedmap.org> (accessed on 4 October 2022) adapted to the rat brain [67].

4.8. Statistical Analysis

Data were analyzed using GraphPad Prism 9 and RStudio (v. 1.1.463) by R (v. 4.0.2). Differences in the mean NF-L plasma levels between groups were assessed with the Mann-Whitney U test (unpaired data) or the Wilcoxon matched-pairs signed rank test (paired data). Differences in mean NF-L plasma levels in TBI rats over different time points were assessed by the Friedman test followed by the Wilcoxon *post hoc* test. Correlations between the plasma NF-L levels and behavioral outcome measures or lesion size in MRI or histology were assessed with the Spearman rank correlation test (ρ). Evolution of the composite neuroscore over the testing period was assessed by the Friedman test followed by the Wilcoxon *post hoc* test. Categorization of rats with TBI into those with or without cognitive impairment (CI+ or CI-, respectively) on D35-D39 was performed with the cut-point analysis, using the cutpointr package in R. The optimal cut-off value for each parameter was defined as the maximal sum of sensitivity and specificity. The sensitivity and specificity of plasma NF-L as a prognostic biomarker for cognitive impairment and epileptogenesis were assessed with receiver operating characteristic (ROC) analysis using the pROC package in R. Statistical significance of the AUC was evaluated by the Mann-Whitney U test. A *p*-value less than 0.05 was considered significant. Data are expressed as the mean \pm standard deviation of the mean (SD).

5. Conclusions

This is the first systematic study of plasma NF-L levels in a model of PTE with structural, behavioral, and vEEG follow-up. Our data show that TBI and even a craniotomy lead to an increase in plasma NF-L levels. After lateral FPI, the higher the NF-L levels, the greater the cortical brain damage and somatomotor impairment. We did not find an association between plasma NF-L levels and the evolution of chronic hippocampus-dependent memory impairment. Nor did we find a correlation between plasma NF-L and somatomotor recovery or epileptogenesis. Our data indicate that although the dynamics of post-injury plasma NF-L levels seem faster in the rat model compared with that in

human TBI, the association of plasma NF-L with TBI-related factors such as severity of TBI and brain damage and magnitude of functional impairments is similar between the rat model and human TBI. Our data show that plasma NF-L is a sensitive biomarker to monitor post-injury structural and functional severity after lateral FPI and could serve as a promising noninvasive response biomarker in preclinical treatment trials.

Supplementary Materials: The following supporting information can be downloaded at: <https://www.mdpi.com/article/10.3390/ijms232315208/s1>.

Author Contributions: Conceptualization, M.H., S.D.G., N.P. and A.P.; software, P.A. and R.C.; formal analysis, M.H. and E.M.; investigation, O.J., E.M. and P.A.; resources, O.G., S.-K.H. and A.P.; writing—original draft preparation, M.H. and A.P.; writing—review and editing, M.H. and A.P.; visualization, M.H. and E.M.; supervision, O.G., S.-K.H., N.P. and A.P.; project administration, A.P.; funding acquisition, O.G. and A.P. All authors have read and agreed to the published version of the manuscript.

Funding: This research was funded by The Medical Research Council of the Academy of Finland (Grants 272249, 273909, 2285733-9, 298007), The Sigrid Jusélius Foundation, the European Union's Seventh Framework Programme (FP7/2007-2013) under grant agreement n°602102 (EPITARGET), and the National Institute of Neurological Disorders and Stroke (NINDS) Center without Walls of the National Institutes of Health (NIH) under Award Number U54NS100064 (EpiBio54Rx).

Institutional Review Board Statement: All animal experiments were approved by the Animal Ethics Committee of the Provincial Government of Southern Finland and performed in accordance with the guidelines of the European Community Council Directives 2010/63/EU.

Informed Consent Statement: Not applicable.

Data Availability Statement: The data presented in this study are available on request from the corresponding author.

Acknowledgments: We thank Jarmo Hartikainen and Merja Lukkari for their excellent technical assistance, and Niina Lapinlampi for her help in setting up the RedCap database for data collection.

Conflicts of Interest: The authors declare no conflict of interest.

References

1. Dewan, M.C.; Rattani, A.; Gupta, S.; Baticulon, R.E.; Hung, Y.C.; Punchak, M.; Agrawal, A.; Adeleye, A.O.; Shrime, M.G.; Rubiano, A.M.; et al. Estimating the Global Incidence of Traumatic Brain Injury. *J. Neurosurg.* **2019**, *130*, 1080–1097. [\[CrossRef\]](#)
2. Pitkänen, A.; Paananen, T.; Kyyriäinen, J.; Das Gupta, S.; Heiskanen, M.; Vuokila, N.; Bañuelos-Cabrera, I.; Lapinlampi, N.; Kajevu, N.; Andrade, P.; et al. Biomarkers for Posttraumatic Epilepsy. *Epilepsy Behav.* **2021**, *121*, 107080. [\[CrossRef\]](#)
3. Mozaffari, K.; Dejam, D.; Duong, C.; Ding, K.; French, A.; Ng, E.; Preet, K.; Franks, A.; Kwan, I.; Phillips, H.W.; et al. Systematic Review of Serum Biomarkers in Traumatic Brain Injury. *Cureus* **2021**, *13*, e17056. [\[CrossRef\]](#)
4. Krausz, A.D.; Korley, F.K.; Burns, M.A. The Current State of Traumatic Brain Injury Biomarker Measurement Methods. *Biosensors* **2021**, *11*, 319. [\[CrossRef\]](#)
5. Smith, D.H.; Kochanek, P.M.; Rosi, S.; Meyer, R.; Ferland-Beckham, C.; Prager, E.M.; Ahlers, S.T.; Crawford, F. Roadmap for Advancing Pre-Clinical Science in Traumatic Brain Injury. *J. Neurotrauma* **2021**, *38*, 3204–3221. [\[CrossRef\]](#)
6. Dulla, C.G.; Pitkänen, A. Novel Approaches to Prevent Epileptogenesis after Traumatic Brain Injury. *Neurotherapeutics* **2021**, *18*, 1582–1601. [\[CrossRef\]](#)
7. Teunissen, C.E.; Verberk, I.M.W.; Thijssen, E.H.; Vermunt, L.; Hansson, O.; Zetterberg, H.; van der Flier, W.M.; Mielke, M.M.; del Campo, M. Blood-Based Biomarkers for Alzheimer's Disease: Towards Clinical Implementation. *Lancet Neurol.* **2022**, *21*, 66–77. [\[CrossRef\]](#)
8. Wang, K.K.; Yang, Z.; Zhu, T.; Shi, Y.; Rubenstein, R.; Tyndall, J.A.; Manley, G.T. An Update on Diagnostic and Prognostic Biomarkers for Traumatic Brain Injury. *Expert Rev. Mol. Diagn.* **2018**, *18*, 165–180. [\[CrossRef\]](#)
9. Rogan, A.; O'Sullivan, M.B.; Holley, A.; McQuade, D.; Larsen, P. Can Serum Biomarkers Be Used to Rule out Significant Intracranial Pathology in Emergency Department Patients with Mild Traumatic Brain Injury? A Systemic Review & Meta-Analysis. *Injury* **2021**, *53*, 259–271. [\[CrossRef\]](#)
10. Shultz, S.R.; McDonald, S.J.; Vonder Haar, C.; Meconi, A.; Vink, R.; van Donkelaar, P.; Taneja, C.; Iverson, G.L.; Christie, B.R. The Potential for Animal Models to Provide Insight into Mild Traumatic Brain Injury: Translational Challenges and Strategies. *Neurosci. Biobehav. Rev.* **2017**, *76*, 396–414. [\[CrossRef\]](#)

11. Khalil, M.; Teunissen, C.E.; Otto, M.; Piehl, F.; Sormani, M.P.; Gattringer, T.; Barro, C.; Kappos, L.; Comabella, M.; Fazekas, F.; et al. Neurofilaments as Biomarkers in Neurological Disorders. *Nat. Rev. Neurol.* **2018**, *14*, 577–589. [[CrossRef](#)]
12. Gafson, A.R.; Barthélemy, N.R.; Bomont, P.; Carare, R.O.; Durham, H.D.; Julien, J.P.; Kuhle, J.; Leppert, D.; Nixon, R.A.; Weller, R.O.; et al. Neurofilaments: Neurobiological Foundations for Biomarker Applications. *Brain* **2020**, *143*, 1975–1998. [[CrossRef](#)]
13. Rosengren, L.E.; Karlsson, J.E.; Karlsson, J.O.; Persson, L.I.; Wikkelsö, C. Patients with Amyotrophic Lateral Sclerosis and Other Neurodegenerative Diseases Have Increased Levels of Neurofilament Protein in CSF. *J. Neurochem.* **1996**, *67*, 2013–2018. [[CrossRef](#)]
14. Norgren, N.; Sundström, P.; Svenningsson, A.; Rosengren, L.; Stigbrand, T.; Gunnarsson, M. Neurofilament and Glial Fibrillary Acidic Protein in Multiple Sclerosis. *Neurology* **2004**, *63*, 1586–1590. [[CrossRef](#)]
15. al Nimer, F.; Thelin, E.; Nyström, H.; Dring, A.M.; Svenningsson, A.; Piehl, F.; Nelson, D.W.; Bellander, B.M. Comparative Assessment of the Prognostic Value of Biomarkers in Traumatic Brain Injury Reveals an Independent Role for Serum Levels of Neurofilament Light. *PLoS ONE* **2015**, *10*, e0132177. [[CrossRef](#)]
16. Shahim, P.; Gren, M.; Liman, V.; Andreasson, U.; Norgren, N.; Tegner, Y.; Mattsson, N.; Andreassen, N.; Öst, M.; Zetterberg, H.; et al. Serum Neurofilament Light Protein Predicts Clinical Outcome in Traumatic Brain Injury. *Sci. Rep.* **2016**, *6*, 36791. [[CrossRef](#)]
17. Ljungqvist, J.; Zetterberg, H.; Mitsis, M.; Blennow, K.; Skoglund, T. Serum Neurofilament Light Protein as a Marker for Diffuse Axonal Injury: Results from a Case Series Study. *J. Neurotrauma* **2017**, *34*, 1124–1127. [[CrossRef](#)]
18. Thelin, E.; al Nimer, F.; Frostell, A.; Zetterberg, H.; Blennow, K.; Nyström, H.; Svensson, M.; Bellander, B.M.; Piehl, F.; Nelson, D.W. A Serum Protein Biomarker Panel Improves Outcome Prediction in Human Traumatic Brain Injury. *J. Neurotrauma* **2019**, *36*, 2850–2862. [[CrossRef](#)]
19. Shahim, P.; Politis, A.; van der Merwe, A.; Moore, B.; Chou, Y.Y.; Pham, D.L.; Butman, J.A.; Diaz-Arrastia, R.; Gill, J.M.; Brody, D.L.; et al. Neurofilament Light as a Biomarker in Traumatic Brain Injury. *Neurology* **2020**, *95*, e610–e622. [[CrossRef](#)]
20. Bramlett, H.M.; Dietrich, W.D. Long-Term Consequences of Traumatic Brain Injury: Current Status of Potential Mechanisms of Injury and Neurological Outcomes. *J. Neurotrauma* **2015**, *32*, 1834–1848. [[CrossRef](#)]
21. Pitkänen, A.; Kempainen, S.; Ndode-Ekane, X.E.; Huusko, N.; Huttunen, J.K.; Gröhn, O.; Immonen, R.; Sierra, A.; Bolkvadze, T. Posttraumatic Epilepsy-Disease or Comorbidity? *Epilepsy Behav.* **2014**, *38*, 19–24. [[CrossRef](#)]
22. Lapinlampi, N.; Andrade, P.; Paananen, T.; Hämäläinen, E.; Ekolle Ndode-Ekane, X.; Puhakka, N.; Pitkänen, A. Postinjury Weight Rather than Cognitive or Behavioral Impairment Predicts Development of Posttraumatic Epilepsy after Lateral Fluid-Perfusion Injury in Rats. *Epilepsia* **2020**, *61*, 2035–2052. [[CrossRef](#)]
23. O'Brien, W.T.; Pham, L.; Brady, R.D.; Bain, J.; Yamakawa, G.R.; Sun, M.; Mychasiuk, R.; O'Brien, T.J.; Monif, M.; Shultz, S.R.; et al. Temporal Profile and Utility of Serum Neurofilament Light in a Rat Model of Mild Traumatic Brain Injury. *Exp. Neurol.* **2021**, *341*, 113698. [[CrossRef](#)]
24. Pham, L.; Wright, D.K.; O'Brien, W.T.; Bain, J.; Huang, C.; Sun, M.; Casillas-Espinosa, P.M.; Shah, A.D.; Schittenhelm, R.B.; Sobey, C.G.; et al. Behavioral, Axonal, and Proteomic Alterations Following Repeated Mild Traumatic Brain Injury: Novel Insights Using a Clinically Relevant Rat Model. *Neurobiol. Dis.* **2021**, *148*, 105151. [[CrossRef](#)]
25. Wong, K.R.; O'Brien, W.T.; Sun, M.; Yamakawa, G.; O'Brien, T.J.; Mychasiuk, R.; Shultz, S.R.; McDonald, S.J.; Brady, R.D. Serum Neurofilament Light as a Biomarker of Traumatic Brain Injury in the Presence of Concomitant Peripheral Injury. *Biomark. Insights* **2021**, *16*, 15–18. [[CrossRef](#)]
26. Scrimgeour, A.G.; Condlin, M.L.; Loban, A.; DeMar, J.C. Omega-3 Fatty Acids and Vitamin D Decrease Plasma T-Tau, GFAP, and UCH-L1 in Experimental Traumatic Brain Injury. *Front. Nutr.* **2021**, *8*, 685220. [[CrossRef](#)]
27. Cheng, W.H.; Stukas, S.; Martens, K.M.; Namjoshi, D.R.; Button, E.B.; Wilkinson, A.; Bashir, A.; Robert, J.; Crompton, P.A.; Wellington, C.L. Age at Injury and Genotype Modify Acute Inflammatory and Neurofilament-Light Responses to Mild CHIMERA Traumatic Brain Injury in Wild-Type and APP/PS1 Mice. *Exp. Neurol.* **2018**, *301*, 26–38. [[CrossRef](#)]
28. Barry, D.M.; Millecamps, S.; Julien, J.-P.; Garcia, M.L. New Movements in Neurofilament Transport, Turnover and Disease. *Exp. Cell Res.* **2007**, *313*, 2110–2120. [[CrossRef](#)]
29. Akamine, S.; Marutani, N.; Kanayama, D.; Gotoh, S.; Maruyama, R.; Yanagida, K.; Sakagami, Y.; Mori, K.; Adachi, H.; Kozawa, J.; et al. Renal Function Is Associated with Blood Neurofilament Light Chain Level in Older Adults. *Sci. Rep.* **2020**, *10*, 20350. [[CrossRef](#)]
30. Rebelos, E.; Rissanen, E.; Bucci, M.; Jääskeläinen, O.; Honka, M.-J.; Nummenmaa, L.; Moriconi, D.; Laurila, S.; Salminen, P.; Herukka, S.-K.; et al. Circulating Neurofilament Is Linked with Morbid Obesity, Renal Function, and Brain Density. *Sci. Rep.* **2022**, *12*, 7841. [[CrossRef](#)]
31. Thelin, E.P.; Zeiler, F.A.; Ercole, A.; Mondello, S.; Büki, A.; Bellander, B.M.; Helmy, A.; Menon, D.K.; Nelson, D.W. Serial Sampling of Serum Protein Biomarkers for Monitoring Human Traumatic Brain Injury Dynamics: A Systematic Review. *Front. Neurol.* **2017**, *8*, 300. [[CrossRef](#)]
32. McDonald, S.J.; Shultz, S.R.; Agoston, D.V. The Known Unknowns: An Overview of the State of Blood-Based Protein Biomarkers of Mild Traumatic Brain Injury. *J. Neurotrauma* **2021**, *38*, 2652–2666. [[CrossRef](#)]
33. Pierce, J.E.S.; Smith, D.H.; Trojanowski, J.Q.; McIntosh, T.K. Enduring Cognitive, Neurobehavioral and Histopathological Changes Persist for up to One Year Following Severe Experimental Brain Injury in Rats. *Neuroscience* **1998**, *87*, 359–369. [[CrossRef](#)]
34. Laitinen, T.; Sierra, A.; Bolkvadze, T.; Pitkänen, A.; Gröhn, O. Diffusion Tensor Imaging Detects Chronic Microstructural Changes in White and Gray Matter after Traumatic Brain Injury in Rat. *Front. Neurosci.* **2015**, *9*, 128. [[CrossRef](#)]

35. Dickstein, D.L.; de Gasperi, R.; Gama Sosa, M.A.; Perez-Garcia, G.; Short, J.A.; Sosa, H.; Perez, G.M.; Tschiffely, A.E.; Dams-O'Connor, K.; Pullman, M.Y.; et al. Brain and Blood Biomarkers of Tauopathy and Neuronal Injury in Humans and Rats with Neurobehavioral Syndromes Following Blast Exposure. *Mol. Psychiatry* **2020**, *26*, 5940–5954. [[CrossRef](#)]
36. Koivikko, P.; Posti, J.P.; Mohammadian, M.; Lagerstedt, L.; Azurmendi, L.; Hossain, I.; Katila, A.J.; Menon, D.; Newcombe, V.F.J.; Hutchinson, P.J.; et al. Potential of Heart Fatty-Acid Binding Protein, Neurofilament Light, Interleukin-10 and S100 Calcium-Binding Protein B in the Acute Diagnostics and Severity Assessment of Traumatic Brain Injury. *Emerg. Med. J.* **2021**, *39*, 206–212. [[CrossRef](#)]
37. Manninen, E.; Chary, K.; Lapinlampi, N.; Andrade, P.; Paananen, T.; Sierra, A.; Tohka, J.; Gröhn, O.; Pitkänen, A. Early Increase in Cortical T₂ Relaxation Is a Prognostic Biomarker for the Evolution of Severe Cortical Damage, but Not for Epileptogenesis, after Experimental Traumatic Brain Injury. *J. Neurotrauma* **2020**, *37*, 2580–2594. [[CrossRef](#)]
38. Shahim, P.; Tegner, Y.; Marklund, N.; Blennow, K.; Zetterberg, H. Neurofilament Light and Tau as Blood Biomarkers for Sports-Related Concussion. *Neurology* **2018**, *90*, E1780–E1788. [[CrossRef](#)]
39. Cole, J.T.; Yarnell, A.; Kean, W.S.; Gold, E.; Lewis, B.; Ren, M.; McMullen, D.C.; Jacobowitz, D.M.; Pollard, H.B.; O'Neill, J.T.; et al. Craniotomy: True Sham for Traumatic Brain Injury, or a Sham of a Sham? *J. Neurotrauma* **2011**, *28*, 359–369. [[CrossRef](#)]
40. McIntosh, T.K.; Vink, R.; Noble, L.; Yamakami, I.; Fernyak, S.; Soares, H.; Faden, A.L. Traumatic Brain Injury in the Rat: Characterization of a Lateral Fluid-Perfusion Model. *Neuroscience* **1989**, *28*, 233–244. [[CrossRef](#)]
41. Lin, C.H.; Li, C.H.; Yang, K.C.; Lin, F.J.; Wu, C.C.; Chieh, J.J.; Chiu, M.J. Blood NfL: A Biomarker for Disease Severity and Progression in Parkinson Disease. *Neurology* **2019**, *93*, e1104–e1111. [[CrossRef](#)]
42. Zhu, Y.; Yang, B.; Wang, F.; Liu, B.; Li, K.; Yin, K.; Yin, W.F.; Zhou, C.; Tian, S.; Ren, H.; et al. Association between Plasma Neurofilament Light Chain Levels and Cognitive Function in Patients with Parkinson's Disease. *J. Neuroimmunol.* **2021**, *358*, 577662. [[CrossRef](#)]
43. Mattioli, F.; Bellomi, F.; Stampatori, C.; Mariotto, S.; Ferrari, S.; Monaco, S.; Mancinelli, C.; Capra, R. Longitudinal Serum Neurofilament Light Chain (SNfL) Concentration Relates to Cognitive Function in Multiple Sclerosis Patients. *J. Neurol.* **2020**, *267*, 2245–2251. [[CrossRef](#)]
44. Mattsson, N.; Andreasson, U.; Zetterberg, H.; Blennow, K.; Weiner, M.W.; Aisen, P.; Toga, A.W.; Petersen, R.; Jack, C.R.; Jagust, W.; et al. Association of Plasma Neurofilament Light with Neurodegeneration in Patients with Alzheimer Disease. *JAMA Neurol.* **2017**, *74*, 557–566. [[CrossRef](#)]
45. Thompson, H.J.; LeBold, D.G.; Marklund, N.; Morales, D.M.; Hagner, A.P.; McIntosh, T.K. Cognitive Evaluation of Traumatically Brain-Injured Rats Using Serial Testing in the Morris Water Maze. *Restor. Neurol. Neurosci.* **2006**, *24*, 109–114.
46. Pitkänen, A.; McIntosh, T.K. Animal Models of Post-Traumatic Epilepsy. *J. Neurotrauma* **2006**, *23*, 241–261. [[CrossRef](#)]
47. Huusko, N.; Römer, C.; Ndode-Ekane, X.E.; Lukasiuk, K.; Pitkänen, A. Loss of Hippocampal Interneurons and Epileptogenesis: A Comparison of Two Animal Models of Acquired Epilepsy. *Brain Struct. Funct.* **2015**, *220*, 153–191. [[CrossRef](#)]
48. Sierra, A.; Laitinen, T.; Gröhn, O.; Pitkänen, A. Diffusion Tensor Imaging of Hippocampal Network Plasticity. *Brain Struct. Funct.* **2015**, *220*, 781–801. [[CrossRef](#)]
49. Pitkänen, A.; Immonen, R. Epilepsy Related to Traumatic Brain Injury. *Neurotherapeutics* **2014**, *11*, 286–296. [[CrossRef](#)]
50. Bragin, A.; Li, L.; Almajano, J.; Alvarado-Rojas, C.; Reid, A.Y.; Staba, R.J.; Engel, J.J. Pathologic Electrographic Changes after Experimental Traumatic Brain Injury. *Epilepsia* **2016**, *57*, 735–745. [[CrossRef](#)]
51. Giovannini, G.; Bedin, R.; Ferraro, D.; Vaudano, A.E.; Mandrioli, J.; Meletti, S. Serum Neurofilament Light as Biomarker of Seizure-Related Neuronal Injury in Status Epilepticus. *Epilepsia* **2021**, *63*, e23–e29. [[CrossRef](#)]
52. Nass, R.D.; Akgün, K.; Dague, K.O.; Elger, C.E.; Reichmann, H.; Ziemssen, T.; Surges, R. CSF and Serum Biomarkers of Cerebral Damage in Autoimmune Epilepsy. *Front. Neurol.* **2021**, *12*, 647428. [[CrossRef](#)]
53. Ouédraogo, O.; Rébillard, R.M.; Jamann, H.; Mamane, V.H.; Clénet, M.L.; Daigneault, A.; Lahav, B.; Uphaus, T.; Steffen, F.; Bittner, S.; et al. Increased Frequency of Proinflammatory CD4 T Cells and Pathological Levels of Serum Neurofilament Light Chain in Adult Drug-Resistant Epilepsy. *Epilepsia* **2021**, *62*, 176–189. [[CrossRef](#)]
54. Eriksson, H.; Banote, R.K.; Larsson, D.; Blennow, K.; Zetterberg, H.; Zelano, J. Brain Injury Markers in New-Onset Seizures in Adults: A Pilot Study. *Seizure* **2021**, *92*, 62–67. [[CrossRef](#)]
55. Nass, R.D.; Akgün, K.; Elger, C.; Reichmann, H.; Wagner, M.; Surges, R.; Ziemssen, T. Serum Biomarkers of Cerebral Cellular Stress after Self Limited Tonic Clonic Seizures: An Exploratory Study. *Seizure* **2021**, *85*, 1–5. [[CrossRef](#)]
56. Evers, K.S.; Hügli, M.; Fouzas, S.; Kasser, S.; Pohl, C.; Stoecklin, B.; Bernasconi, L.; Kuhle, J.; Wellmann, S. Serum Neurofilament Levels in Children with Febrile Seizures and in Controls. *Front. Neurosci.* **2020**, *14*, 579958. [[CrossRef](#)]
57. Andrade, P.; Banuelos-Cabrera, I.; Lapinlampi, N.; Paananen, T.; Cizek, R.; Ndode-Ekane, X.E.; Pitkänen, A. Acute Non-Convulsive Status Epilepticus after Experimental Traumatic Brain Injury in Rats. *J. Neurotrauma* **2019**, *36*, 1890–1907. [[CrossRef](#)]
58. Khalil, M.; Pirpamer, L.; Hofer, E.; Voortman, M.M.; Barro, C.; Leppert, D.; Benkert, P.; Ropele, S.; Enzinger, C.; Fazekas, F.; et al. Serum Neurofilament Light Levels in Normal Aging and Their Association with Morphologic Brain Changes. *Nat. Commun.* **2020**, *11*, 812. [[CrossRef](#)]
59. Lindblad, C.; Nelson, D.W.; Zeiler, F.A.; Ercole, A.; Ghatan, P.H.; von Horn, H.; Risling, M.; Svensson, M.; Agoston, D.V.; Bellander, B.-M.; et al. Influence of Blood-Brain Barrier Integrity on Brain Protein Biomarker Clearance in Severe Traumatic Brain Injury: A Longitudinal Prospective Study. *J. Neurotrauma* **2020**, *37*, 1381–1391. [[CrossRef](#)]

60. van Vliet, E.A.; Puhakka, N.; Mills, J.D.; Srivastava, P.K.; Johnson, M.R.; Roncon, P.; Das Gupta, S.; Karttunen, J.; Simonato, M.; Lukasiuk, K.; et al. Standardization Procedure for Plasma Biomarker Analysis in Rat Models of Epileptogenesis: Focus on Circulating MicroRNAs. *Epilepsia* **2017**, *58*, 2013–2024. [[CrossRef](#)]
61. Wilson, D.H.; Rissin, D.M.; Kan, C.W.; Fournier, D.R.; Piech, T.; Campbell, T.G.; Meyer, R.E.; Fishburn, M.W.; Cabrera, C.; Patel, P.P.; et al. The Simoa HD-1 Analyzer: A Novel Fully Automated Digital Immunoassay Analyzer with Single-Molecule Sensitivity and Multiplexing. *J. Lab. Autom.* **2016**, *21*, 533–547. [[CrossRef](#)]
62. Rissin, D.M.; Fournier, D.R.; Piech, T.; Kan, C.W.; Campbell, T.G.; Song, L.; Chang, L.; Rivnak, A.J.; Patel, P.P.; Provuncher, G.K.; et al. Simultaneous Detection of Single Molecules and Singulated Ensembles of Molecules Enables Immunoassays with Broad Dynamic Range. *Anal. Chem.* **2011**, *83*, 2279–2285. [[CrossRef](#)]
63. Manninen, E.; Chary, K.; Lapinlampi, N.; Andrade, P.; Paananen, T.; Sierra, A.; Tohka, J.; Gröhn, O.; Pitkänen, A. Acute Thalamic Damage as a Prognostic Biomarker for Post-Traumatic Epileptogenesis. *Epilepsia* **2021**, *62*, 1852–1864. [[CrossRef](#)]
64. Benjamini, Y.; Hochberg, Y. Controlling the False Discovery Rate: A Practical and Powerful Approach to Multiple Testing. *J. R. Stat. Soc. Ser. B (Methodol.)* **1995**, *57*, 289–300. [[CrossRef](#)]
65. Kharatishvili, I.; Nissinen, J.P.; McIntosh, T.K.; Pitkänen, A. A Model of Posttraumatic Epilepsy Induced by Lateral Fluid-Perfusion Brain Injury in Rats. *Neuroscience* **2006**, *140*, 685–697. [[CrossRef](#)]
66. Ekolle Ndode-Ekane, X.; Kharatishvili, I.; Pitkänen, A. Unfolded Maps for Quantitative Analysis of Cortical Lesion Location and Extent after Traumatic Brain Injury. *J. Neurotrauma* **2017**, *34*, 459–474. [[CrossRef](#)]
67. Andrade, P.; Ciszek, R.; Pitkänen, A.; Ndode-Ekane, X.E. A Web-Based Application for Generating 2D-Unfolded Cortical Maps to Analyze the Location and Extent of Cortical Lesions Following Traumatic Brain Injury in Adult Rats. *J. Neurosci. Methods* **2018**, *308*, 330–336. [[CrossRef](#)]



METTE HEISKANEN

Post-traumatic epilepsy (PTE) is a seizure disorder that can develop months or even years after a traumatic brain injury (TBI). The lack of biomarkers to identify epileptogenesis after TBI has hindered the development of antiepileptogenic treatments to prevent PTE. This thesis investigated the potential of plasma microRNAs and neurofilament light chain protein to act as biomarkers for the severity of the brain injury and the development of post-traumatic epileptogenesis in an animal model of PTE.



UNIVERSITY OF
EASTERN FINLAND

uef.fi

**PUBLICATIONS OF
THE UNIVERSITY OF EASTERN FINLAND**
Dissertations in Health Sciences

ISBN 978-952-61-5193-9
ISSN 1798-5706